The Use of Ultrasonics for Characterising Fats and Emulsions

by

David Julian McClements

Submitted in accordance with the requirements for the degree of
Doctor of Philosophy

Procter Department of Food Science
University of Leeds
LS2 9JT

November 1988

SUMMARY

Ultrasonics has not found widespread use in the food industry, despite having considerable potential for characterising food materials. This is due to the complexity and diversity of food materials, the lack of suitable instrumentation and a poor understanding of how ultrasound interacts with many food components. In this work it is shown how a good appreciation of the theories describing ultrasonic propagation in heterogeneous materials, coupled with careful experimental design, leads to many new applications of ultrasonics for characterising fats and emulsions. Ultrasonic measurements were made using either a pulse echo technique (1-10MHz), or a pulse echo interferometric technique (5-55MHz).

The ultrasonic velocities of a series of 0-30% w/w glyceride/oil mixtures and some commercial fats were measured with varying temperature (0-70°C) at 1MHz. Ultrasonic scattering was not important in these systems and so empirical equations or simple theoretical formulae could be used to relate the measured velocities to the solid fat contents (SFC) of the samples. There were very significant correlations between the SFCs determined using ultrasonics and those determined using pulsed NMR ($r > 0.99$), and so ultrasonics should prove a useful adjunct or alternative to NMR. Velocity measurements also proved useful for characterising vegetable oils since the velocity of an oil could be related to its glyceride composition.

The ultrasonic velocity and attenuation of a series of sunflower oil and water emulsions were measured with varying frequency (1-55MHz), droplet size (0.1-0.9μm), disperse phase mass fraction (0-0.5) and emulsion type (O/W and W/O). Scattering was significant in these emulsions and could be used to measure their disperse phase mass fractions and particle size distributions. Ultrasonics has important advantages over existing techniques for this type of measurement since it can be used in emulsions which are optically opaque, in a non-intrusive, non-invasive manner.

ACKNOWLEDGEMENTS

Thanks are due to my supervisor, Dr. Malcolm Povey, for advice and encouragement throughout my research; to all the members of staff and technicians at the Procter Department for academic and technical support; to the Ministry of Agriculture, Fisheries and Foods for funding my research; to Unilever Research for financial and technical support and in particular D. Moran, I. Campbell, F. Padlee, R. Bee and D. Cebula; to Professor Richmond for kindly allowing Dr. Povey and myself access to the facilities at the AFRC Institute of Food Research (Norwich) to carry out a series of valuable experiments; to N. Gladwell, D. Hibberd, A. Howe, C. Javanaud and M. Robbins for helpful discussions and technical assistance during these experiments; and finally to my family and friends for support and encouragement over the last three years.

ASIDE

The fundament upon which all our knowledge and learning rests is the inexplicable. It is to this that every explanation, through few or many intermediate stages, leads; as the plummet touches the bottom of the sea now at a greater depth, now at a less, but is bound to reach it somewhere sooner or later.

Arthur Schopenhauer

CONTENTS

TABLES

FIGURES

Chapter 1

INTRODUCTION

1.1 Ultrasonics

Ultrasonics is the name given to the study and application of sound waves having frequencies higher than those to which the human ear can respond (≈ 16kHz) (Blitz 1963). A general history of its development can be found in the review article by Karl Graff (1981), whilst its development in the food industry is discussed in the articles by McCann (1986), Javanaud (1988) and Povey and McClements (1988a).

The use of ultrasonics in the food industry can be divided into two distinct areas: high and low intensity applications. High intensity ultrasound is characterised by relatively high power levels (10mW-1kW) and low frequencies (usually < 100kHz) and often causes permanent changes in the materials through which it propagates. Typical applications of high intensity ultrasound in the food industry include emulsification (Sajas et al 1978) and cleaning (Lambert 1982). Low intensity applications use lower power levels (1μW-100mW) and higher frequencies (0.5- 100MHz) and leave the material through which they propagate unaltered. Typical applications of low intensity ultrasonics are level detection (Asher 1982, Kress-Rogers 1986), doppler flow metering (Lynnworth 1979, Sanderson 1982), molecular relaxation studies (Wyn-Jones et al 1982) and non-destructive testing (NDT) (Povey and McClements 1988a, Povey 1988). It is this latter application which is of interest in this work.

Low intensity ultrasonic waves can be used to determine various characteristics of materials through which they propagate. In the food industry ultrasonic compressional waves are most frequently used for this purpose, however, shear and surface waves may also be used for certain applications (Asher 1983). Compressional waves pass through materials

by successive compressions and rarefactions (figure 1.1) and leave the material unaltered if the amplitude of the deformations is small enough to be within the elastic region of the material. Compressional waves are usually generated using piezo-electric transducers, however other methods are also available, and these have been reviewed by Silk (1984). The two ultrasonic parameters which are most frequently measured are ultrasonic velocity and attenuation. These parameters are characteristic of a material and can be related to its physical properties e.g. elastic constants, density, composition and micro-structure (chapter 2). There are a variety of techniques available for measuring the ultrasonic velocity and attenuation of materials and the choice of a particular technique depends on the material under test and the requirements of the investigator. Detailed accounts of the techniques available for ultrasonic NDT in general are contained in the articles by Breazeale et al (1981) and Papadakis (1976), whilst McCann (1986) and Povey and McClements (1988a) have reviewed a number of the techniques most suitable for use in the food industry.

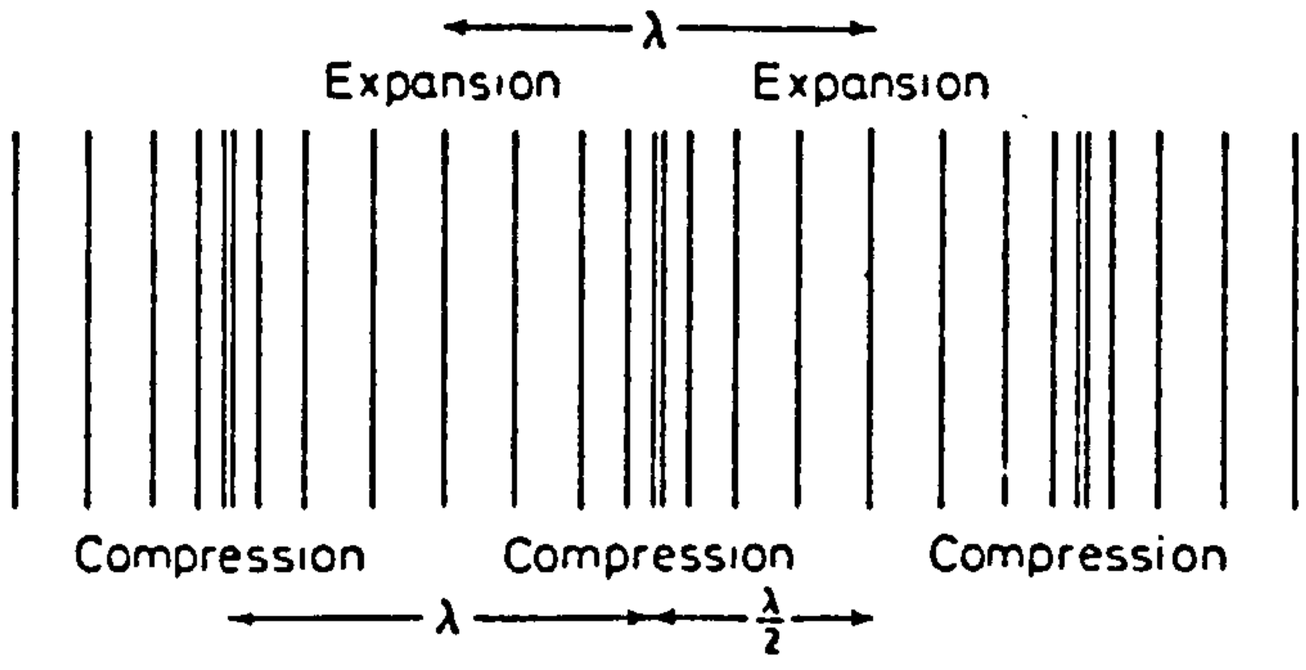

Figure 1.1: Propagation of a compressional wave in a material. Layers expand and contract as wave passes through.
(λ = Wavelength of compressional wave)

1.2 Ultrasonic sensors in the food industry

Sensors are required in the food industry in order to provide information about the properties of food materials. This information is essential in the competitive environment of the food industry today, since it helps manufacturers to develop new products, improve existing products and optimise manufacturing costs. Sensors are needed in the laboratory to establish the factors which influence product quality, and in the factory, to monitor these factors during processing. At present there is a lack of suitable sensors for use in the food industry and so there is considerable interest in the development of new sensors or the adaptation of existing sensors (Agricultural Research Council 1982, Food and Drink Federation 1985).

A number of workers have highlighted the potential of ultrasonics as a probe of food materials (e.g. McCann 1986, Povey and McClements 1988a, Javanaud 1988). The technique can be used to measure the physical properties of materials in-line, in a non-invasive, non-intrusive manner (Asher 1982, 1983). It can be fully automated; is capable of rapid and precise measurements; is robust; has relatively low capital and running costs and is non-hazardous (Povey and McClements 1988a). It also lends itself well to translation from the laboratory to a factory environment (Papadakis 1976). Ultrasonics would therefore seem to have many of the qualities of the 'ideal sensor' outlined by the Food and Drink Federation (1985). However, the complexity and diversity of food materials, coupled with the lack of information on the interaction between food components and ultrasound, means that a considerable amount of research is still required before the technique can be applied successfully to many food materials.

1.3 Ultrasonic measurements in fats and emulsions

Over the past 30 years or so there have been a variety of applications of ultrasonics to food fats and emulsions (see sections 4.1 and 5.1). The majority of these have been preliminary experiments whose aim was to establish whether ultrasonics was suitable for a particular application. With the exception of meat inspection, few of these preliminary investigations

have led to the development of ultrasonic techniques for use in the food industry. This is surprising since ultrasonics is a well established means of characterising materials in other areas such as medical physics, geology and materials testing. There are a number of reasons which might explain this apparent discrepancy. Firstly, many of the ultrasonic instruments which are suitable for measurements in the laboratory are not suitable for use in the environments often encountered in the food industry. Secondly, many investigators working in this area are not aware of the theories describing ultrasonic propagation in heterogeneous systems. Finally, food emulsions and fats contain a variety of different components and it is often difficult to isolate the effect each component has on ultrasonic measurements.

The aim of this work was to establish the factors which affect ultrasonic propagation in fats and emulsions and thus highlight the potential of the ultrasonic technique as a tool for characterising these systems. For this reason a significant proportion of this work was spent developing a reliable measuring technique (chapter 3) and in understanding the theories which describe ultrasonic propagation in heterogeneous materials (chapter 2). The majority of the experimental measurements were carried out using simple binary fat/oil mixtures (chapter 4) and oil/water emulsions (chapter 5) rather than multi-component food systems since the factors which affect measurements could be isolated more easily. However, a number of experiments were also carried out using commercial fats, margarines and low fat spreads to demonstrate the usefulness of the technique for characterising real food materials.

Chapter 2

ULTRASONIC PROPAGATION IN EMULSIONS AND SUSPENSIONS

2.1 Introduction

There have been many applications of ultrasonics to non-food emulsions and suspensions over the past 50 years or so. The majority of these have involved comparisons between experimental measurements of ultrasonic velocity and attenuation and various theoretical formulations (e.g. see the articles by Allegra and Hawley 1972, Kuster and Toksoz 1974, Anderson and Hampton 1980, McClements and Povey 1987a, Harker and Temple 1987). A number of workers have also examined specific applications of the technique, such as particle sizing (Ohsawa 1969, Rozhlenko et al 1974, Ballaro et al 1980, Javanaud et al 1986, Rokhlenko 1986), determination of disperse phase volume fractions (Hussin and Povey 1984, Howe et al 1986, Hibberd et al 1987a,b) and measurement of particle compressibilities (Urick 1947, Barret-Gultepe et al 1980, 1983, Shung et al 1982).

To measure any of these properties it is necessary to relate some parameter which can be measured using ultrasonics (e.g. velocity or attenuation) to the property of interest. This can either be done by carrying out many experiments and establishing empirical relationships or by using theoretical equations available in the literature. In complex systems or in systems where there is no appropriate theory the former approach may be the only alternative. However, a theoretical approach should be used where possible since it leads to a better appreciation of the factors which influence measurements and because it has predic-tive power.

There are many theoretical equations available in the literature which attempt to describe the propagation of ultrasound in emulsions and suspensions. Different equations

can be categorised by the mathematical approach used to derive them, the assumptions underlying them and the systems they apply to. Useful reviews of the subject can be found in the articles by Ahuja (1971), Anderson and Hampton (1980), McClements and Povey (1987a) and Harker and Temple (1987). The most comprehensive treatments of the problem for dilute systems appear to be those based on scattering theory, and this approach is discussed in some detail in section 2.4. The mathematical approach required to describe ultrasonic scattering is fairly complicated and tends to obscure the physical significance of the results. For this reason the origin of the various scattering mechanisms is also discussed in section 2.4 and their practical significance is highlighted by numerical calculation of the velocity and attenuation in some model systems. Before considering ultrasonic scattering theory, however, it is useful to examine ultrasonic propagation in isotropic, homogeneous materials (section 2.2) and in simple two phase systems which do not scatter ultrasound (section 2.3) so as to establish the basic relationships which will be used in the later sections. In section 2.5 a number of other factors which may effect ultrasonic measurements in food dispersions are discussed. These include propagation in concentrated systems, the effects of particle interaction and the presence of air cells and strong scatterers. A list of symbols used in the equations in this chapter is included in Appendix I.

2.2 Propagation through isotropic homogeneous materials

2.2.1 Ultrasonic velocity

To obtain a relationship between the ultrasonic velocity and the physical properties of a material a mathematical description of the propagation of ultrasonic waves is necessary. By consideration of plane compressional waves travelling through an isotropic liquid it is possible to show that (Appendix II):

$$\frac{\delta^2\xi}{\delta x^2}+\frac{\delta^2\xi}{\delta y^2}+\frac{\delta^2\xi}{\delta z^2}=\left(\frac{\rho}{\varepsilon}\right)\frac{\delta^2\xi}{\delta t^2} \qquad (2.1)$$

where ξ is the displacement of an element of the liquid from its equilibrium position, x, y, and z are directions in three dimensional space, t is the time, ρ is the density of the material and ε is the appropriate elastic modulus. The general differential equation for the propagation of waves in three dimensions is:

$$\frac{\delta^2\xi}{\delta x^2}+\frac{\delta^2\xi}{\delta y^2}+\frac{\delta^2\xi}{\delta z^2}=\left(\frac{k}{\omega}\right)^2\frac{\delta^2\xi}{\delta t^2} \qquad (2.2)$$

where k is the wave number and ω is the angular frequency. For non-attenuating media $k=\frac{\omega}{v}$, where v is the velocity of ultrasound in the material. By comparing equations 2.1 and 2.2 a simple relationship between the ultrasonic velocity and the physical properties of a material can be derived:

$$v=\sqrt{\frac{\varepsilon}{\rho}} \qquad (2.3)$$

For compressional waves propagating in a liquid or a gas the appropriate elastic modulus is the bulk modulus K (which is the reciprocal of the adiabatic compressibility κ), and for bulk solids it is $E+\frac{4}{3}\bar{G}$ Shear waves will propagate through most solids ($\varepsilon=G$), however, they are highly attenuated in liquids and gasses and usually do not travel far enough to be detected ($\approx\mu m$). Emulsions and suspensions are predominantly liquid and so it is compressional waves which are of primary concern to this work.

2.2.2 Absorption

As an ultrasonic wave travels through a material it is attenuated, i.e. its amplitude decreases with distance travelled. The major causes of attenuation in general are due to absorption of ultrasound by the material it passes through and deflection of ultrasound out of its original path by scattering, reflection, refraction or diffraction (Blitz 1963). In isotopic homogeneous materials absorption is the predominant form of attenuation. Absorption occurs to some extent in all materials and is due to mechanisms which convert energy from the ultrasonic wave into some other form, ultimately heat. In liquids and gasses the most important forms

of absorption are due to shear and bulk viscosity, thermal conduction and molecular relaxation (Bhatia 1967). In solids the situation is more complex and there are many more forms of absorption which have to be considered (Bhatia 1967).

The wave number of an attenuating material is complex: $k = \frac{\omega}{v} + i\alpha$. Here α is the attenuation coefficient which has units of Nepers per metre (Np/m) when defined by the equation:

$$A = A_0 e^{-\alpha x} \tag{2.4}$$

where x is the distance the wave has travelled through the material (in m), A_0 is the initial amplitude of the wave and A is the amplitude at position x. By convention the attenuation coefficient is usually defined in units of decibels per metre (dB/m), where 1dB = 8.686Np.

2.2.3 Frequency dependence of velocity and absorption

The overall absorption of a material increases with increasing frequency. The absorption due to the classical absorption mechanisms, viscosity and thermal conduction, increases with the square of frequency, whilst absorption due to molecular relaxation has a maximum value of absorption per cycle ($\alpha\lambda$) at some characteristic frequency, which depends on the relaxation time of the absorption process. The ultrasonic velocity of a material also varies with frequency due to molecular relaxation. At low frequencies the velocity has a constant value, as the frequency increases the velocity increases until it reaches another constant value at high frequencies. For solids and liquids the high frequency limit is usually only a few percent larger than the low frequency limit (Bhatia 1967). The dependence of ultrasonic velocity on frequency is called *velocity dispersion*.

2.3 Propagation in non-scattering emulsions and suspensions

2.3.1 Velocity

Assuming that the wavelength of sound is much greater than the particle size, the velocity of a non-scattering system can be described by an equation derived by Wood (1941):

$$v^2 = \frac{1}{\kappa_0 \rho_0} \tag{2.5}$$

where

$$\kappa_0 = \kappa'\phi + \kappa(1-\phi) \tag{2.6}$$

$$\rho_0 = \rho'\phi + \rho(1-\phi) \tag{2.7}$$

Here κ_0 and ρ_0 are simply the volume average values of adiabatic compressibility and density of the component phases and ϕ is the disperse phase volume fraction. Thus if the adiabatic compressibilities and densities of the component phases are known the variation of velocity with ϕ can be calculated using equation 2.5. Figure 2.1 shows a graph of velocity versus ϕ for a model emulsion where the velocity of the disperse phase is larger than that of the continuous phase. It can be seen that by measuring the velocity through the emulsion it is possible to determine its disperse phase volume fraction. Alternatively, the adiabatic compressibility of a disperse phase of an emulsion or suspension could be calculated by measuring the velocity through it, once the values of κ, ρ', ρ and ϕ are known. This may be useful for measuring compressibilities of materials which cannot be measured directly in their bulk form e.g. blood cells (Shung et al 1982), powders or granular material (Urick 1947, 1948).

The velocity dispersion in a non-scattering system is due to the velocity dispersion of the component phases and is therefore independent of factors such as particle size and the relative theromophysical properties of the component phases. For many emulsions, ultrasonic scattering is important, and the velocity is dependent on these factors (section 2.4).

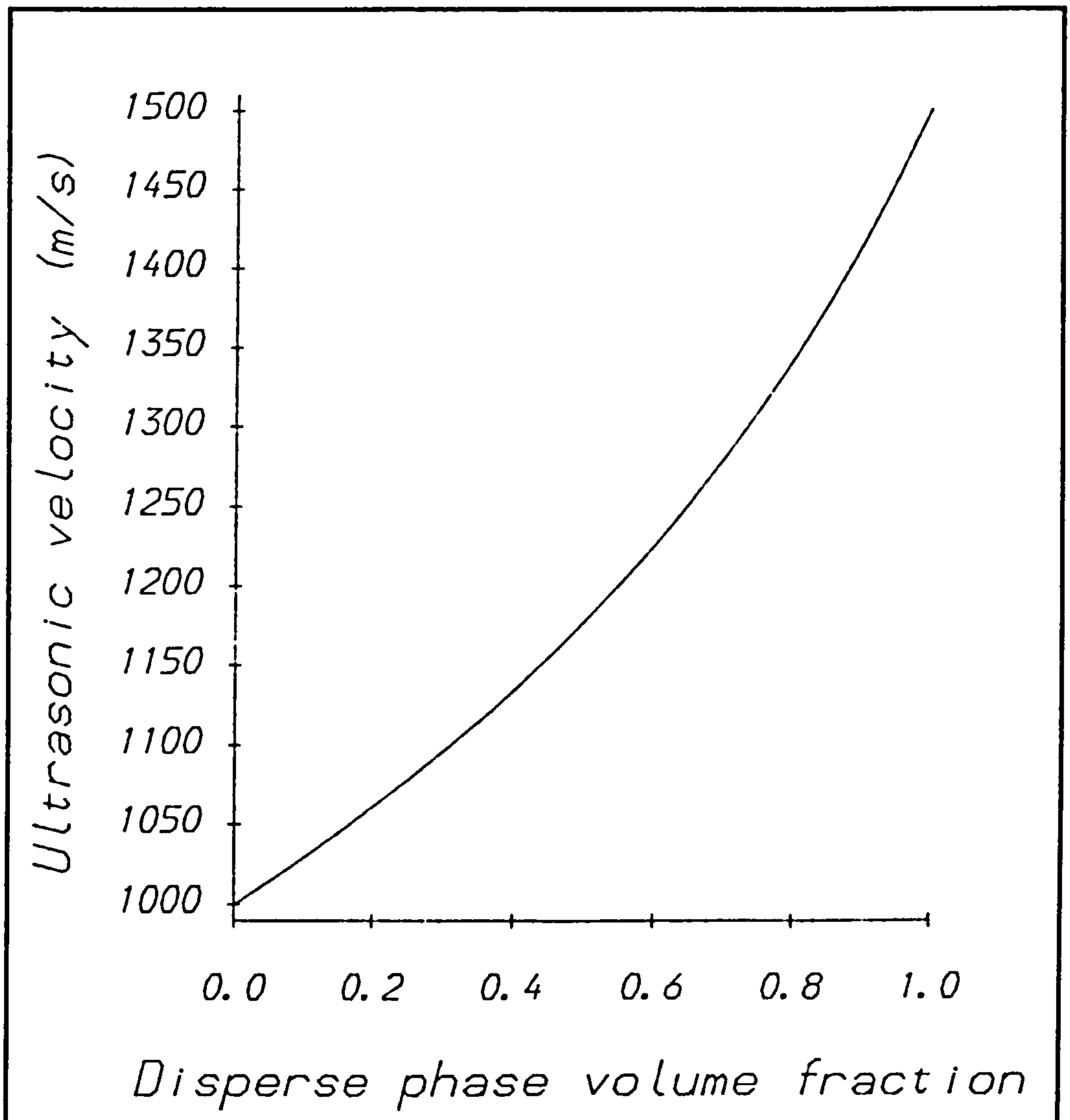

Figure 2.1: Ultrasonic velocity of a non-scattering emulsion. Variation of ultrasonic velocity with disperse phase volume fraction was calculated using equation 2.5 and the parameters: $v' = 1500$ m/s, $v = 1000$ m/s, $\rho' = \rho = 1000$ kg/m^3.

2.3.2 Attenuation

The attenuation of ultrasound in a non-scattering system is given by the equation (Allegra and Hawley 1972):

$$\alpha_0 = \alpha'\phi + \alpha(1-\phi) \qquad (2.8)$$

Where α_0 is the volume average value of the intrinsic absorption coefficients of the component phases. Once the absorption coefficients of the component phases are known, it is simple to calculate the variation of the overall attenuation with ϕ (figure 2.2). By measuring the attenuation of an emulsion or suspension it should therefore be possible to determine its disperse phase volume fraction. For real systems the overall attenuation is due to both absorption and scattering of ultrasound and may be considerably larger than that predicted by equation 2.8. Unlike absorption, when ultrasound is scattered, the ultrasonic energy is not converted into some other form of energy, but is redirected in directions which are different from that of the incident wave. The difference between the overall attenuation and that due to absorption alone (equation 2.8) is termed the *excess attenuation* and is made up of contributions from a number of scattering mechanisms (section 2.4).

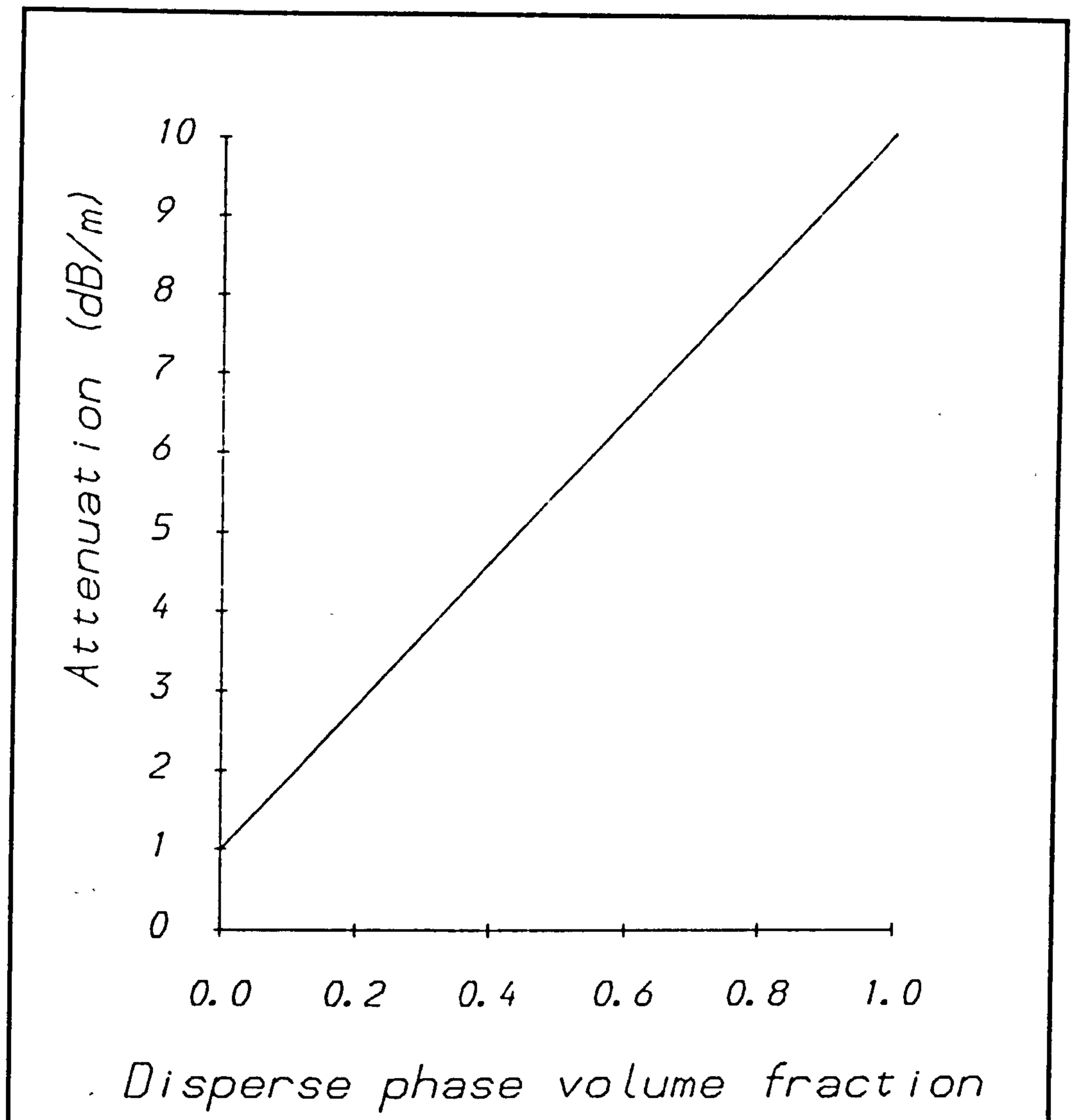

Figure 2.2: Attenuation of a non-scattering emulsion. Variation of attenuation coefficient with disperse phase volume fraction was calculated using equation 2.8 and the parameters $\alpha = 1$ dB/m and $\alpha' = 10$ dB/m.

2.4 *Scattering by emulsions and suspensions*

2.4.1 Introduction

When an ultrasonic wave is incident on a particle some of the ultrasound passes through the particle and some is scattered (figure 2.3). The theories discussed in this section are only applicable to weakly scattering particles, i.e. the amplitude of the scattered wave is much smaller than the amplitude of the incident wave. Scattering reduces the amount of ultrasonic energy detected in the forward direction and so increases the attenuation. It also effects the ultrasonic velocity since scattered waves interact with the incident wave, altering the phase of the detected wave.

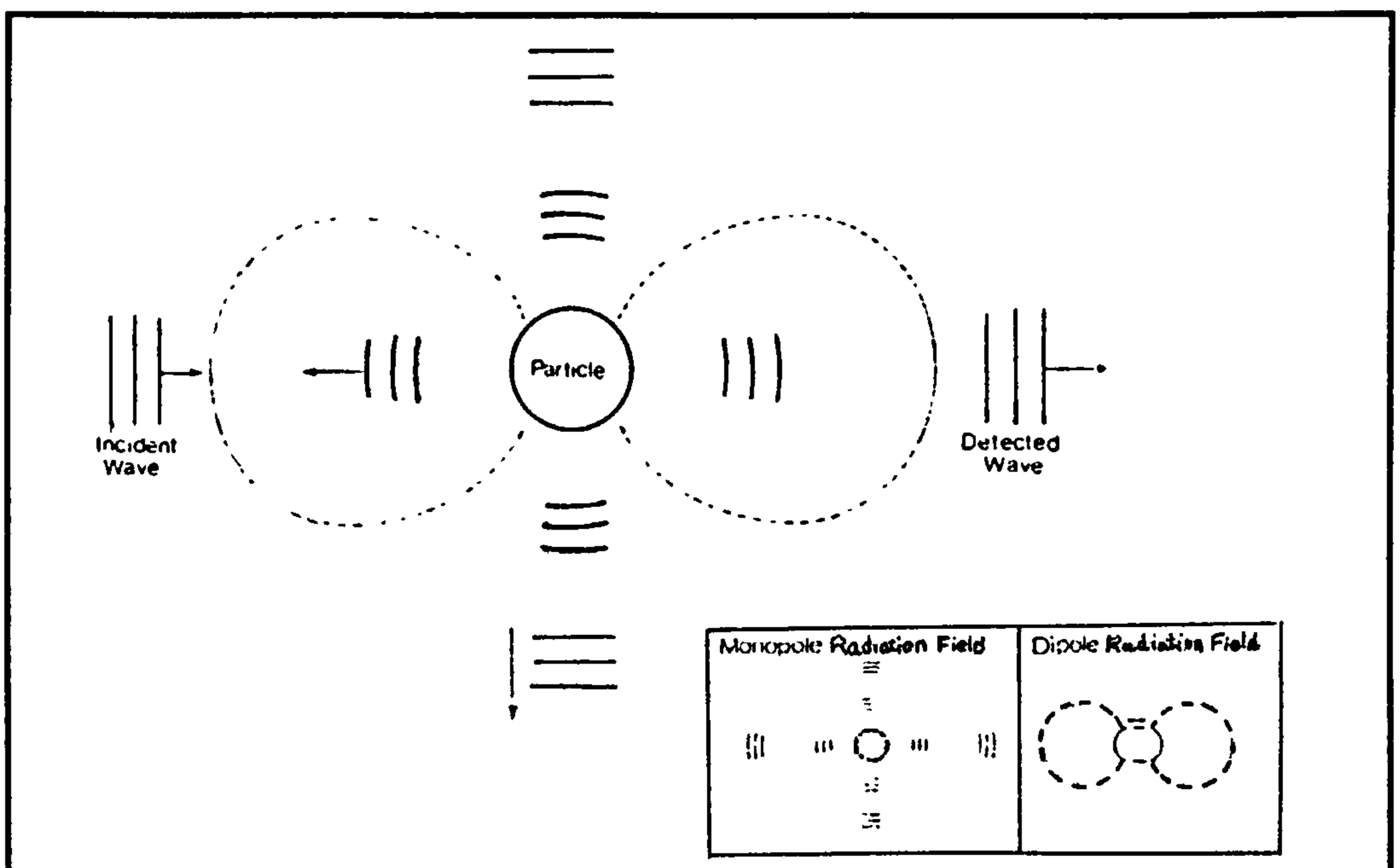

Figure 2.3: Ultrasonic scattering by a spherical particle.

The major developments in scattering theory from the pioneering work of Rayleigh to the early 1970's have been reviewed by Allegra and Hawley (1972), whilst more recent work has been reviewed by Harker and Temple (1987). One of the most important

publications in this area was that of Epstein and Carhart (1953) dealing with ultrasonic propagation in aerosols and emulsions. They showed that the two most important sources of scattering were due to viscous and thermal transport mechanisms which occur at the interface of the inhomogenities. Chow (1964) extended this work to include the effects of surface tension, and demonstrated that these were significant for gas bubbles suspended in fluid media, but were not important for emulsions due to the low compressibility of emulsion droplets. Allegra and Hawley (1972) further extended the formulations of Epstein and Carhart to include solid particles suspended in liquid continuum. All of these workers considered the problem of scattering from a single particle suspended in a fluid continuum and assumed the effects of scattering were linearly related to the number of particles present, and so their formulations are only strictly applicable to dilute systems. For more concentrated systems, ultrasound scattered from one particle may be incident on another and so the effects of multiple scattering must be considered (Waterman and Truell 1961, Twersky 1962, and Lloyd and Berry 1967). A number of workers have used ultrasonic scattering theory to describe ultrasonic propagation in a variety of disperse systems (e.g. Davies 1978, Datta and Pethrick 1980, Hay and Burling 1982, Lin and Raptis 1983, Habeger 1982, Hay and Mercer 1985, Gladwell et al 1987).

In this work scattering coefficients were calculated from the formulations of Epstein and Carhart (1953) and the velocity and attenuation were calculated from these using the multiple scattering theory of Lloyd and Berry (1967). This approach is slightly different from that which is usually used, since the multiple scattering theory of Lloyd and Berry (1967) was used rather than that of Waterman and Truell (1961). This was because Lloyd and Berry (1967) have shown that the Waterman and Truell approach is a limiting case of their more general approach.

2.4.2 Determination of scattering coefficients.

When a compressional wave is incident on a particle it gives rise to a reflected compressional wave, a compressional wave in the particle and viscous and thermal waves in both the fluid and particle. Wave equations for the propagation of these waves in viscous isotropic heat conducting media are derived from the conservation laws, a stress-strain relation and two thermodynamic equations of state (Allegra and Hawley 1972) and can be written as follows:

$$(\nabla^2 + k_c^2)\phi_c = 0$$

$$(\nabla^2 + k_t^2)\phi_t = 0$$

$$(\nabla^2 + k_s^2)A = 0$$

$$k_c = \frac{\omega}{v} + i\alpha$$

$$k_t = (1+i)\sqrt{\frac{\omega}{2\sigma}}$$

$$k_s = (1+i)\sqrt{\frac{\omega}{2v}}$$

These equations are solved in spherical co-ordinates in terms of series expansions of spherical Bessel functions and spherical harmonics with undetermined coefficients.

In the continuous phase:

$$\phi_0 = \sum_{n=0}^{\infty} i^n (2n+1) j_n(k_c r) P_n(\cos\theta)$$

$$\phi_r = \sum_{n=0}^{\infty} i^n (2n+1) A_n h_n(k_c r) P_n(\cos\theta)$$

$$\phi_t = \sum_{n=0}^{\infty} i^n (2n+1) B_n h_n(k_t r) P_n(\cos\theta)$$

$$A = \sum_{n=0}^{\infty} i^n (2n+1) C_n h_n(k_s r) P_n^1(\cos\theta)$$

In the disperse phase:

$$\phi'_r = \sum_{n=0}^{\infty} i^n (2n+1) A'_n j_n(k'_c r) P_n(\cos\theta)$$

$$\phi'_t = \sum_{n=0}^{\infty} i^n (2n+1) B'_n j_n(k'_t r) P_n(\cos\theta)$$

$$A' = \sum_{n=0}^{\infty} i^n (2n+1) C'_n j_n(k'_s r) P^1_n(\cos\theta)$$

By considering the boundary conditions at the surface of the droplet - the velocity and stress components, the temperature, and the heat flow are continuous - a set of six complex simultaneous equations are obtained which can be solved for the unknown coefficients, A_n, B_n, C_n, A'_n, B'_n, C'_n, as shown below.

$$aj'_n(a)+A_n ah'_n(a)+B_n bh'_n(b)-C_n n(n+1)h_n(c) = A'_n a'j'_n(a')+B'_n b'j'_n(b')-C'_n n(n+1)j_n(c')$$

$$j_n(a)+A_n h_n(a)+B_n h_n(b)-C_n[h_n(c)+ch'_n(c)] = A'_n j(a')+B'_n j_n(b')-C'_n[j_n(c')+c'j'_n(c')]$$

$$g[j_n(a)+A_n h_n(a)]+GB_n h_n(b) = g'A'_n j_n(a')+G'B'_n j_n(b')$$

$$\tau\{g[aj'_n(a)+A_n ah'_n(a)]+GB_n bh'_n(b)\} = \tau'\{g'A'_n a'j'_n(a')+G'B'_n b'j'_n(b')\} \qquad (2.9)$$

$$\eta\{[aj'_n(a)-j_n(a)]+A_n[ah'_n(a)-h_n(a)]+B_n[bh'_n(b)-h_n(b)]-\frac{1}{2}C_n[c^2h''_n(c)+(n^2+n-2)h_n(c)]\}$$

$$= \eta'\{A'_n[a'j'_n(a')-j_n(a')]+B'_n[b'j'_n(b')-j_n(b')]-\frac{1}{2}C'_n[c'^2j''_n(c')+(n^2+n-2)j_n(c')]\}$$

$$\eta\{[c^2j_n(a)-2a^2j''_n(a)]+A_n[c^2h_n(a)-2a^2h''_n(a)]+B_n[Mc^2h_n(b)-2b^2h''_n(b)]+2n(n+1)C_n[ch'^{(c)}_{n_\lambda}-h_n(c)]\}$$

$$= \eta'\{A'_n[c'^2j_n(a')-2a'^2j''_n(a')]+B'_n[M'c'^2j_n(b')-2b'^2j''_n(b')]+2n(n+1)C'_n[c'j'_n(c')-j_n(c')]\}$$

where the following abbreviations have been used for both primed and unprimed quantities:

$$g = \frac{-i\omega\rho\kappa(\gamma-1)}{\beta}$$

$$G = \frac{\gamma p\kappa}{i\omega\beta}\left[\omega^2-\left(\frac{1}{\gamma p\kappa}-\frac{4i\omega\eta}{3\rho}\right)k_t^2\right]$$

$$M = 1-2\frac{\nu}{\sigma}$$

$$\gamma = 1 + \frac{T_o \beta^2}{C_p \rho \kappa}$$

For the special case when n = 0, the second and fifth equations of equation 2.9 are not valid, and all the other n terms vanish from the remaining equations. In this case the problem reduces to four equations with four unknowns. Equation 2.9 is suitable for determining the scattering coefficients of fluid particles suspended in fluid media i.e. emulsions. For suspensions the equations of Allegra and Hawley (1972) should be used. These can be obtained from the above equations by making the substitution $\eta' = \frac{\mu'}{-i\omega}$ where ever η' appears, and by multiplying the right hand side equations of equation 2.9 by $-i\omega$. The Bessel functions used in equation 2.9 are included in Appendix III.

2.4.3 Relationship of scattering coefficients to velocity and attenuation

Once the scattering coefficients of a single particle have been determined they need to be related to the velocity and attenuation of an emulsion or suspension. This is done using the complex propagation constant B ($=\frac{\omega}{v} + i\alpha$), derived from consideration of multiple scattering effects of a random assembly of spherical particles (Lloyd and Berry 1967):

$$\left(\frac{B}{k_c}\right)^2 = 1 + \frac{3\phi f(0)}{k_c^2 r^3} + \frac{9\phi^2}{4k_c^4 r^6}\left[f^2(\pi) - f^2(0) - \int_{\theta=0}^{\pi} \frac{1}{\sin\frac{1}{2}\theta} \frac{d}{d\theta} f^2(\theta) d\theta\right] \qquad (2.10)$$

where f(0) and f(π) are the far-field scattering amplitudes:

$$f(0) = \frac{1}{ik_c} \sum_{n=0}^{\infty} (2n+1) A_n$$

$$f(\pi) = \frac{1}{ik_c} \sum_{n=0}^{\infty} (-i)^n (2n+1) A_n$$

The term containing ϕ in equation 2.10 describes the contribution due to single scattering (Foldy 1945) whilst the terms containing ϕ^2 describe the contribution due to multiple scattering (Lloyd and Berry 1967). These multiple scattering terms become increasingly important as the particle concentration increases.

The majority of ultrasonic measurements carried out in this work were in the frequency range 1-10 MHz. In this range the wavelength of ultrasound ($\lambda \approx$ 1500-150μm for water) is considerably larger than the radius of the dispersed particles (usually less than 5 μm) and so the long wavelength approximation is valid (i.e. $a^2 << 1$). The orders n = 0 and 1 are then sufficient to describe the problem since every additional A_n term contains an extra a^2 factor and convergence of the series is rapid. Equation 2.10 can then be rewritten in the following form, by substituting in the far-field scattering amplitudes:

$$(\frac{B}{k_c})^2 = 1 - \frac{3i\phi}{(k_c r)^3}(A_0 + 3A_1) - \frac{27\phi^2}{(k_c r)^6}(A_0 A_1 + 2A_1^2) \qquad (2.11)$$

This equation is the same as that calculated by Waterman and Truell (1961) apart from the additional $2A_1^2$ term contained in the multiple scattering contribution. Lloyd and Berry (1967) have shown that this term may become significant as the volume fraction increases. The ultrasonic velocity and attenuation of an emulsion or suspension are calculated from equation 2.11 using the relationships: $v = \frac{\omega}{\mathrm{Re}(B)}$ and $\alpha = \mathrm{Im}(B)$. The computer program used for numerical solution of equations 2.9 and 2.11 is discussed in Appendix IV.

It is useful to list the assumptions implicit in equation 2.11. These are a) the particles are spherical, weak scatterers whose radii are much smaller than the compressional wavelength in the continuous phase ($r << \lambda$); b) the distance between the particles d, is much greater than the viscous and thermal wavelengths in the continuous phase ($d >> \delta_t$ and $d >> \delta_s$); c) no relaxation or mass transfer mechanisms occur; d) the distribution of the particles in the emulsion or suspension is random. It should also be noted that equation 2.11 does not define the medium surrounding the particles self consistently and may thus only have limited application at higher particle concentrations (section 2.5.2).

2.4.4 Physical significance of scattering mechanisms

An examination of equations 2.9 and 2.11 reveals that the ultrasonic velocity and attenuation of an emulsion or suspension depends on the thermophysical properties of its component phases, the volume fraction of particles present, the particle size and the frequency used. However, the rigorous mathematical approach required to formulate a general theory of ultrasonic scattering in these systems tends to obscure the physical significance of the scattering mechanisms. To gain an intuitive understanding of the factors which influence scattering in emulsions and suspensions it is necessary to highlight the physical processes involved.

Thermal scattering An adiabatic pressure wave passing through a medium causes fluctuations in temperature around the equilibrium value due to pressure-temperature coupling. In a two phase system, where the thermal properties of the component phases are different, the temperature fluctuations in the particle and the surrounding fluid will be different and a temperature gradient will exist in a layer of thickness δ_t from the interface. As a result the particle will pulsate, and heat energy will flow between the components. If this heat flow is not in phase with the incident compressional wave, the effective compressibility of the emulsion becomes a complex quantity and velocity dispersion and excess attenuation occur (Ahuja 1973). The magnitude of the resultant thermal scattering depends on the difference in temperature between the particle and the surrounding fluid, which is contained in the term $\left[\frac{\beta}{\rho C_p} - \frac{\beta'}{\rho' C'_p}\right]^2$. The ultrasound scattered by a pulsating particle is spherically symmetric i.e. it is monopole (figure 2.3).

Visco-inertial scattering Visco-inertial scattering occurs when particles have a different density to the surrounding fluid. In the presence of a compressional wave a net inertial force acts on the particles which causes them to oscillate, and this oscillation is damped by the viscosity of the surrounding fluid. When the oscillations of the particle are out of phase with the incident wave the effective density of the system becomes a complex quantity and visco-inertial scattering occurs which also leads to velocity dispersion and excess attenuation

(Ahuja 1972a,b). The magnitude of visco-inertial scattering depends on the density difference between the component phases. The ultrasound scattered by an oscillating particle has a cosϕ dependence on angle i.e. it is dipole (figure 2.3).

2.4.5 Explicit expressions for ultrasonic propagation parameters

In general the effects of visco-inertial and thermal scattering are intermingled, however, in the long wavelength regime ($r << \lambda$) they can be considered to act independently of one another and explicit expressions for the A_s terms can be obtained (Allegra and Hawley 1972). Examination of these expressions reveal that thermal scattering is associated with the A_0 term, whilst visco-inertial scattering is associated with the A_1 term (Ahuja 1973). By inserting these expressions into the complex propagation constant calculated by Waterman and Truell (1961) (which is equivalent to equation 2.11 at low particle concentrations), expressions for the effective compressibility and density of an emulsion (or suspension) can be derived:

$$\kappa = \kappa_0 - \frac{3\kappa\phi(\gamma-1)}{b^2 F}\left(1-\frac{\beta'\rho C_p}{\beta\rho' C_p}\right)^2 \tag{2.12}$$

$$\rho = \rho_0 - \frac{\phi(\rho'-\rho)^2}{\rho'+\rho T+i\rho s} \tag{2.13}$$

Similarly the contributions of the visco-inertial and thermal scattering mechanisms to the overall excess attenuation can be isolated assuming the multiple scattering contribution is negligible, i.e. the droplet concentration is small:

$$\alpha_{th} = \frac{3\phi k_c i(\gamma-1)}{2b^2 F}\left(1-\frac{\beta'\rho C_p}{\beta\rho' C_p}\right)^2 \tag{2.14}$$

$$\alpha_{vis} = \frac{1}{2}\frac{\phi k_c s(\rho'-\rho)^2}{(\rho'+T\rho)^2+s^2\rho^2} \tag{2.15}$$

where the following abbreviations have been used:

$$F = \frac{(1-\frac{\tau}{\tau'}Z)}{(1-ib)}$$

$$Z = \frac{(1-ib)\sin b'}{\sin b' - b'\cos b'}$$

$$T = \frac{1}{2} + \frac{9\delta_g}{4r}$$

$$s = \frac{9\delta_g}{4r}\left(1 + \frac{\delta_g}{r}\right)$$

The values of T and s are for rigid particles (i.e. $\frac{\eta'}{\eta} \to \infty$); for viscous particles the values of T and s must be modified (Ahuja 1972a,b).

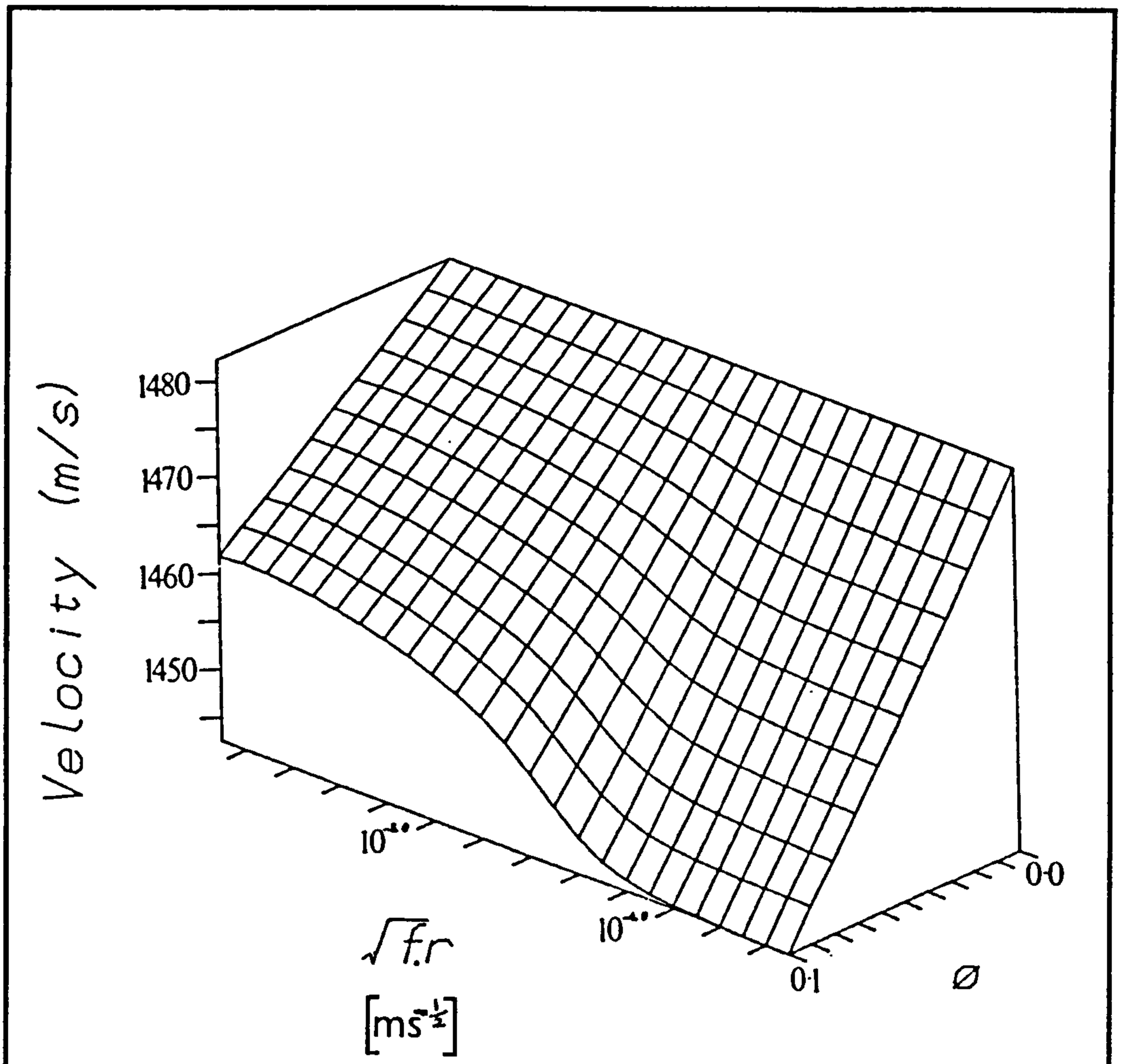

Figure 2.4: Ultrasonic velocity of a scattering emulsion. Three dimensional plot of velocity against ϕ and $\sqrt{fr}$ for a hexadecane in water emulsion.

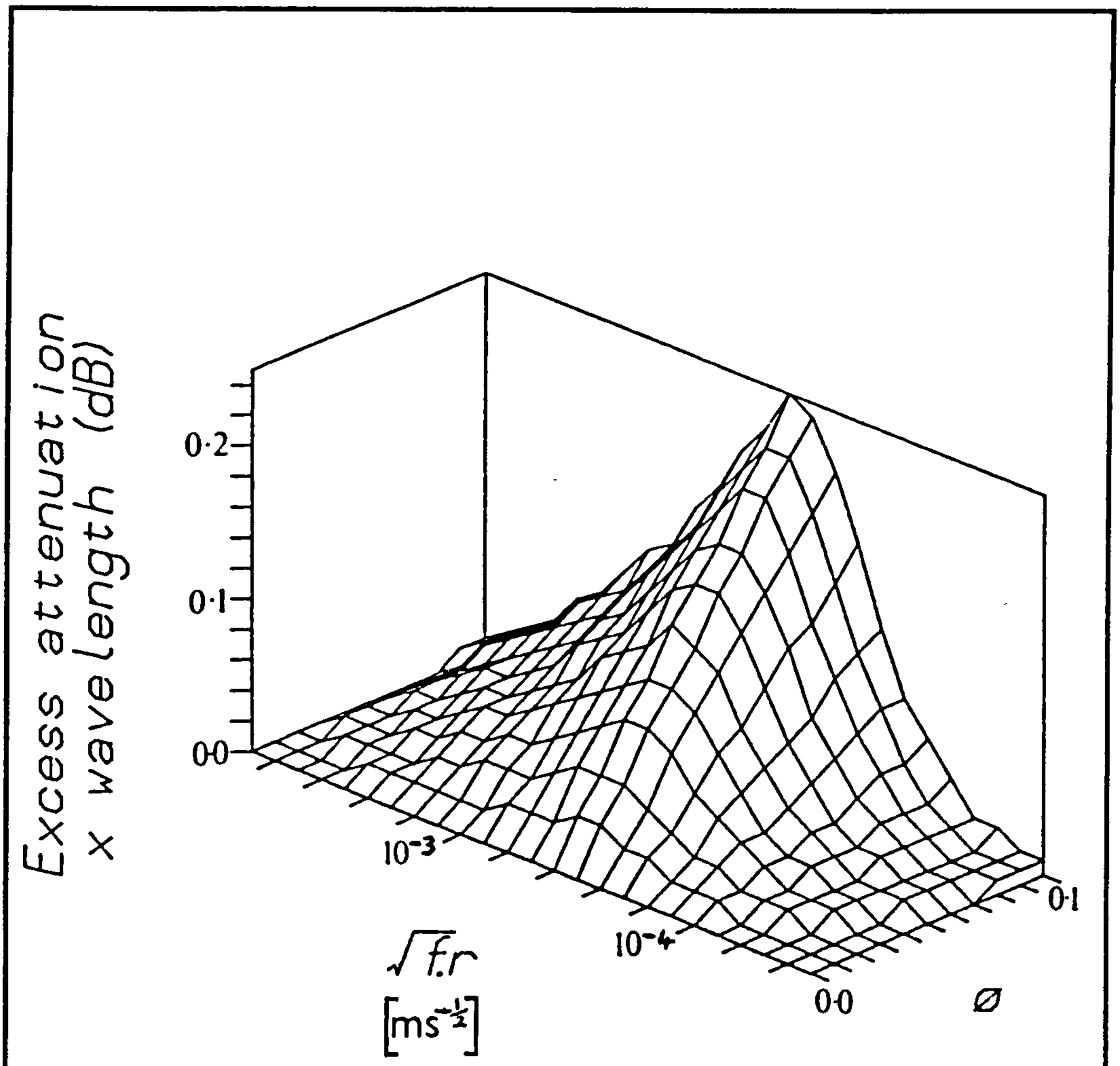

Figure 2.5: Attenuation of a scattering emulsion. Three dimensional plot of excess attenuation per cycle against ϕ and $\sqrt{fr}$ for a hexadecane in water emulsion.

2.4.6 Numerical calculations of ultrasonic propagation parameters

Figures 2.4 and 2.5 show three dimensional plots of ultrasonic velocity and excess attenuation per cycle versus disperse phase volume fraction and $\sqrt{fr}$ for a hexadecane in water emulsion where both visco-inertial and thermal scattering are important. The thermophysical properties of hexadecane were taken from Allegra and Hawley (1972). The velocity and attenuation were plotted against $\sqrt{fr}$ since this term is proportional to the b, b', c and c' terms which determine the magnitude of visco-inertial and thermal scattering. The graphs show that the velocity and attenuation of a system which scatters ultrasound depend on the particle size and frequency as well as the disperse phase volume fraction (cf. figures 2.1 and 2.2). The velocity is independent of particle size and frequency for small values of $\sqrt{fr}$, but increases as $\sqrt{fr}$ increases until it reaches an upper limit where it is again independent of particle size and frequency. The excess attenuation per cycle is small for very small and very large values of $\sqrt{fr}$ but has a maximum value in the intermediate region. The dependence of the ultrasonic velocity and attenuation on $\sqrt{fr}$ means that it should be possible to determine both the particle size and ϕ of an emulsion or suspension using ultrasonic measurements depending on which parameters are known. Figures 2.4 and 2.5 show the overall velocity dispersion and excess attenuation of an emulsion. It is useful to isolate the contributions of the visco-inertial and thermal scattering mechanisms to the overall scattering.

2.4.6.1 Emulsion where scattering is appreciable

To demonstrate the practical significance of the visco-inertial and thermal scattering mechanisms the dependence of the various ultrasonic propagation parameters (equations 2.12-2.15) on frequency and droplet size is presented graphically (figures 2.6 and 2.7) for a hexadecane in water emulsion where visco-inertial and thermal scattering are appreciable. The values of velocity, effective compressibility and effective density were normalised with respect to their non-scattering values (equations 2.5-2.7) so as to illustrate the effects of scattering more clearly.

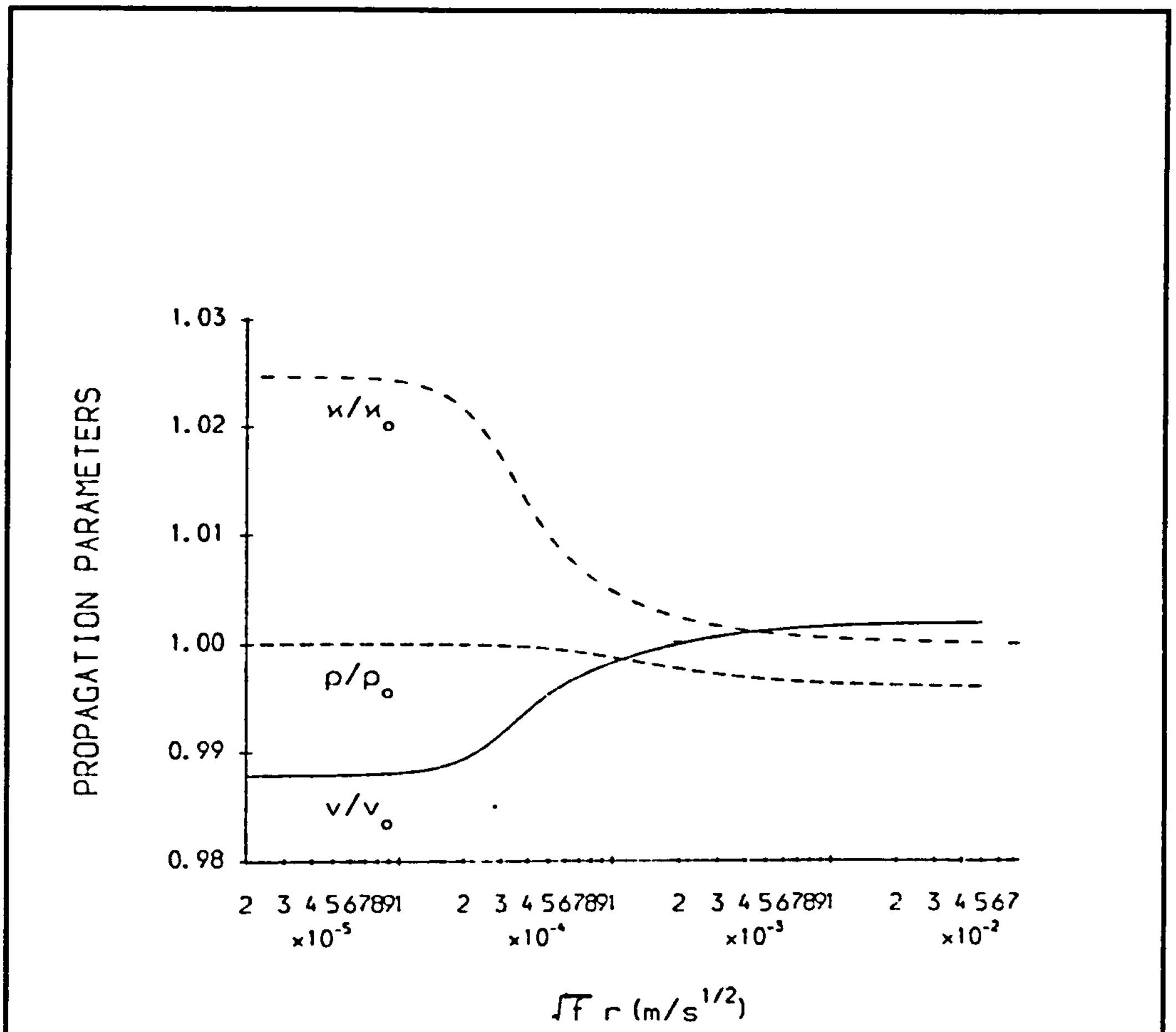

Figure 2.6: Ultrasonic propagation parameters of a hexadecane in water emulsion. Normalised ultrasonic velocity, adiabatic compressibility and density are plotted against $\sqrt{f}r$ (ϕ = 0.1) at 20°C.

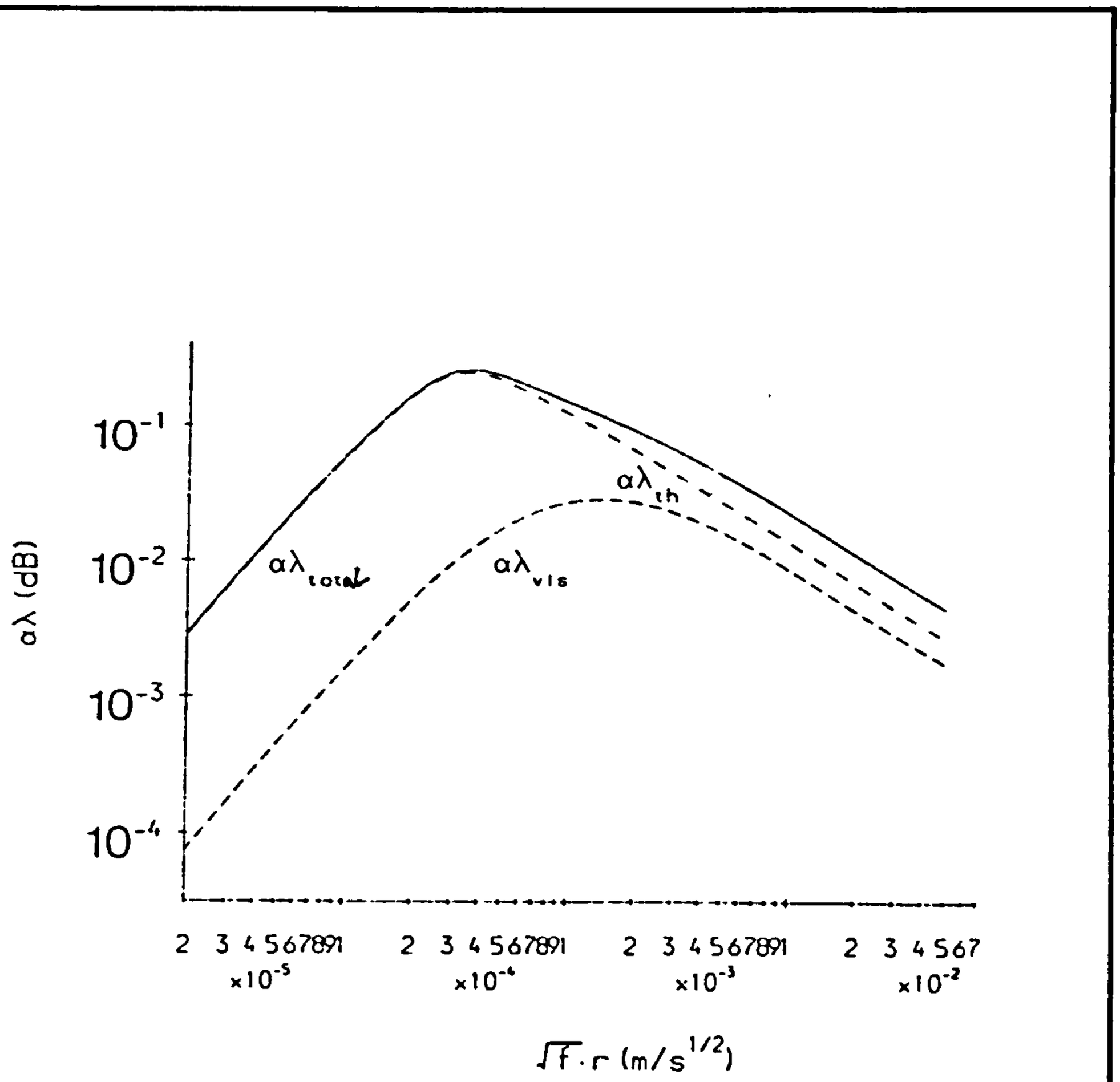

Figure 2.7: Attenuation of a hexadecane in water emulsion. Excess attenuation per cycle is plotted against $\sqrt{fr}$ ($\phi = 0.1$) at 20°C.

Figure 2.6 shows that as the frequency or droplet size decreases the effective density tends to its volume average value (equation 2.7) whilst the effective compressibility tends to a value which is greater than its volume average value:

$$\kappa = \kappa_0 + \kappa\phi(\gamma-1)\frac{\rho' C'_p}{\rho C_p}\left(1-\frac{\beta'\rho C_p}{\beta\rho' C'_p}\right)^2 \qquad (2.16)$$

Thus the velocity has a lower limit, for small droplet sizes and low frequencies, which depends on the difference in thermal properties of the component phases, and is below that predicted assuming no scattering. As the frequency or droplet size increases the effective compressibility tends to its volume average value (equation 2.6), whilst the effective density tends to a value which is lower than its volume average value:

$$\rho = \rho_0 - \frac{\phi(\rho'-\rho)^2}{\rho'+\frac{\rho}{2}} \qquad (2.17)$$

Thus the velocity also has an upper limit for large droplet sizes and high frequencies, which depends on the density difference between the component phases, and is greater than that predicted assuming no scattering. In the intermediate region the ultrasonic velocity depends on the relative magnitude of the visco-inertial and thermal scattering mechanisms.

The dependence of the visco-inertial ($\alpha_{vi}\lambda$) and thermal ($\alpha_{th}\lambda$) attenuation per cycle on droplet size and frequency is illustrated in figure 2.7. The excess attenuation per cycle is small for high and low values of frequency and droplet size, but has a maximum value in the intermediate region. The magnitude of the visco-inertial attenuation depends on the density difference between the droplets and surrounding fluid, and its maximum value occurs when the viscous skin depth δ_v, is approximately equal to the droplet radius (Ahuja 1973). The magnitude of the thermal attenuation depends on the magnitude of the $\left[\frac{\beta}{\rho C_p}-\frac{\beta'}{\rho' C'_p}\right]^2$ term, and its maximum value occurs when the thermal skin depth δ_t, is approximately equal to the droplet radius (Ahuja 1973). The overall excess attenuation in the emulsion is the sum of the visco-inertial and thermal attenuations.

After examining the predictions for a model system where both visco-inertial and thermal scattering are important it is useful to examine some of the systems which were used in the experimental work in this thesis (see chapters 4 and 5).

Table 2.1: Thermophysical properties of component phases

Values for water were taken from Kaye and Laby (1986), the rest of the values were taken from section 4.2.2.5. All values are quoted at 20°C and 1.25 MHz.

		Water	Sunflower oil	Paraffin oil	Tristearin
v	(m/s)	1482.3	1469.9	1472.0	2077.4
ρ	(kg/m^3)	998.2	919.6	876.3	1082.6
η	($kg.m^{-1}s^{-1}$)	0.001	0.054	0.164	∞
C_p	($J.kg^{-1}K^{-1}$)	4182	1980	2135	1488
τ	($J.s^{-1}m^{-1}K^{-1}$)	0.591	0.170	0.125	0.18
β	(/K)	0.00021	0.00071	0.00070	0.00035
α	(dB/m)	3.6	15	35	390

2.4.6.2 Sunflower oil in water emulsion

Theoretical predictions of the normalised propagation parameters of a 0.1 volume fraction sunflower oil in water emulsion are plotted in figures 2.8 and 2.9. The effective compressibility and density were calculated using equations 2.12 and 2.13, and the resultant velocity by substituting these values into equation 2.5. α_{vis} and α_{th} were calculated using equations 2.14 and 2.15. The thermophysical properties of the sunflower oil and water used in the predictions are listed in table 2.1.

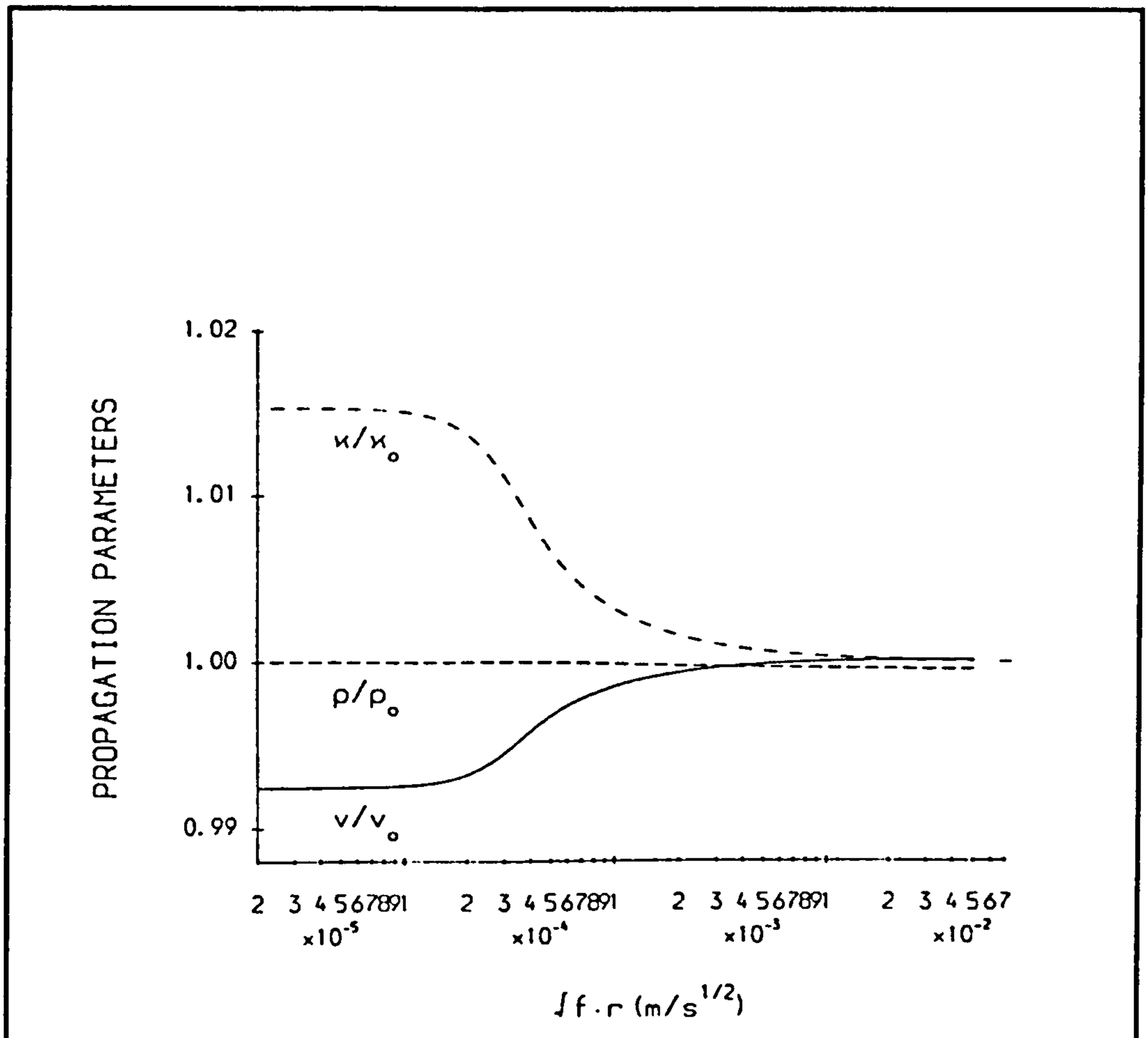

Figure 2.8: Ultrasonic propagation parameters of a sunflower oil in water emulsion. Normalised ultrasonic velocity, adiabatic compressibility and density are plotted against $\sqrt{fr}$ ($\phi = 0.1$) at 20°C.

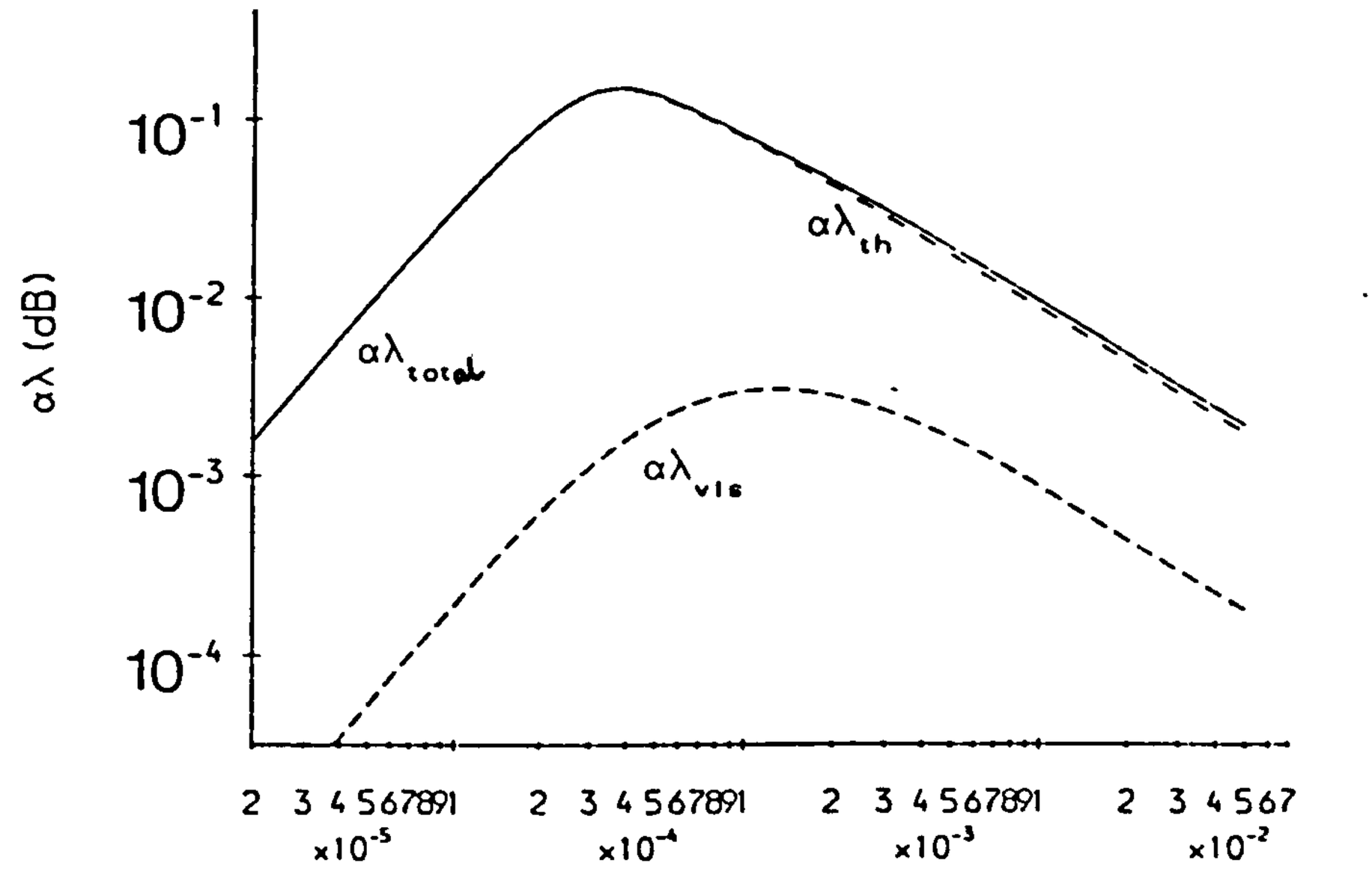

Figure 2.9: Attenuation of a sunflower oil in water emulsion. Excess attenuation per cycle is plotted against $\sqrt{fr}$ ($\phi = 0.1$) at 20°C.

Figures 2.8 and 2.9 show that visco-inertial scattering has little effect on the velocity and attenuation of ultrasound in sunflower oil in water emulsions. This is because the densities of the component phases are similar ($\frac{\rho'}{\rho} \approx 0.92$) and therefore scattering due to the viscous transport processes is negligible. The effects of thermal scattering, however, are significant, and may lead to appreciable excess attenuation and velocity dispersion, especially at the lower frequencies and droplet sizes. The dependence of the velocity and attenuation on $\sqrt{fr}$ means that it should be possible to determine the particle size of a sunflower oil and water emulsion from ultrasonic measurements.

2.4.6.3 Tristearin in paraffin oil suspension

Similar calculations as those described above were carried out for a 0.1 volume fraction solid tristearin in paraffin oil suspension using the properties of the component phases shown in table 2.1. The results are plotted in figures 2.10 and 2.11. The theoretical predictions show that both visco-inertial and thermal scattering make significant contributions to the overall velocity dispersion and excess attenuation. However, the magnitude of the scattering effects is much smaller than for the emulsions examined. In the frequency (1-10MHz) and particle size (0.3-10μm) ranges of interest in this work (e.g. $3 \cdot 10^{-4} < \sqrt{fr} < 3 \cdot 10^{-2}$ $m s^{-\frac{1}{2}}$) the velocity dispersion is less than 1m/s. This is because the densities and thermal properties of the solid fat and liquid oil phases are similar and so scattering is not significant. To measure the particle size of the crystals in this system accurate velocity measurements are needed (± 0.1m/s). In practice the effects of scattering can usually be ignored and the simple Wood equation, which assumes no scattering, may be used to interpret velocity measurements (equation 2.5).

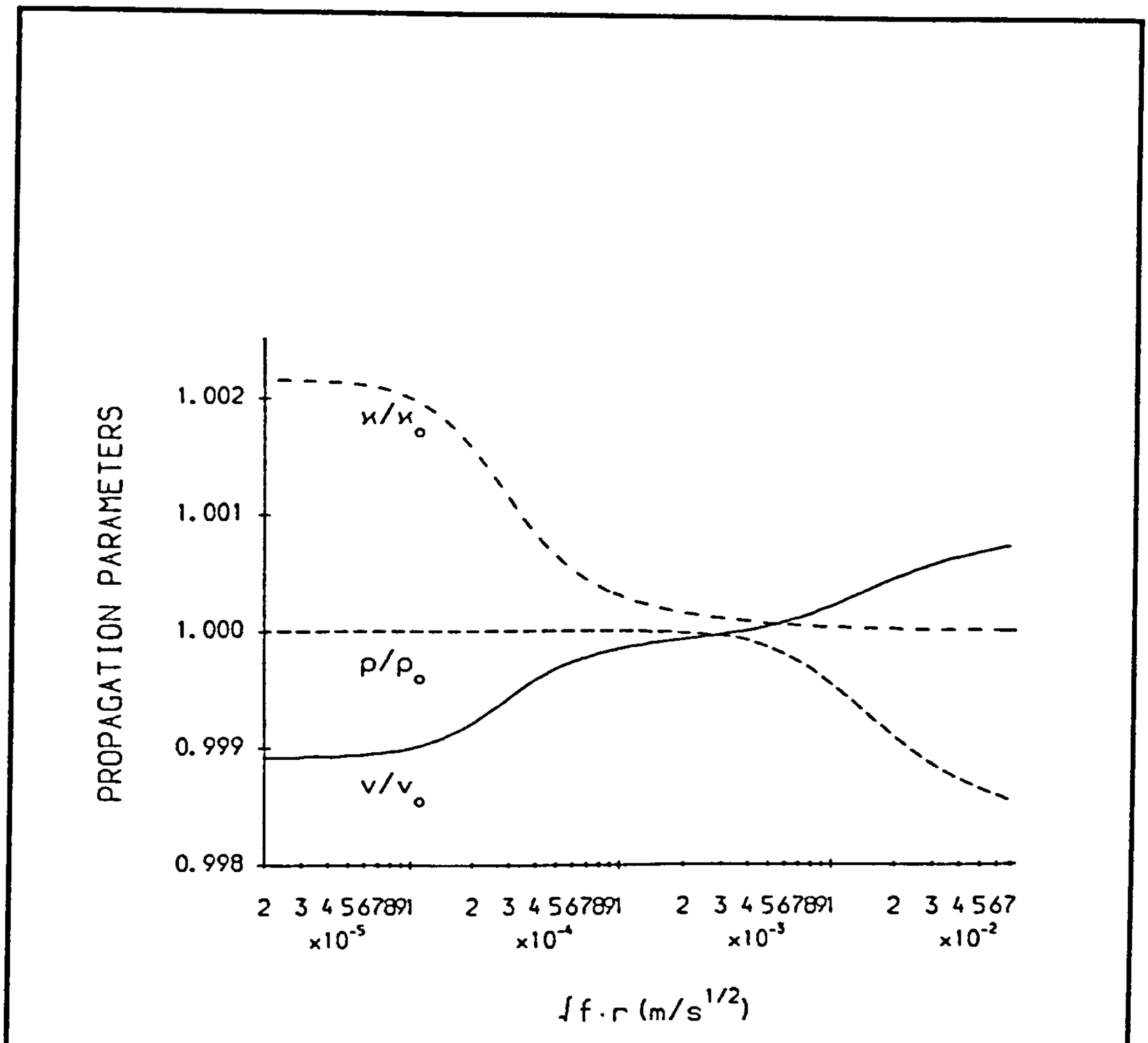

Figure 2.10: Ultrasonic propagation parameters of a tristearin in paraffin oil suspension. Normalised ultrasonic velocity, adiabatic compressibility and density are plotted against $\sqrt{fr}$ ($\phi = 0.1$) at 20°C.

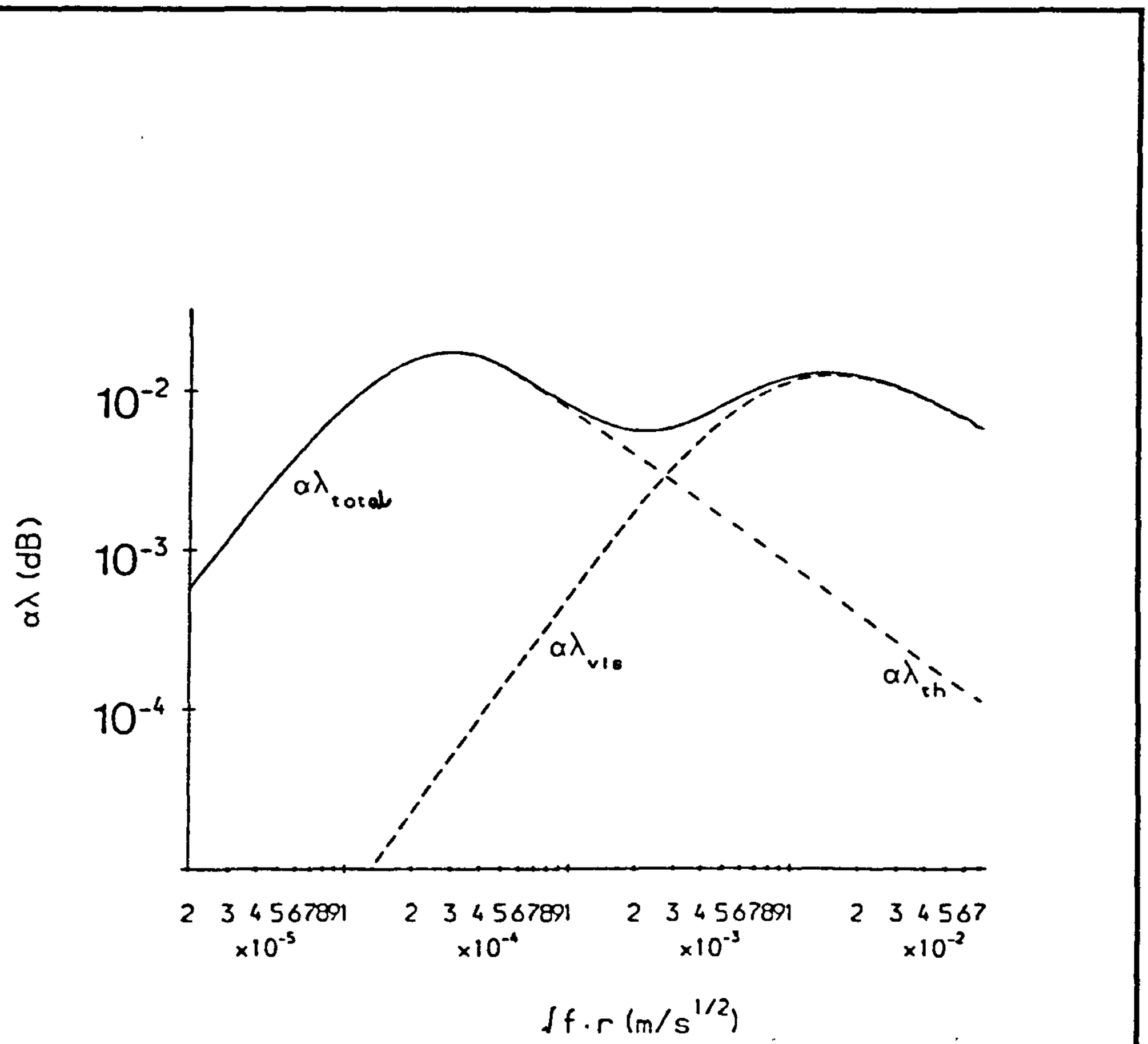

Figure 2.11: Attenuation of a tristearin in paraffin oil suspension. Excess attenuation per cycle is plotted against $\sqrt{fr}$ ($\phi = 0.1$) at 20°C.

2.5 *Other factors which effect ultrasonic propagation*

In section 2.4 the effects of visco-inertial and thermal scattering on the velocity and attenuation of ultrasound in dilute emulsions and suspensions were examined. In this section a number of other factors which may have an effect on ultrasonic propagation in disperse systems are discussed.

2.5.1 Particle shape

The scattering theory presented in the previous section was applicable to spherical particles. Due to the effects of surface tension, emulsion droplets can usually be considered to be spherical, however, they may be deformed under shear flow or in concentrated systems where they are close packed. Solid particles are rarely spherical; more often they are granular, crystalline or fibrous. The effects of non-sphericity on ultrasonic propagation in dispersions has been demonstrated by a number of workers theoretically and experimentally. Blue and McLeroy (1968) have measured the absorption coefficients of disk-like and needle shaped particles whose density was much larger than that of the surrounding media and have shown that they may have attenuations up to 40% less than those of spheres of equivalent volume. For systems such as these the effects of non-sphericity must be included in the formulations describing ultrasonic propagation.

Due to the formidable calculation required for a treatment of irregularly shaped particles, orientated at various angles in an acoustic field, workers have tended to use systems with simpler geometries. Ahuja and Hendee (1978) have used a phenomological approach to examine the effects of oblate and prolate spheroids suspended either parallel or perpendicular to an acoustic field. They showed that the effective density of an emulsion or suspension could still be calculated using equation 2.13, by modifying the values of the parameters T and s. For small density differences between the component phases (e.g. blood cells suspended in plasma, $\frac{\rho'}{\rho} \approx 1.03$) they were able to show that the effects of particle shape are negligible, however, for systems where the density difference between the phases

is relatively large (e.g. kaolin in water, $\frac{\rho'}{\rho} \approx 2.5$) then the shape and orientation of the particles can have a significant effect on velocity and attenuation. Due to the complexity of the mathematics involved it is more difficult to include non- spherical particles in scattering theory formulations, however, a number of workers have extended the formulations of Allegra and Hawley (1972) to include infinitely long cylindrical particles (Habeger 1982, Lin and Raptis 1983).

2.5.2 Multiple scattering and self consistency

Multiple scattering occurs when ultrasound scattered from one particle is incident on a neighbouring particle. This extra excitation of the particle must be included in the calculations of velocity and attenuation for concentrated systems. It was included in equation 2.11 by using the multiple scattering formulations of Lloyd and Berry (1967). This approach was used since it is more mathematically precise than the approaches of either Waterman and Truell (1961) or Twersky (1962), which are more frequently used to interpret results (e.g. Davies 1979, Datta and Pethrick 1980, Gladwell et al 1987). Other workers to have considered ultrasonic scattering and its effects on velocity and attenuation measurements include Sayers (1980), Davies (1979), Mehta (1983) and Schwartz and Johnson (1984).

Scattering theory does not define the medium surrounding the particles in a self-consistent manner and may therefore be limited to fairly dilute systems. It is assumed in the calculations that the medium surrounding the particles consists of continuous phase only, and so its thermo-physical properties are the same as those of the continuous phase. For practical purposes this may be true for dilute systems, however, as the concentration increases the particles pack closer together and the medium surrounding them will contain more and more of the neighbouring particles. Thus its thermophysical properties will be different from those of the pure continuous phase. Scattering theory does not take this phenomena into account and therefore tends to over estimate the degree of scattering in

concentrated emulsions and suspensions. The lack of self-consistency is demonstrated clearly at volume fractions of 1.0, since the equations do not predict the velocity and attenuation of the pure disperse phase.

A number of workers have attempted to describe emulsions and suspensions self-consistently using a variety of mathematical techniques (Berryman 1980). Due to the complexity of the problem, a number of assumptions have to be made which often limit the range of application of the formulations and frequently it is only possible to obtain upper and lower limits for the effective density and moduli of a system. Recently, however, McClements and Povey (1987a) have shown that an equation derived by Ahuja (1973) can be used to define the effective density of emulsions and suspensions self consistently in the long wavelength regime:

$$\rho = \rho_0 - \frac{(1-\phi)\phi(\rho'-\rho)^2}{\rho'+\rho T+i\rho s-(\rho'-\rho)\phi} \tag{2.18}$$

similarly, the attenuation due to visco-inertial scattering can also be defined self-consistently (Ahuja 1973):

$$\alpha_{vis} = \frac{k_c(\phi-\phi^2)s(\rho'-\rho)^2}{2[(\rho'+T\rho-\phi(\rho'-\rho))^2+s^2\rho^2]} \tag{2.19}$$

Equations 2.18 and 2.19 give similar predictions to those of 2.13 and 2.15 for dilute emulsions and suspensions but may give significantly different values at larger particle concentrations. Sayers (1980) has attempted to define the effective compressibility of a medium self consistently using scattering theory, however, his formulations are limited in practice, since they only apply to systems where the particle and the surrounding media have the same density and shear modulus.

2.5.3 Particle Interaction

As the concentration of suspended particles in an emulsion or suspension increases, the particles get closer together until eventually they touch. Contact between particles will introduce a frame bulk modulus into a system. A number of workers have considered the effects of particle interaction on ultrasonic propagation. Anderson and Hampton (1980) have reviewed much of the work in this area and have shown that particle interaction may have a significant effect on both the attenuation and velocity of ultrasound. They demonstrated that a simple equation derived by Gassman (1951) could be used to estimate the frame bulk modulus of a sediment from ultrasonic velocity and density measurements. Another popular approach often used to describe the propagation of ultrasound in systems where the particles touch is that of Biot (1956 a,b, 1962a,b). Biot used a phenomological model to consider ultrasonic propagation through porous media and saturated sediments, where the solid particles form a matrix of interconnecting particles. Many workers have since utilised Biot's formulations for describing ultrasonic propagation in systems containing interconnecting particles e.g. Stoll (1971), Ogushwitz (1985), Johnson and Plona (1982) and Schwartz and Johnson (1984).

2.5.4 Strong scattering

Strong scattering occurs when the amplitude of an ultrasonic wave scattered by a particle is of the same order as the amplitude of the incident wave. This occurs when the scattering particle and the surrounding media have appreciably different acoustic impedances. All the equations discussed so far are applicable to systems of weak scatterers and may break down when applied to strongly scattering systems. For systems such as fats and emulsions strong scattering is not important, however, for systems such as sugar crystals suspended in fat (as in chocolate), strong scattering may be appreciable. Indeed it may be impossible to get a signal through chocolate at normal ultrasonic frequencies (Povey 1988). This is because the ultrasonic energy in the sample bounces around between individual scatterers and so the scattered wave becomes in-coherent and phase correlation between different parts of the

signal is lost. Under these circumstances the ultrasonic energy, whilst still being present in the system is undetectable by normal means. In addition, strong scattering problems are difficult to describe theoretically. For this reason one must be extremely careful when interpreting measurements from systems which contain strong scatterers.

2.5.5 Resonant scattering by gas bubbles

Experimental and theoretical work has shown that the presence of gas bubbles can have a significant effect on the propagation of ultrasound in materials (Anderson and Hampton 1980). Since many foods contain gas bubbles it is useful to examine the work carried out in this area. In the presence of an acoustic field gas bubbles are capable of vibratory motion with a sharply peaked resonance at their fundamental pulsation frequency. This resonance has a dramatic effect on both the ultrasonic velocity and attenuation (figure 2.12). The frequency at which resonance occurs depends on the physical properties of the component phases and the bubble size. The larger the bubble size the lower is the resonant frequency. Gaunaurd and Uberall (1981) have shown that for large bubbles ($r > 3\mu m$) the resonance is most intense at the Minnaert frequency ω_m:

$$\omega_m = \sqrt{\frac{3\rho' v'^2}{4\rho r^2}} \qquad (2.20)$$

Here ρ' is the bubble density, ρ is the density of the fluid continuum, r is the bubble radius and v' is the velocity of sound in the bubble. For smaller bubbles the effects of fluid viscosity, thermal conductivity and surface tension have to be included in equation 2.20 (Nishi 1975).

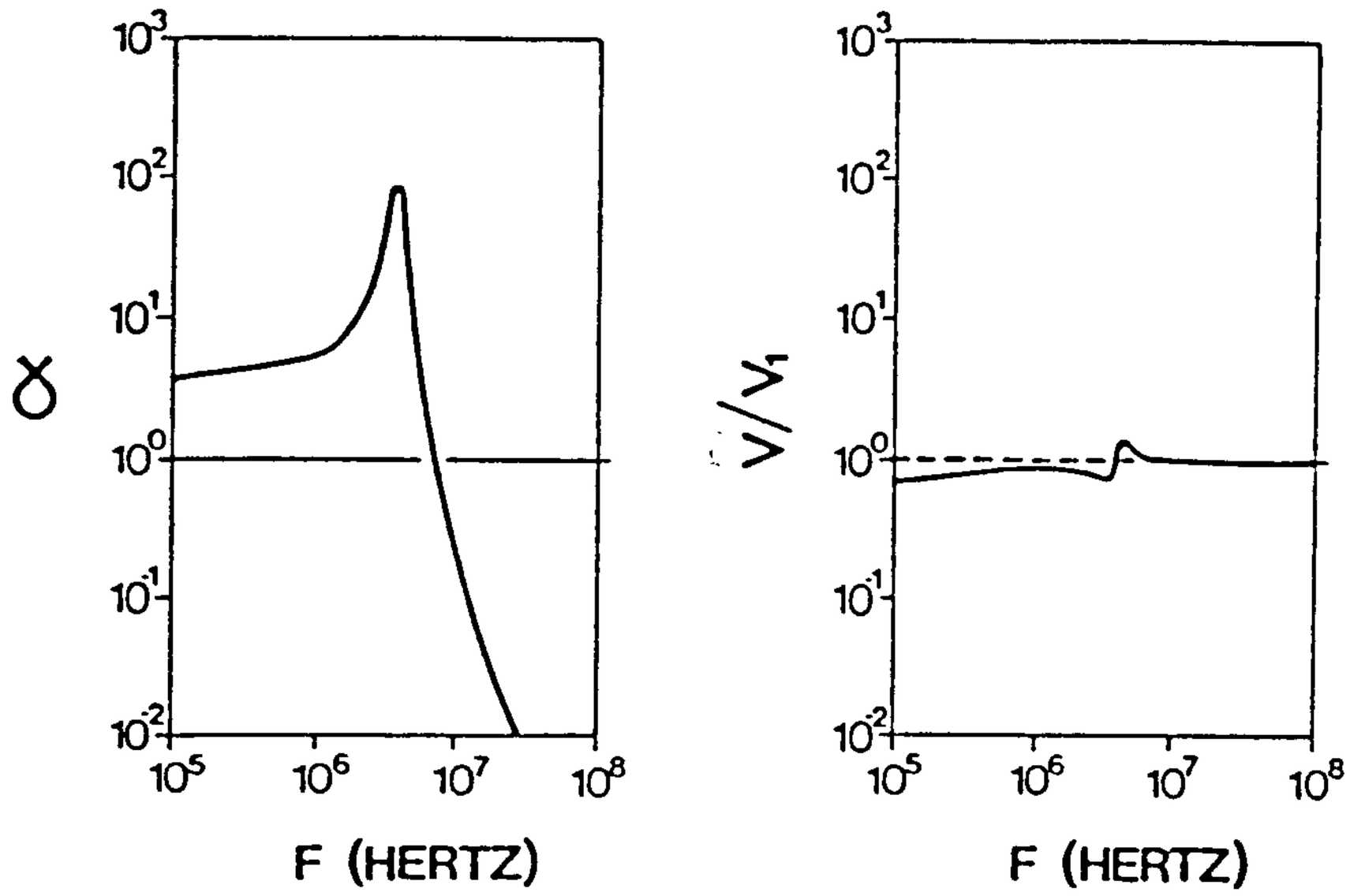

Figure 2.12: Ultrasonic velocity and attenuation of a bubbly liquid. (ϕ = 0.00001, r = 1 μm).

Figure 2.12 illustrates the variation of normalised ultrasonic velocity and excess attenuation with frequency for bubbly water calculated using the formulations of Gaunaurd and Uberall (1981). In practice the resonant peaks may not be so sharply defined due to bubble size distribution. The attenuation of sound in bubbly liquids is greatest at frequencies near resonance. The ultrasonic velocity is independent of frequency far below resonance and can be described approximately by the Wood equation; its value being lower than that of the pure fluid by an amount depending on the volume fraction of gas present. In the vicinity of resonance the ultrasonic velocity is highly frequency dependent. At frequencies above resonance the velocity tends to the continuum value. These theoretical observations have been confirmed experimentally by a number of workers using air bubbles suspended in water (e.g. Gibson 1970, Medwin 1974). Recently, Gaunaurd and Uberall (1982, 1983) have generalised their theory so as to include resonance in perforated solids and in particulate materials, and so their formulations can be used to model the ultrasonic behaviour of a wide range of materials.

In some food systems gas bubbles may be undesirable to ultrasonic measurements since they interfere with the measurement of some other quantity. In these systems it may be necessary to remove the gas bubbles if possible or to reduce their effect by measuring the ultrasonic velocity and attenuation at a frequency much larger than the resonant frequency of the gas bubbles. On the other hand, ultrasonics may prove useful as a means of characterising aerated materials such as foams, doughs, fruits, vegetables and animal tissues. By measuring the velocity and attenuation as a function of frequency it should be possible to estimate both the volume fraction and particle size distribution of the gas bubbles present.

2.6 Implications of ultrasonic scattering

The work presented in this chapter has demonstrated the complex nature of ultrasonic propagation in emulsions and suspensions; the velocity and attenuation depend on many factors. If the technique is to be applied successfully to these systems it is essential to understand the basic physical processes occurring and to appreciate the theories describing these processes. For some systems, simple theoretical equations may be used to interpret results since scattering is negligible (e.g. fat/oil mixtures). For others, where scattering is important, it is necessary to use more complex equations e.g. emulsions. It is also essential to appreciate the range of applicability of the equations used and to be aware of the many other factors which may influence measurements.

Chapter 3

ULTRASONIC MEASUREMENTS

3.1 Introduction

As well as a good understanding of the theories describing ultrasonic propagation in materials (chapter 2), a successful application of ultrasonics also relies on the development of a suitable measuring technique. There are a variety of techniques which can be used for ultrasonic measurements and the choice of a particular technique depends on the material under test, the property to be measured and the requirements of the investigator e.g. cost, accuracy, measurement time, environmental conditions. A technique which is suitable for one type of measurement may be unsuitable for another. Often techniques have to be tailored for each particular application. A number of techniques which are frequently used for non-destructive testing (NDT) in general have been reviewed by Breazeale et al (1981) and Papadakis (1976), whilst those techniques which are suitable for use in the food industry have been reviewed by McCann (1986) and Povey and McClements (1988a).

Most of the techniques used for NDT utilize either continuous wave (c.w.) or pulsed ultrasound. Instruments which utilise c.w. ultrasound are capable of the most accurate measurements (Inoue et al 1986), however, they are sophisicated in design, rely on precise mechanical adjustments and are time consuming to operate. Consequently c.w. techniques are not usually suitable for use in industrial environments. Although pulsed techniques are less accurate than c.w. techniques, the variability of most food materials means that they are still accurate enough for most applications in the food industry. Pulse techniques are simple to design and operate, are robust and are capable of rapid and precise measurements in a non-intrusive, non-invasive manner. They are therefore more suitable for use in industrial applications than c.w. techniques. For these reasons a pulse echo technique, which is

described in section 3.2, was used for most of the measurements carried out in this work. A small number of measurements were also made using a pulse echo interferometry technique similar to that described by Andreae et al (1958). The actual apparatus used was a modern version of the Andreae technique and was designed and developed at the AFRC Institute of Food Research, Norwich (Rahalkar et al 1986). This technique is described in more detail in section 5.2.2.

3.2 Description of pulse echo technique

The pulse echo technique used in this work is based on the standard pulse echo technique described in many text books (e.g. Blitz 1963), however there are a number of points which are specific to this particular application of the technique and these are discussed below. Initial measurements were carried out at a frequency of 1 MHz using the experimental arrangement illustrated in figure 3.1. A Hewlett Packard Function generator (3312A) was used in conjunction with two 1 MHz piezo-electric transducers and a Tektronix 468 digital storage oscilloscope (DSO). As the work proceeded it became apparent that measurements would have to be made over a range of frequencies and so transducers of different resonant frequency would have to be used (table 3.1). In some cases there was only one transducer of the appropriate frequency available in the laboratory and so later measurements were made using a single transducer as both generator and receiver. For these experiments a Sonatest Ultrasonic Flaw Detector (U.F.D. 1) was used as the signal generator and the Tektronix D.S.O was used to display the signal (figure 3.2). In practice velocity and attenuation measurements can be made in exactly the same way using either technique.

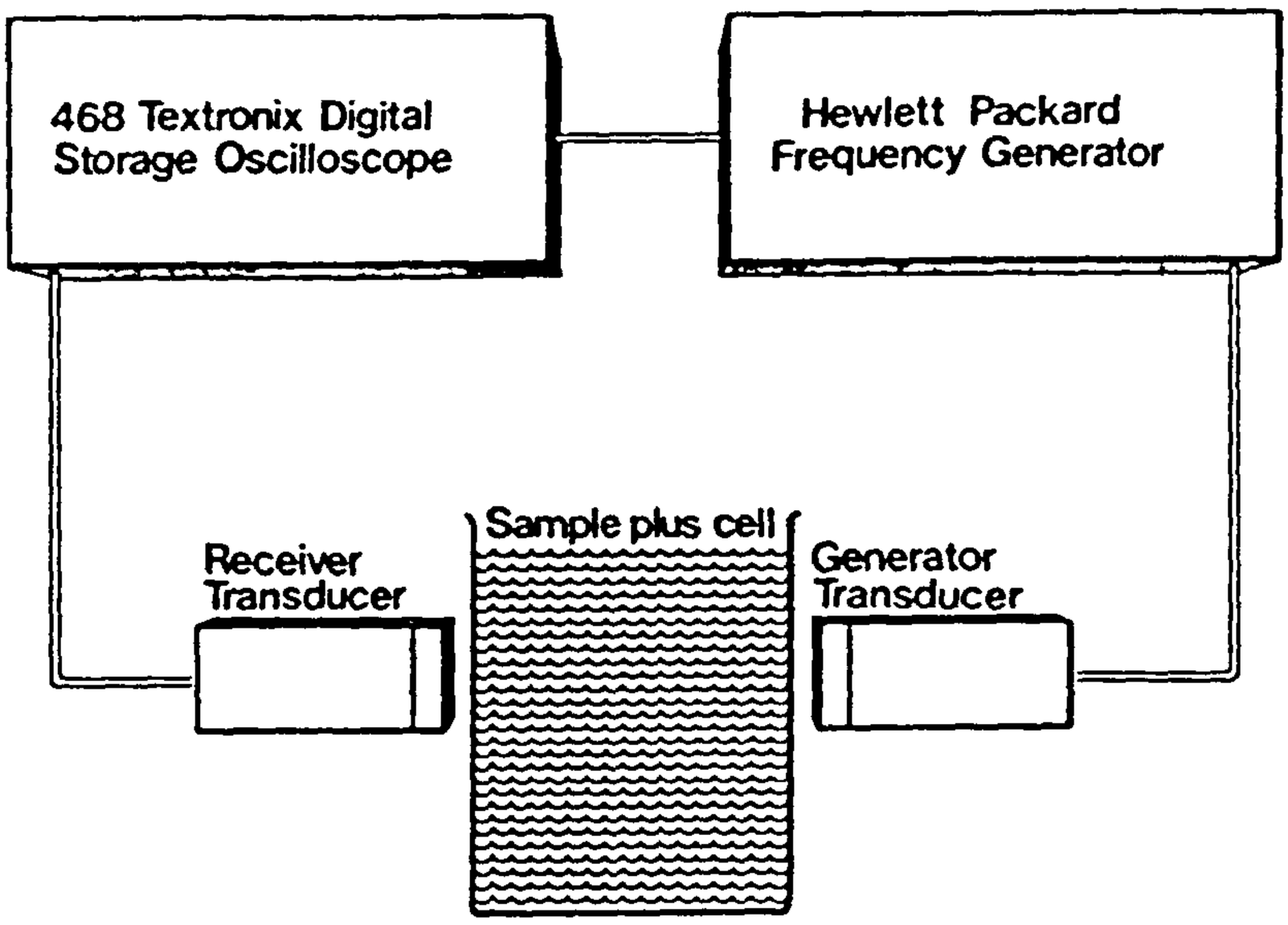

Figure 3.1: Block diagram of double transducer pulse echo technique

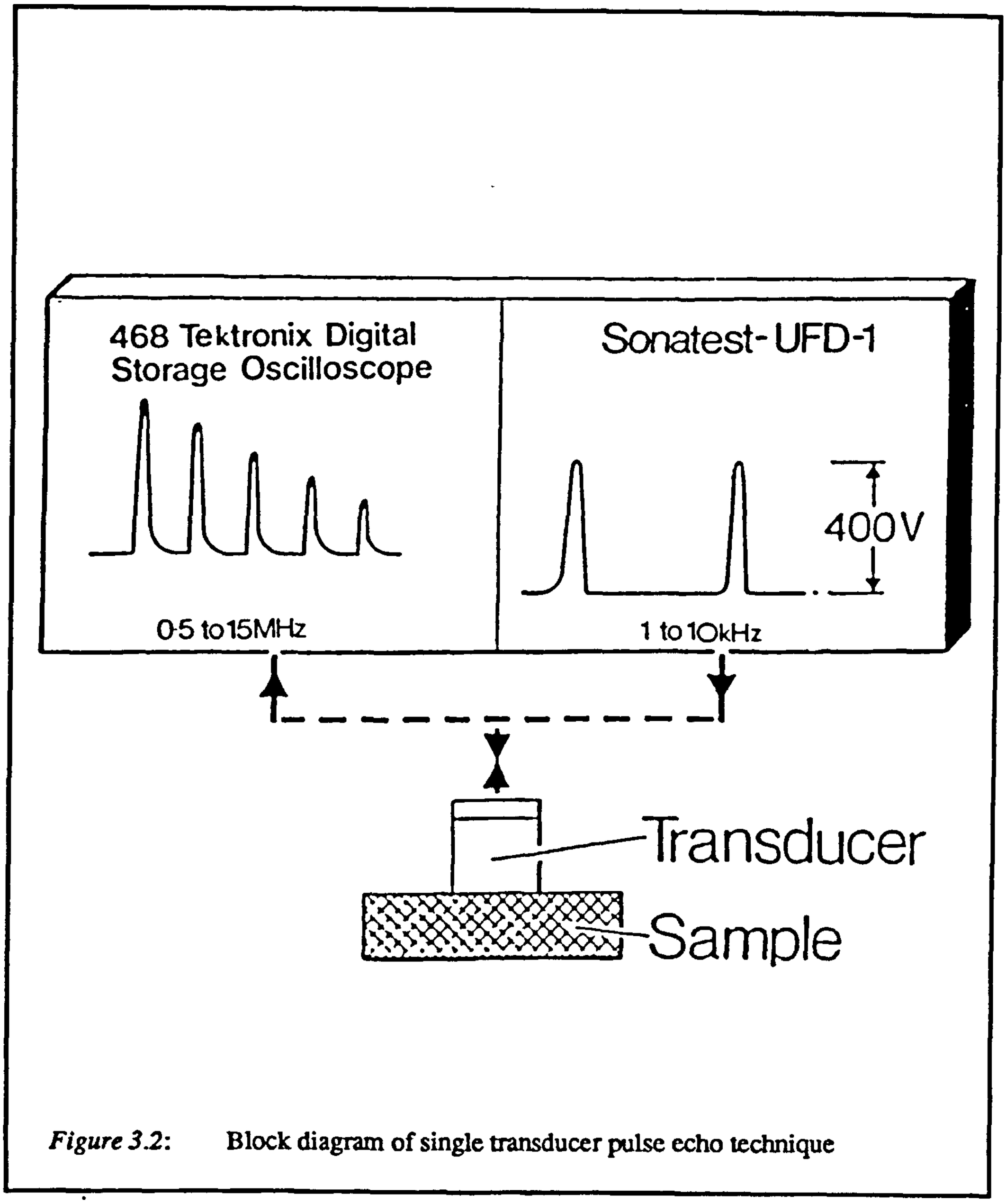

Figure 3.2: Block diagram of single transducer pulse echo technique

Table 3.1: Characteristics of transducers used in experiments.

The wavelength λ, of ultrasound is calculated assuming that the sample is distilled water at 20°C (i.e. v = 1482.3 m/s).

Manufacturer	f (MHz)	D (mm)	$D^2/4\lambda$ (mm)	D/λ
Mateval	1.0	10	17	7
Sonatest	1.25	20	84	17
Sonatest	2.25	10	38	15
Mateval	6.0	5	25	20
Mateval	10.0	10	170	68

Samples were contained in small glass cuvettes which had path lengths of about 10mm and held about 12cm^3 of material. During measurements the cuvettes were held between the transducers using a specially designed perspex sample holder. The cuvettes could be easily slipped in and out from the sample holder which meant that measurements of successive samples could be made quickly and simply. The temperature of the samples was controlled by placing them in water baths equilibrated to the appropriate temperature (± 0.1°C). Precise temperature control is important since the ultrasonic velocity of many materials is particularly sensitive to temperature, e.g. for water and oil the temperature coefficient of the velocity is about |3| $ms^{-1}°C^{-1}$ The technique was optimised for velocity measurements since these can be measured more accurately than attenuation measurements and are easier to interpret.

3.2.1 Double transducer technique

A sinusoidally varying electrical potential is produced by the Hewlett Packard frequency generator whose frequency is chosen to be equivalent to the resonant frequency of the transducers. This sine wave is electronically 'chopped' into pulses of a few cycles duration, with a repetition rate of between about 1-100 kHz. Each pulse is converted into a mechanical pulse by a piezo-electric transducer (the generator) and passes through the cuvette wall and into the sample. The pulse propagates through the sample until it reaches

the opposite cuvette wall where it is partially transmitted, partially reflected. After passing through the cuvette, the transmitted portion is detected by another piezo-electric transducer (the receiver) where it is converted back into an electrical pulse and displayed on an oscilloscope. The reflected part travels back through the sample until it reaches the initial cuvette wall, where it is again partially reflected, partially transmitted. An ultrasonic pulse therefore travels backwards and forwards across the sample, its amplitude decreasing due to attenuation in the sample, transmission at the sample/cuvette interface and diffraction. The part detected by the receiver is displayed on the oscilloscope as a series of echoes of decreasing amplitude (figure 3.3).

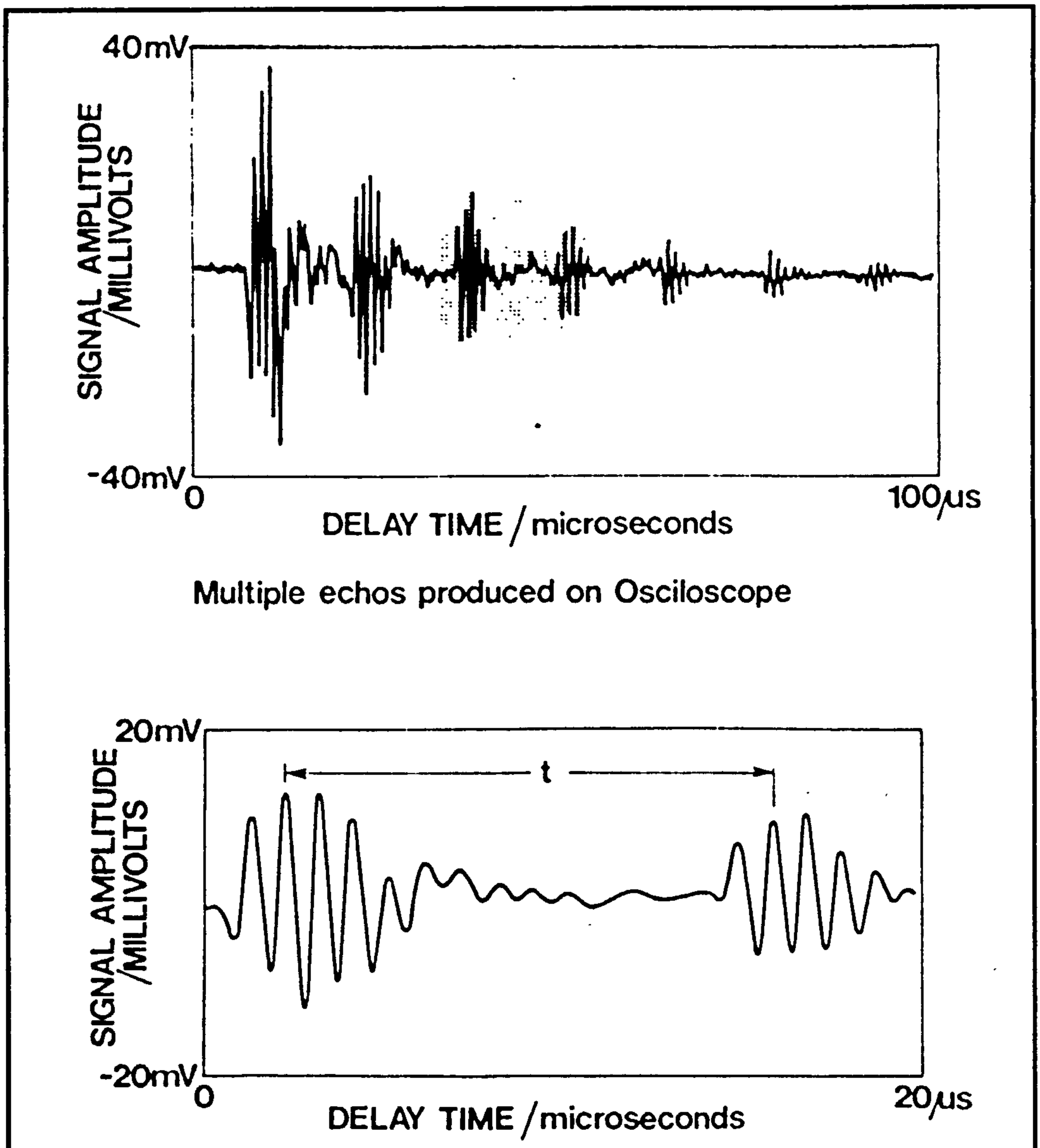

Figure 3.3: Multiple echoes observed on oscilloscope. Lower diagram shows how the time is measured by resolving succesive echoes of upper diagram (shaded area).

Velocity measurements. Each echo observed on the oscilloscope has travelled a distance twice the cuvette path length (d) further than the previous one and so the ultrasonic velocity v can be calculated by measuring the time difference (t) between similar positions on successive peaks ($v = 2d/t$). This time difference is measured accurately by using the cursors on the oscilloscope and by resolving successive echoes (figure 3.3). The quality of the signal is improved by using the digital averaging facility of the oscilloscope. Any background noise which is randomly distributed in time and amplitude is then averaged out leaving the genuine signal. The cuvette path length is determined precisely by calibration with a liquid of known ultrasonic velocity (see worked example below). In many commercial ultrasonic instruments, the ultrasonic velocity is calculated from the time a pulse takes to travel from the generator to the receiver transducer, after allowing for corrections for the time the pulse spends in the cuvette walls and the transducers. The advantage of measuring the time between successive peaks is that no correction to the measured time is required; the only difference in time between successive peaks is the time it takes a pulse to travel twice the length of the sample.

Attenuation measurements. The attenuation coefficient (α) of a sample is calculated by measuring the amplitude of successive echoes (e.g. figure 3.3), and finding the best least squares fit of the measurements to the equation: $A_n = A_0 e^{-\alpha x}$, where A_0 is the amplitude of the initial peak, A_n is the amplitude of the n^{th} peak and x is the distance between the initial and the n^{th} peak. The measured attenuation of a sample includes losses due to transmission at the sample/cuvette interface and diffraction which have to be accounted for. This was done by calibrating each cuvette with distilled water (see worked example below).

Worked example of velocity and attenuation measurements. To demonstrate how the velocity and attenuation were calculated an example calculation is worked through. Measurements of the time difference (t) between successive echoes and the relative

amplitudes ($\frac{A_n}{A_0}$) of the echoes for distilled water and a 8.4% w/w sunflower oil in water emulsion (Sauter mean radius = 0.748μm) at 20°C and 1.25 MHz are presented in table 3.2. Only measurements in the far-field are included, i.e. echoes which have travelled further than 80 mm (see section 3.3.2). Distilled water was used as a calibrant since the velocity of ultrasound in it has been measured accurately to within 0.003% using an interferometric technique (Del Grosso and Mader 1972) and its attenuation coefficient is also known (Kaye and Laby 1986).

Table 3.2: Time and amplitude measurements for water and an emulsion

The measurements for distilled water and a 8.4% w/w sunflower oil in water emulsion are at 20°C and 1.25 MHz.

		Water		Emulsion	
Peak no.	x	t (μs)	A_n/A_o	t (μs)	A_n/A_o
0	0	-	1.00	-	1.00
1	2d	13.49	0.89	13.54	0.78
2	4d	13.48	0.78	13.52	0.63
3	6d	13.48	0.69	13.54	0.50
4	8d	13.47	0.61	13.52	0.42
5	10d	13.49	0.56	13.54	0.34
6	12d	13.48	0.50	13.53	0.26
7	14d	13.47	0.47	13.53	0.20

The path length ($d = \frac{1}{2}vt$) of the cuvette was calculated to be 9.991 ± 0.003 mm from the known velocity of distilled water (1482.34 ± 0.02 m/s at 20°C) and the measured time difference between successive echoes (t_{mean} = 13.480 ± 0.011 μs). The ultrasonic velocity of the emulsion was then calculated (v = 2d/t) from the mean time difference between successive echoes (t = 13.532 ± 0.009μs) and the cuvette path length and was found to be 1476.6 ± 1.1 m/s.

The major source of error in the velocity measurements is the accuracy to which the time and the cuvette path lengths can be measured ($v = 2d/t$). The error in the time measurements is determined by the accuracy to which the oscilloscope can measure time differences (0.05%). The error in the cuvette path lengths is determined by the accuracies of the literature value of ultrasonic velocity (0.01%) and the time measurements (0.05%). The overall accuracy of the ultrasonic velocity measurements was therefore about 0.1%, which corresponds to an error in velocity of about 1.5 m/s. If the error in the measuring temperature is 0.1°C then there will be an additional error due to the temperature coefficient of the velocity. For oils and water this value is about .3 m/s/°C and so the overall accuracy is about 1.8 m/s. The reproducibility of the velocity measurements was calculated from the average of at least five measurements per sample and was found to be typically about 1.0 m/s (e.g. see velocity of emulsion calculated above).

The attenuation coefficient of the samples was determined by calculating the best least squares fit of the measured values of $\frac{A_n}{A_0}$ (table 3.2) to the equation: $A_n = A_0 e^{-\alpha x}$. The attenuation coefficients of the distilled water and the emulsion calculated from these measurements were 5.5 ± 0.2 Np/m (48.0 ± 1.7 dB/m) and 11.2 ± 0.2 Np/m (97.3 ± 1.7 dB/m) respectively. These measured values ($\alpha_{measured}$) are partly due to the attenuation of the sample (α_{sample}) and partly due to transmission which occurs at the sample/cuvette interface and diffraction (α_{expt}) i.e. $\alpha_{measured} = \alpha_{expt} + \alpha_{sample}$. These additional sources of attenuation are accounted for by subtracting the known attenuation of distilled water from the measured value ($\alpha_{expt} = \alpha_{measured} - \alpha_{water}$). The attenuation coefficient of distilled water at 20°C is 0.35 dB/m (Kaye and Laby 1986) and so the value of α_{expt} is 47.7 ± 1.7 dB/m. By subtracting this value from the measured attenuation of the emulsion, the attenuation due to the emulsion alone can be calculated: 49.6 ± 2.6 dB/m. This approach can only be used if the value of α_{expt} is the same for the distilled water and for the emulsion. In fact the value of α_{expt} will be different since the velocity and acoustic impedances of the sample and distilled water are

different and so the extent of the diffraction and transmission losses will be different. However, the difference in the acoustic properties of the water and the samples used in this work are not large and therefore α_{expt} is not expected to vary much.

It is difficult to assess the absolute accuracy of the attenuation measurements since there are many factors which contribute to the overall attenuation which are difficult to quantify. In general the reproducibility of the attenuation measurements was worse than that calculated for the emulsion above. This was because the energy losses at the interface between the transducer and the cuvette were sensitive to the thickness of the thin layer of water between the cuvette and the transducer (section 3.3.3) and this was difficult to control precisely. The overall reproducibility of the attenuation measurements was calculated to be about 10-20%, which is considerably worse than that of the velocity measurements (0.1%).

3.2.2 Single transducer technique

The measuring principle of the single transducer technique (figure 3.2) is exactly the same as that described for the double transducer technique (figure 3.1). However, the way the pulses are generated is different. For the single transducer system it is necessary to isolate the initial electrical excitation from the received signal so that the oscilloscope is not saturated by the relatively large amplitude of the excitation signal. The Hewlett Packard function generator does not have this facility and so a Sonatest U.F.D. 1 was used. The Sonatest U.F.D. 1 uses high voltage *shock excitation* to produce the electrical excitation pulse, which therefore contains a broad band of frequencies. The appropriate ultrasonic frequency is then selected by the resonant frequency of the transducer.

3.3 Practical considerations

In principle the ultrasonic measurements described in section 3.2 are fairly straightforward to carry out; in practice, however, there are a number of factors which have to be considered when designing the technique if it is to be applied successfully.

3.3.1 Choice of transducer

Choice of a suitable transducer is central to any successful application of ultrasonics. There are many types of ultrasonic transducer which can be used for the NDT of materials (Silk 1984). Piezo-electric transducers are the most commonly used at present, however there is considerable interest in the development of alternative types, such as laser and electromagnetic transducers (Silk 1984), and these may become of greater importance in the future. In this work lead zirconate titanate (PZT) piezo-electric transducers were used, since they could be purchased off-the-shelf at relatively low costs (< 100 £/transducer). These transducers operated at single frequencies between 1 and 10 MHz (see table 3.1) and were purchased from either Balteau Sonatest (Milton Keynes, U.K.) or MatEval Ltd (U.K.).

The transducers were highly damped in order to produce pulses of short time duration which could be resolved on the oscilloscope. They were also water-proofed so that they could be immersed in a water bath during measurements. Transducers of different resonant frequency were used so that the velocity and attenuation could be measured as a function of frequency. The lower limit of frequency was determined by the ratio of sample size to ultrasonic wavelength; as the frequency decreases the wavelength increases and it becomes more difficult to resolve successive pulses. The upper limit of frequency is determined by the attenuation coefficient of the sample; as the frequency increases the attenuation coefficient may become so large that the signal cannot be detected. This is accentuated when samples are contained in cuvettes because the transmission of ultrasonic energy from transducer to sample is reduced as the frequency is increased.

3.3.2 Ultrasonic diffraction

The theoretical formulations discussed in chapter 2 assume that the ultrasonic wave passes through a material in the form of a plane, compressional wave. In practice, the finite size of an ultrasonic transducer means that the ultrasonic beam spreads out into a diffraction field (figure 3.4). Various methods of describing diffraction fields have been reviewed by Silk (1984). The most common approach is to assume that the transducer consists of a disc

oscillating in a piston-like manner which exerts pressure in the direction of wave propagation. Such a device produces a parallel beam of plane waves which diverge after travelling a distance d from the source. This distance depends on the diameter of the transducer face D and the wavelength of the ultrasound in the sample ($d \approx \frac{D^2}{4\lambda}$). The parallel portion of the beam is called the near-field or Fresnel Zone, and the divergent part the far-field or Fraunhofer Zone. If the ratio of the transducer diameter to the ultrasonic wavelength ($\frac{D}{\lambda}$) is greater than about 10 the influence of diffraction effects can usually be ignored and it can be assumed to a first approximation that the field produced is about the same as that of an ideal plane wave. The values of $\frac{D}{\lambda}$ for the transducers used in this work are included in table 3.1. With the exception of the 1 MHz transducers all the transducers satisfy the condition $\frac{D}{\lambda} > 10$, and even for the 1MHz transducers the condition is almost satisfied.

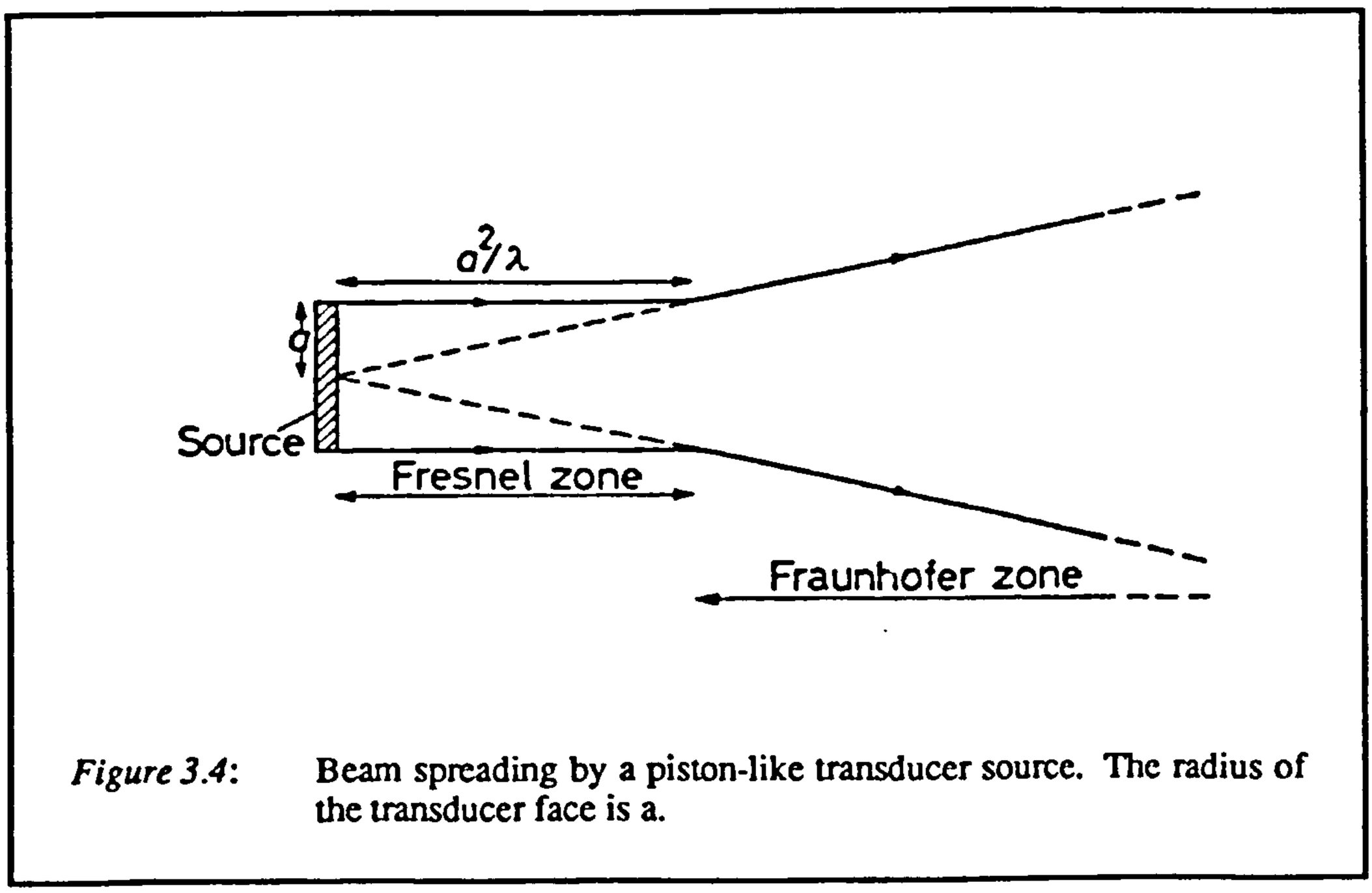

Figure 3.4: Beam spreading by a piston-like transducer source. The radius of the transducer face is a.

The average intensity over any given cross section in the near field remains constant (assuming no absorption occurs), but there are cyclical intensity changes along any line in the direction of wave motion (see figure 3.5). In the far-field the intensity decreases inversely with the square of the distance from the source. Due to the sensitivity of the intensity to distance in the near-field it is usually advisable to make measurements in the far-field. However, measurements at 6 and 10 MHz had to be made in the near-field due to the relatively large attenuation of some of the samples at these frequencies. These measurements could still be used because the signal detected by a transducer is an average over the whole of its face and since the transducers were aligned to a high degree of parallelism and had similar diameters the intensity of the beam should remain fairly constant. Indeed there was no evidence of cyclical intensity changes when the separation between the receiver and generator was varied in the near field.

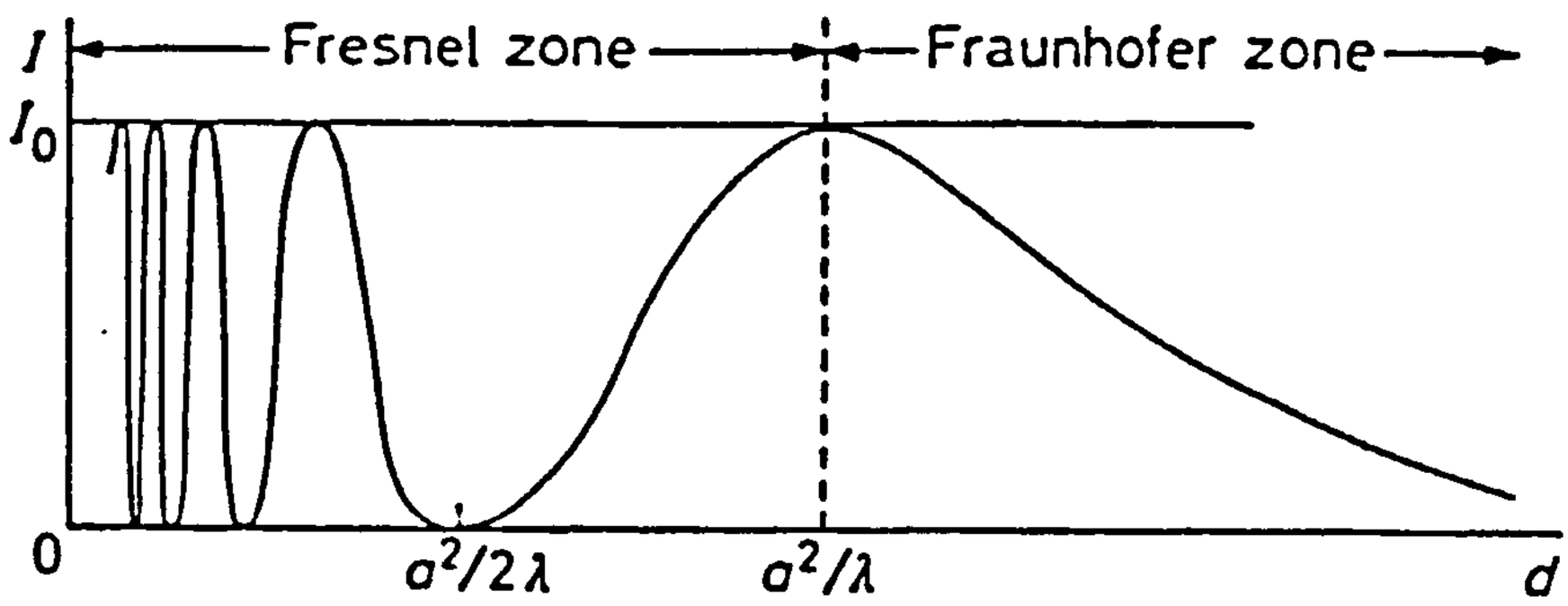

Figure 3.5: Intensity along the axis of a vibrating piston-like source. (Blitz 1963)

3.3.3 Coupling of the transducer to the sample

The fraction of ultrasonic energy transferred from a transducer to a sample (and visa versa) depends primarily on the acoustic impedances of the sample and transducer and the thickness and impedances of any intervening materials (Asher 1982, 1983). The fraction of acoustical energy transmitted (F_t) on normal incidence of a plane wave at a boundary between two materials a and b can be calculated from the acoustic impedances of the two materials (w_a and w_b) (Blitz 1963);

$$F_t = \frac{4w_a w_b}{(w_a + w_b)^2} \tag{3.1}$$

This equation shows that optimum transmission is obtained when the materials have similar acoustic impedances. In practice materials have different impedances and it is the aim of the ultrasonicist to obtain the best possible acoustic match between the materials. Values of F_t from 0.1 to 1.0 are often considered to constitute good acoustic coupling (Blitz 1963).

In this work the transducer and sample were separated by a glass cuvette. There is also a thin layer of water between the cuvette and the transducer face since the samples were contained in a water bath. Thus transmission through a multi-layer system must be considered. Kinsler and Frey (1950) have calculated the fraction of energy transmitted when an ultrasonic wave passes through three media separated by plane parallel boundaries. For normal incidence:

$$F_t = \frac{4w_a w_b}{(w_a + w_b)^2 \cos^2 k'l + \left(w' + \frac{w_a w_b}{w'}\right)^2 \sin^2 k'l} \tag{3.2}$$

Here l, w' and k' are the thickness, impedance and wave number of the intervening layer. Equation 3.2 shows that the amount of energy transmitted depends on the thickness of the intervening material, as well as the relative magnitude of the impedances of the three materials. When the intervening material is very thin (i.e. $k'l \ll 1$) then equation 3.2 reduces to that of 3.1 and the intervening material should have no effect on the overall transmission. This is only the case when the three materials have similar acoustic

impedances. If the intervening material is air, which has a much lower acoustic impedance than either solids or liquids the energy transmitted may be much less than that predicted by equation 3.1 even when k'l << 1 (Blitz 1963). In this work the cuvettes and transducers were submerged in a water bath during measurements and so there is a thin layer of water between the cuvette and the transducer face. The value of k' for water at 20°C and 1 MHz is 4238.8 m and so for k'l to be less than 0.1 the thickness of the water layer will have to be less than 0.02 mm. Although the transducers were held against the side of the cuvettes by the perspex sample holders the gap between a transducer face and a cuvette may still be of the order of 0.02 mm or greater and so the water layer may have an effect on the fraction of energy transmitted. It was difficult to control the thickness of this gap precisely and so the fraction of energy transmitted may vary slightly depending on the relative positions of a transducer and a cuvette. As mentioned in section 3.2 this may cause variation in the attenuation measurements.

For optimum transmission of ultrasound the acoustic impedance of the cuvette should be equal to the geometric mean of the acoustic impedances of the surrounding materials and its thickness should be equal to an odd number of quarter wavelengths (Blitz 1963). The thickness of the cuvettes used in this work (1.5 mm) was chosen as a compromise between optimum transmission and the robustness of the cuvettes (section 3.3.5). Ultrasonic transducers are usually manufactured with a thin epoxy coating over the piezo-electric crystal. By varying the type of material used as a coating and its thickness a transducer can be *acoustically matched* to a particular type of material. Most commercial transducers are either matched to water or to steel. In this work samples are contained in glass cuvettes and so it is best to use transducers which are acoustically matched to steel, since this has an acoustic impedance similar to that of glass.

Once the pulse has entered the cuvette it passes through the sample and is partly reflected, partly transmitted at the cuvette walls. To obtain a series of echoes we do not want 100% transmission at the walls (i.e. 0% reflection), nor do we want 0% transmission (or the

signal will never be detected). An intermediate value is required which depends on the amplitude of the signal and the number of echoes required. The fraction of energy transmitted at an oil-glass boundary was calculated to be about 0.67, and this value was sufficient to give a number of easily distinguishable echoes on the oscilloscope (see figure 3.3). Indeed in low attenuating samples such as water up to 20 peaks could be observed. Other sources of error associated with the coupling of the transducer to the sample include, variable delays, pulse broadening, dispersion and sample loading and these are considered by McSkimin (1961) and Papadakis (1976).

3.3.4 Velocity dispersion

In a dispersive material, such as an emulsion, different frequency components travel at different velocities. Thus the velocity measured is the group velocity which may be different from that of the phase velocity (the velocity of a single frequency component) (Pierce 1981). The pulses used in this work were of short duration (≈ 2 to 3 cycles) and so contain a range of frequency components. Velocity dispersion may therefore lead to errors in both velocity and attenuation measurements. A Fast Fourier Transform of the echoes received from an emulsion which was known to be dispersive was carried out using a Lecroy oscilloscope. These measurements indicated that the majority of the signal observed was at the stipulated frequency. Also measurements of the time difference between successive echoes of a dispersive emulsion showed no apparent effects of velocity dispersion; the time differences between consecutive peaks were similar. Thus it was assumed that errors due to velocity dispersion were small.

3.3.5 Cuvette design

Rather than having the samples in direct contact with the transducers, they were contained in cuvettes. This was so that many samples could be prepared and measured together, the apparatus did not have to be cleaned after each measurement, and because it is easier to align the sides of a cuvette to a high degree of parallelism than it is to align the faces of

transducers. Initially it was hoped that some existing spectroscopic cuvette might be utilised. A number of these were obtained from various manufacturers, however none proved to be suitable and so it was necessary to design and manufacture the cuvettes specially. After some consideration it was decided to use glass cuvettes of the following specification 1.5mm thick walls, 10mm path length, 30mm wide and 50mm high which contained about 12 cm^3 of sample. These were manufactured by Chandos Intercontinental U.K. The factors considered when designing the cuvettes are discussed below.

Material for cuvette Ideally, the material used to construct a cuvette should be fairly low cost, robust, chemically unreactive, easily manufactured and have a suitable acoustic impedance. There are a number of materials which may be suitable e.g. glass, quartz and some types of metals and plastics. Glass proved to be a convenient material for the samples used in this work, which was useful since it meant cuvettes could be manufactured by existing glass-ware suppliers.

Cuvette path length The longer the path length of a cuvette the greater is the time difference between successive echoes and so the better is the resolution of the time measurements. However, small cuvettes are easier to handle and manufacture; are more robust and require smaller sample sizes. A path length of 10mm was a good balance between accuracy and convenience.

Cuvette width Better signals were obtained when the face of a transducer was narrower than the width of a cuvette. This was probably because less of the ultrasonic energy can pass through the side walls of the cuvettes and be detected by the receiver, thus obscuring the signal which has travelled directly through the sample. It is also necessary to have the cuvette sufficiently wide to reduce the possibility of side wall reflections produced by beam spreading in the far field region (figure 3.4). This effect can also be reduced by roughening the inside faces of the cuvette side walls so that any diffracted ultrasonic waves are scattered in all directions rather than being directed, thus reducing the possibility of interference with the wave which has travelled directly through the sample.

Cuvette wall thickness For optimum transmission of ultrasound from transducer to sample it is best to have a cuvette thickness of an odd number of quarter wavelengths of ultrasound in glass (section 3.3.3). Taking the velocity of ultrasound in glass to be 5660 m/s (Kaye and Laby 1986) the optimum cuvette thickness was calculated to be 1.4mm at 1MHz, 1.1mm at 1.25 MHz, 0.63mm at 2.25 MHz, 0.24mm at 6 MHz and 0.14mm at 10 MHz. It would therefore be best to use different cuvette thicknesses for each frequency used which is impractical. Experiments with a number of cuvettes of different thickness, indicated that the best transmission was achieved for cuvettes with thin walls. This is probably because for thin walled cuvettes less of the ultrasonic signal can pass through the cuvette walls and obscure the signal which has travelled directly through the sample. However, cuvettes with thin walls are difficult to manufacture and are fragile. The thickness chosen (1.5mm) was a compromise between the optimum transmission of acoustic energy and the robustness of the cuvette.

Parallelism It is essential to have the front and back cuvette walls aligned to a high degree of parallelism so that phase cancellation does not occur; phase cancellation can cause appreciable errors in velocity and attenuation measurements (McSkimin 1961). For this reason cuvettes were manufactured to a high degree of parallelism; the angle between the opposite faces of a cuvette was less than 0.02°.

Chapter 4

ULTRASONIC MEASUREMENTS IN FATS AND OILS

4.1 Introduction

4.1.1 Edible fats and oils

Fats and oils play a vital role in the human diet. They provide an important source of energy, having a higher calorific value than either proteins or carbohydrates, and contain a number of fatty acids which are essential to human health but which cannot be synthesised by the human metabolism. They are also used extensively for their characteristic heat transfer, organoleptic and rheological properties (Pomeranz 1985). Edible fats and oils are usually obtained from animal, marine or vegetable sources, the latter being the most important at present (Weiss 1983). Chemically, they are esters of the trihydric alcohol glycerol and fatty acids and belong to the group of compounds called 'lipids'. Different members of the lipid group have little in common with each other apart from the fact that they are all insoluble in water but soluble in organic solvents (Fox and Cameron 1970). By definition a fat is solid (or semi-solid) at the temperature of interest, whilst an oil is liquid.

Triglycerides are the major constituents of most edible fats and oils and largely determine their overall bulk properties (Hampson and Hudson 1961). However, small amounts of mono- and diglycerides may also be present and these can play an important role in some applications e.g. emulsification (Dickinson and Stainsby 1982). The physical and chemical properties of glyceride molecules depend on the type, the number and the position of the fatty acid molecules attached to the glycerol. The fatty acids found in natural fats and oils are generally straight chained with an even number of carbon atoms in the range 4-24 per molecule, and may be either saturated or unsaturated. The most commonly occurring

saturated fatty acids in edible fats and oils are mysteric, lauric, palmitic and stearic acids, whilst the most common unsaturated fatty acids are oleic, linoleic and linolenic acids (Hampson and Hudson 1961). Processing of natural fats and oils may alter the structure of some of the fatty acids present. During catalytic hydrogenation some of the unsaturated molecules may be converted from a cis to a trans configuration and some iso-acids may also be formed (Hampson and Hudson 1961). The chemical composition of edible fats and oils is therefore extremely complex (Walstra 1987a).

4.1.2 Physical properties of fats

Many of the physical properties of fats which are important commercially, such as texture, spreadability and consistency, depend on their characteristic plastic properties (Prentice 1984). Plasticity occurs in fats because they contain a mixture of triglycerides each with its own melting point and so a range of temperatures exist where some of the triglycerides are crystalline and the rest are liquid. In this range the fat consists of a matrix of inter-locking crystals surrounded by a liquid oil phase. Below a certain yield stress this matrix behaves elastically, however, when the yield stress is exceeded the crystals slide over one another and permanent deformation occurs. The plasticity of fats depends primarily on the type and proportion of triglycerides present as well as their thermal and shear history (Walstra 1987a).

If the tempering procedure used to prepare a fat is kept constant, its consistency is directly related to the amount of solid fat present; the so called 'solid fat content' (SFC) (Lefebvre 1983). The variation of SFC with temperature is an important property of many commercial fats and often determines their suitability for particular applications. For example, margarines must not collapse under their own weight, yet spread upon application of a given stress and 'melt' in the mouth. Consequently, there has been considerable interest in the development of techniques for measuring SFC and a number of these are discussed in section 4.1.3.

The physical properties of fats also depend on their thermal and shear history; two fats which have the same SFC may have different rheological properties due to the method used to prepare them. This is because fat crystals can exist in more than one crystalline form - they are polymorphic (Lutton 1972). The polymorphic form of fat crystals depends on the tempering procedure used to produce them, their tendency towards a particular polymorphic form and the presence of various additional ingredients (Gunstone and Norris 1983). An increasing number of polymorphic forms are being identified, however, the three principle forms are the α, β' and β forms. The α form has the lowest melting point and is the least stable, the β form has the highest melting point and is the most stable, whilst the β' form is an intermediate form. In general rapidly cooled, stirred samples tend to form matrices of small needle like crystals, whilst slower cooled, unstirred samples tend to form larger isolated crystals. In margarines and some other edible fats these large crystals are undesirable since they impart a 'grainy' mouth-feel to the product (Merker et al 1958). The polymorphic form of fat crystals is characterised by the way the molecules are packed in the crystal lattice, and is usually determined by one of the spectroscopic techniques X-ray, infra-red, ultraviolet (Chapman 1969), however, other techniques can also be used e.g. microscopy, melting point and differential thermal analysis.

4.1.3 Instrumental methods of determining SFC

The methods available for measuring SFC can be divided into two groups: 'traditional' and 'modern' methods. The traditional methods include various melting point techniques, penetrometer measurements and dilatometry (Rossel 1986). Although these methods proved useful in the past they are time consuming, laborious and subjective and are therefore not suitable for modern process control purposes, which rely on rapid and precise measurements. Consequently, there has been interest in the development of alternative instrumental techniques for measuring SFC. The essential requirements of any new technique have been discussed by Waddington (1986). He suggests that new techniques should be capable of rapid and reliable measurements over a range of temperatures and should be easy to operate and calibrate.

Differential thermal analysis (DTA) was initially proposed as an alternative to the traditional methods of determining SFC (Hannewijk and Haighton 1958, Lavery 1958). However, DTA measurements require minute sample sizes (≈10μg) and the value of SFC determined depends on the type and amount of fat crystals present as well as their thermal and shear histories (Hagemann et al 1972). Thus the technique is not really suitable as a routine quality control device, but is still useful in research laboratories where precise measurements of the enthalpy-temperature profiles of fats are important (Sleeter 1985).

The technique which is most widely used for SFC determinations in the food industry at present is low resolution nuclear magnetic resonance (NMR). The first commercial instruments utilising this technique were based on continuous-wave NMR, however, these have largely been replaced by pulsed NMR instruments which are capable of faster sampling rates and have greater sensitivity (Sleeter 1985). Pulsed NMR has been used to estimate SFCs in a wide variety of partially solidified fats and emulsions over the past 15 years or so (Sleeter 1985). The technique is rapid, non-intrusive, easily adaptable to in-line measurements and has proved reliable. It does, however, have a number of limitations: it is relatively expensive to purchase, it is not applicable to some systems of interest and it cannot determine the SFC directly due to the inherent 'dead' time of the instrument (Waddington 1986). The limitations of this technique and the fact that alternative techniques may offer wider scope and better insight into particular problems has led to renewed interest in the development of techniques for determining SFCs (Sleeter 1985).

4.1.4 Application of ultrasonics to fats and oils

In recent years there has been increasing interest in the use of ultrasonics as a means of characterising fatty materials. The most frequent application of ultrasonics in this area is for the determination of back-fat thickness and tissue composition in animals (Lister 1984). Due to the complex structure of animal tissue workers have usually tried to establish empirical relationships between the ultrasonic velocity and the composition of the animal tissue. Recently however, Povey (1984), Hussin and Povey (1984) and Miles et al (1985)

have used simple theoretical equations, which assume no scattering of ultrasound by the systems, to predict the variation of ultrasonic velocity with SFC for a number of animal and vegetable fats. Their results suggest that ultrasonics may prove a useful means of determining SFCs in these materials.

The ultrasonic technique has also been used to investigate various properties of liquid oils. The ultrasonic velocity of a number of liquid triglycerides and fatty acid methyl esters has been empirically related to their chemical formula (Gouw and Vlugter 1964, 1967, Javanuad and Rahalkar 1988). Empirical formula have also been used to relate the ultrasonic velocity of vegetable oils to their constituent components (Javanuad and Rahalkar 1988). The dependence of the ultrasonic velocity and attenuation on temperature and frequency has been measured for a number of animal and vegetable oils (Hustad et al 1970, Kuo 1971, 1975, Grigorev et al 1976, Bhattachayra and Deo 1981, Hussin and Povey 1984, Gladwell et al 1985, Miles et al 1985, Javanuad and Rahalkar 1988) and the technique has been used to detect adulteration in oils (Rao et al 1980).

4.2 Ultrasonic investigations of glyceride/oil mixtures

4.2.1 Introduction

The majority of the investigations discussed in section 4.1.4 concentrated on naturally occurring animal or vegetable fats, whose principal constituents are the glycerides. To appreciate the factors which influence ultrasonic measurements in these fatty materials it is useful to examine ultrasonic propagation in their constituent glycerides. For this reason the ultrasonic velocity of a series of glyceride in oil mixtures was measured with varying temperature (0-70°C) and glyceride type and concentration (0-30% w/w). The glycerides were diluted with liquid paraffin oil or with sunflower oil so that the amount of glyceride present could be controlled and to prevent vacuole formation (Hvolby 1974) which can cause large attenuation of ultrasound. The aim of the experiments presented in this section was to identify the factors which affect ultrasonic measurements in fat/oil mixtures and thus

highlight the potential of the ultrasonic technique for characterising these systems. Some of the results presented is this section, as well as some complementary results have recently been published (McClements and Povey 1987 b,c, 1988 a,b,c).

4.2.2 Materials and Methods

4.2.2.1 Materials

Tristearin (SSS), tripalmitin (PPP), trilaurin (LLL), Glycerol 1,3 dipalmitate-2-oleate (POP), Glycerol 2,3 dipalmitate-1-oleate (OPP), Glycerol 1,3 dipalmitate-2-stearate (PSP), Glycerol 1- palmitate 2-oleate 3-stearate (POS), Glycerol 1,3, distearate-2- oleate (SOS) and distearate (SS) were supplied by Unilever Research Laboratories (URL), Colworth House, U.K. Stearic acid (SA) and triolein (OOO) were obtained from BDH Chemicals Ltd., U.K. The purity of the mono-acid saturated triglycerides was determined at URL using high pressure liquid chromatography of the fatty acid methyl esters (FAME). The results are presented in table 4.1.

Table 4.1: FAME analysis of mono-acid saturated triglycerides

Results are presented as the weight percentage of fatty acids determined (tr = trace amounts found).

	10:0	12:0	14:0	16:0	17:0	18:0	18:1	20:0
SSS	-	-	tr	0.5	-	98.8	-	0.6
PPP	-	-	0.4	97.7	tr	1.2	-	-
LLL	0.4	96.2	0.5	1.1	-	1.7	tr	-

Paraffin oil was obtained from Boots Company, Nottingham, U.K. Silica treated sunflower oil was obtained from URL. The physical properties of these oils varied slightly from batch to batch, and so each batch was characterised individually before use. Corn oil, grape seed oil, ground nut oil, olive oil, palm oil, rape seed oil, safflower oil and soybean oil were obtained from Wm. Morrisons Ltd., U.K.

4.2.2.2 Sample preparation

The physical properties of fat/oil mixtures depend on their thermal and shear histories and so samples were prepared using a constant tempering procedure. Solid glyceride and/or liquid oil were weighed into a glass cuvette and mixed thoroughly. This mixture was melted at 80°C in a vacuum oven, stirred to ensure homogeneity and then placed under vacuum at 650 mmHg for 30 mins to remove any air. The sample was then cooled rapidly by placing it in a 5° C water bath, where it was left overnight to ensure complete crystallisation. Ultrasonic velocity and attenuation measurements were then made with increasing temperature. The samples were allowed to equilibrate for at least 30 mins at each temperature before measurements were made.

This tempering procedure produced samples which contained a fine matrix of glyceride crystals surrounded by a liquid oil phase (photograph 4.1). The formation of a matrix is useful since it prevents fat crystals from sedimenting during measurements. The most significant problem encountered when preparing the samples was due to vacuole formation in some of the larger SFC samples (>15% w/w). Vacuoles are cavities formed in the samples due to the contraction or expansion of fats on cooling (Hvolby 1974). They have a large acoustic mismatch with fats and can attenuate the ultrasonic signal so much that it cannot be detected. This problem was partially overcome by rapidly removing heat from the bottom of the sample; any cavities formed are then filled in by the hot oil above.

Samples of solid tristearin and tripalmitin were prepared using the same technique, however, some important difficulties were encountered. On solidification both the tristearin and tripalmitin expanded slightly (Hvolby 1974) which caused the glass cuvettes they were stored in to break. Thus the samples had to be removed from their cuvettes before measurements were made. The samples were left for at least four weeks at room temperature before ultrasonic measurements were made so that the crystals had time to convert from the unstable α polymorphic form, which is formed on rapid cooling of these pure triglycerides, to the stable β form (Garti et al 1982).

4.2.2.3 Characterisation of samples

Polymorphic form. The polymorphic forms of the crystalline tristearin, tripalmitin and trilaurin in oil mixtures were determined using X-ray diffraction and differential scanning calorimetry (DSC). X-ray measurements were carried out at 20°C using a Phillips Constant Potential Generator which utilises Cu_{KL} radiation (λ = 0.1541nm). Wide angle diffraction measurements were made using a proportional counter at a scan rate of 2°/min. Figure 4.1. shows a typical wide angle diffraction pattern obtained for the samples, whilst table 4.2 summarises the results for the three triglycerides investigated. The d-spacings were calculated from Bragg diffraction angles and correspond to the β polymorphic form (Chapman 1969). These results were confirmed using a Perkin-Elmer DSC-2. A few micrograms of triglyceride in oil mixture were placed in a small aluminium pan and heated from 10-80°C at a rate of 10°C/min. A typical DSC curve obtained is shown in figure 4.2. Similar, curves were also obtained for the other triglycerides. The large exothermic peak at about 65°C corresponds to the β polymorphic form of the crystals (taking into account the solubility of tristearin in paraffin oil, Lutton 1955). The rapid transformation of these triglycerides to their most stable form in binary triglyceride/oil mixtures has also been noted elsewhere in the literature (Van Boekel 1981, Norton et al 1985). The polymorphic form of the pure solid triglycerides was determined from their melting point. Both were found to be in the β form at the time of measurements.

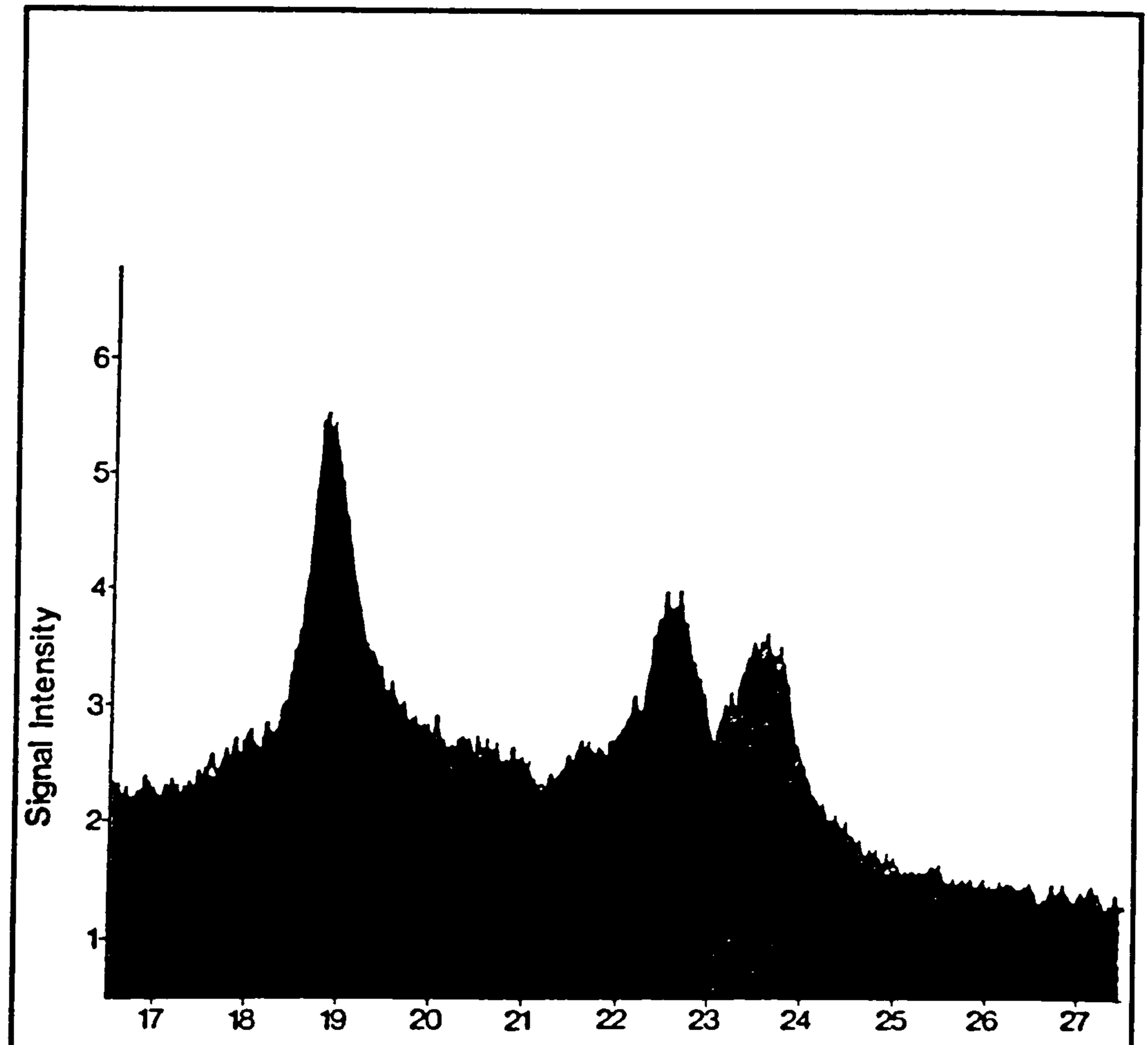

Figure 4.1: X-ray diffraction pattern of tristearin in paraffin oil mixture. (45% w/w)

Table 4.2: D-spacings of tristearin, tripalmitin and trilaurin in paraffin oil mixtures

	D-spacings (Å)		
Tristearin	3.72	3.88	4.63
Tripalmitin	3.73	3.88	4.62
Trilaurin	3.75	3.88	4.65

Microscopic examination of fat crystals The crystalline tristearin, tripalmitin and trilaurin in paraffin oil mixtures were examined using polarised light microscopy. Samples were prepared using the modified smear technique first suggested by Hoerr (1955). A small amount of sample (≈10μg) was placed on a glass slide using a micro-spatula and a cover slip was carefully pressed down on it so as to reduce distortion of the crystal structure. The sample thickness was controlled by placing narrow strips of sellotape at either side of the sample, between the cover slip and the slide. The depth of the sample was then equal to the thickness of the sellotape. Polarised light allows the solid and liquid phases to be distinguished since solid fat is anisotropic and is therefore birefringent whereas liquid oil is isotropic and appears dark in polarised light (Berger et al 1979).

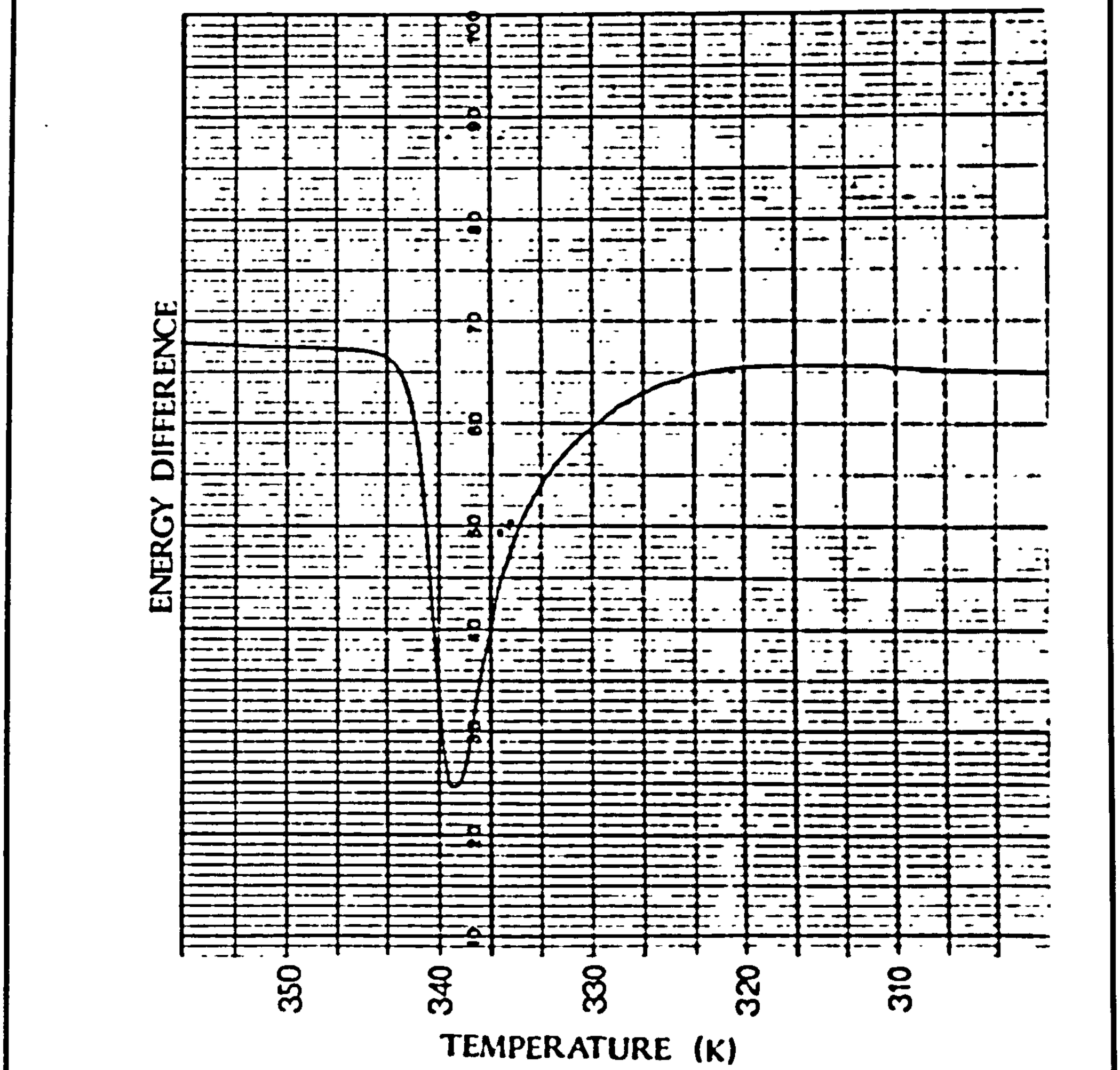

Figure 4.2: DSC thermogram of 45% w/w tristearin in paraffin oil mixture

Photograph 4.1. Photograph of 5% tristearin in paraffin oil mixture at room temperature under polarised light (x 500 magnification). Notice matrix of interlocking needle-like crystals.

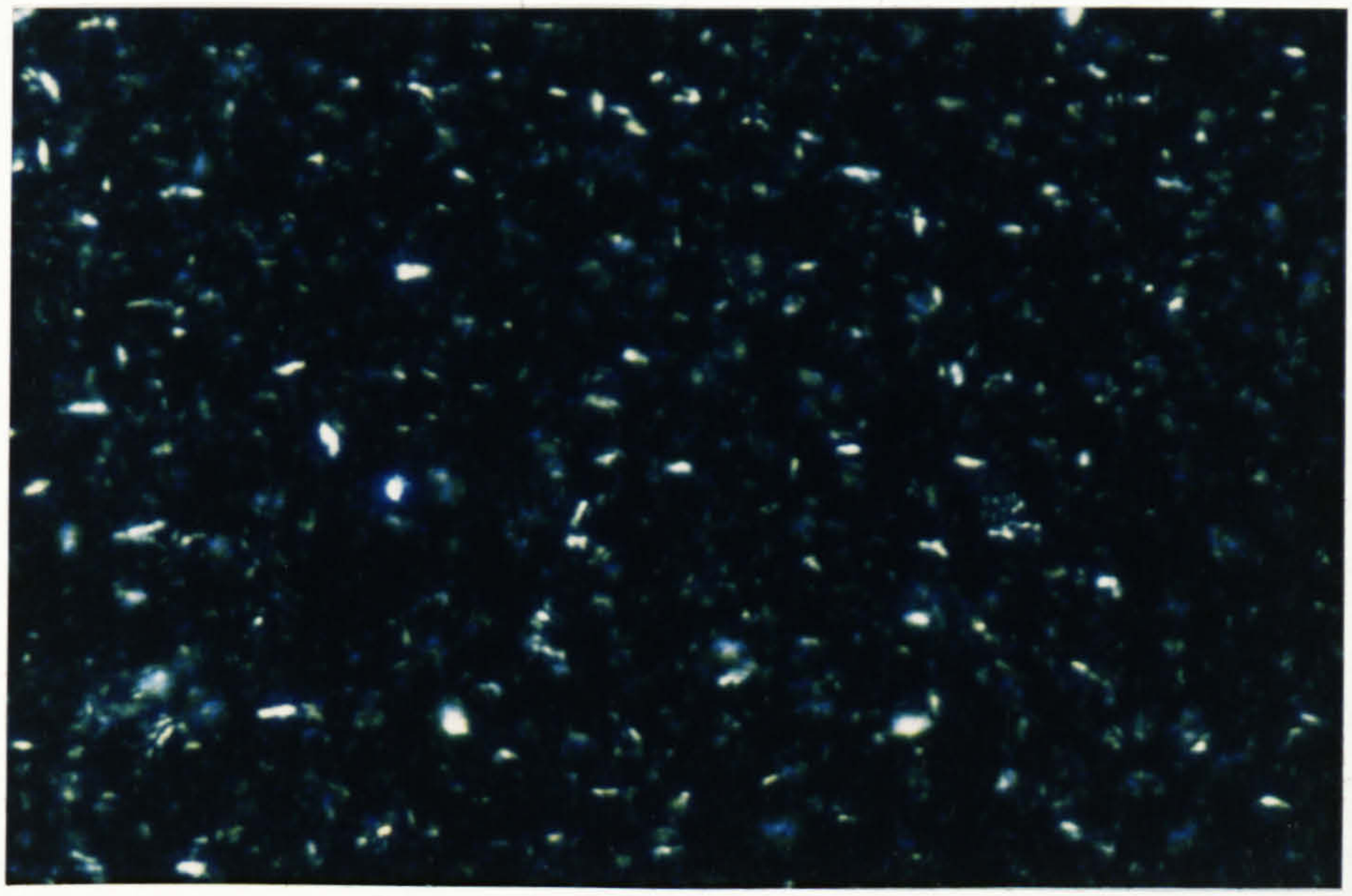

Photograph 4.2. Photograph of 10% tristearin in paraffin oil mixture at room temperature under polarised light (x 500 magnification). Spherulites start to appear.

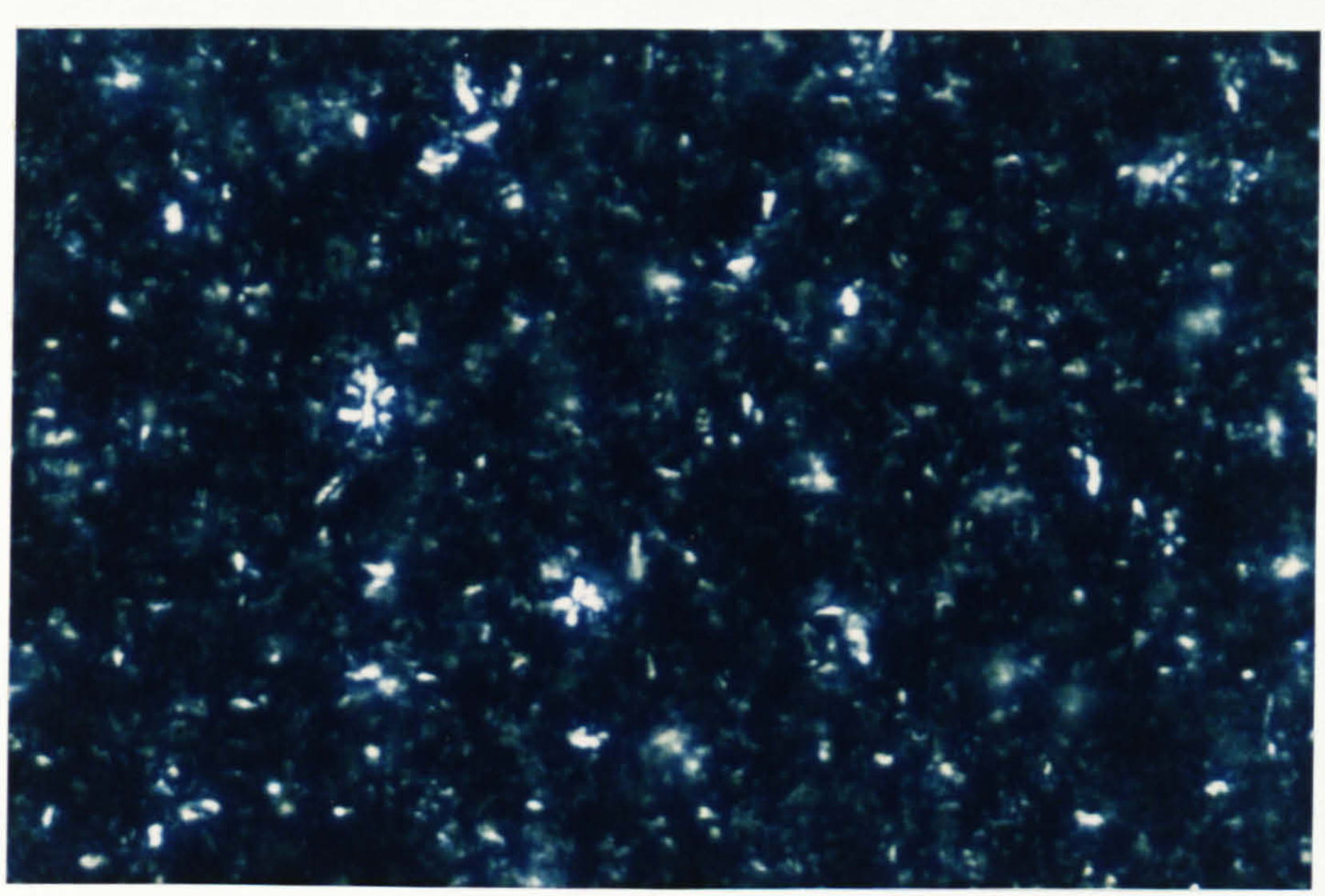

Photograph 4.3. Photograph of 5% trilaurin in paraffin oil mixture at room temperature under polarised light (x500 magnification).

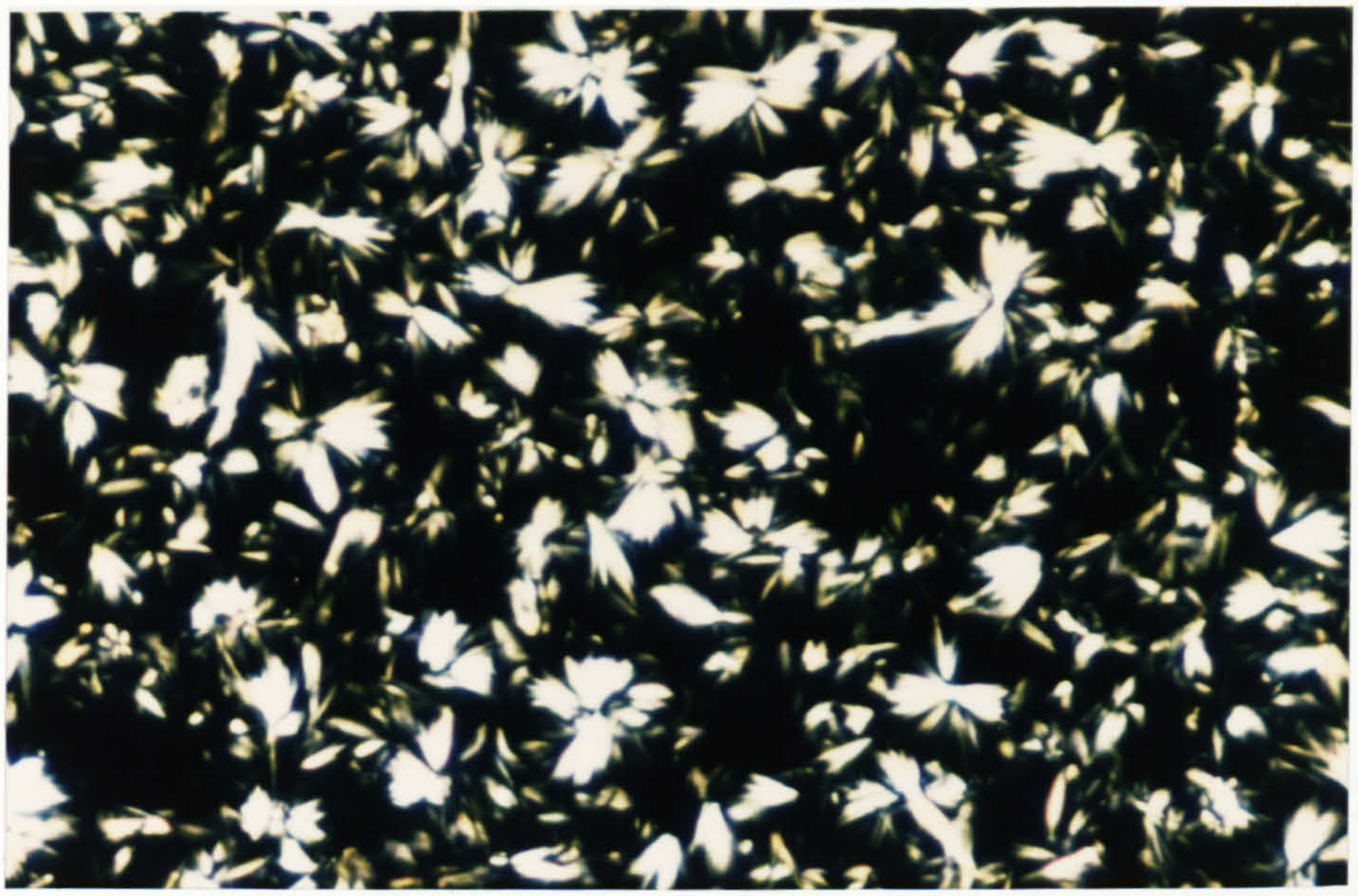

For SFCs between about 1 and 10% the tristearin in paraffin oil mixtures formed a gel matrix of needle-like crystals surrounded by liquid oil (photograph 4.1). Above SFCs of about 10% spherulites started to appear (photograph 4.2). These are clusters of individual crystals into loosely spherical shapes (Berger et al 1979). The photographs are blurred because the thickness of the samples makes it difficult to focus on any one plane. The sizes of the individual needle-like crystals could not be determined accurately but were estimated to be about 1μm in length and about 0.2μm in width. The size of the spherulite clusters were larger having diameters between about 3 and 4μm (photograph 4.2). The tripalmitin in paraffin oil mixtures were observed to have a similar crystal structure as the tristearin in paraffin oil mixtures. The trilaurin in paraffin oil mixtures still formed gel matrices,

however, the crystals tended to aggregate into 'fan' shapes which were about 5μm in length (photograph 4.3).

Crystallisation rate To ensure the glycerides had fully crystallised out when the ultrasonic measurements were made the variation of SFC with time was determined using pulsed NMR (see section 4.3). For all the samples the SFC determined after 6 days at 5°C was within 0.3% of that determined after 2 hrs at the same temperature. The samples were therefore assumed to be fully crystalline when measurements were made.

4.2.2.4 Ultrasonic measurements

The ultrasonic velocity and attenuation of the liquid oils and the glyceride in oil mixtures were measured using the pulse echo technique described in chapter 3. These measurements were made at 1MHz unless otherwise stated. The attenuation measurements in the fat/oil mixtures proved to be unreliable and prone to large experimental errors. This was partly because of difficulties in separating the attenuation due to the sample from that caused by beam spreading and transmission losses (section 3.2.1), and partly because many of the samples contained vacuoles which can highly attenuate ultrasound and thus obscure the signal from the samples themselves.

The ultrasonic velocity and attenuation of the solid glycerides is required for the theoretical calculations of ultrasonic velocity in the glyceride/oil mixtures (chapter 2). The technique described in chapter 3 could not be used to measure the ultrasonic velocity of the solid glycerides because the samples expanded on cooling, breaking the cuvettes. For this reason the ultrasonic velocity was measured using a technique similar to that described by Hussin (1982). A single 1MHz transducer, used as both generator and receiver, was pressed against the surface of a 10 mm thick slab of solid triglyceride. The ultrasonic velocity ($v = 2d/t$) was then calculated by measuring the time difference between successive echoes t, and the length of the slab d, using vernier callipers. The attenuation of the solid tripalmitin was so great that no signal could be observed on the oscilloscope. This phenomena has also been observed by Hussin (1982) and is probably caused by excessive vacuole formation in the

samples. The ultrasonic velocity of the solid tripalmitin could therefore not be measured. The attenuation of the solid tristearin was also large (390 dB/m at 1.25MHz and 20°C): only three successive echoes could be observed, however, measurements of the velocity could still be obtained.

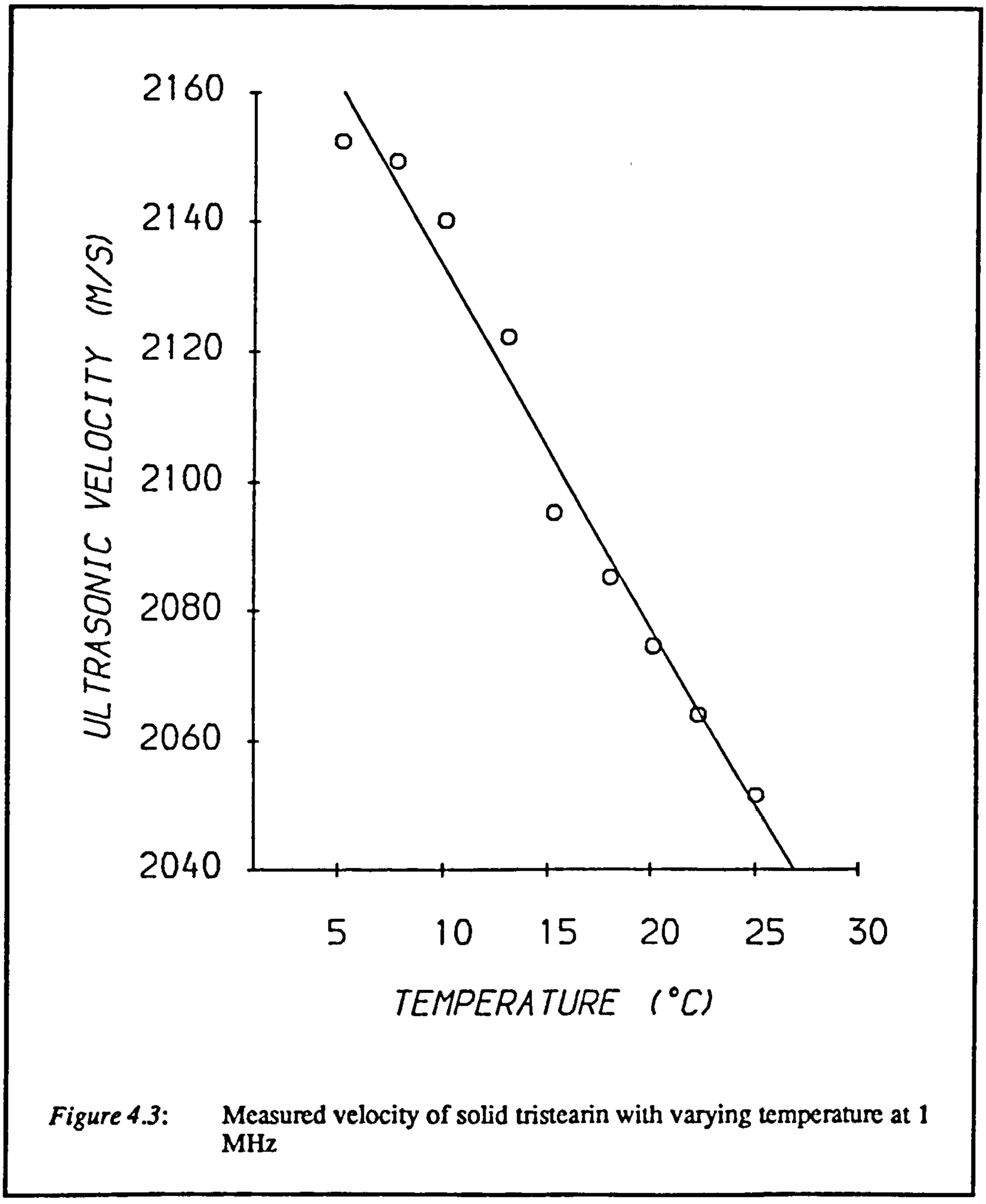

Figure 4.3: Measured velocity of solid tristearin with varying temperature at 1 MHz

The ultrasonic velocity of the solid tristearin was measured with increasing temperature (5-25°C) by placing it in a water bath which was equilibrated to the appropriate temperatures. Due to the low solubility of solid tristearin in water at these temperatures (Formo 1979) it was safe to assume that the tristearin would not dissolve in the water during the measurements. The results of the velocity measurements are presented in figure 4.3. The precision of the measurements was calculated from the standard error of the mean of at least five measurements of the velocity and was found to be ± 5m/s. The curve through the experimental measurements was calculated by finding the best least squares fit of the measurements to the equation $v = ae^{bT}$, where v is the measured velocity, T is the temperature and a and b are constants. The values of a and b were calculated as 2190.0 ± 0.7 m/s and -0.00264 ± 0.00014 $ms^{-1}°C^{-1}$ respectively.

4.2.2.5 Thermophysical properties required in theoretical calculations

As well as the ultrasonic velocities and attenuations of the component phases, a number of other thermophysical properties are needed in order to use the theoretical equations discussed in chapter 2.

Densities and coefficients of volume expansion The densities of the glycerides were extracted from the literature whilst the densities of sunflower oil and paraffin oil were measured with varying temperature using 50 cm^3 density bottles (figure 4.4). The volume of the density bottles was measured accurately over a range of temperatures by calibrating them with distilled water whose density is known (Kaye and Laby 1986). The variation of density with temperature for a material depends on its coefficient of volume expansion β (= $\frac{1}{V}\left(\frac{\partial V}{\partial T}\right)_p$). For some substances β can be considered to be constant over quite wide ranges of temperature and pressure (Zemansky 1957) and the variation of density with temperature can be described by the equation:

$$\rho = \rho_0(1 + \beta T)^{-1}$$

Here ρ is the density, T is the temperature and ρ_0 and β are constants which are determined by calculating the best least squares fit of this equation to experimental measurements. In general, however, the coefficient of volume expansion is temperature dependent. Miles et al (1985) have shown that the variation of density with temperature for many fats and oils can be described using Taylor series expansions of the form:

$$\rho = \rho_0(1 + \beta(T-T_0) + \beta_1(T-T_0)^2)^{-1} \qquad (4.1)$$

Where T_0 is the reference temperature and β_1 is a constant. The values of ρ_0, β and β_1 calculated from the density measurements of sunflower oil and paraffin oil shown in figure 4.4 are presented in table 4.3. The values for the solid and liquid tristearin are also included, these were taken from Lutton (1955). The value of β at 20°C was calculated from the density measurements between 10 and 30°C only. The value for sunflower oil was 7.11 $\cdot 10^{-4}$ whilst that for paraffin oil was 6.97 $\cdot 10^{-4} K^{-1}$.

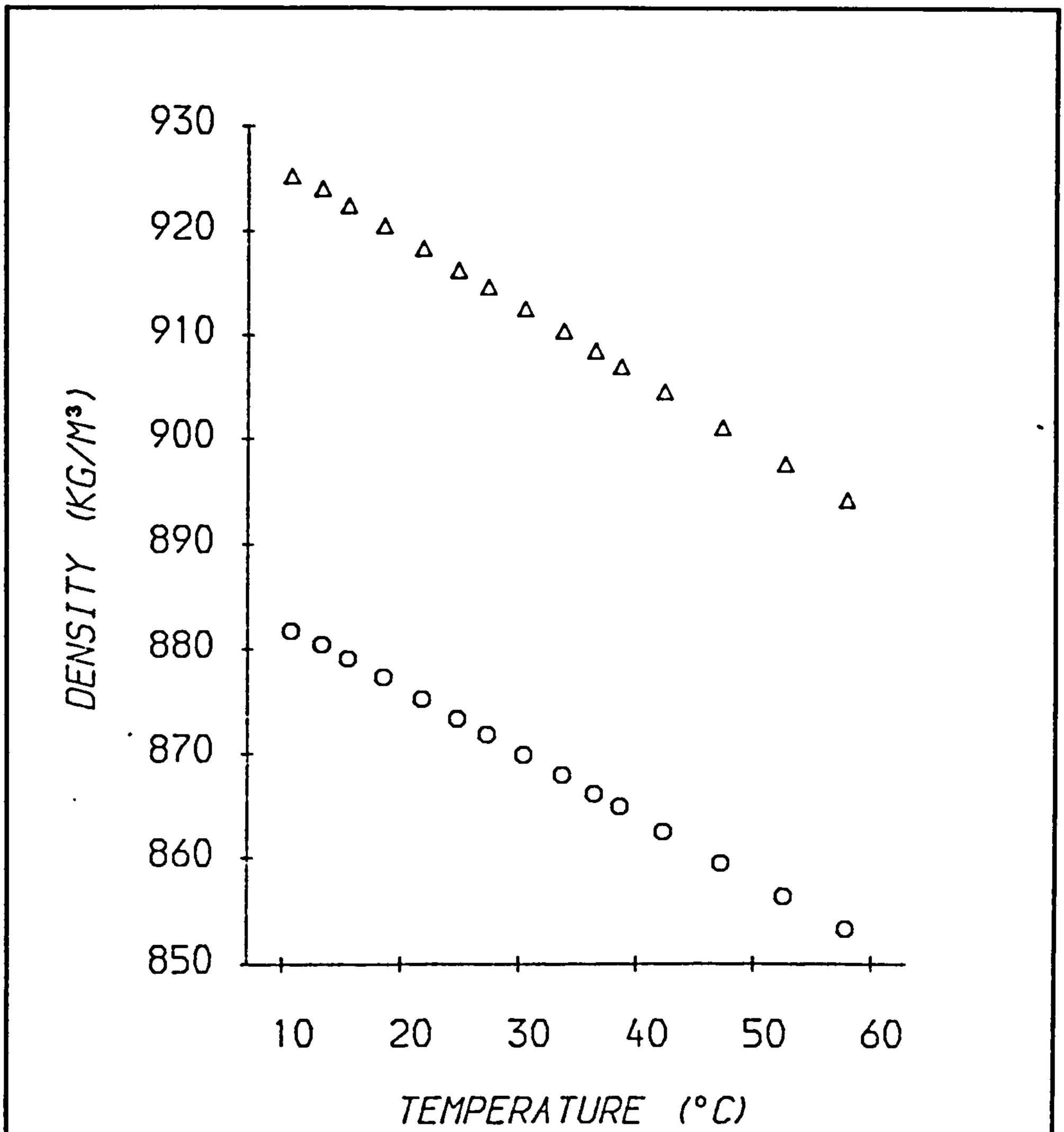

Figure 4.4: Measured densities of paraffin oil and sunflower oil. Annotation: paraffin oil = o, sunflower oil = Δ.

Table 4.3: Densities of paraffin oil, sunflower oil and tristearin

Parameters calculated using equation 4.1.

	n	T (°C)	ρ (kg/m^3)	β (10^{-4} °C^{-1})	β_1 (10^{-7} °C^{-2})
Paraffin oil	15	31.4	869.3	7.03	4.3
Sunflower oil	15	31.4	912.0	7.28	7.8
SSS (solid)	-	0.0	1090.2	3.51	0.0
SSS (liquid)	-	0.0	969.8	7.98	0.0

Specific Heat Capacity The variation of specific heat capacity with temperature for a number of triglycerides, including tristearin, can be found in an article by Hagemann et al (1972). The specific heat capacity of paraffin oil (Raznjevic 1976) and sunflower oil (Mohsenin 1980) were also taken from the literature. The values at 20°C were 2135 and 1980 J kg^{-1} K^{-1} respectively.

Thermal conductivity The thermal conductivities of the fats and oils were also taken from the literature. The value for paraffin oil at 20°C was obtained from Raznjevic (1976): 0.124 W m^{-1} K^{-1} The value for sunflower oil could not be found in the literature, however, many vegetable oils have similar thermal conductivities, between 0.16 and 0.18 W m^{-1} K^{-1} at 20°C (Qashou et al 1972) and so an average value of 0.17 W m^{-1} K^{-1} was used. The thermal conductivity of solid triglycerides could also not be found in the literature, however, values for a number of animal fats are available (Qashou et al 1972). It was therefore assumed that the thermal conductivity of the solid triglycerides was similar to that of solid beef fat i.e. τ = 0.19 W m^{-1} K^{-1}

4.2.3 Results and discussion

Measurements of ultrasonic velocity with increasing temperature for 0-30% w/w tristearin, tripalmitin and trilaurin in paraffin oil mixtures are presented in Appendix V, tables V.1-V.3. The variation of ultrasonic velocity with temperature for a number of 15% w/w glyceride in

paraffin oil mixtures is represented graphically in figures 4.5-4.9. The marked regions in these figures (i.e. | -- II -- |) signify the temperature range where the glycerides are partially soluble in the oil phase (see below). Figure 4.5 shows the results for a 15% w/w tristearin in paraffin oil mixture and for pure paraffin oil, which is liquid across the whole temperature range. These results are included in figures 4.6-4.9 in the form of cubic polynomial curves for comparative purposes. The effect of glyceride concentration on the ultrasonic velocity is illustrated in figure 4.10, which illustrates the variation of ultrasonic velocity with temperature for 0, 10, 20 and 30% w/w tristearin in paraffin oil mixtures.

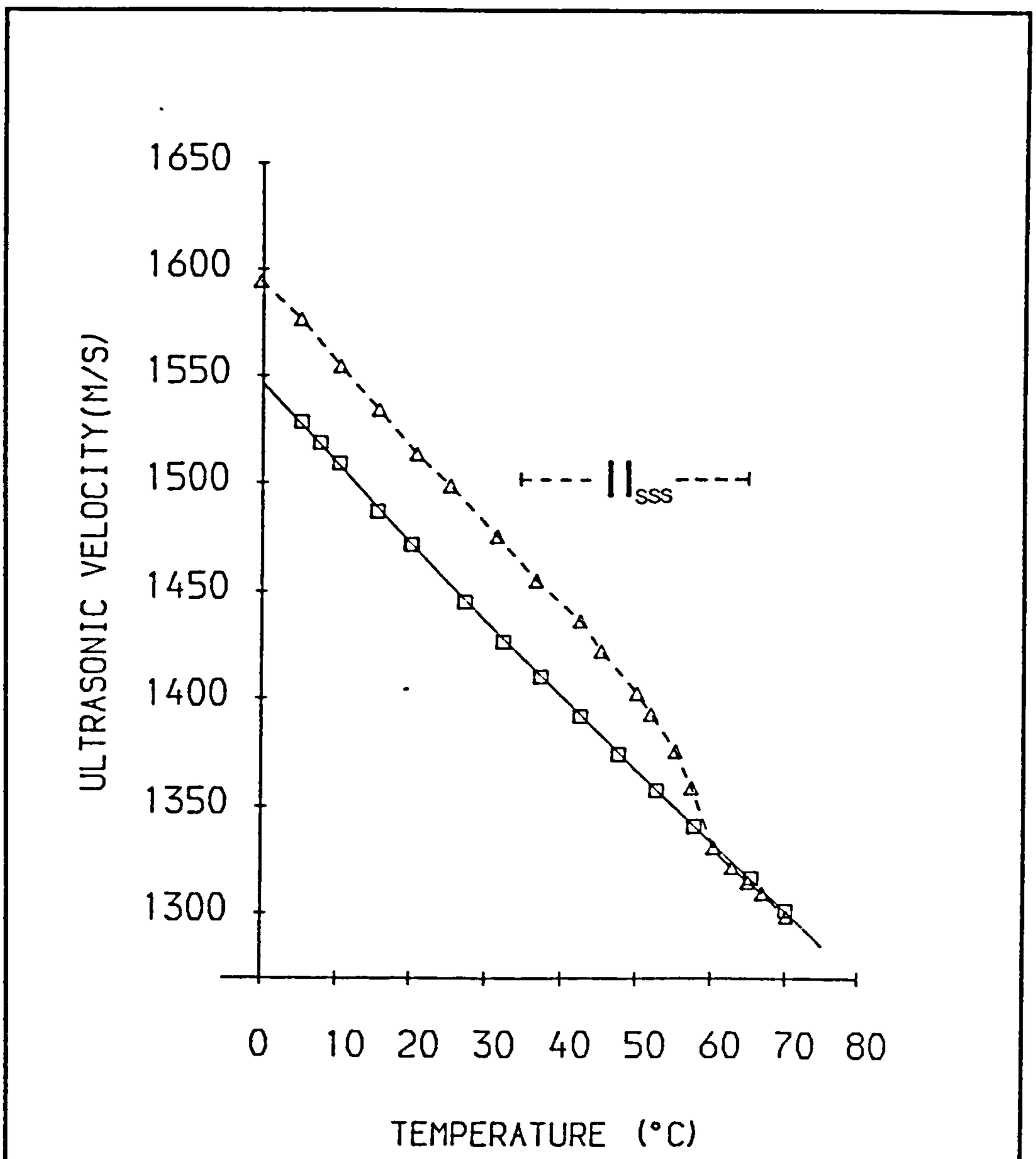

Figure 4.5: Velocity-temperature profiles of 15% w/w glyceride/oil mixtures. Experimental measurements: paraffin oil (□) and 15% w/w tristearin in paraffin oil (△).

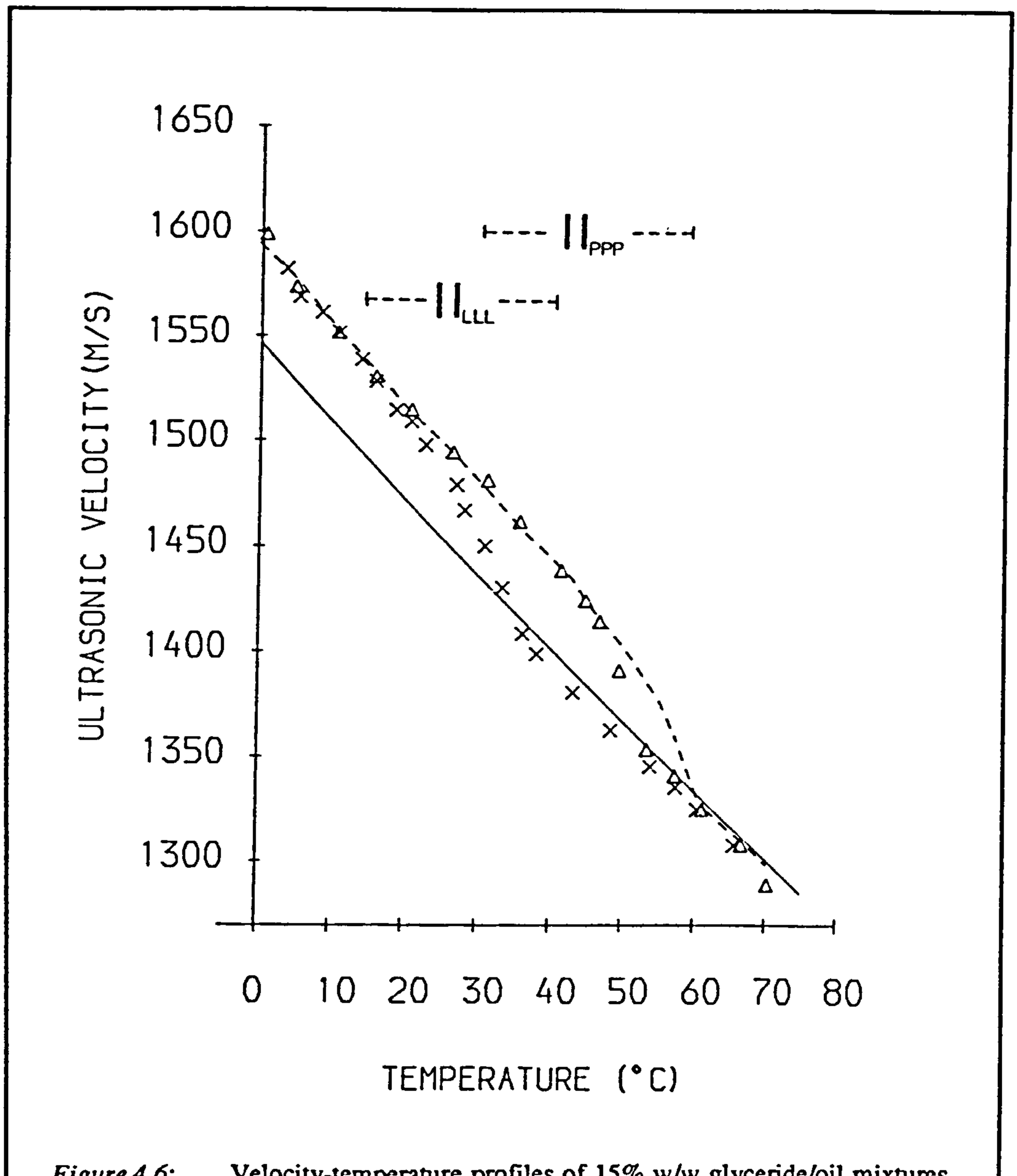

Figure 4.6: Velocity-temperature profiles of 15% w/w glyceride/oil mixtures. Experimental measurements: 15% w/w tripalmitin (△) and trilaurin in paraffin oil (X) mixtures. The full curve represents liquid paraffin oil, the broken curve represents 15% tristearin in paraffin oil.

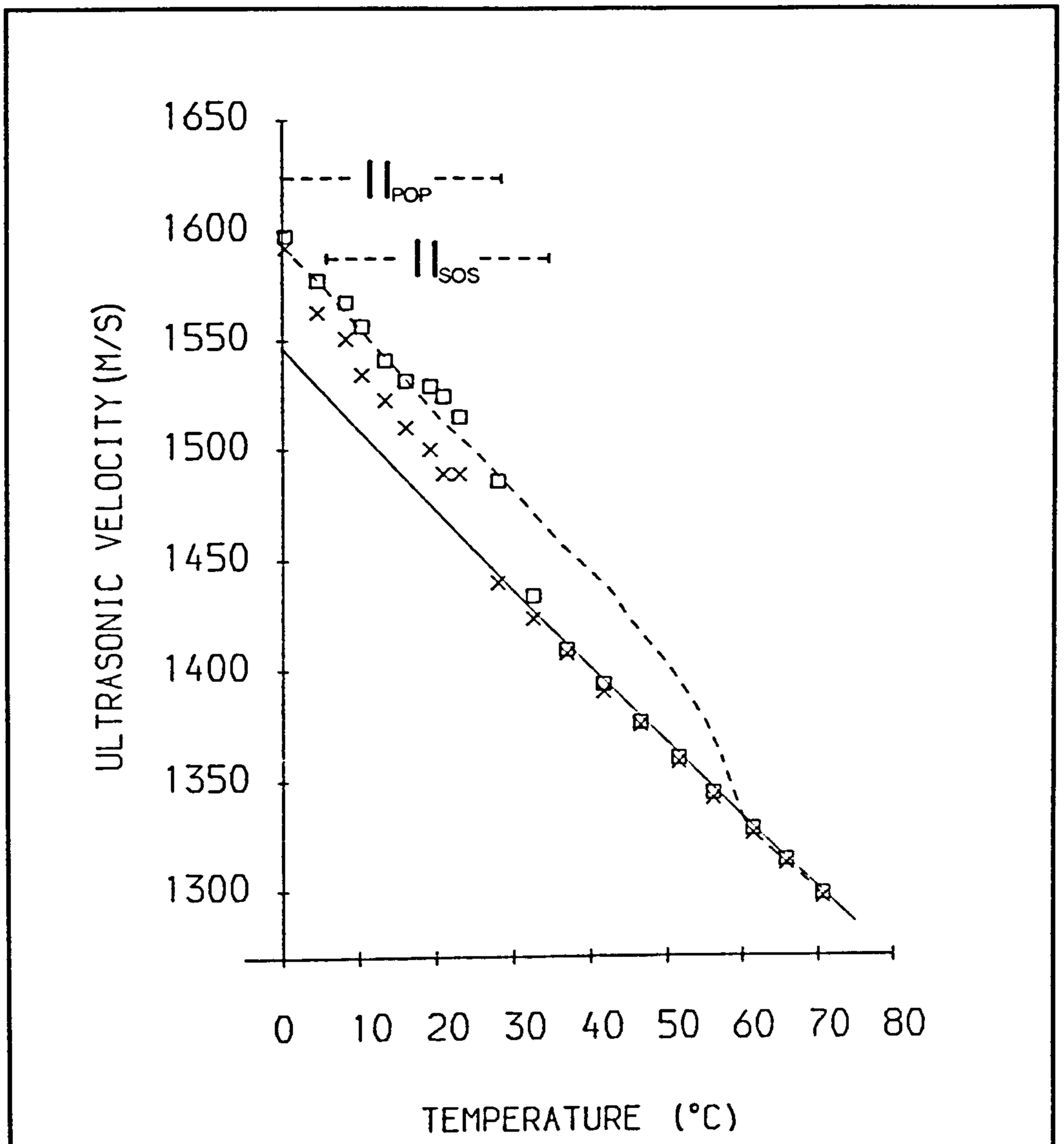

Figure 4.7: Velocity-temperature profiles of 15% w/w glyceride/oil mixtures. Experimental measurements: 15% w/w SOS (□) and POP (X) in paraffin oil mixtures. The full curve represents liquid paraffin oil, the broken curve represents 15% tristearin in paraffin oil.

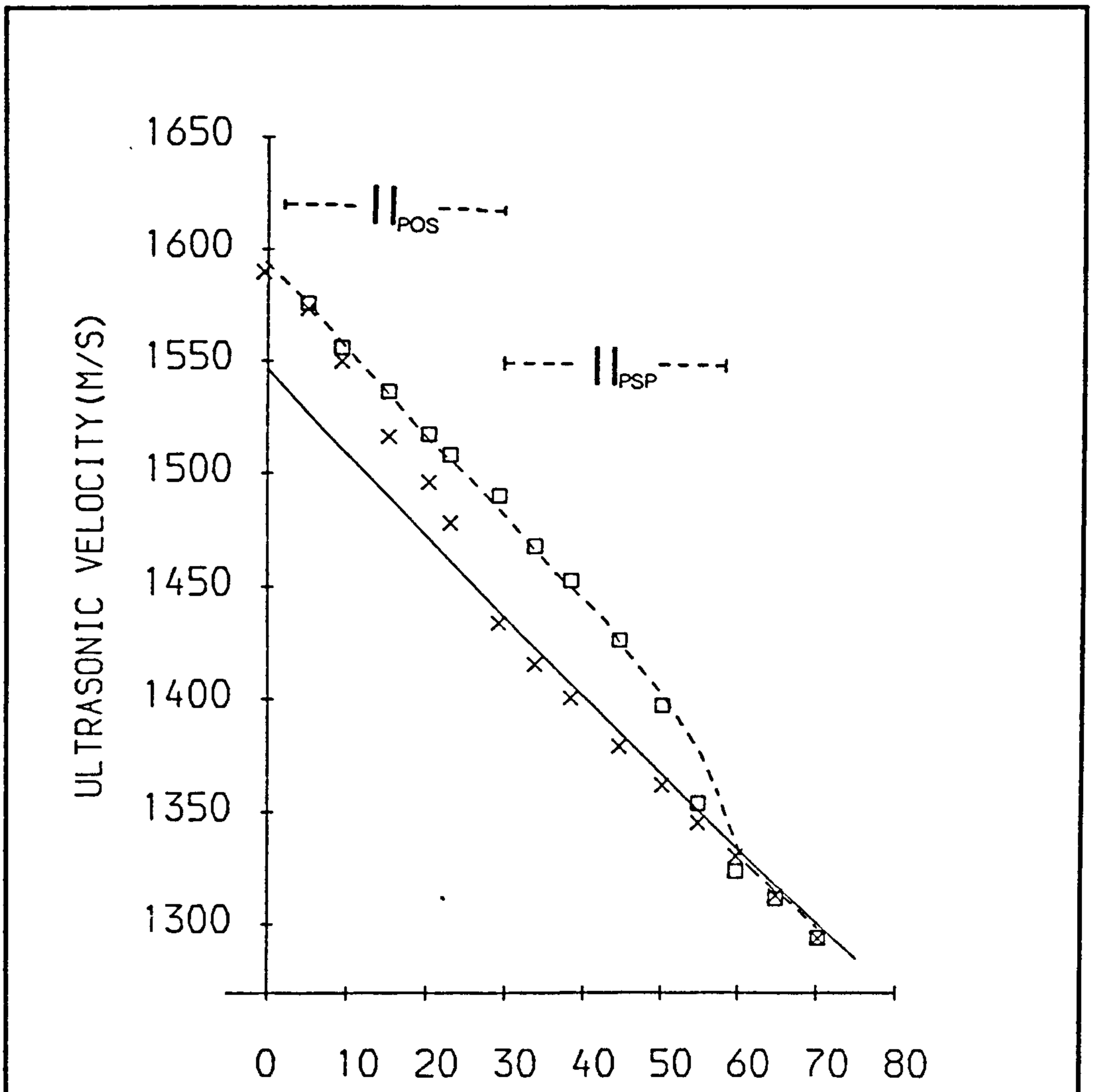

Figure 4.8: Velocity temperature profiles of 15% w/w glyceride/oil mixtures. Experimental measurements: 15% w/w POS (X) and PSP (□) in paraffin oil mixtures. The full curve represents liquid paraffin oil, the broken curve represents 15% tristearin in paraffin oil.

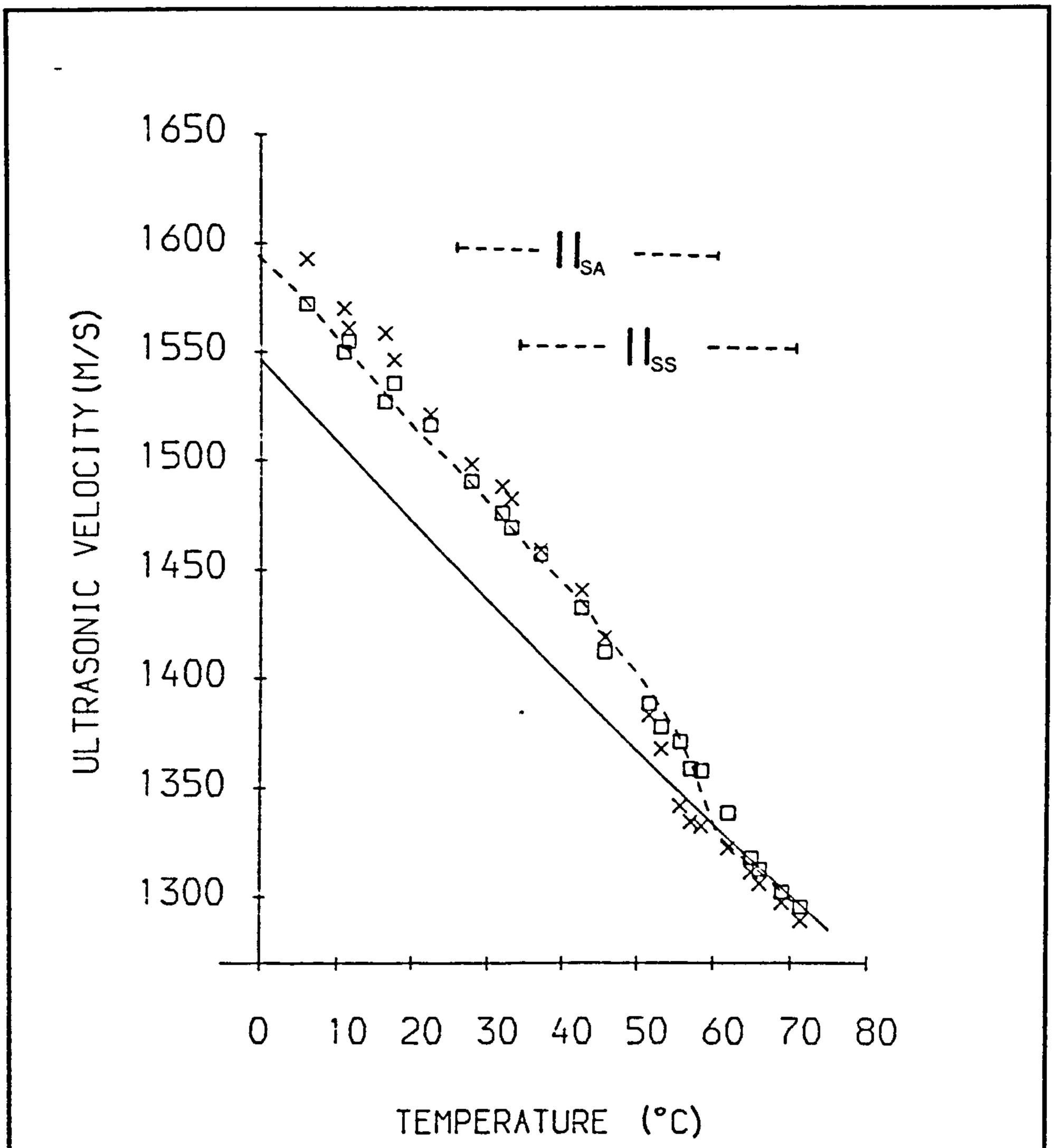

Figure 4.9: Velocity-temperature profiles of 15% w/w glyceride/oil mixtures. Experimental measurements: 15% w/w distearin (□) and stearic acid (X) in paraffin oil mixtures. The full curve represents liquid paraffin oil, the broken curve represents 15% tristearin in paraffin oil.

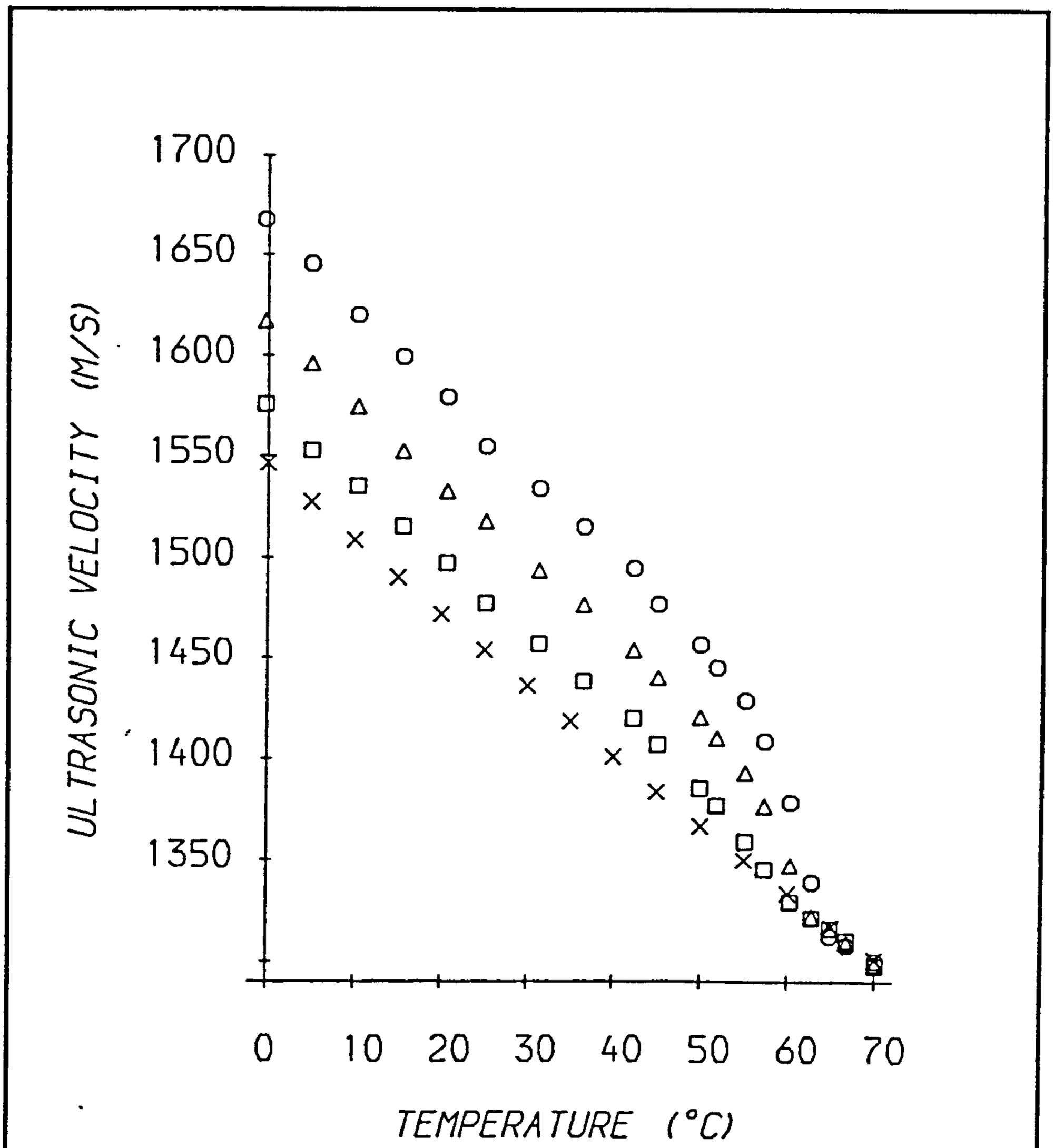

Figure 4.10: Dependence of velocity-temperature profile on triglyceride content. Variation of ultrasonic velocity with increasing temperature for paraffin oil (X) and 10% (□), 20% (△) and 30% (O) w/w tristearin in paraffin oil mixtures.

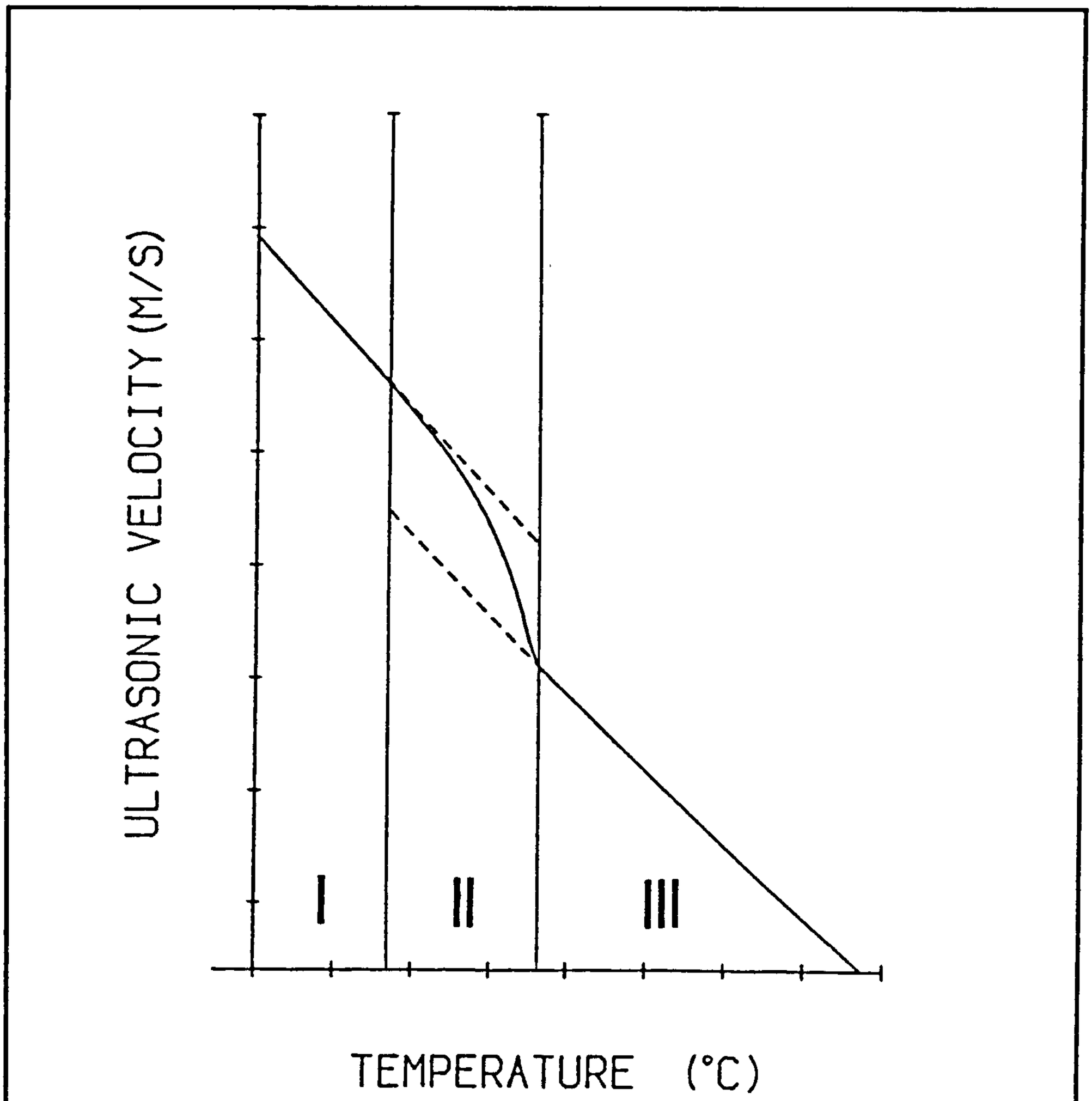

Figure 4.11: Typical velocity-temperature profile for a fat/oil mixture. In region I the glyceride is completely solid, in region II it is part solid, part liquid, in region III it is completely liquid.

The velocity-temperature profiles of all the mixtures follow a similar trend represented diagramatically by figure 4.11. At the lower temperatures, the glyceride component is completely solid and there is a fairly constant decrease in velocity with increasing temperature (region I). As the temperature rises, the glycerides become increasingly soluble in the oil phase and the velocity decreases more rapidly (region II). Once the glyceride reaches a temperature where it is completely liquid the decrease in velocity with temperature is again fairly constant (region III). The exceptions to this trend are the POP and POS in paraffin oil mixtures. This is because these triglycerides are still partially soluble at the lower temperatures (figures 4.7 and 4.8). In the following sections the factors which influence the ultrasonic velocity in each of the three regions is discussed.

4.2.3.1 Measurements in solid glyceride/oil mixtures (region I)

Temperature dependence The variation of ultrasonic velocity with temperature in region I can be described using Taylor series expansions (Miles et al 1985). However, a better fit to the measurements was obtained using an exponential function of the form:

$$v = ae^{bT} \tag{4.2}$$

Here v is the velocity, T is the temperature and a and b are constants which are determined by finding the best least squares fit of equation 4.2 to experimental measurements of velocity with temperature. The values of a and b, calculated from the measurements shown in figures 4.5-4.9 are listed in table 4.4 for those mixtures where there was sufficient data ($n > 3$). The variation of ultrasonic velocity with temperature ($\frac{\partial v}{\partial T}$) for the mixtures was calculated assuming a linear relationship between the velocity and the temperature, which was roughly approximated over the temperature ranges examined ($r > 0.993$).

An examination of region I in figures 4.5-4.8 and table 4.4 indicates that the type of solid triglyceride present does not greatly influence the velocity through a sample; all the triglyceride mixtures examined have similar variations of velocity with temperature ($\approx$ -3.8m s^{-1}°C^{-1}). The variation of the ultrasonic velocity with SFC for a number of triglyceride

Table 4.4: Velocity-temperature dependence of glyceride/paraffin oil mixtures

Coefficients were calculated from velocity measurements in regions I and III of figures 4.5-4.9 using equation 4.2.

Region I

	n Data points	a (m/s)	b (°C)	dv/dT $(ms^{-1}\,°C)^{-1}$
SSS	8	1594.6	-0.00249	-3.8
PPP	7	1595.2	-0.00246	-3.8
LLL	4	1593.8	-0.00250	-3.9
PSP	6	1594.2	-0.00243	-3.7
SS	11	1599.1	-0.00252	-3.8
SA	11	1614.5	-0.00260	-4.0
s.e.m.		0.5	0.00007	0.1

Region III

	n	a (m/s)	b (°C)	dv/dT $(ms^{-1}\,°C)^{-1}$
P.O.	15	1546.5	-0.00247	-3.5
SSS	5	1548.2	-0.00251	-3.3
PPP	4	1545.4	-0.00249	-3.3
LLL	8	1534.3	-0.00244	-3.3
POP	6	1537.9	-0.00242	-3.3
SOS	6	1529.0	-0.00241	-3.2
POS	6	1540.6	-0.00247	-3.2
SS	5	1553.6	-0.00254	-3.3
SA	10	1540.7	-0.00249	-3.3
s.e.m.		0.5	0.00007	0.1

in oil mixtures has also been found to be similar (McClements and Povey 1987b,c). This is important if the technique is going to be used to determine SFCs in fatty materials, which are complex mixtures of glycerides, since it is usually assumed that, "each component, in relation to its amount, yields a linear contribution to the solid content" (Haighton 1976). However, figure 4.9 and table 4.4 show that the velocities of the distearin and the stearic acid in paraffin oil mixtures are significantly larger than those of the triglyceride mixtures.

Triglycerides, however, are the major constituents of most edible fats and oils and so it seems reasonable to assume that the variation of ultrasonic velocity with SFC is independent of the type of solid fat present.

Variation of ultrasonic velocity with SFC To examine the relationship between the ultrasonic velocity and the solid fat content (SFC), additional measurements of ultrasonic velocity were made at 25°C in a series of tristearin in paraffin oil mixtures of varying triglyceride content (0-30%). At this temperature the tristearin is practically insoluble in paraffin oil (Lutton 1955) and so the amount of triglyceride added is equivalent to the SFC. The experimental measurements are presented in figure 4.12.

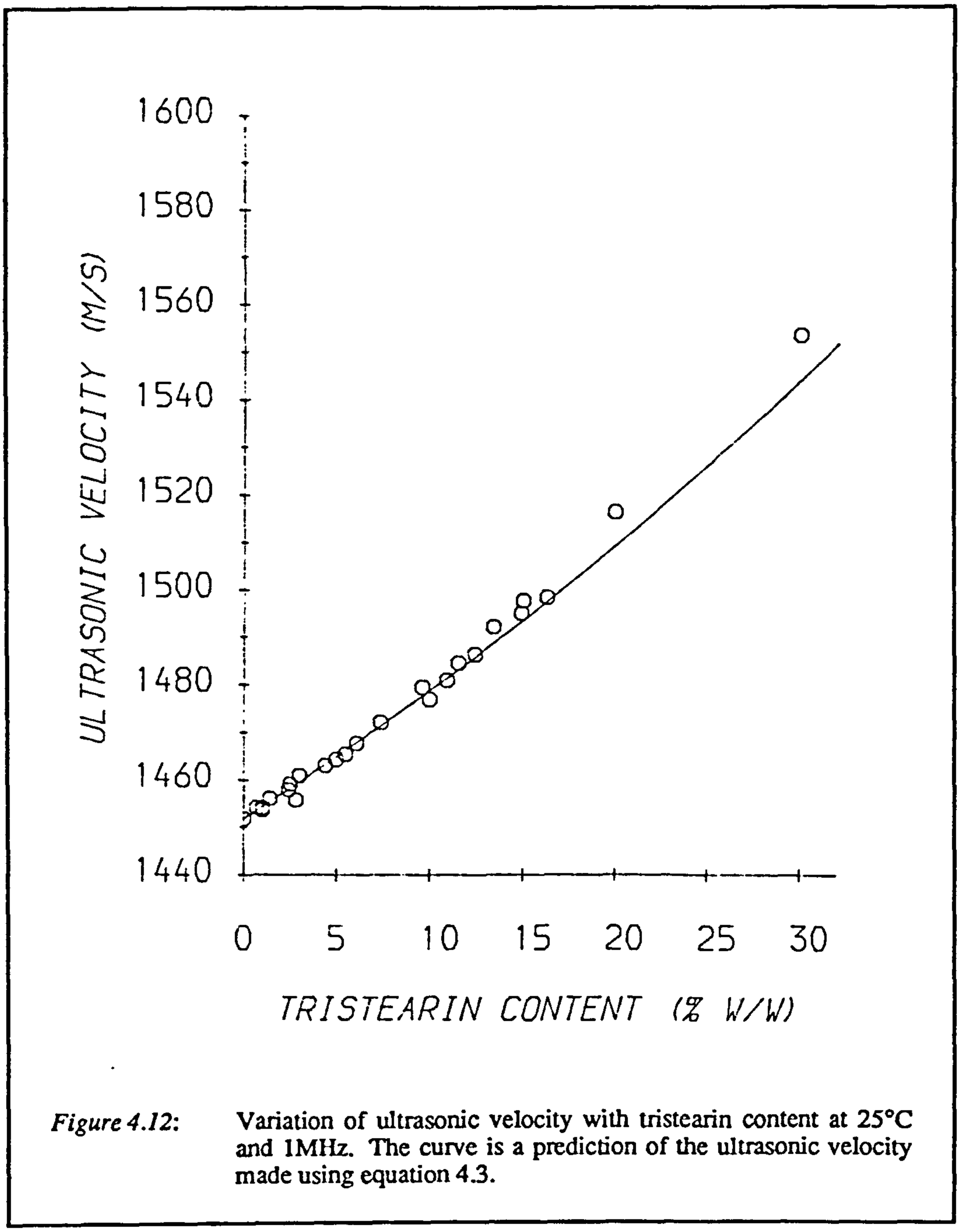

Figure 4.12: Variation of ultrasonic velocity with tristearin content at 25°C and 1MHz. The curve is a prediction of the ultrasonic velocity made using equation 4.3.

The velocity increases by about 2.9 m/s per percent of tristearin added. Since the ultrasonic velocity can be measured to within 1.0 m/s it should be possible to determine the SFC of a fat/oil mixture to within 0.3% by measuring the velocity through it. To do this it is necessary to relate the ultrasonic velocity to the SFC. This can either be done by measuring the velocity through many samples of varying SFC and establishing an empirical relationship between the velocity and the SFC or by using the theoretical formula discussed in chapter 2. The former approach will be called the 'empirical approach' whilst the latter will be called the 'theoretical approach'.

Theoretical approach Although an empirical approach is useful for many applications, a theoretical approach should be used where possible since the factors which effect measurements can be identified more easily and it is possible to extract more information from a system. The variation of ultrasonic velocity with SFC may be described using the theortical formulations discussed in chapter 2. For tristearin in paraffin oil mixtures, visco-inertial and thermal scattering are not significant at the frequencies and particle sizes used in this work (section 2.4.6.3) and so the Wood equation (equation 2.5) which assumes no scattering should be applicable:

$$\frac{1}{v_{mix}^2} = (\rho'\phi+\rho(1-\phi))(\kappa'\phi+\kappa(1-\phi)) \tag{4.3}$$

Where v_{mix} is the velocity of the mixture, ρ is the density, κ is the adiabatic compressibility and ϕ is the volume fraction of disperse phase. In order to determine the range of applicability of this equation to the triglyceride/oil mixtures used in this work, predicted values of the ultrasonic velocity were compared with experimentally measured values (figure 4.12). The ultrasonic velocities of the solid tristearin and the paraffin oil used in equation 4.3 were 2049.9 and 1451.7 m/s respectively. The densities of the solid tristearin (Lutton 1955) and the paraffin oil were 1022.2 and 880.7 kg/m^3 respectively. There is good agreement between the measured and predicted values of ultrasonic velocity upto SFCs of about 15%. At larger values the measured velocities lie increasingly above the predicted values. Possible reasons for this phenomenon are discussed below.

An increase in ultrasonic velocity above that predicted by the Wood equation at high solid contents is often encountered in geological materials such as sands and clays, where it has been attributed to particle interaction (Anderson and Hampton 1980). As the concentration of particles in a suspension increases, the particles get closer together until eventually they touch. An elastic framework is then introduced into the system which modifies the elastic properties of the aggregate; the shear modulus increases above zero (the value for a true suspension) and the adiabatic compressibility of the system decreases below its volume average value. Thus the ultrasonic velocity increases above that predicted by the Wood equation, which is consistent with the results shown in figure 4.12. If this is the reason for the observed deviations it may not be possible to use the Wood equation to interpret results in concentrated systems (e.g. SFC > 15%) and so it may be necessary to determine the relationship between SFC and velocity empirically. On the other hand it may be possible to use ultrasonics to measure the degree of interaction between fat crystals in fat/oil mixtures.

Alternatively, the deviations observed in figure 4.12 may be due to difficulties in preparing solid tristearin. The tristearin expanded on solidification, when it would be expected to contract ($\rho_{solid} > \rho_{liquid}$), and so the solid tristearin must contain some vacuoles. The presence of vacuoles may cause the measured velocity of the solid tristearin to be lower than the actual value depending on their size and this would account for the deviations in figure 4.12. It may be possible to account for the presence of vacuoles in the tristearin by using the formulations of Gaunaurd and Uberall (section 2.5.5), however, the size and concentration of the vacuoles must be known. Cebula, Povey and McClements (1987) have recently examined the possiblility of using neutron scattering for characterising vacuoles in solid triglycerides but this work is in its preliminary stages at present. Indeed it may also be possible to use ultrasonic measurements for the same purpose, however, this is out of the scope of the present work but may provide a useful area for future work.

The agreement between the measured and predicted values of ultrasonic velocity up to SFCs of about 15% means the theoretical approach may still be used for fairly dilute systems. To determine the SFC of a fat/oil mixture using the theoretical approach equation 4.3 must be re-written in terms of ϕ. For fat/oil mixtures this leads to a quadratic equation which has one solution in the range $0 \leq \phi \leq 1$:

$$\phi = \frac{-B-\sqrt{(B^2-4AC)}}{2A} \tag{4.4}$$

where,

$$A = v^2\left(1-\frac{\rho}{\rho'}\right) + v'^2\left(1-\frac{\rho'}{\rho}\right)$$

$$B = v'^2\left(\frac{\rho'}{\rho}-2\right)+v^2\frac{\rho}{\rho'}$$

$$C = v'^2\left(1-\frac{v^2}{v_{mix}^2}\right)$$

The SFC is then calculated by converting the volume fraction ϕ into a mass percentage:

$$SFC = 100\left[\frac{\phi\rho'}{\phi\rho'+(1-\phi)\rho}\right] \tag{4.5}$$

Thus, if the densities and velocities of the component phases are known the SFC of a fat/oil mixture can be determined by measuring the velocity through it. The SFCs of the 0-15% tristearin in paraffin oil mixtures shown in figure 4.12 were calculated using this method, and are compared with the actual amount of tristearin added in figure 4.13. There is a very significant correlation between the SFCs measured using ultrasonics and the amount of triglyceride added initially ($r = 0.997$, $n = 22$). The theoretical approach should therefore prove a useful means of determining SFC in these systems.

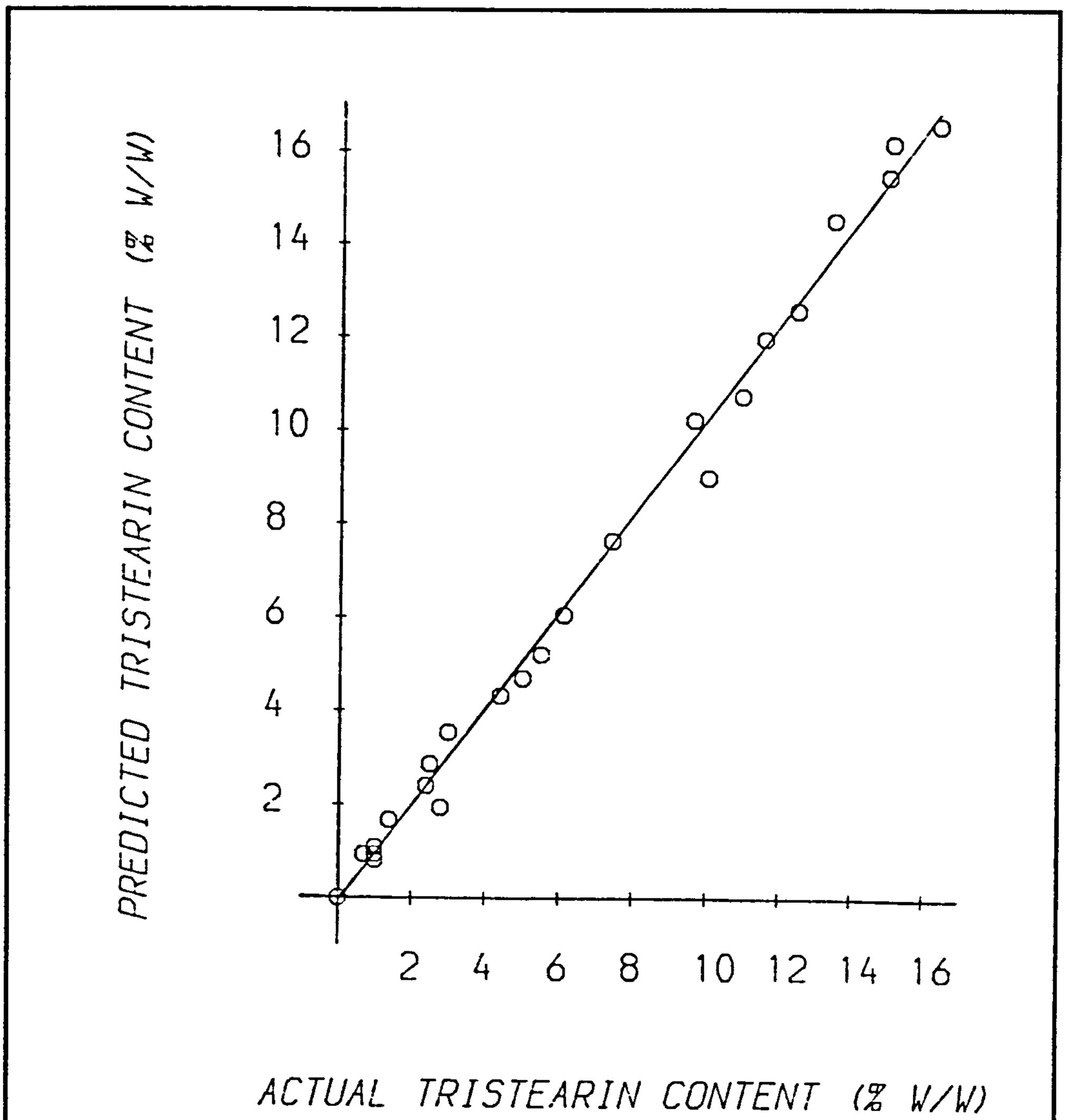

Figure 4.13: SFC of tristearin in paraffin oil mixtures determined by ultrasonic technique. The line through the experimental results is the best least squares fit calculated using linear regression analysis.

Empirical approach As already mentioned in this section it may be necessary to use an empirical approach to relate the ultrasonic velocity to the SFC for some systems. Tables V.1-V.3 in Appendix V contain measurements of the ultrasonic velocity with varying triglyceride content and temperature for a series of tristearin, tripalmitin and trilaurin in paraffin oil mixtures. At the lower temperatures (region I) the triglycerides are completely solid and so the triglyceride content is equivalant to the SFC. Thus the measurements in region I can be used to obtain emprical relationships between ultrasonic velocity, SFC and temperature. Figure 4.12 shows that the relationship between velocity and SFC is not linear and so an empirical relation which reflects this is required. Miles et al (1985) have shown that the following equation can be used to relate ultrasonic velocity measurements to SFCs:

$$\frac{1}{v_{mix}^2} = \frac{\left(1-\frac{SFC}{100}\right)}{v_{oil}^2} + \frac{\left(\frac{SFC}{100}\right)}{v_{fat}^2} \qquad (4.6)$$

Here v_{mix} is the velocity of a fat/oil mixture, v_{oil} is the velocity of the oil phase and v_{fat} is an adjustable parameter which is related to the velocity of the fat phase and is determined empirically from experimental measurements. The values of v_{mix}, v_{oil} and v_{fat} decrease with increasing temperature, and so a different value of v_{fat} is needed at each temperature. By calculating the best least squares fit of the above equation to the experimental measurements of velocity included in Appendix V, tables V.1-V.3, the value of v_{fat} was determined as a function of temperature. The temperature dependence of the v_{fat} parameter was then described using equation 4.2 as $v_{fat} = 1999.1e^{-0.00274 8T}$, n = 70, r = 0.7. Thus it should be possible to measure the SFC of a fat/oil mixture at any temperature by measuring its velocity and the velocity of the oil phase. It should be noted however, that this equation is only strictly applicable to fat/oil mixtures with SFCs from 0-30% over the temperature range 0-30°C.

4.2.3.2 Ultrasonic propagation in liquid oils (Region III)

In this section the factors which affect the ultrasonic velocity in liquid oils is examined. As well as considering the measurements for the triglyceride/oil mixtures shown in figures 4.5-4.9, additional measurements were made at 1.25MHz for nine commercially available vegetable oils. These are presented in tables V.4 and V.5, Appendix V.

Temperature dependence The variation of ultrasonic velocity with temperature in region III of figures 4.5-4.9 can be described in exactly the same way as in region I, by using equation 4.2. Table 4.4 lists the values of the constants a and b for the various glyceride/paraffin oil mixtures, calculated using least squares regression analysis of the experimental measurements shown in figures 4.5-4.9. The variation of ultrasonic velocity with temperature for sunflower oil is presented graphically in figure 4.14, whilst the results for all the oils are summarised in the form of exponential equations in table 4.5. The values of a and b were calculated using least squares regression analysis of the velocity measurements shown in tables V.4 and V.5, Appendix V.

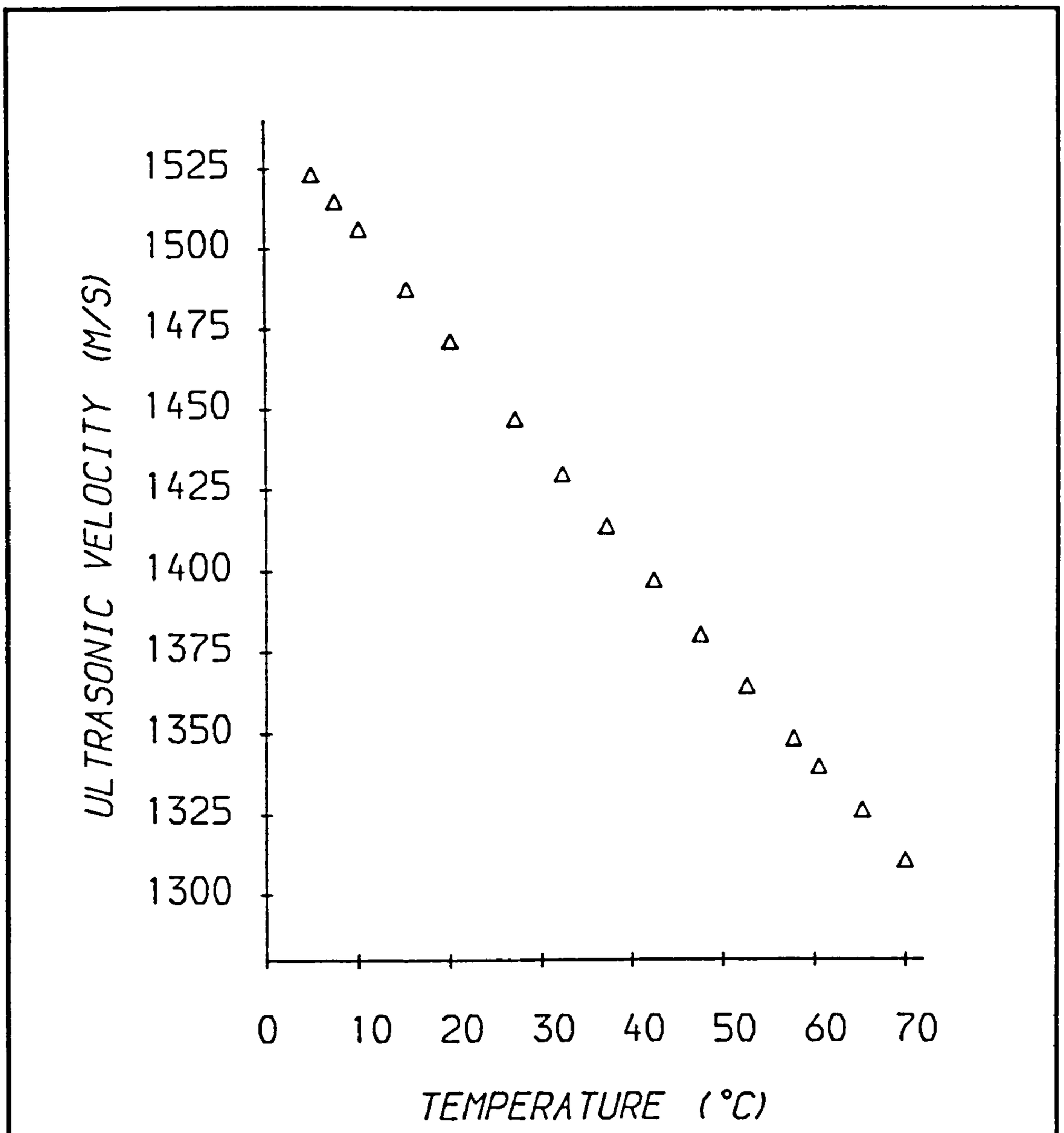

Figure 4.14: Measured velocity-temperature profile of sunflower oil at 1.25MHz

Table 4.5: Ultrasonic velocities of nine vegetable oils

Results are presented in the form of exponential equations: $v = a\ e^{bT}$. The correlations were always better than -0.9995. (n = number of data points).

Oil	T (°C)	n	a (m/s)	b ($ms^{-1}\,°C^{-1}$)	dv/dT ($ms^{-1}\,°C^{-1}$)
Corn	20-70	36	1539.3	-0.00232	-3.2
Grapeseed	20-70	36	1540.9	-0.00233	-3.2
Groundnut	20-70	36	1535.8	-0.00233	-3.2
Olive	20-70	36	1536.1	-0.00237	-3.3
Palm	50-70	10	1529.2	-0.00234	-3.1
Rapeseed	20-70	36	1539.8	-0.00234	-3.2
Safflower	20-70	36	1541.3	-0.00232	-3.2
Soybean	5-70	30	1539.6	-0.00232	-3.3
Sunflower	5-70	30	1541.5	-0.00232	-3.3

The temperature coefficients of velocity of the various glyceride/paraffin oil mixtures are similar ($\approx -3.3 ms^{-1}°C^{-1}$), however, they have significantly different absolute values (table 4.4). Similarly, the various vegetable oils have similar temperature coefficients ($\approx$ -3.1 to 3.3 $ms^{-1}°C^{-1}$) but different absolute velocities (table 4.5) This is because the glyceride components of the oils have different ultrasonic velocities (Gouw and Vlugter 1967) and the velocity of an oil depends on the type and amount of glycerides present (Javanaud and Rahalkar 1988). In the following sections the dependence of the ultrasonic velocity on the type and amount of triglycerides in liquid oils is examined.

Type of triglyceride A number of workers have attempted to empirically relate the ultrasonic velocity of triglycerides to their chemical formula. The two most frequently used approaches are those of Gouw and Vlugter (1967) and Javanaud and Rahalkar (1988). In this work the approach of Javanaud and Rahalkar (1988) was used rather than that of Gouw and Vlugter (1967) since the former gave a better fit to the results and because the constants used have more physical significance, relating velocity differences directly to differences in chemical structure.

Javanaud and Rahalkar (1988) have suggested that a simple empirical formula may be used to relate the ultrasonic velocity v of many triglycerides to their molecular formula:

$$v = V_0 + nV_1 + mV_2 \qquad (4.7)$$

Here V_0, V_1 and V_2 are constants, where V_1 corresponds to the increase in velocity per additional carbon atom in the triglyceride, V_2 corresponds to the increase in velocity per additional unsaturated bond, n is the total number of carbon atoms in the triglyceride molecule and m is the total number of unsaturated bonds. This equation assumes that the ultrasonic velocities of triglyceride isomers are similar (e.g. POP is equivalent to OPP). Although isomers do generally have different ultrasonic velocities the difference is usually small (see table 4.6 and Gouw and Vlugter 1967).

Table 4.6: Ultrasonic velocities and densities of a number of liquid triglycerides

All values are at 70°C and 1.25 MHz. Here n is the number of carbon atoms in the triglyceride molecule and m is the number of double bonds. Densities were either taken from Formo (1979) or calculated from these values using the additive property, molar volume ($V_m = \frac{MW}{\rho}$) suggested by Gouw and Vlugter (1966) (e.g. $V_{mPOS} = \frac{1}{3}(V_{mPPP}+V_{mOOO}+V_{mSSS})$)

Oil	n	m	(kg/m^3)	v(m/s)
LLL	36	0	887.1a	1262.7
PPP	48	0	873.3a	1290.2
PSP	50	0	872.3b	1292.3
SSS	54	0	870.2a	1301.0
POP	50	1	877.6b	1293.4
OPP	50	1	877.6b	1294.8
POS	52	1	876.5b	1297.3
SOS	54	1	875.3b	1301.5
OOO	54	3	885.7a	1303.5

To determine whether this relationship was applicable to the systems used in this work, the ultrasonic velocity of nine liquid triglycerides was measured at 70°C (table 4.6) and the values of the three constants calculated using multiple linear regression. These were found to

be; $V_0 = 1187.1 \pm 3$ m/s; $V_1 = 2.12 \pm 0.07$ m/s and $V_2 = 0.7 \pm 0.4$ m/s.

In this work only triglycerides containing mono-unsaturated fatty acids were examined. Gouw and Vlugter (1967) have measured the velocity in triolein and trilinolein at 20 and 40°C and have found that the difference in velocity between them is about 10.4m/s at both temperatures, corresponding to an increase in velocity per unsaturated bond of about 3.5m/s. This value is significantly larger than the value of V_2 calculated from the measurements in this work (0.7m/s) and therefore it was assumed that the addition of an unsaturated bond to an unsaturated fatty acid chain leads to a greater increase in velocity than the addition of an unsaturated bond to a saturated fatty acid chain. Equation 4.7 must therefore be modified:

$$v = V_0 + nV_1 + mV_2 + oV_3 \tag{4.8}$$

now V_2 is the increase in velocity due to the addition of an unsaturated bond to a saturated fatty acid chain, V_3 is the increase in velocity due to the addition of an unsaturated bond to an unsaturated fatty acid chain, m is the number of unsaturated fatty acids per triglyceride molecule and o is the total number of unsaturated bonds on the triglyceride, excluding the first on each unsaturated fatty acid chain. The value of V_3 at 70°C was calculated from the measurements of Gouw and Vlugter (1967) at 20 and 40°C assuming that the temperature coefficient of velocity of triolein and trilinolein are similar, and was found to be about 3.5m/s.

Using these values of V_0, V_1, V_2 and V_3 and equation 4.8 it is possible to predict the ultrasonic velocity of a triglyceride at 70°C from a knowledge of its molecular formula. This may be useful if the velocity of a particular glyceride is not known or is difficult to measure.

Amount of glyceride The ultrasonic velocity of a liquid oil depends on the velocities and relative proportions of its constituent components. Javanaud and Rahalkar (1988) have suggested that the Wood equation (equation 2.5) can be used to relate the ultrasonic velocity of many vegetable oils to the velocities of their constituent triglycerides. In this section the suitability of this equation for predicting the velocity of ultrasound of oil mixtures is

examined by measuring the velocity through binary triglyceride/oil mixtures of varying triglyceride content (0-100%) at 70°C. Tristearin, tripalmitin and trilaurin in paraffin oil and in sunflower oil were used as examples (figures 4.15 and 4.16).

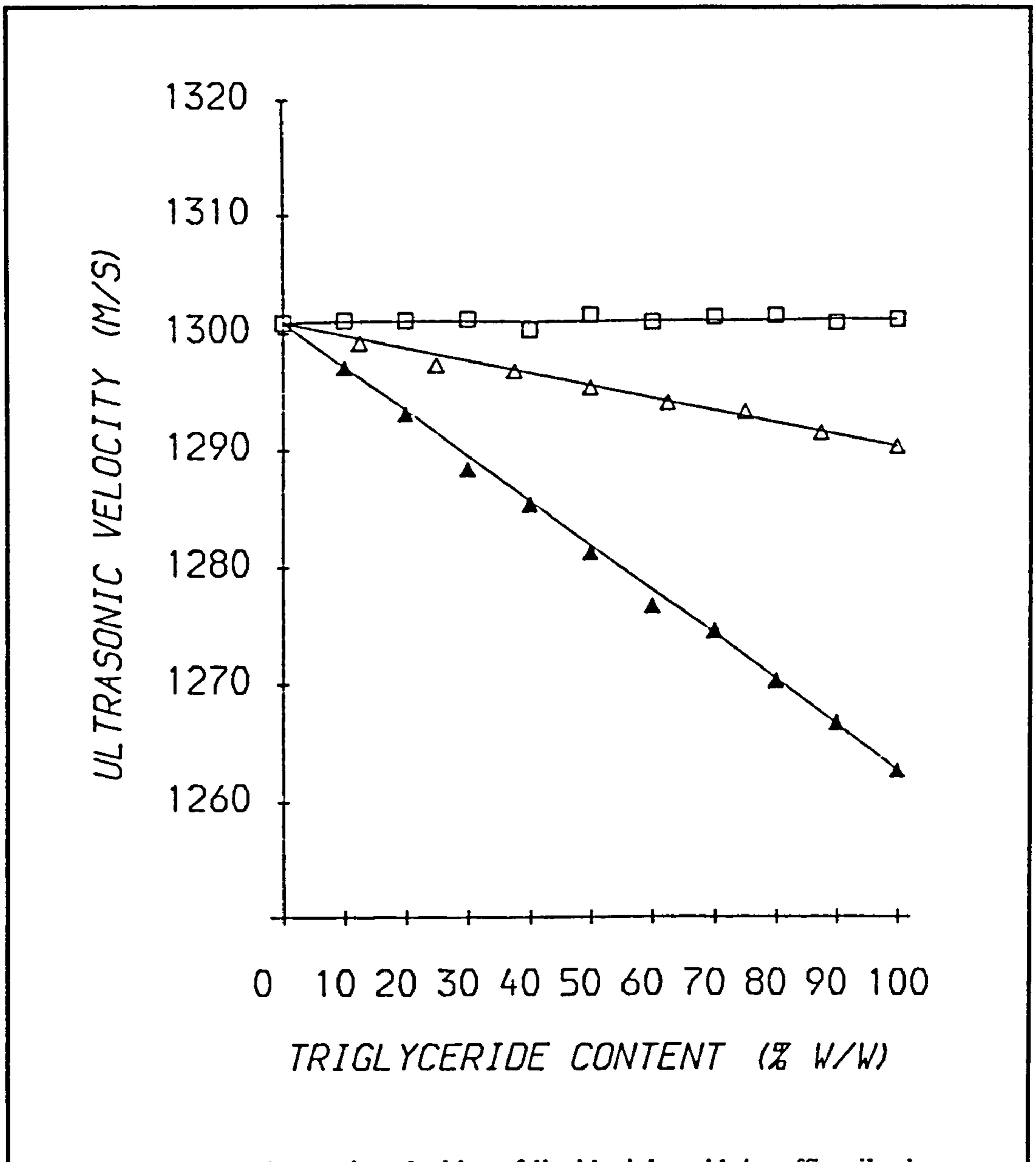

Figure 4.15: Ultrasonic velocities of liquid triglyceride/paraffin oil mixtures at 70°C and 1.25MHz. Annotation: tristearin (□), tripalmitin (△) and trilaurin (▲) in paraffin oil mixtures.

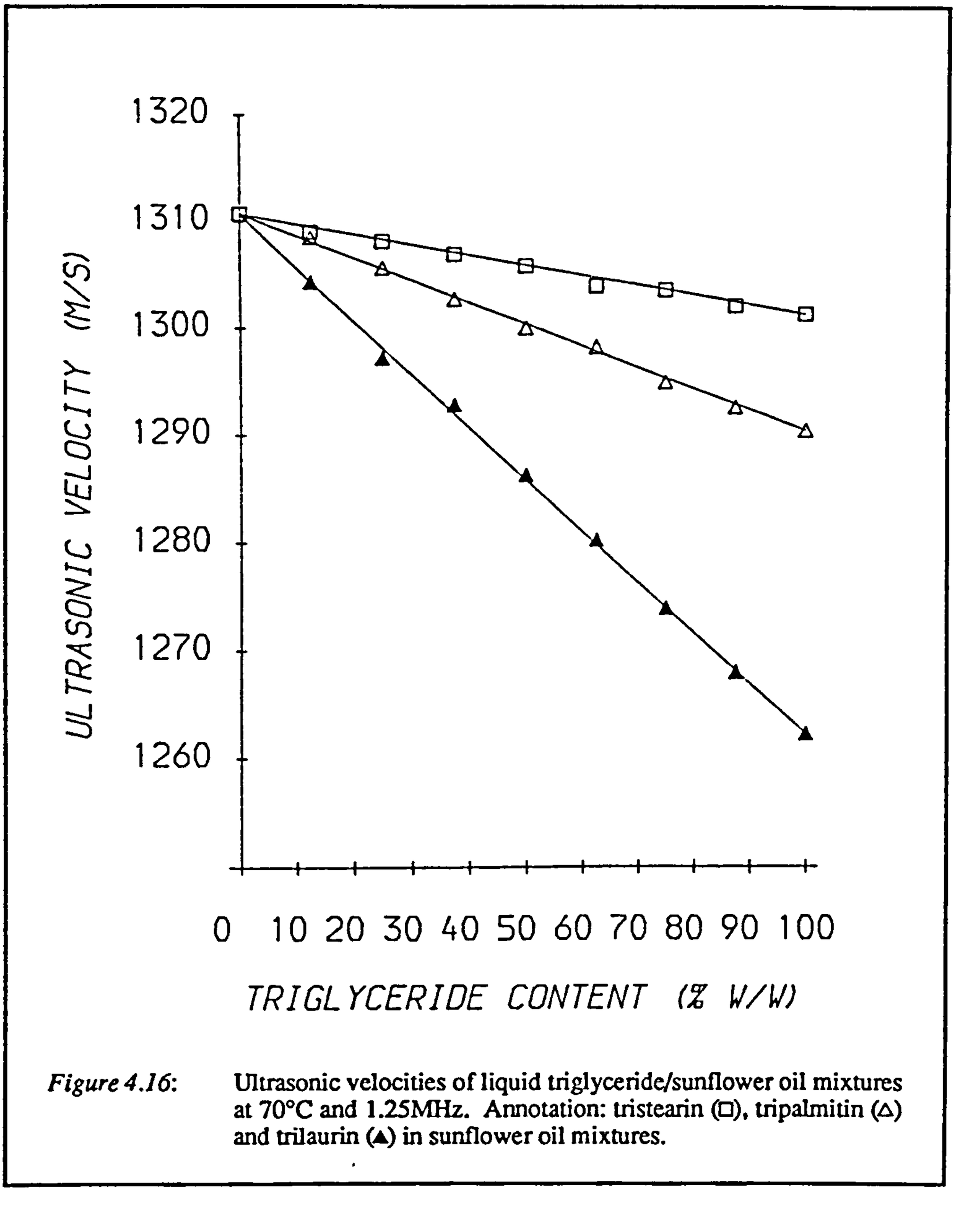

Figure 4.16: Ultrasonic velocities of liquid triglyceride/sunflower oil mixtures at 70°C and 1.25MHz. Annotation: tristearin (□), tripalmitin (△) and trilaurin (▲) in sunflower oil mixtures.

The Wood equation can be written in its most general form as follows:

$$\frac{1}{v_{mix}^2} = \left(\sum_{i=1}^{n} \frac{\phi_i}{v_i^2 \rho_i}\right)\left(\sum_{i=1}^{n} \phi_i \rho_i\right) \tag{4.9}$$

Here n is the number of components and i represents the i^{th} component. This equation assumes that $\sum_{i=1} \phi_i = 1$, i.e. the components form an ideal mixture. For many oils the density of the component phases is similar and so the velocity can be described by a simpler relationship which depends on ultrasonic velocity measurements only (Miles et al 1985);

$$\frac{1}{v_{mix}^2} = \sum_{i=1}^{n} \frac{\phi_i}{v_i^2} \tag{4.10}$$

The difference between the velocities of the oil mixtures calculated using this equation and those calculated using equation 4.9 were always less than 0.2 m/s even when the mass fraction of the components was used in the equations instead of the volume fraction. This equation may therefore prove a more practical means of relating the velocity of an oil to the velocities of its constituent components since it relies on ultrasonic measurements only.

The agreement between the experimentally measured velocities of the triglyceride/oil mixtures investigated and those predicted by equation 4.10 using the velocities of the component phases is excellent (figures 4.15 and 4.16). The Wood equation should therefore be a useful means of estimating the composition of binary oil mixtures once the velocities of the component phases are known, or for calculating the velocity of vegetable oils from their triglyceride composition once the velocities of the various triglycerides are known.

Relationship between velocity and oil composition To ascertain whether equations 4.8 and 4.10 can be used to relate the ultrasonic velocity of vegetable oils to their composition, predicted values of the ultrasonic velocity were compared with experimentally measured values (table 4.7). The predicted values were calculated from typical triglyceride compositions found in the literature (table 4.8), using equation 4.8 to calculate the velocity of the various triglycerides present and equation 4.10 to calculate the velocity of the

triglyceride mixture. Table 4.7 shows that there is good agreement between the predicted and the experimental values of velocity for the various vegetable oils investigated. The slight discrepencies between the predicted and calculated values are probably because the actual composition of the oils was not known and the fatty acid distribution of a given oil may vary significantly (Javanaud and Rahalkar 1988).

Table 4.7: Predicted and experimental velocities of nine vegetable oils

Predicted values were calculated using equations 4.8 and 4.10 and the triglyceride compositions shown in table 4.8. All values are at 70°C and 1.25 MHz.

	Measured velocity (m/s)	Predicted velocity (m/s)
Corn	1308.4	1308.2
Grapeseed	1309.3	1308.7
Groundnut	1304.9	1305.9
Olive	1301.5	1302.4
Palm	1298.3	1297.2
Rapeseed	1307.6	1307.6
Safflower	1310.1	1310.4
Soybean	1308.7	1309.3
Sunflower	1310.7	1310.4

These results suggest that the ultrasonic velocities of many oils can be related to their chemical composition using simple empirical formula[e] and that the composition of binary oil mixtures may be estimated from velocity measurements once the velocities of the component phases are known. Ultrasonics may therefore prove a useful means of charactersing liquid oils or of monitoring processess where there is a change in the degree of unsaturation or chain length of the fatty acids present or of processess which involve the separation of one oil component from another.

Table 4.8: Typical triglyceride compositions of the vegetable oils□

All values extracted from Weiss (1983) apart from that for grapeseed oil which was taken from Sonntag (1979).

Oils	Saturated fatty acids						Unsaturated fatty acids				
	14:0	16:0	18:0	20:0	22:0	24:0	16:1	18:1	18:2	18:3	20:1
Corn	-	11	2	-	-	-	-	27	59	1	-
Grapeseed	-	8	4	-	-	-	-	27	60	1	-
Groundnut	-	11	3	1	2	1	-	51	31	-	-
Olive	-	17	3	-	-	-	2	62	15	1	-
Palm	1	47	4	-	-	-	-	38	10	-	-
Rapeseed	-	4	2	1	-	1	-	59	23	8	2
Safflower	-	7	3	-	-	-	-	13	77	-	-
Soybean	-	11	3	1	-	-	-	22	55	8	-
Sunflower	-	7	3	-	-	-	-	14	76	-	-

□ – w/w%

4.2.3.3 Investigation of phase transitions (Region II)

In region II the decrease in ultrasonic velocity with increasing temperature is greater than in regions I and III (figure 4.11). This is because the amount of solid glyceride present decreases with increasing temperature and so there is an additional decrease in velocity superimposed on that due to the negative temperature coefficients of the velocities of the solid and liquid phases. The temperature range where a glyceride is partially soluble in paraffin oil (region II) depends on the type of glyceride present (figures 4.5-4.9). The solubility of glycerides in oil can be described, to a first approximation, by the following equation, which assumes that the mixture follows ideal solubility behaviour (Hannewijk et al 1964).

$$\ln(x) = \frac{\Delta H_f}{R}\left(\frac{1}{T} - \frac{1}{T_{mp}}\right) \tag{4.11}$$

Here x is the mole fraction of glyceride in the liquid phase, ΔH_f is the enthalpy change per mole of crystallising material, R is the gas constant, T_{mp} is the melting point (in K) and T is the temperature (in K). The mass fraction ϕ_m of glyceride in the solid state can then be calculated at any temperature from the relation:

$$\phi_m = \frac{\phi_g - \frac{xMW_g(1-\phi_g)}{MW_o(1-x)}}{\phi_g} \tag{4.12}$$

where MW_g and MW_o are the molecular weights of the glyceride and oil phases respectively and ϕ_g is the total mass fraction of glyceride present in the mixture. The position of region II for a particular glyceride/oil mixture therefore depends primarily on the melting point and heat of fusion of the glyceride component.

Solubility determinations The effects of glyceride solubility are clearly illustrated in figure 4.17. Here the ultrasonic velocity has been measured in a series of tristearin in paraffin oil mixtures with increasing tristearin content at 1MHz and 57.3°C. At this temperature the tristearin is partially soluble in the paraffin oil (≈ 6% w/w as calculated by equations 4.11 and 4.12) and so there is a minim$^{um}_{\lambda}$ in the ultrasonic velocity versus tristearin content curve. This is because the first few percent of tristearin added are soluble in the paraffin oil and so the velocity decreases because liquid tristearin has a lower velocity than liquid paraffin oil. However, as the tristearin content is increased above the clear point of the mixture (the point where all the added fat is just soluble), crystalline tristearin appears and the velocity starts to increase because solid tristearin has a larger velocity than liquid paraffin oil. By making many measurements of the ultrasonic velocity near to the minim$^{um}_{\lambda}$ it is possible to determine the solubility of a glyceride accurately.

Calculation of the variation of solid glyceride content with temperature for the 15% w/w tristearin in paraffin oil mixtures The dependence of the ultrasonic velocity on the amount of solid glyceride present suggests that the ultrasonic velocity may prove a useful tool for investigating phase transitions (Miles et al 1985, Hussin and Povey 1984). To do this it is necessary to relate the ultrasonic velocity of a mixture to the amount of solid glyceride present over a range of temperatures. Rather than use the empirical approach described in section 4.2.3.1 an approach similar to that suggested by Miles et al (1985) was used. This approach was pref$^{f}_{\lambda}$ered since it is more suitable for fundamental investigations of phase transitions when the velocities of the solid and liquid phases can be measured.

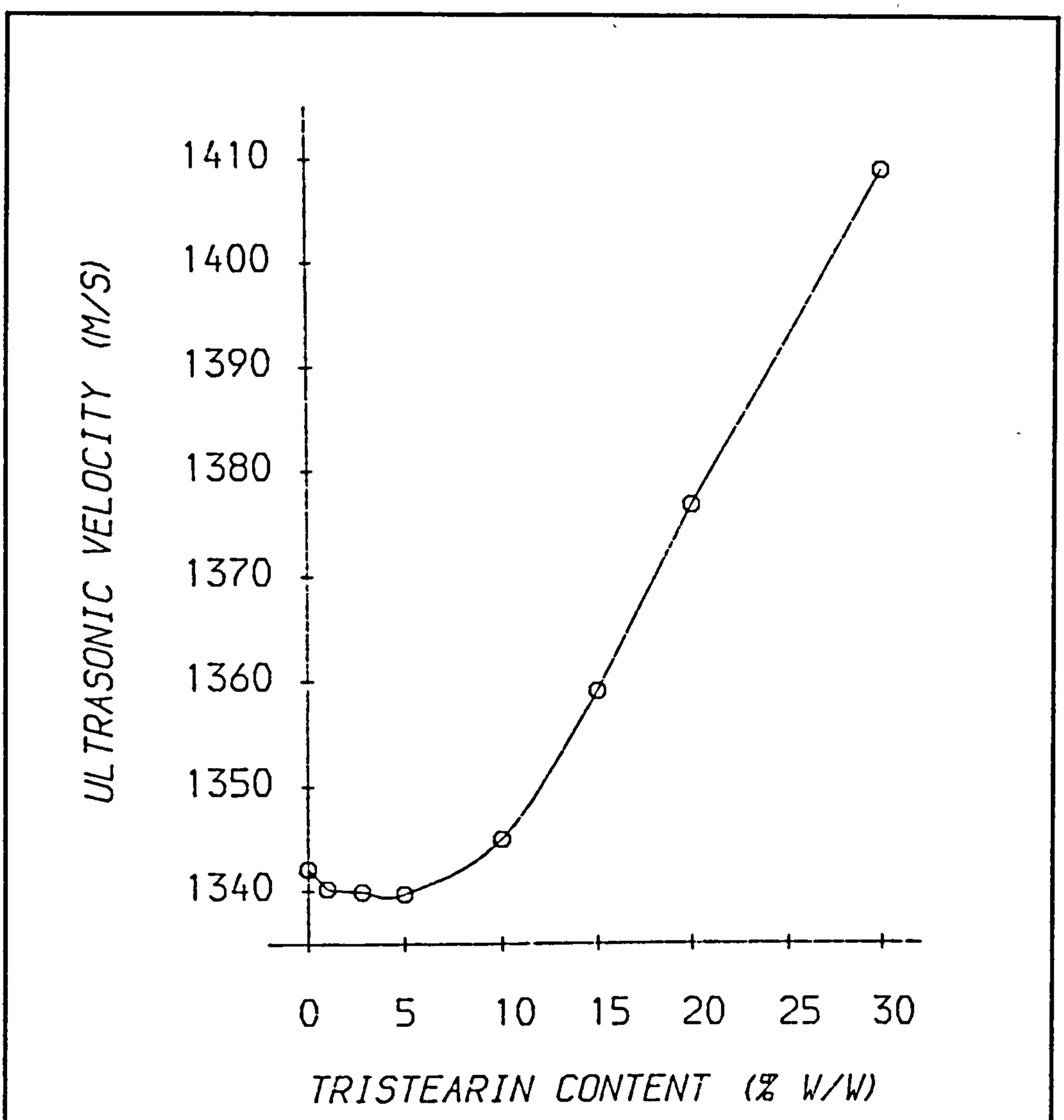

Figure 4.17: Effect of glyceride solubility on velocity at 57.3°C and 1 MHz.

In region I the glyceride component is completely solid, in region III it is completely liquid, and in the intermediate region it is partly solid, partly liquid (region II). To estimate the amount of solid glyceride in region II it is assumed that the mixture consists of a 'solid' and a 'liquid' phase whose velocities and densities are the same as those found by extrapolation from regions I and III respectively. Thus the variation of velocity with temperature of the

'solid' and 'liquid' phases in region II can be described by equation 4.2 (e.g. see figure 4.11). Whilst the variation of density with temperature for the 'solid' and 'liquid' phases can be described using equation 4.1. The velocity of a mixture can then be related to the ratio of solid to total glyceride using the Wood equation:

$$\frac{1}{v_{mix}^2} = (\phi\rho_I+(1-\phi)\rho_{III})\left(\frac{\phi}{\rho_I v_I^2}+\frac{(1-\phi)}{\rho_{III} v_{III}^2}\right) \tag{4.13}$$

Where the subscripts I and III represent the extrapolated values of the relevant parameters from regions I and III respectively and ϕ is the ratio of solid to total glyceride (v/v). This equation assumes that $\sum_{i=1}^{n}\phi_i = 1$, that the fat crystals are much smaller than the ultrasonic wavelength, that no scattering of ultrasound occurs and that there is no interaction between the fat crystals (see chapter 2). If the densities of the 'solid' and 'liquid' phases are similar (i.e. $\rho \approx \rho'$) then a simpler form of equation 4.13 can be used which depends on velocity measurements only (see equation 4.10);

$$\frac{1}{v_{mix}^2} = \frac{\phi}{v_I^2}+\frac{(1-\phi)}{v_{III}^2} \tag{4.14}$$

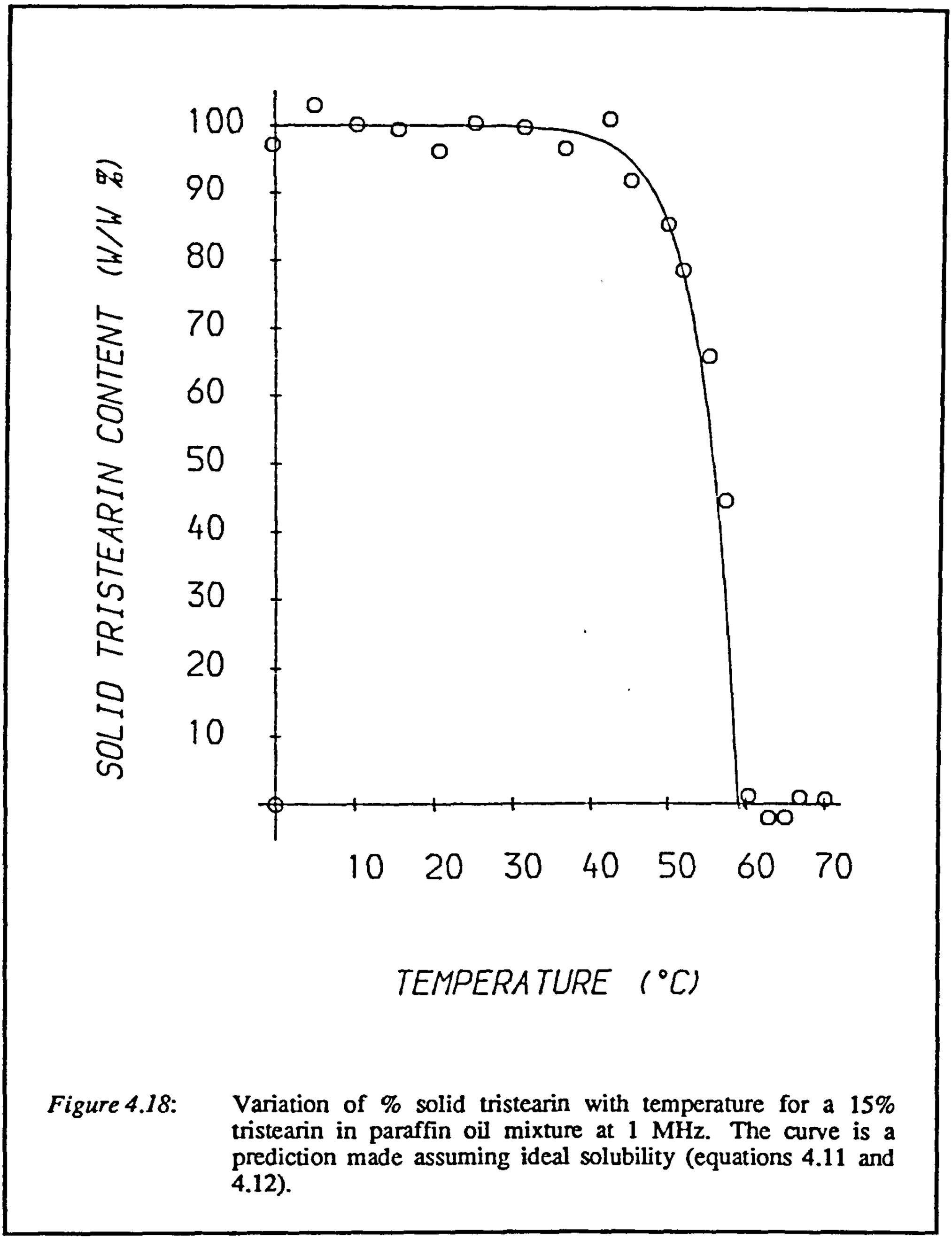

Figure 4.18: Variation of % solid tristearin with temperature for a 15% tristearin in paraffin oil mixture at 1 MHz. The curve is a prediction made assuming ideal solubility (equations 4.11 and 4.12).

Using this technique the variation of % solid glyceride with temperature was calculated for the 15% w/w tristearin in paraffin oil mixture. The variation of velocity with temperature for the 'solid' and 'liquid' phases was calculated using equation 4.2 and the parameters given in table 4.4. The densities were calculated from the volume average values of the experimentally measured paraffin oil densities and values of tristearin density found in the literature (table 4.3). Least squares regression analysis gave the constants ρ_0 = 907.7 kg/m^3, β = 0.000672 °C^{-1} (T_0 = 0.0°C) for region I and ρ_0 = 893.0 kg/m^3, β = 0.000732 °C^{-1} (T_0 = 0.0°C) for region III. The variation of % solid tristearin content with temperature was then calculated from the experimental velocity measurements shown in figure 4.5 using a rearranged form of equation 4.13 (see equations 4.4 and 4.5). The results are plotted in figure 4.18. For comparison the solid tristearin content predicted using the ideal solubility equation (equations 4.11-4.12) are also included in figure 4.18 (using the values T_{mp} = 72.4°C, ΔH_f = 180J/g (Norton et al 1985) and $MW_{paraffin\ oil}$ = 440 gmol^{-1} (Skoda and Van den Tempel 1963)). There is good agreement between the experimentally measured values and the predictions of the ideal solubility equation. However, the values of % solid tristearin content determined by the ultrasonic technique are slightly above the predicted values. This may be due to impurities in the sample (section 4.2.2.1) or due to demixing (Norton et al 1985).

Predictions of the solid tristearin content calculated using equation 4.13 and 4.14 agreed to within 1%, and so equation 4.14 may prove a more practical means of relating the ultrasonic velocity to the SFC since it requires velocity measurements only.

4.3 Comparison of ultrasonic and NMR methods of determining SFC

4.3.1 Introduction

The pulsed NMR technique is the established method of determining SFCs in the fats and oils industry at present (section 4.1.3). If ultrasonics is going to prove a useful adjunct or alternative to pNMR it is necessary to compare the SFCs determined by each technique. In this section SFCs determined using the ultrasonic velocity technique described in section 4.2 are compared with those determined using two frequently used pNMR techniques, the so called 'weight' and 'direct' methods (Van Boekel 1981). Measurements were made at 18°C using 0-20% samples of tristearin in paraffin oil, tristearin in sunflower oil and tripalmitin in paraffin oil.

4.3.2 Materials and Methods

4.3.2.1 Materials

The tristearin, tripalmitin, sunflower oil and paraffin oil used in these experiments were the same as those described in section 4.2.2.1.

4.3.2.2 Sample preparation

A slightly different tempering procedure than that described in section 4.2.2.2 was used to prepare the samples. This tempering procedure was used so as to conform with that usually used in the Unilever laboratories for preparing glyceride/oil mixtures for pNMR measurements (Unilever - private communication). Like the tempering procedure described earlier, it involved heating the samples to a temperature where they were molten and then cooling them rapidly so that they crystallised in the form of a gel matrix. The samples produced had the same polymorphic form (β) and appeared similar to the samples produced using the earlier tempering procedure (section 4.2.2) when examined under the microscope.

4.3.2.3 Ultrasonic measurements

The ultrasonic velocity was measured at 1 MHz using the pulse echo technique described in section 4.2.2.4. The SFC of the samples was then calculated from these measurements using both the theoretical and empirical approaches described in section 4.2.3.1.

4.3.2.4 The pulsed NMR technique

The physical principles underlying pNMR have been described extensively by previous workers (e.g. Sleeter 1985, Waddington 1986) and so only a brief description of the technique is given here. The method is based on the fact that the NMR signal produced by a solid or a liquid, after a 90° radio frequency (rf) pulse, is proportional to the number of hydrogen atoms present in the sample. In a solid/liquid mixture the signal is the sum of two components; one from the solid, the other from the liquid. Due to the rapid decay of the solid signal compared with the liquid signal, the amount of solid and liquid in the sample can be deduced by measuring the intensity of the signal at different times after the initial pulse (figure 4.19). The signal amplitude at zero time (S_0) is proportional to the total amount of sample, whilst the signal at time t_2 (S_2) is proportional to the amount of liquid. The difference S_0–S_2 should therefore be proportional to the amount of solid. Unfortunately, there is an inherent 'dead-time' in the receiver, before which the signal cannot be measured. The signal can therefore only be measured some time t_1 after the initial pulse. In this time the solid signal has decayed somewhat, and so it is necessary to multiply the amplitude (S_1–S_2) by a previously determined correction factor (the f-factor) in order to estimate (S_0–S_2).

Two pulsed NMR methods were used in this work: the first, the so called 'direct method', uses the ratio of solid to liquid signal and therefore requires the f-factor, whilst the second, the 'weight method', uses only the liquid signal and therefore requires no correction factor. For both methods, a Brucker Minispec PC20 was used with an operating frequency of 20MHz. The sample holder was thermostated at 18°C, and the sample tubes used were 100mm long and had an internal diameter of 6mm.

Weight method For this method, all the sample (approx. 0.2g) is present within the NMR coil and only the signal due to the liquid (time t_2 of figure 4.19, 70μs) is measured. This signal is converted into a mass of oil in the sample, by using a previously prepared calibration curve of NMR signal per mass of pure oil within the coil. The SFC is then determined by weighing the total mass of the sample, and using the following equation:

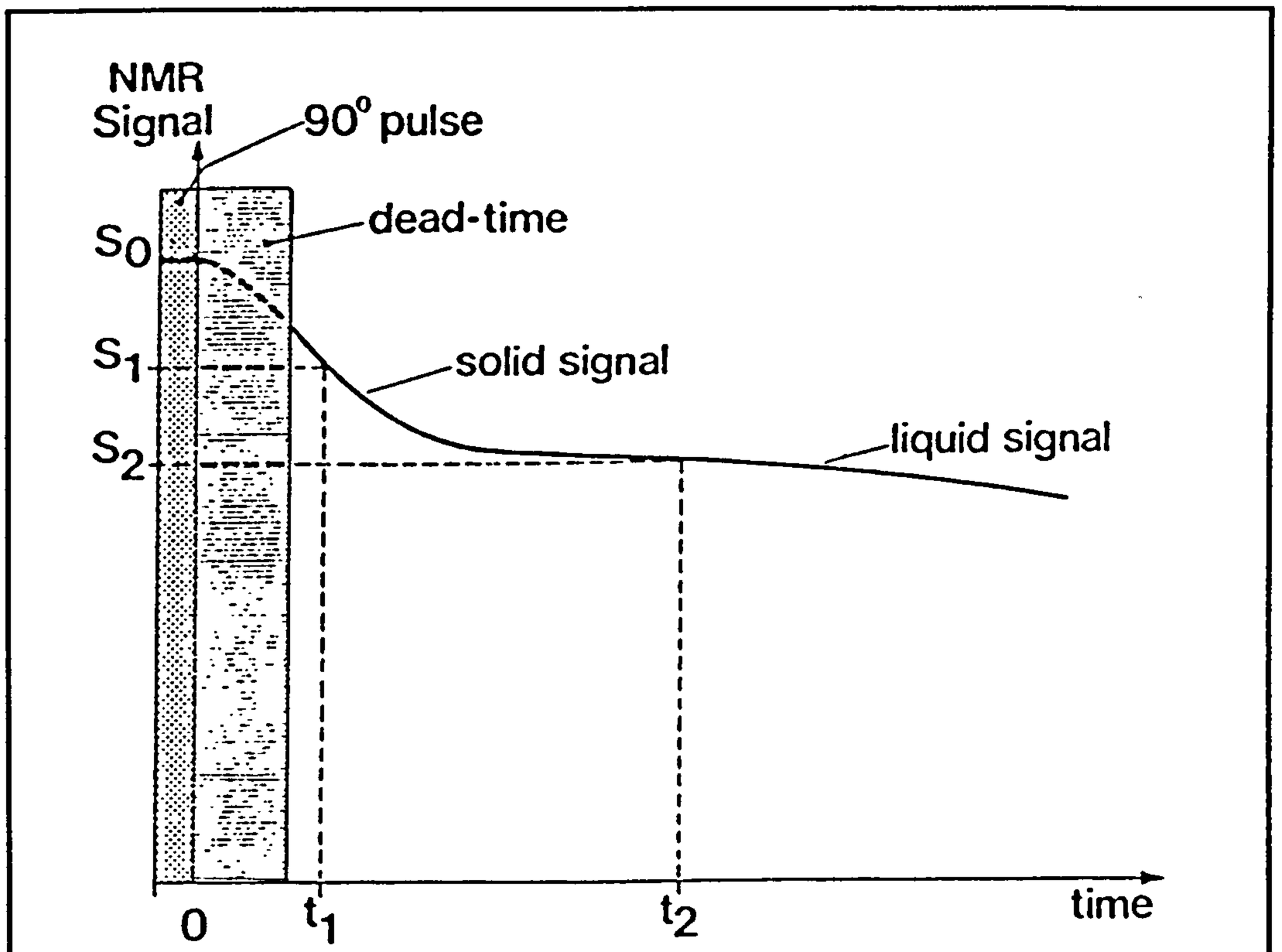

Figure 4.19: Schematic representation of NMR signal decay for a fat/oil mixture after a 90° rf pulse

$$SFC = \frac{100(M_{tot} - M_{liq})}{M_{tot}} \tag{4.15}$$

Here M_{tot} is the total mass of the sample and M_{liq} is the mass of the liquid determined by the NMR. A four decimal place balance was used to measure the masses of the samples.

Direct method In this method, the SFC is determined by measuring the NMR signal at 11 and 70μs after the initial pulse (times t_1 and t_2 of figure 4.19) and using the following equation:

$$SFC = \frac{100(S_1 - S_2)F}{(S_1 - S_2)F + S_2} \tag{4.16}$$

Alternatively, if the actual SFC of a sample is known (SFC_a) its f-factor (F_{sam}), can be calculated. From this value, the SFC which would have been predicted for the system, had the established f-factor for that system (F_{sys}) been used, can be determined:

$$SFC = \frac{SFC_a F_{sys}}{F_{sam} + SFC_a(F_{sys} - F_{sam})} \tag{4.17}$$

4.3.3 Results

The experimental results, and the calculated SFCs for each technique, are shown in tables 4.9-4.11. The precisions of the weight and direct methods were calculated from the standard error of the mean (s.e.m.) of three SFC determinations (nine measurements per determination, 2 sec per measurement), and were found to be 0.3% and 0.7% respectively. The precision of the ultrasonic technique was calculated from the s.e.m. of five SFC determinations and was found to be 0.2%. The total measurement times of the three techniques were similar, being about 1 min/sample. However, the ultrasonic measurements were made manually, and the measurement time could be reduced significantly if the technique were automated: the oscilloscope sampling rate was 50kHz.

Table 4.9: Comparison of SFCs determined by ultrasonic and pNMR techniques

Tristearin in paraffin oil mixtures at 18°C.

	NMR				Ultrasonic		
SSS	weight	direct			v	theory	empir.
(%w/w)	SFC	F	SFC		(m/s)	SFC	SFC
0.53	0.2	0.54	0.2		1477.8	0.1	0.1
1.19	0.7	0.99	2.1		1479.5	0.7	0.6
1.71	1.2	0.94	3.2		1482.1	1.6	1.5
2.33	1.4	1.04	3.9		1484.1	2.3	2.2
2.67	2.4	1.08	4.3		1483.0	2.4	2.5
3.55	3.4	1.32	4.7		1486.9	3.2	3.1
3.71	2.4	1.12	5.8		1487.3	3.7	3.3
5.30	4.7	1.32	7.0		1491.1	5.0	4.5
6.49	5.3	1.36	8.3		1493.4	5.6	5.3
7.73	6.9	1.36	9.9		1500.0	7.8	7.5
7.87	6.2	1.53	9.0		1499.1	7.5	7.2
8.23	8.0	1.64	8.9		1499.3	7.5	7.2
9.17	7.8	1.46	11.0		1502.5	8.7	8.3
10.54	10.0	1.53	12.4		1508.0	10.5	10.1
11.21	10.9	1.54	12.9		1510.0	11.7	10.7
11.98	11.8	1.52	13.6		1511.7	11.8	11.2
12.47	11.8	1.56	14.0		1516.4	13.8	12.6
14.10	13.2	1.53	16.0		1519.4	14.3	13.7
14.38	13.9	1.66	15.3		1520.1	14.6	13.9
15.98	15.6	1.59	17.6		1524.3	16.0	15.2
16.43	16.7	1.58	18.1		1528.4	17.6	16.5
18.40	17.9	1.57	20.4		1537.4	20.0	19.2
sem*	0.3	0.05	0.7		0.7	0.2	0.2
r+	0.997		0.996			0.997	0.997
A	-0.8		1.2			-0.6	-0.6
B	1.02		1.03			1.08	1.03

* standard error of the mean (see section 4.3.3)
\+ Correlation between the amount of triglyceride added and the predicted SFC

Table 4.10: Comparison of SFCs determined by ultrasonic and pNMR techniques

Tristearin in sunflower oil mixtures at 18°C.

	NMR			Ultrasonic		
SSS	weight	direct		v	theory	empir.
(%w/w)	SFC	F	SFC	(m/s)	SFC	SFC
0.43	0.7	0.42	1.6	1478.5	0.2	0.2
1.15	1.0	0.77	2.6	1479.9	0.7	0.7
2.06	2.4	0.85	3.4	1484.6	2.3	2.3
3.60	3.4	0.99	5.2	1489.5	4.0	3.9
4.71	5.8	1.14	6.4	1493.8	5.4	5.4
5.39	5.6	1.14	7.0	1495.9	6.1	6.1
5.64	6.1	1.10	7.2	1496.1	6.2	6.1
7.81	8.8	1.19	10.1	1504.7	8.9	8.9
9.56	10.4	1.19	11.5	1510.5	10.7	10.8
12.26	12.6	1.16	14.7	1517.1	12.8	12.9
14.68	15.8	1.22	15.8	1528.6	16.2	16.5
15.12	16.0	1.27	16.5	1536.0	18.3	18.7
18.55	19.8	1.36	19.8	1544.4	20.7	21.3
sem*	0.3	0.05	0.7	0.7	0.2	0.2
r+	0.998	0.998			0.997	0.997
A	0.1		1.6		-0.2	-0.4
B	1.06		1.00		1.14	1.17

* standard error of the mean (see section 4.3.3)
\+ Correlation between the amount of triglyceride added and the predicted SFC

Table 4.11: Comparison of SFCs determined by ultrasonic and pNMR techniques

Tripalmitin in paraffin oil mixtures at 18°C.

	NMR			Ultrasonic		
PPP	weight	direct		v	theory	empir.
(%w/w)	SFC	F	SFC	(m/s)	SFC	SFC
0.57	0.4	0.75	1.4	1478.7	0.1	0.4
1.20	0.3	1.35	2.0	1481.0	1.0	1.2
1.26	0.2	0.84	2.9	1481.2	1.1	1.2
1.49	0.4	1.05	2.7	1480.0	0.6	0.8
2.40	1.7	1.35	3.4	1484.3	2.2	2.3
2.65	1.5	1.44	3.5	1484.3	2.2	2.3
3.83	3.0	1.35	5.4	1486.8	3.2	3.1
4.32	3.4	1.45	5.5	1488.7	3.9	3.7
4.90	4.1	1.51	6.2	1490.7	4.3	4.4
5.97	5.2	1.57	7.2	1493.7	5.8	5.4
6.08	5.0	1.57	7.4	1496.8	6.5	6.4
7.29	6.4	1.54	9.9	1496.7	6.5	6.9
7.63	7.0	1.53	9.4	1498.4	7.4	8.3
9.00	7.9	1.65	10.4	1502.6	8.9	8.5
9.01	8.1	1.69	10.2	1503.1	9.1	10.1
10.65	9.8	1.66	12.2	1508.2	10.9	10.2
10.69	9.8	1.61	12.6	1508.5	11.0	11.8
12.05	11.0	1.70	13.3	1513.4	12.7	12.6
12.50	11.6	1.65	14.3	1515.9	13.5	12.6
13.71	12.4	1.67	15.5	1515.9	13.5	13.8
14.51	12.6	1.71	16.1	1519.9	14.5	14.1
15.72	14.6	1.65	17.8	1520.8	15.1	15.2
16.67	14.9	1.72	18.3	1524.3	15.9	17.4
17.53	16.0	1.73	19.2	1531.3	18.4	17.6
17.78	16.9	1.76	19.2	1532.2	18.7	17.9
19.51	18.3	1.76	21.0	1540.5	20.7	20.2
sem*	0.3	0.05	0.7	0.7	0.2	0.2
r+	0.999		0.998		0.997	0.996
A	-0.7		1.2		-0.5	-0.4
B	0.97		1.03		1.06	1.04

* standard error of the mean (see section 4.3.3)
\+ Correlation between the amount of triglyceride added and the predicted SFC

4.3.3.1 Weight method

The NMR signal per gram of the paraffin oil and sunflower oil were determined from calibration curves of NMR signal versus mass of oil present. The values for the two oils were found to be 13.41±0.07 and 11.22±0.07 respectively.

4.3.3.2 Direct method

The f-factors, calculated from equation 4.16, were found to increase with increasing SFC up to values of about 15%, where they levelled off (Tables 4.9-4.11 and figure 4.20). They were also found to vary with time: e.g., for a 20% tristearin in paraffin oil mixture, the f-factor increased from 1.58 at 2hr to 1.77 at 24hr and 1.78 after 6 days. For this reason, the actual f-factor (F_{act}) for a system was determined from the 6-day-old mixtures with triglyceride contents greater than 15%. The f-factors were 1.78±0.03 for tristearin in paraffin oil, 1.42±0.03 for tristearin in sunflower oil and 1.93±0.03 for tripalmitin in paraffin oil. Possible reasons for the variation of f-factor with time and type and amount of triglyceride are discussed below.

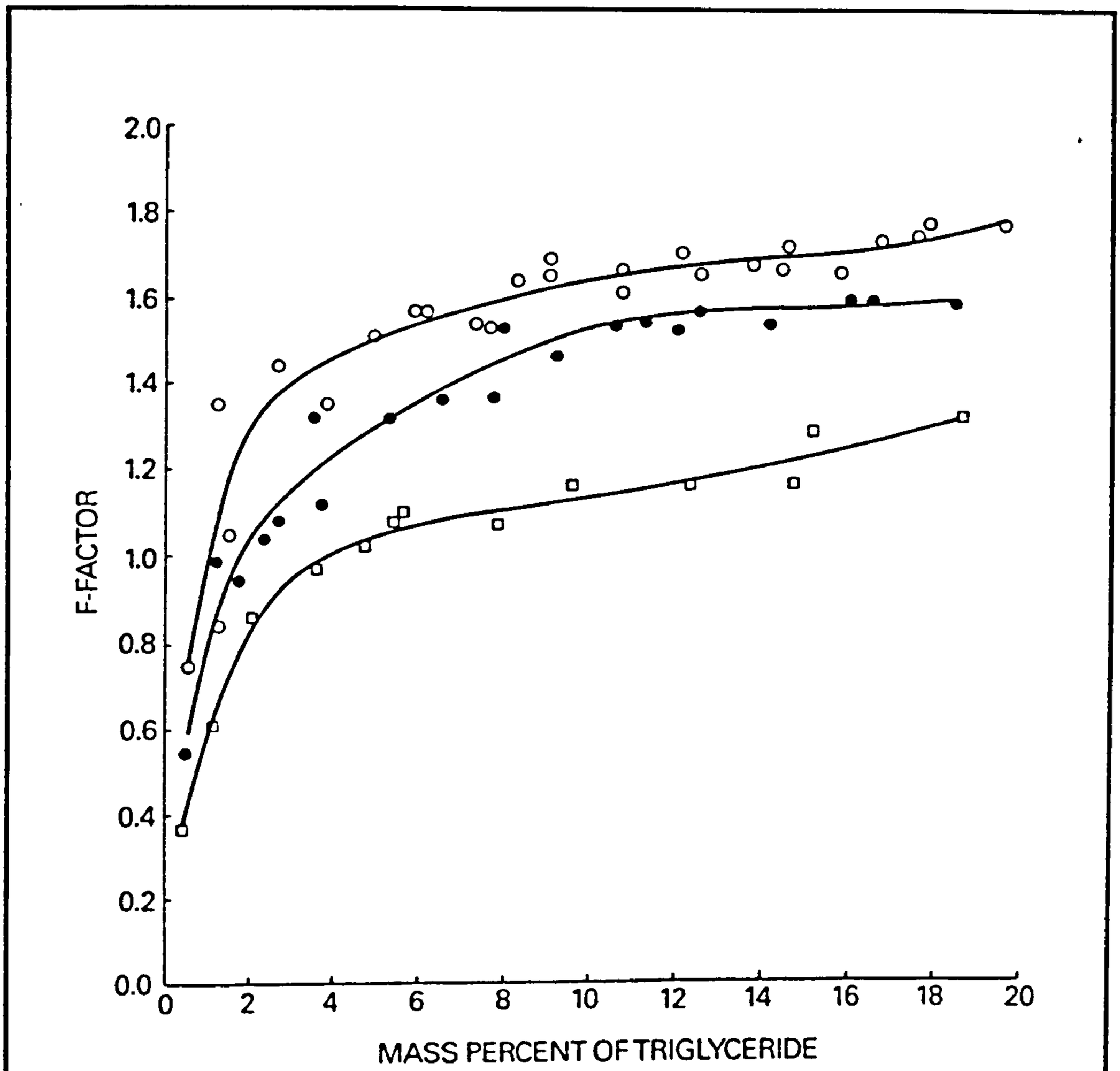

Figure 4.20: Variation of f-factor with triglyceride content at 18°C for tristearin in paraffin oil (●), tripalmitin in paraffin oil (○) and tristearin in sunflower oil (□). Curves are cubic spline fits.

4.3.3.3 Ultrasonic technique

The SFC of the mixtures was calculated using both the theoretical and the empirical approaches discussed in section 4.2.3.1. For the empirical approach the SFC was determined from the velocities of the pure oil (v_{oil}) and the fat/oil mixtures (v_{mix}) using a rearranged form of equation 4.6:

$$SFC = 100\left(\frac{\frac{1}{v_{mix}^2} - \frac{1}{v_{oil}^2}}{\frac{1}{v_{fat}^2} - \frac{1}{v_{oil}^2}}\right) \tag{4.18}$$

and the value of v_{fat} at 18°C (1902.6 m/s). To calculate the SFC using the theoretical approach the velocities and densities of the tristearin, tripalmitin, paraffin oil and sunflower oil are needed in equations 4.4 and 4.5. These are included in table 4.12. The velocity of the tripalmitin was assumed to be the same as that of the tristearin. This was because its velocity could not be measured directly, probably because of vacuole formation during crystallisation which can highly attenuate ultrasound (section 4.2.3.1). The density of solid tripalmitin at 18°C could not be found in the literature, however it is known to be slightly larger than that of tristearin at lower temperatures (Formo 1979) and so the value 1030 kgm^{-3} was used.

Table 4.12: Physical properties of component phases

Velocities and densities of tristearin, tripalmitin, paraffin oil and sunflower oil at 18°C.

Material	Velocity (m/s)	Density (kg/m^3)
Tristearin	2085	1025
Tripalmitin	2085	1030
Paraffin oil	1477.6	882.8
Sunflower oil	1477.8	917.9

4.3.3.4 Linear regression

The relationship between the amount of triglyceride added and the SFC predicted by the techniques was determined by linear regression using the equation:

$$y = A + Bx \tag{4.19}$$

where x is the amount of triglyceride added (the independent variable), y is the predicted SFC (the dependent variable), A is the regression constant and B is the regression

coefficient. In the ideal case y = x (i.e. A = 0, B = 1). The actual values are included in tables 4.9-4.11.

4.3.4 Discussion

The correlations between the amount of triglyceride added and the SFCs predicted by each of the techniques were very significant, always being better than 0.995 (tables 4.9-4.11). However, there was a significant difference between the expected (A = 0, B = 1) and the measured regression constants and coefficients, which is discussed below.

4.3.4.1 Weight method

The SFCs determined by the weight method indicated that the tristearin and the tripalmitin were slightly soluble in the paraffin oil (≈ 0.3 and 0.6% respectively, tables 4.9 and 4.11). This might be caused by slight impurities in the triglyceride samples (table 4.1) or by incomplete crystallisation of the triglycerides at the time of measurement. Indeed, there was a slight increase in the measured SFC a day after the initial measurements (≈ 0.2-0.3%). In the tristearin in sunflower oil the SFC was overestimated, probably because impurities in the oil crystallised with the tristearin.

As the weight method uses only the NMR signal from the liquid component, the results should be independent of the type of triglyceride present and the polymorphic form. Once the instrument has been calibrated for a particular liquid, the SFC can be determined without any information other than the mass of the sample, assuming that the signal per gram of liquid in the mixture is the same as that in the pure liquid used to calibrate the instrument. The fully automated weight method gives rapid, accurate determinations and can be used for non-intrusive, in-line measurements. It can also be used across the whole SFC range, although its accuracy will decrease near 0 and 100% due to errors associated with weighing. Other disadvantages are that it has a relatively high capital cost, and is more time consuming than the other two methods, requiring accurate weighings of the samples. The method also depends on the composition of the liquid phase present; if the liquid phase consists of more

than one component and they have different NMR signals per gram there are problems associated with the determination of SFCs.

4.3.4.2 Direct Method

Although there are very significant correlations between the amount of triglyceride added and the SFCs determined, the direct method appears to consistently over-predict the SFC (Tables 4.9-4.11). This is probably a result of the variation in sample f-factors with time and the amount of triglyceride present, and accounts for the relatively large regression constants (A). The change of f-factor with time is probably due to some rearrangement of the fat crystals in the samples. On rapid cooling the crystals tend to form a disordered gel matrix; however, with time they tend to rearrange themselves to form a more ordered arrangement. This will change their proton environment, and hence, also the f-factor.

There are a number of possible reasons for the variation of f-factor with triglyceride content. At low SFCs, the signal measured at time t_1 will be similar to that at t_2, and therefore the percentage errors in equation 4.16 will be larger. Also any effect due to the slight decay of the liquid signal will be magnified, and may cause appreciable errors. Another possible reason is that at low SFCs the crystals are mainly surrounded by the oil phase; however, as the SFC increases the crystals become closer together and their proton environment will be changed. Van Putte and Van den Enden (1974) have also noted large inaccuracies of f-factors in fat/oil mixtures with SFCs below 5%.

There are also other problems associated with the direct method. Equation 4.16 assumes that the proton densities of the solid and liquid phases are similar, so that the ratio of solid to total signal is equal to the SFC. For natural fatty materials the proton densities of the phases may be similar, but this is less likely for a system such as triglyceride in paraffin oil. The relatively large proton density of the paraffin oil, compared to that of a natural fat, means the SFC predicted by equation 4.16 will be slightly in error. To account for this, the proton density of the component phases would have to be determined. The f-factor also depends on the adjustment of the instrument, fat composition, formation of compound

crystals, polymorphism and temperature (Sleeter 1985, Waddington 1986) and, therefore, a different f-factor is required for each system investigated. For complicated systems such as margarines or shortenings it is usually necessary to determine the f-factor empirically for each formulation and tempering procedure.

4.3.4.3 Ultrasonic technique

There were very significant correlations between the SFCs determined using the ultrasonic technique and the amount of triglyceride in the samples for both the theoretical and empirical approach (tables 4.9-4.11). The relatively high values of the regression coefficients (B) are probably a combination of the slight solubility of the triglycerides, and, in the case of the theoretical approach, the breakdown of the Wood equation (equation 4.3) at SFCs around 15%. It would seem that either approach could be used to determine the SFCs for the systems examined. At higher SFCs, however, the theoretical approach may not prove suitable and an empirical approach may be the only alternative (section 4.2.3.1). The empirical approach also has the advantage that it relies on velocity measurements only (no density measurements are required) which makes it simpler to use. For fundamental studies, however, a theoretical approach should be used if possible since it allows more information to be obtained from a system.

A significant limitation of the ultrasonic technique noted in this work was that it was restricted to SFCs less than about 40%, probably because of vacuole formation in the samples during cooling (Hvolby 1974). Vacuoles have a large acoustic mismatch with the rest of the sample, and cause the ultrasonic pulse to be highly attenuated. Any air trapped in the system may also have a significant effect on the velocity and attenuation of the signal, the magnitude depending on the bubble size and volume fraction (Gaunaurd and Uberall 1981). To overcome these problems, vacuoles and air bubbles should be removed from the samples before any measurements are made or measurements should be made as a function of frequency (section 2.5.5).

Like NMR, the ultrasonic technique is capable of rapid and precise measurements, however, it is much cheaper to install, and once automated may be capable of faster sampling rates (50kHz). In addition pNMR has been reported to give poor predictions of the SFC at low SFCs (<5%) (Van Putte and Van den Enden 1974) and so for these systems the ultrasonic technique may prove more useful. Since the ultrasonic velocity depends on the physical properties of the component phases, it also has to be calibrated for each particular system under investigation. However, in section 4.2.3. it was shown that the velocities of many solid triglycerides and of many liquid oils are similar and so the use of average values for the velocities of solid triglycerides and liquid oils may not cause much loss of accuracy in SFC determinations.

4.4 SFC determinations in commercial fats

4.4.1 Introduction

In the previous sections ultrasonic propagation in binary glyceride/oil mixtures was examined. Commercial fats consist of a complex mixture of glycerides and melt over a range of temperatures. In this section the use of ultrasonic velocity measurements as a means of determining SFCs in some commercially available fats is examined. The fats used were Co-op Cooking Oil and Silver Medal Lard which are both animal fats which are partially solid below temperatures of 40°C. The SFCs determined by the ultrasonic technique were compared with those determined using the pNMR 'direct' method.

4.4.2 Materials and Methods

4.4.2.1 Materials

The two commercial fats were obtained from the Co-operative Wholesale Society Ltd., New Century House, Manchester. Before being used they were stored in a 5°C refrigerator to prevent melting and subsequent supercooling/recrystallisation of their constituent triglycerides.

4.4.2.2 Ultrasonic measurements

The fats were partially solid at 5°C and so care had to be taken when they were placed in the cuvettes. This was so that no air pockets were incorporated, which may highly attenuate the ultrasonic signal, and because the cuvettes were fragile and so broke easily if a semi-solid sample were forced in. Once in the cuvettes the samples were placed in a water bath and allowed to equilibrate to the appropriate temperature before measurements were made. Velocity measurements were made at 1.25 MHz over the temperature range 5-65°C using the pulse-echo apparatus described in chapter 3.

4.4.2.3 pNMR measurements

The pNMR 'direct' method was used to determine the variation of SFC with temperature for the two fats. These measurements were carried out by Unilever Research Laboratories (Colworth House, Sharnbrook, Bedford) using a Brucker PC20 Minispec. The f-factor used in the calculation of the SFC was 1.5345 which is determined by calibrating the instrument with the standards supplied by the manufacturer.

4.4.3 Results and discussion

The measured variation of ultrasonic velocity with temperature for the two fats is shown in figures 4.21 and 4.22. At temperatures below about 40°C the ultrasonic velocity decreases rapidly with increasing temperature because the ratio of solid to liquid glyceride is decreasing. Above temperatures of 40°C the glycerides are completely liquid and the decrease of ultrasonic velocity with temperature is less rapid. This variation of ultrasonic velocity with temperature is similar to that for the glyceride/oil mixtures represented by figure 4.11. The commercial fats, however, melt over a wider temperature range because they consist of a mixture of glycerides each with its own melting point. There is also no temperature range in figures 4.21 and 4.22 where the fats are completely solid. This is because the samples could not be cooled to a low enough temperature with the equipment available.

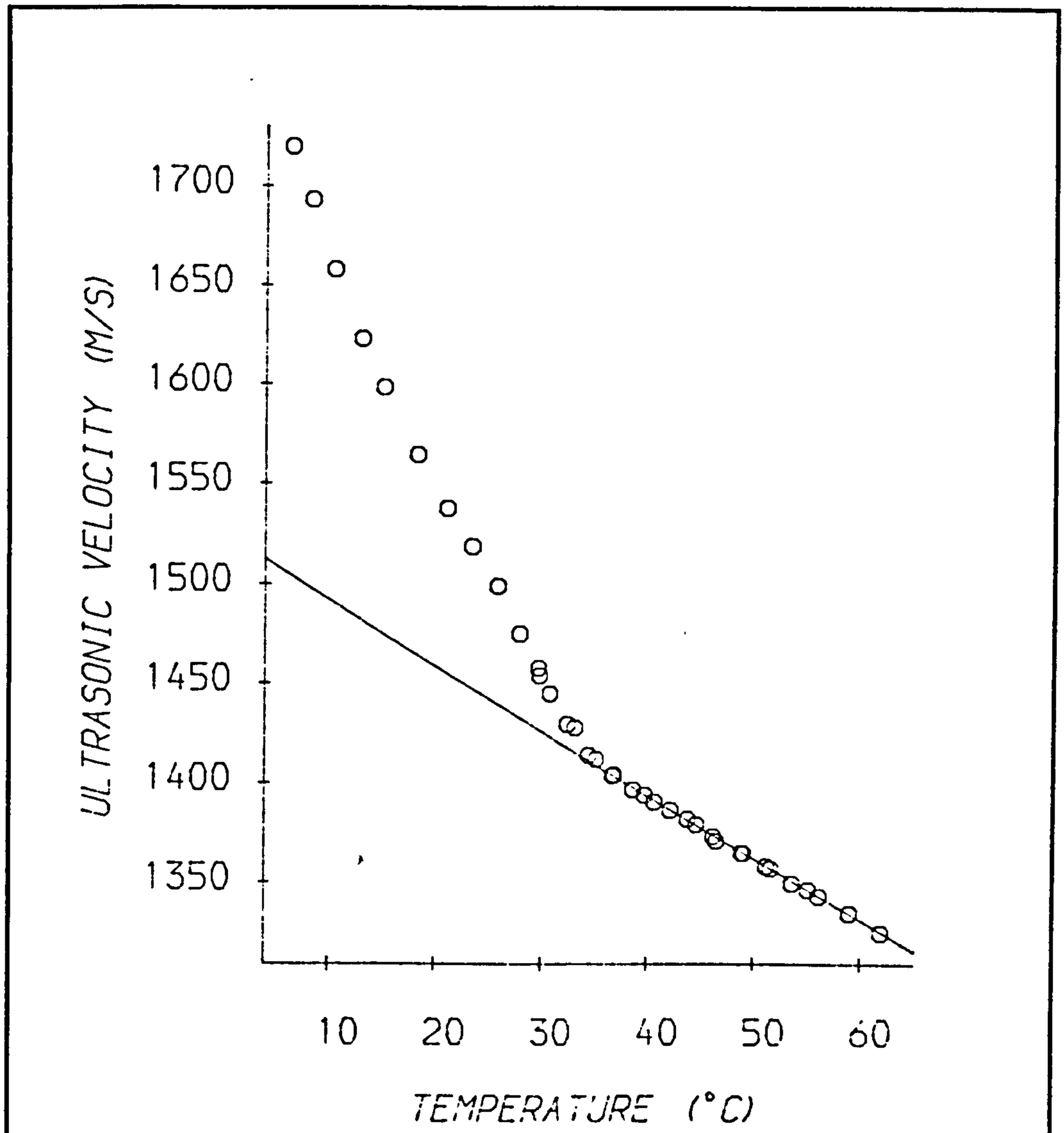

Figure 4.21: Velocity-temperature profile of Co-op Cooking Oil at 1.25MHz

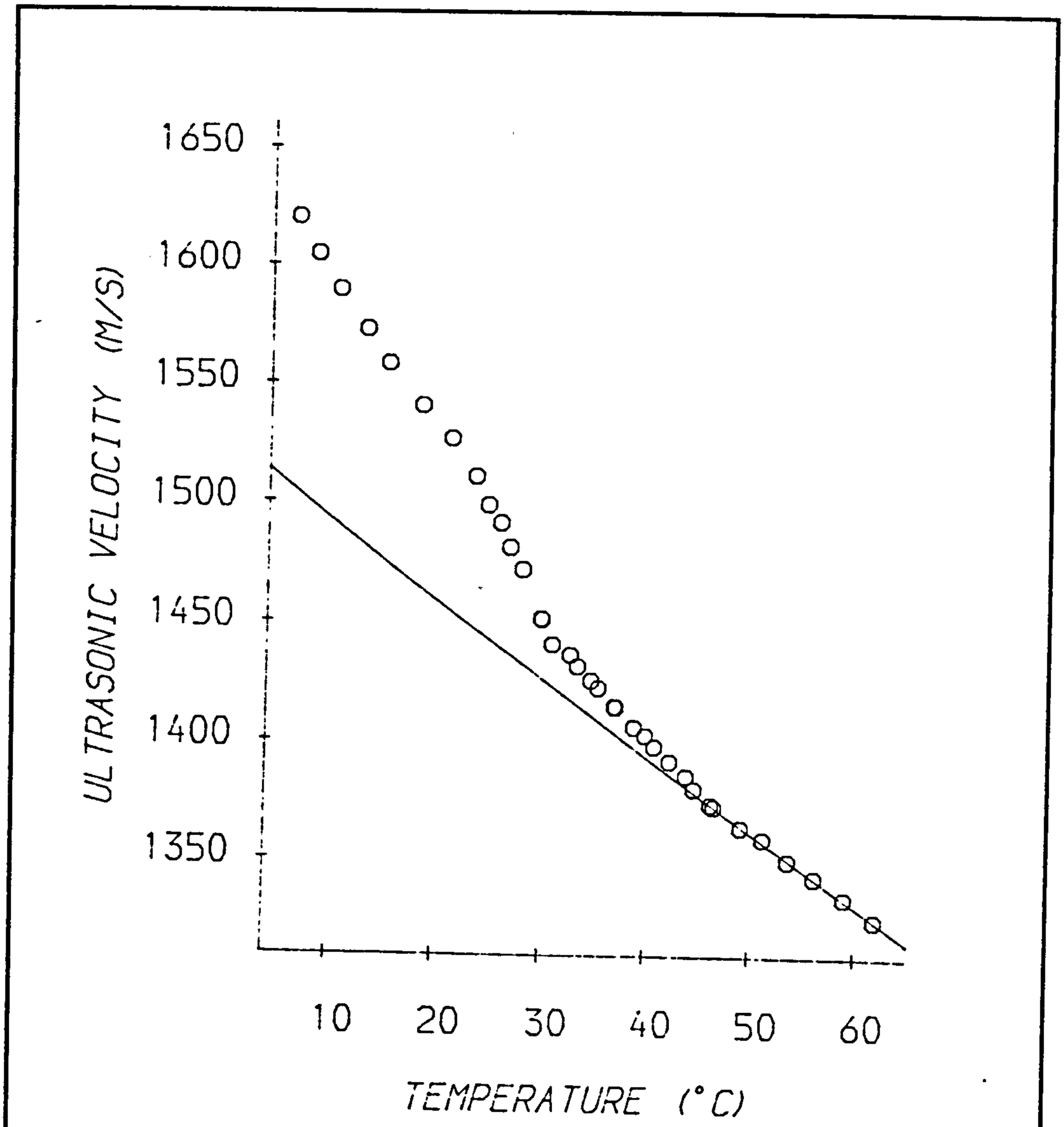

Figure 4.22: Velocity-temperature profile of Silver Medal Lard at 1.25MHz

The technique used in section 4.2.3.3 to determine the variation of SFC with temperature of the glyceride/oil mixtures cannot be used for the commercial products since the variation of ultrasonic velocity with temperature for the solid phase cannot be calculated from the experimental measurements. However, the empirical approach described in section 4.2.3.1 should prove useful. The variation of ultrasonic velocity with temperature for the region where the commercial fats were completely liquid (see figures 4.21 and 4.22) were determined by calculating the best least squares fit of the experimental measurements to equation 4.2. The calculated constants are shown in table 4.13 and as curves in figures 4.21 and 4.22.

Table 4.13: Velocities of liquid oil phase of commerical fats

Temperature dependence of velocity measurements in figures 4.21 and 4.22 was calculated using equation 4.2. The correlation coefficient was always better than -0.9995.

	T(°C)	n	a(m/s)	b($°C^{-1}$)	dV/dT
Co-op Cooking Oil	46-62	19	1526.8	-0.00228	-3.12
Silver Medal Lard	46-62	8	1527.5	-0.00229	-3.13
s.e.m.			0.2	0.00002	0.03

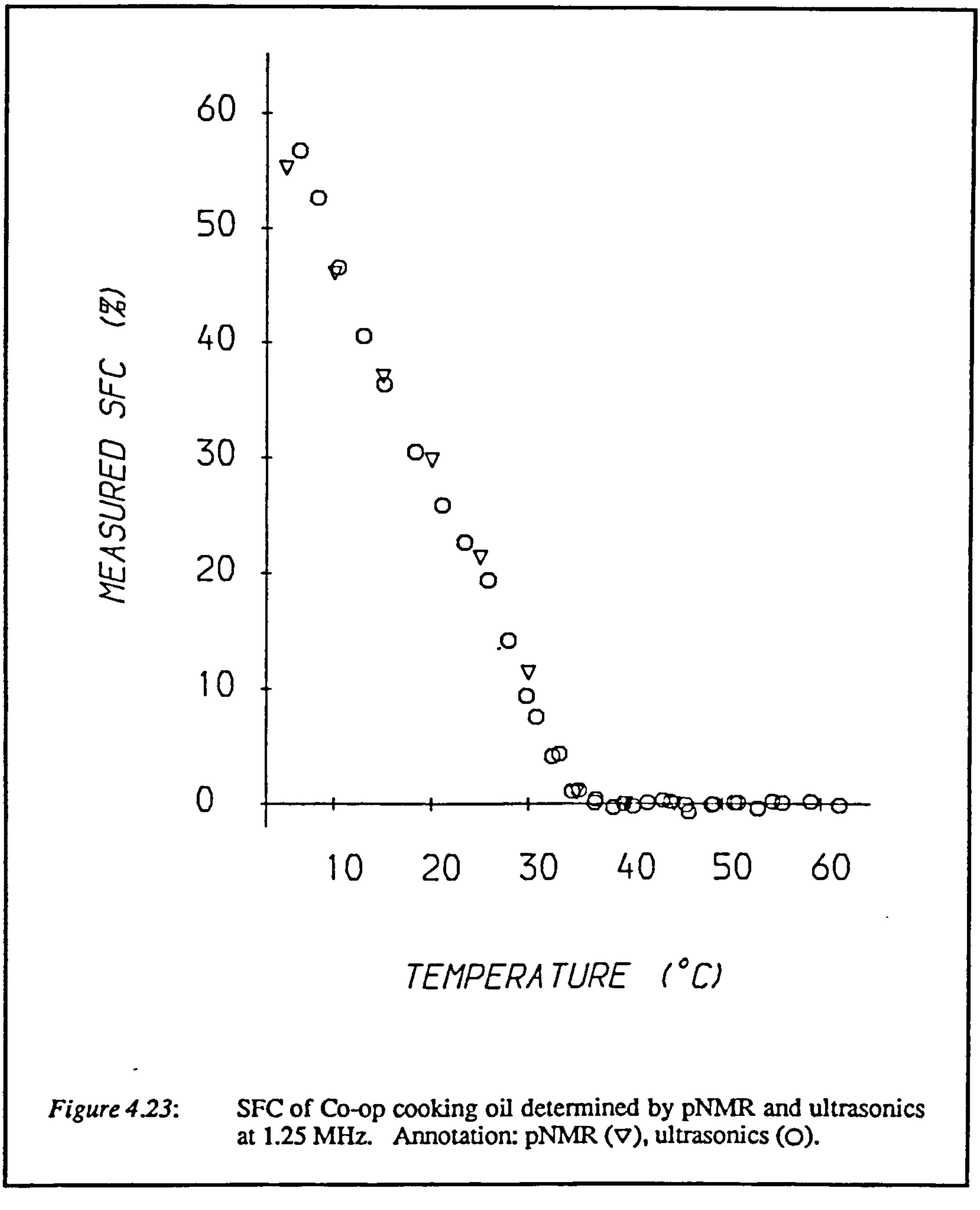

Figure 4.23: SFC of Co-op cooking oil determined by pNMR and ultrasonics at 1.25 MHz. Annotation: pNMR (▽), ultrasonics (O).

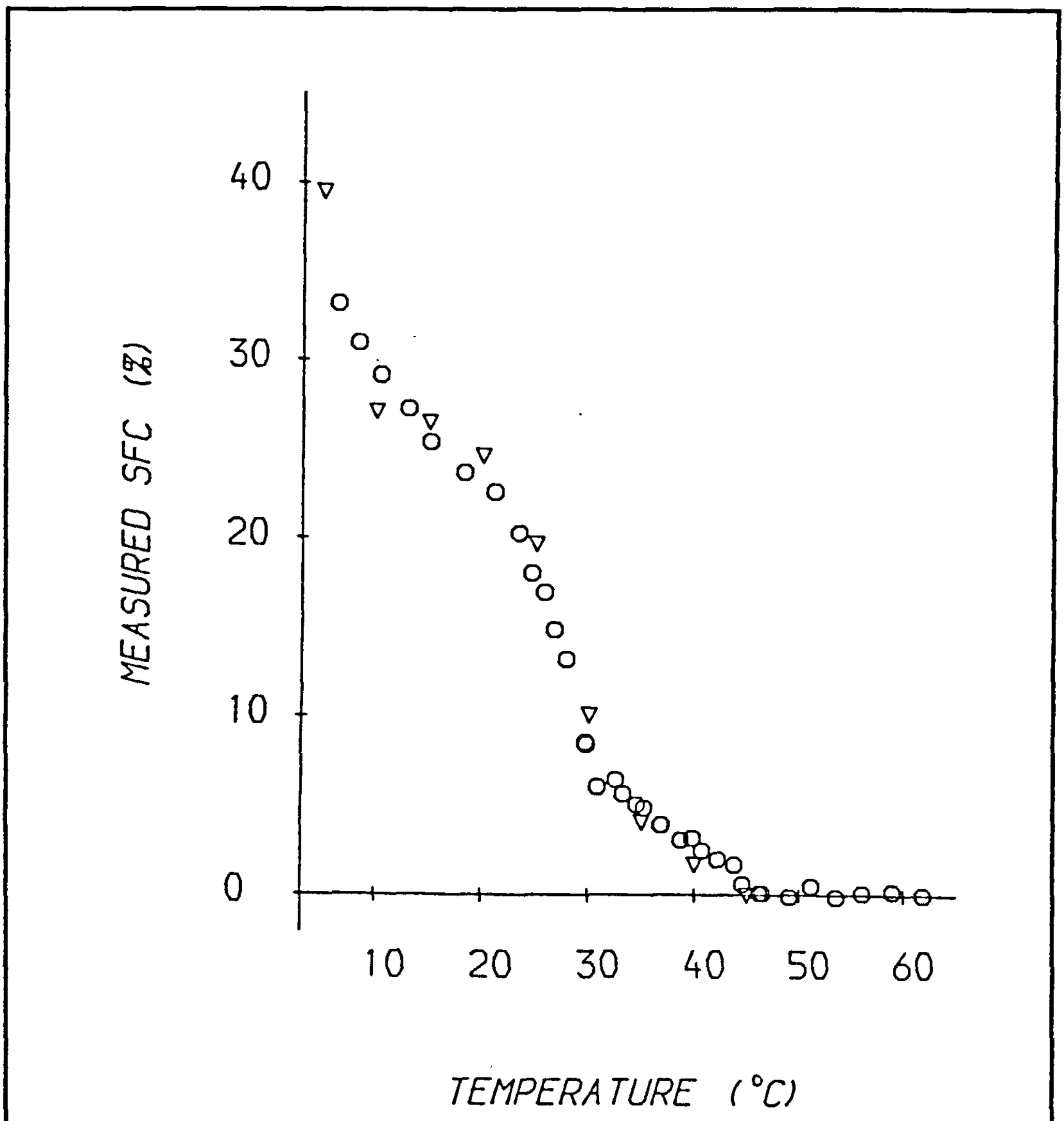

Figure 4.24: SFC of Silver Medal lard determined by pNMR and ultrasonics at 1.25 MHz. Annotation: pNMR (∇), ultrasonics (O).

The variation of the SFC of the fats with temperature was then calculated by using equation 4.18

$$SFC = 100\left(\frac{\frac{1}{v_{mix}^2} - \frac{1}{v_{oil}^2}}{\frac{1}{v_{fat}^2} - \frac{1}{v_{oil}^2}}\right)$$

where v_{mix} is the measured velocity of the mixture, v_{oil} is the velocity of the oil phase calculated from equation 4.2 and the constants shown in table 4.13 and v_{fat} is the same as that calculated in section 4.2.3.1. The values of SFC calculated using this technique for the two commercial fats are presented in figures 4.23 and 4.24 along with the values determined by pulsed NMR. There is good agreement between the SFCs determined by the two techniques. Ultrasonics therefore seems to be a useful adjunct to or alternative to the pNMR technique for this type of measurement. Both techniques can be fully automated and used for in-line measurements of the SFC, however, the ultrasonic technique has a lower capital cost and has faster sampling rates than the pNMR technique, although it may not be suitable for products which contain many air cells or vacuoles (section 4.2.2).

To determine the SFC of a fat/oil mixture by the method described above it is necessary to measure the velocity across a range of temperatures so the variation of the velocity with temperature for the liquid oil region can be determined. Ideally, we would like a single equation which can be used to describe the variation of ultrasonic velocity with SFC at any temperature. This would require that the variation of ultrasonic velocity with temperature for all solid glycerides and for all liquid glycerides were the same so we could use average values for v_{oil} and v_{fat}. In practice this is not the case, however, many solid triglycerides (table 4.4) have similar velocities as do many liquid oils (tables 4.5 and 4.13). Thus it may be possible to use a single equation to determine the SFC of many fatty materials. The value of v_{fat} has already been calculated in section 4.2.3.1. The average value for the variation of ultrasonic velocity with temperature of the liquid oil phase was calculated from the measurements shown in tables 4.5 and 4.13 and was found to be $v = 1536.6e^{-0.00234T}$. Thus

the following equation can be used to calculate the SFC of an unknown fat/oil mixture at any temperature:

$$SFC = 100\left(\frac{1-\frac{2.36x10^{6}e^{-0.00468T}}{v_{mix}^{2}}}{1-0.591e^{0.00082T}}\right)$$

The SFCs of the two commercial products were calculated from the ultrasonic velocity measurements shown in figures 4.21 and 4.22 using this equation and were found to agree to within 5 % of those shown in figures 4.23 and 4.24. The above equation may therefore be used to provide a rough indication of the SFC of many fat/oil mixtures.

4.5 Ultrasonic characterisation of fats and oils

The work in this chapter has shown that ultrasonics can be used to characterise a number of properties of fats and oils. The SFC or solubility of fat/oil mixtures can be determined by measuring their ultrasonic velocity. Phase transitions can be monitored by measuring the velocity as a function of temperature. The technique may also be used to characterise many liquid oils, since the ultrasonic velocity is related to the type and amount of triglycerides present. Ultrasonics should therefore prove a useful adjunct or alternative to the existing techniques for characterising fats and oils (e.g. NMR, DSC, dilatometry, RI, SV etc.). It can be used to make rapid and precise measurements in a non-intrusive, non-invasive manner, and should therefore prove useful for both fundamental investigations and as a tool for monitoring process control.

Chapter 5

ULTRASONIC MEASUREMENTS IN EMULSIONS

5.1 Introduction

5.1.1 Emulsions in the Food Industry

An emulsion is usually defined as "an opaque, heterogeneous system of two immiscible phases, with one of the phases being dispersed in the other as droplets of microscopic or colloidal size" (Dickinson 1987). In the food industry, however, the term is often used in a broader sense so as to include systems which contain fat crystals, gas bubbles or various other ingredients, such as macromolecules or starch granules (Dickinson and Stainsby 1982). Emulsions are of considerable importance in the food industry as they contribute to the bulk properties of many food materials. In most food emulsions one of the phases is aqueous, whilst the other is oil. If the oil phase is dispersed in the aqueous phase the emulsion is termed O/W (oil-in-water), if the aqueous phase is dispersed in the oil phase the emulsion is termed W/O (water-in-oil). Mayonnaise, milk and salad cream are examples of O/W emulsions, whilst butter, margarine and low fat spreads are examples of W/O emulsions. Understanding the properties of emulsions and their effect on product quality is a major concern of the food technologist. Which properties are important depends on the nature of the emulsion and its specific application. In some foods it may be the stability to creaming or coalesence which is important, in others it may be the organoleptic, rheological, microbiological or optical properties (Walstra 1987b). These macroscopic properties of emulsions are determined chiefly by the physiochemical properties of the component phases, the droplet shape, size and concentration, the emulsion type (O/W or W/O) and the properties of the oil/water interface (Dickinson and Stainsby 1982). The commercial

importance of emulsions has led to the development of a number of techniques for characterising their properties, e.g. light scattering; neutron scattering; rheological measurements; conductivity measurements; nuclear magnetic resonance; microscopy; interfacial phenomena; X-ray diffraction (Dickinson and Stainsby 1982). However, there are many areas where the development of new techniques would be beneficial. In recent years the potential of ultrasonics as a means of characterising food emulsions has been realised (Povey and McClements 1988b). This technique can be used to make rapid and accurate measurements, in a non-invasive, non-intrusive manner in systems which are optically opaque. Consequently, there is active research into the development of ultrasonic techniques for characterising emulsions by a number of workers in the food industry.

5.1.2 Ultrasonic measurements in food emulsions

The most frequent application of ultrasonics to food emulsions has been for the characterisation of milk and various other dairy products. Hueter et al (1953) showed that measurements of the ultrasonic attenuation of homogenised milk and skimmed milk could be related to their composition. In 1961 Fitzgerald et al developed an ultrasonic instrument, called the 'solution analayser', which used velocity measurements at two temperatures to determine both the butter fat content (BFC) and solids-not-fat (SNF) of milk. Since this early work the solution analyser has been used to measure the BFC and SNF of milk (Winder et al 1961), ice creams, milk shakes (Pulle and Winder 1972), cheese wheys (Wessenti-Pulle 1972) and milk flowing through pipes (Moy and Winder 1971). Tonshev and Grekhova (1976) related the ultrasonic attenuation of milk to the relative composition of its various components. More recently, Saraf and co-workers (1982, 1984) have shown that ultrasonic velocity and attenuation measurements can be used to determine the concentrations of reconstituted milk powders, whilst Bhatti et al (1986) have demonstrated the possibility or using ultrasonic velocity measurements for testing the purity of milks. Most of these workers have used simple empirical relationships to interpret their results. This is partly due to the complex composition of milk and partly due to a poor understanding of the

theories describing ultrasonic propagation in disperse systems. Milk contains both oil droplets and casein micelles which may scatter ultrasound, and so investigations of scattering by milk may prove a useful means of providing additional information about these systems e.g. particle size and concentration of the oil droplets and casein micelles.

Apart from the applications of ultrasonics to dairy systems there are suprisingly few other applications of the technique to food emulsions. This is highlighted by the lack of references to the subject in the recent reviews of ultrasonic applications in the food industry by McCann (1986), Javanaud (1988) and Povey and McClements (1988a). A notable exception is the work carried out by Howe, Mackie, Robins and co-workers at the AFRC Institute of Food Research at Norwich (Howe et al 1986, Hibberd et al 1987a,b). These workers have demonstrated the possibility of using ultrasonic velocity measurements to determine creaming profiles in optically opaque emulsions in a non-invasive, non-intrusive manner, by measuring the ultrasonic velocity as a function of emulsion height. To calculate the creaming profile it is necessary to relate the velocity measurements to the volume fraction of the dispersed droplets. These workers used the Wood equation (equation 2.5), which assumes no scattering of ultrasound, for this purpose. For a number of the emulsions examined by these workers the effects of ultrasonic scattering were small and so this simple approach could be used to interpret results. However, there were also a number of other systems, most notably a soya bean oil in water emulsion (Hibberd et al 1987a), where significant deviations between the measured ultrasonic velocity and the value predicted assuming no scattering were noted. For these systems a semi-empirical approach was used to relate the measured velocities to the disperse phase volume fractions of the emulsions. In section 5.2 it is shown how these deviations may be accounted for by ultrasonic scattering which these workers did not consider. In systems which scatter ultrasound the velocity is dependent on the particle size as well as the disperse phase volume fraction (chapter 2). Thus if there is a change in particle size distribution during creaming e.g. the larger particles cream faster than the smaller particles (Dickinson 1988), there will be no simple relationship

between the measured velocity and the disperse phase volume fraction and the semi-empirical approach described by Hibberd et al (1987a) will not be applicable. However, if scattering is taken into account it may be possible to determine both the disperse phase volume fraction and the particle size distribution as a function of emulsion height by measuring the velocity with varying frequency.

The above discussion has highlighted the poor understanding of the theories describing ultrasonic propagation in disperse systems by many workers in the food industry. A good understanding of ultrasonic scattering theory will facilitate data interpretation and may lead to many interesting new applications of the technique to food emulsions. In chapter 2 it was shown that scattering may have a significant effect on the velocity and attenuation of many emulsions. In systems where the density difference between the component phases is significant, visco-inertial scattering may have an appreciable effect on the measured velocity and attenuation. In food emulsions, however, the densities of the component phases are often similar ($0.9 < \frac{\rho}{\rho'} < 1.1$) and so visco-inertial scattering is not usually important. However, water has significantly different thermal properties to many food oils and so we would expect thermal scattering to be important, particularly at low particles sizes and frequencies (chapter 2). The effects of thermal scattering on excess attenuation in emulsions have been demonstrated experimentally by a number of workers (Ratinskaya 1962, Ohsawa 1969, Koltsova and co-workers 1970, 1974, 1976, 1980, 1985, Allegra and Hawley 1972, Rokhlenko et al 1980, Javanuad et al 1986), however, the author could find no work dealing with its effect on velocity measurements. Ultrasonic velocities can be measured more accurately than attenuation and are easier to interpret and are therefore more useful for application in the food industry. For this reason the effects of thermal scattering on the ultrasonic velocity of emulsions is examined in some detail in section 5.2 and the implications of scattering for characterising emulsions is discussed. In section 5.3 the possibility of using velocity measurements to characterise W/O emulsions which contain a partially crystalline fat phase is examined.

5.2 *Thermal scattering of ultrasound by emulsions*

5.2.1 Introduction

In this section the ultrasonic velocity and attenuation of a series of sunflower oil and water emulsions were measured with varying frequency (1.25-55 MHz), droplet size (0.1-1 μm) and disperse phase mass fraction (0-0.5). The measured values were then compared with the velocity and attenuation predicted by the scattering theory presented in chapter 2. Thus it was hoped to establish the factors which influence ultrasonic propagation in typical food emulsions and to highlight the potential of the ultrasonic technique for characterising these systems. Simple two phase systems were used rather than more complex food emulsions since the results are easier to analyse and because the composition of the emulsions could be controlled.

5.2.2 Materials and Methods

5.2.2.1 Materials

Silica treated sunflower oil (see chapter 4) was used as the oil phase of the emulsions whilst distilled water was used to prepare the aqueous phase. The emulsifiers, Tween 20 and Admol Wol were obtained from Unilever Research Laboratories, Colworth House, UK.

5.2.2.2 Emulsion Preparation

To obtain reliable ultrasonic measurements it is necessary to establish a preparation procedure which produces emulsions which are stable to creaming and aggregation during the measuring period. Emulsion stability can be enhanced by increasing the continuous phase viscosity; decreasing the droplet size; reducing the density difference between the phases; reducing the degree of polydispersity and by using surfactants (Dickinson and Stainsby 1982). Another important factor which had to be considered when preparing the emulsions was the incorporation of air during the homogenisation process. Small volume fractions of air bubbles may have an appreciable effect on the velocity and attenuation of

ultrasound (section 2.5.5). The effects of air were clearly demonstrated when emulsions were prepared using a Silverston blender (which incorporates a considerable amount of air); the ultrasonic signal was so highly attenuated that it could not be detected.

A Shields laboratory homogeniser (Model S 500) was used to prepare the emulsions. This homogeniser works by forcing a course emulsion pre-mix through a small orifice at high pressure, and was used since it produced emulsion droplets which were less than 1μm in radii (and were therefore stable to creaming over the measurement period) and because the amount of air incorporated during the homogenisation process was negligible. The experimental procedure is described below.

1. Oil and aqueous phase were weighed into a 150 cm^3 conical flask, then de-aerated in a vacuum oven (≈ 600 mmHg) at room temperature for 30 min.
2. The flask was stoppered (to prevent losses due to evaporation), placed in a beaker of water equilibrated to 60°C and stirred for 45 min using a magnetic stirrer. Stirring produced a course emulsion pre-mix, without any significant amounts of air being incorporated.
3. The premix was then homogenised by recirculation through a Shields laboratory homogeniser at 60°C whilst being stirred as above. By having the inlet and outlet of the homogeniser under the surface of the emulsion it was possible to reduce the amount of air incorporated. The average droplet size of the emulsions could be varied by varying the homogenisation time or by varying the ratio of surfactant concentration to disperse phase volume fraction.
4. The emulsions were placed in a vacuum oven for 10 min. (at 600 mmHg) in order to remove any air bubbles present.
5. Emulsions of varying disperse phase volume fraction were prepared by dilution of the original emulsion with different amounts of continuous phase. The emulsions were then poured into small glass cuvettes and placed in a water bath to equilibrate to the appropriate temperature before measurements of the ultrasonic velocity and

attenuation were carried out. The emulsions were stirred carefully before each measurement to ensure that the emulsion droplets were distributed homogeneously.

The composition of the original emulsions, which were used to prepare the serial dilutions, are included in table 5.1. O/W emulsions of different average particle size were prepared by either varying the ratio of surfactant (Tween 20) to disperse phase (sunflower oil) or by varying the homogenisation time (H.T.). In general, increasing the homogenisation time reduces the particle size, however, there is a lower limit of particle size which can be achieved, which depends on the ratio of surfactant concentration to the amount of disperse phase added initially. The larger this ratio the smaller the particle size which can be achieved. The lower limit of emulsion droplets sizes was achieved by homogenising the emulsions for longer than 45 mins. In most cases the particle size was varied by varying the amount of disperse phase added initially rather than the surfactant concentration since this meant the properties of the continuous phase remained constant.

Table 5.1: Composition of sunflower oil and water emulsions

	Mass %	Emulsion type	H.T. (mins)	Radii (μm)
A.	43.2	Oil in 2.0% Tween 20/water	10	0.748
B.	50.0	Oil in 2.0% Tween 20/water	60	0.422
C.	37.5	Oil in 2.0% Tween 20/water	60	0.270
D.	25.0	Oil in 2.0% Tween 20/water	60	0.177
E.	12.5	Oil in 2.0% Tween 20/water	60	0.138
F.	10.0	Oil in 1.1% Tween 20/water	120	0.117
G.	20.0	Water in 2.0% Admol Wol/oil	60	0.864

5.2.2.3 Emulsion characterisation

Ideally, the volume fraction of droplets in an emulsion should be the same as the volume fraction of disperse phase added initially. This was checked using density measurements. By measuring the densities of an emulsion and its component phases the disperse phase volume fraction can be calculated:

$$\phi = \frac{\rho_{emul} - \rho}{\rho' - \rho}$$

Density measurements were carried out at 20.0°C using an Anton Paar digital density meter (DMA 40) which is accurate to 0.1kg/m^3. For all the emulsions examined the measured disperse phase volume fraction was found to be within 0.002 of the amount added initially and so the amount of disperse phase added initially was assumed to be equivalent to the volume fraction of the final emulsions.

The technique used to measure the particle size distribution depended on the nature of the emulsion. A Coulter Counter was used to measure the particle size distribution of the O/W emulsions when the majority of the particles were greater than 0.3μm in radius. For smaller droplet sizes a Coulter nano-sizer was used; this gave a mean value of the particle size (d_{30}) and an indication of the polydispersity (the geometric standard deviation, σ_g). Using these parameters the particle size distribution can be calculated by assuming a log-normal distribution (Irani and Callis 1963).

$$\frac{\partial N}{\partial \ln x} = \frac{1}{\sqrt{2\pi}\ln\sigma_g} \exp\left[-\left(\frac{\ln\frac{x}{x_g}}{\sqrt{2}\ln\sigma_g}\right)^2\right] \qquad (5.1)$$

where N is the number frequency, x is the particle size, x_g is the geometric mean of the particle size distribution ($\ln r_{32} = \ln x_g - 2.5\ln^2\sigma_g$) and σ_g is the geometric standard deviation. Figure 5.1 shows the particle size distributions of the O/W emulsions measured using these techniques. The average droplet radius (r_{65}) of the emulsion prepared at the AFRC Institute of Food Research, Norwich (Emulsion F) was measured using photon correlation spectroscopy (PSC) as 0.117 (± 5%) μm. The particle size of the W/O emulsions was

determined by light microscopy using at least 1200 droplets per sample (see table 5.1). Light microscopy was also used to ascertain whether the emulsions contained any air bubbles which may have effected the results: non were found. The average droplet radii of the various emulsions is included in table 5.1. With the exception of emulsion F, these values are given as the Sauter mean radii ($r_{32} = \frac{\sum_{i=1}^{n} N_i r_i^3}{\sum_{i=1}^{n} N_i r_i^2}$).

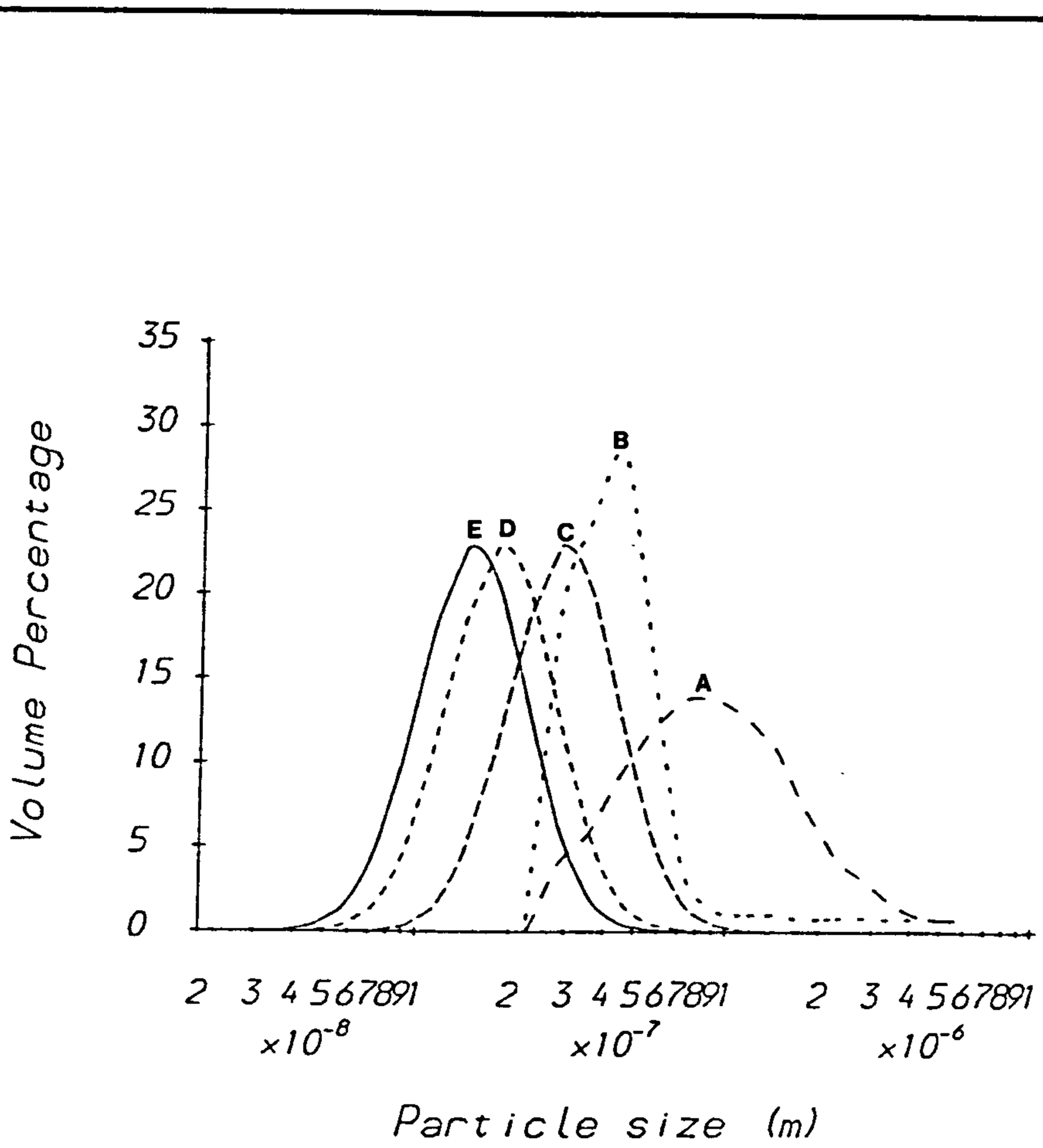

Figure 5.1: Particle size distributions of O/W emulsions. Determined using either the Coulter Counter or the Coulter nanosizer.

5.2.2.4 Ultrasonic measurements

Most of the measurements of velocity and attenuation were made at 1.25, 2.25, 6.0 and 10.0 MHz using the single transducer technique (chapter 3). However, a number of additional measurements were made in the frequency range 5 to 55 MHz using a pulse echo interferometry technique similar to that described by Andreae et al (1958). The actual apparatus used was a modern version of the Andreae technique which was developed at the AFRC Institue of Food Research (Norwich) (Rahalkar et al 1986). The experiments using this technique were carried out with helpful guidance and assistance from N Gladwell, DJ Hibberd, AM Howe, C Javanaud and MM Robbins. The measuring principles of this technique are described briefly below.

Samples were contained in a water jacketed cell, whose temperature was controlled to 20.0 ± 0.1 °C. Two X-cut quartz crystals of fundamental frequency 5 MHz were used as transmitter and receiver. These were coupled to the sample using quartz buffer rods. The upper crystal was moved vertically through the sample and the distance moved was monitored by a micrometer. The crystals were operated at odd harmonics up to 55 MHz where the attenuation in the emulsions became too large for reliable measurements to be made. The emitted and received pulses were displayed on an oscilloscope so that the introduction of 1 dB steps from an attenuator could be compensated for by movements of the upper crystal. The attenuation is then determined from the slope of a plot of attenuation added (in dB) against distance moved (in metres). The velocity is measured by superimposing the unmodulated input pulse upon the received pulse and measuring the seperation between nulls using a micrometer when the distance between the crystals is varied. The instrument was calibrated with distilled water whose velocity and attenuation coefficient are known (Kaye and Laby 1986). Using this technique the velocity could be determined to within 1.0m/s, whilst the attenuation could be measured to within 2% (s.e.m. of at least 20 measurements).

5.2.3 Results and discussion

Measurements of the ultrasonic velocity and attenuation with varying frequency (1.25-55 MHz), droplet size (0.1-1 μm) and disperse phase mass fraction (0-0.5) at 20.0°C for both O/W and W/O emulsions are presented in figures 5.2-5.3 and 5.6-5.13. In figures 5.2 and 5.3 the variation of normalised velocity ($\frac{v}{v_0}$) and excess attenuation per cycle ($\alpha\lambda$) are plotted against $\sqrt{fr}$ for a series of 0.1 mass fraction (ϕ = 0.108) sunflower oil in water emulsions (Emulsions A-F). These values were calculated from the velocity and attenuation measurements included in Appendix VI, tables VI.1 and VI.2. The particle size used in the calculations was the Sauter Mean radius (r_{32}) as has been suggested by Isakovich (1948), however, see also section 5.2.3.1. Figures 5.6-5.13 show the variation of ultrasonic velocity and excess attenuation with droplet mass fraction for three O/W emulsions (Emulsions A, B and D) of different average droplet sizes and a W/O emulsion (Emulsion G) at 1.25 MHz and 20°C.

Numerical calculations of the ultrasonic velocity and attenuation were made using equations 2.9 and 2.11 and are also included in the graphs. The thermophysical properties of sunflower oil and water used in the theoretical calculations at 1.25 MHz are shown in table 2.1. Since measurements were made over a range of frequencies the frequency dependence of the ultrasonic velocities and absorptions of the oil and water phases need to be included in the calculations. The velocity dispersion of distilled water at the frequencies used in this work is negligible, whilst its absorption coefficient can be described by the equation $\alpha_{water} = 2.26 \cdot 10^{-13} f^2$ dB/m (Kaye and Laby 1986). The frequency dependence of the velocity and absorption of sunflower oil were calculated from the measurements shown in Appendix VI, table VI.2. The velocity of the sunflower oil was found to increase slightly over the frequency range 1.25-55 MHz and could be described by the equation $v_{oil} = Af^n$ (where A = 1468.0 m/s, and n = $9.2 \cdot 10^{-5}$), whilst the absorption could be described by the equation $\alpha_{oil} = Af^n$ (where A = $2.50 \cdot 10^{-10}$ dB/m and n = 1.77). The values of A and n being calculated

by finding the best least squares fit of the equations to the experimental measurements of velocity and absorption. The thermophysical properties of the Tween 20 in distilled water and the Admol Wol in sunflower oil surfactant solutions are slightly different to those of the pure distilled water and sunflower oil. The measured values of ultrasonic velocity and density of the surfactant solutions were: $v = v_{water} + 3.29c$ m/s, $\rho = \rho_{water} + 1.35c$ kg/m^3 for Tween 20 in distilled water , and $v = v_{oil}$ m/s, $\rho = \rho_{oil} + 0.3c$ kg/m^3 for the Admol Wol in sunflower oil at 20°C (where c is the surfactant concentration, % w/w). The other thermophysical properties of the aqueous and oil surfactant solutions were assumed to be the same as those of the pure distilled water and sunflower oil respectively (table 2.1).

5.2.3.1 Variation of velocity and attenuation with particle size and frequency

The effects of thermal scattering on the ultrasonic velocity and attenuation are clearly illustrated in figures 5.2 and 5.3. For low frequencies and droplet sizes the ultrasonic velocity falls considerably below that predicted assuming no scattering (figure 5.2). As the frequency or droplet size increases the velocity increases, tending towards its upper limit for high values of these parameters. For sunflower oil in water this upper limit is close to the value predicted assuming no scattering (i.e. $\frac{v}{v_0} \approx 1$), since viscous scattering is negligible (i.e. $\frac{\rho}{\rho'} \approx 1$). The agreement between the experimental measurements of the ultrasonic velocity and the theoretical predictions is very good. The experimental values of excess attenuation per cycle have a maximum value close to that predicted from the scattering theory (figure 5.3). However, there is a considerable amount of scatter in the results and not a particularly good fit between the theoretical predictions and the experimental results, the experimental values being considerably lower than the predicted values. There are a number of possible reasons which may account for the differences between the experimental and theoretical excess attenuations: the attenuation measurements are considerably less accurate than the velocity measurements; the assumptions underlying the scattering theory may not be

valid for this system; an average droplet size was used in the calculations rather than a droplet size distribution; the particle sizes determined by the Coulter Counter and nanosizer may be incorrect.

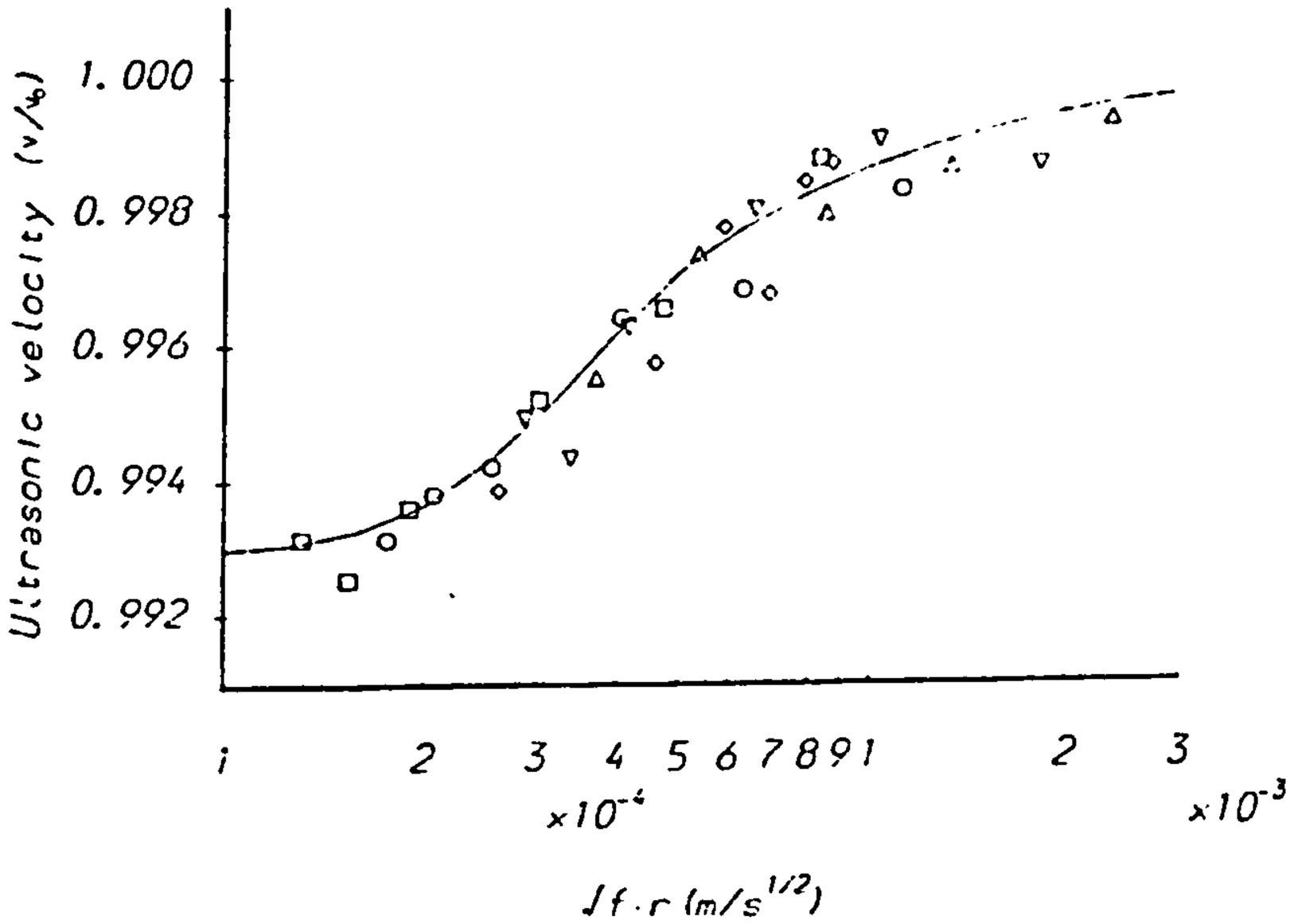

Figure 5.2: Velocity measurements in sunflower oil in water emulsions. The ultrasonic velocity is normalised with respect to its non-scattering value (v_0) and plotted against $\sqrt{fr}$. The experimental measurements were made at 1.25 (□), 2.25 (○), 6.0 (▽) and 10.0 (△) MHz using a pulse echo technique and in the range 5-55 (◇) MHz using a pulse echo interferometric technique. The curve is a prediction made using multiple scattering theory (equation 2.11).

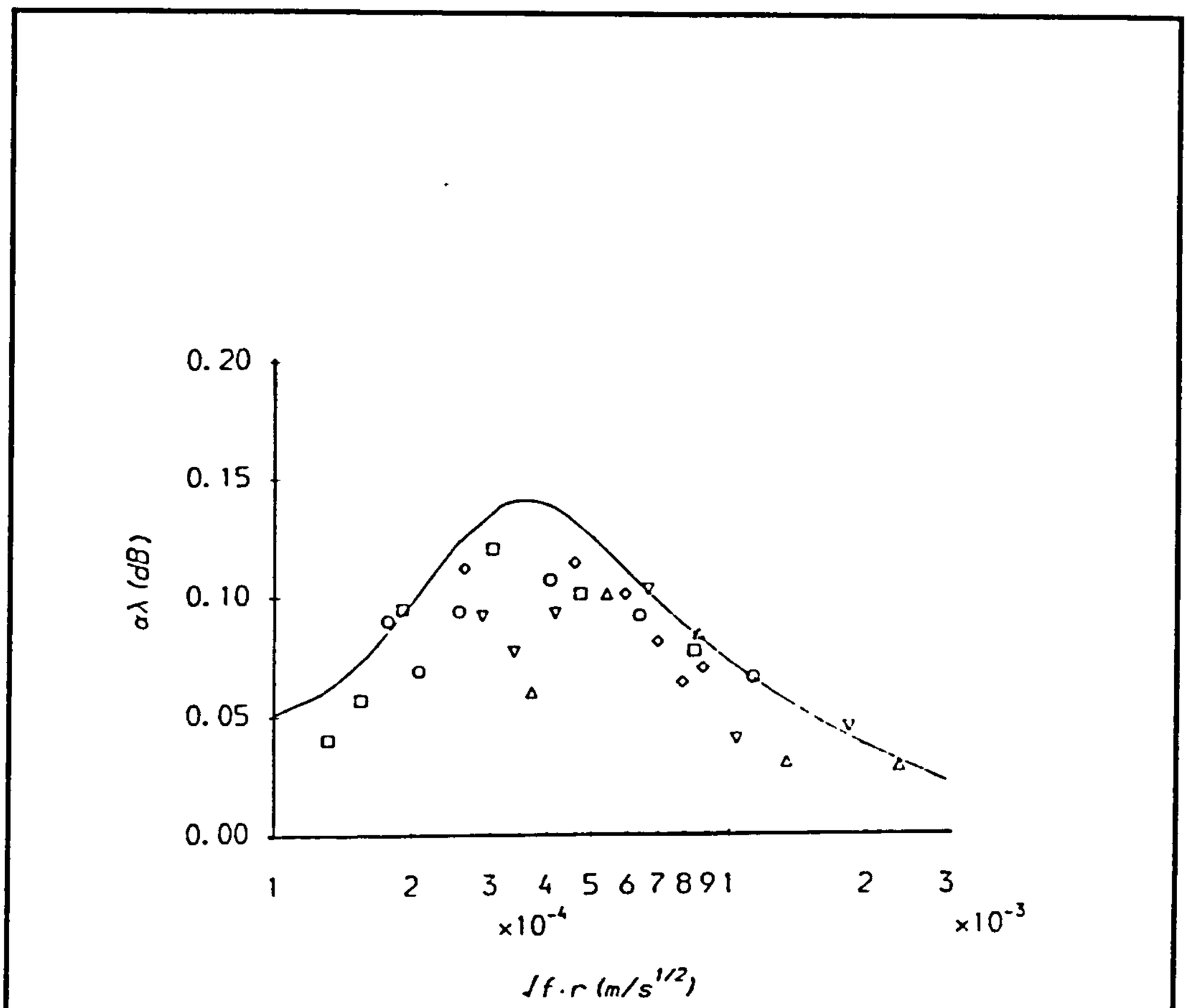

Figure 5.3: Attenuation measurements in sunflower oil in water emulsions. The excess attenuation per cycle is plotted against $\sqrt{fr}$. The experimental measurements were made at 1.25 (□), 2.25 (○), 6.0 (▽) and 10.0 (△) MHz using a pulse echo technique and in the range 5-55 (◇) MHz using a pulse echo interferometric technique. The curve is a prediction made using multiple scattering theory (equation 2.11).

The large experimental errors associated with the attenuation measurements may account for the considerable scatter of the results in figure 5.3, however, they do not explain why the experimental results should fall regularly below the theoretical predictions. The

assumption that the droplet size is much smaller than the ultrasonic wavelength (i.e. $a^2 << 1$) was valid for all the frequencies examined, the A_0 and A_1 scattering coefficients giving an adequate description of the problem. However, the assumption that the viscous and thermal skin depths be much smaller than the distance between the droplets is only roughly approximated for the smaller particles ($r = 0.11\mu m$) and lowest frequency (1.25MHz); d = $0.5\mu m$, $\delta_s = 0.5\mu m$, $\delta_t = 0.2\mu m$. The fact that the assumption $\delta_s << d$ is not satisfied will probably not have a significant effect on the results since the effects of viscous scattering are negligible anyway (see figures 2.8 and 2.9). Whilst figures 5.6-5.13 show that even though the assumption $\delta_t << d$ is not strictly applicable there is still good agreement between the theory and experimental results at mass fractions upto 0.1 at 1.25 MHz. Thus it would seem that the fact that these assumptions are only approximated does not have a significant effect on the results. The most probable reason for the observed deviations is that an average droplet size was used in the calculations rather than the actual droplet size distribution.

Isakovich (1948) has shown that the average particle size required in the equations which describe thermal scattering in emulsions in the limit $\frac{r}{\delta_t} >> 1$ is the Sauter mean radius (r_{32}). As $\frac{r}{\delta_t}$ tends to unity, however, the average particle size needed in the formulations to give the same prediction of velocity and attenuation as an emulsion with a particle size distribution becomes frequency dependent. This can be demonstrated by numerical calculation of the ultrasonic velocity and attenuation in a series of emulsions with different particle size distributions but with the same Sauter mean radius. Figures 5.4 and 5.5 show the variation of ultrasonic velocity and excess attenuation per cycle with frequency for four sunflower oil in water emulsions whose Sauter mean radius is $0.5\mu m$. The particle size distributions were calculated from the parameters listed in table 5.2 assuming a log-normal distribution of droplet sizes (equation 5.1).

A particle size distribution was included in the calculations using the formulation of Urick and Ament (1949) which is equivalent to equation 2.11 when the A_1^2 term is negligible (see

Table 5.2: Four emulsions with different PSDs but the same Sauter mean radii

	W	X	Y	Z
Sauter mean radius (μm)	0.500	0.500	0.500	0.500
Geometric mean x_g (μm)	0.500	0.428	0.268	0.123
Geometric S.D.	1.000	1.284	1.649	2.117

section 5.2.3.3):

$$\left(\frac{B}{k_c}\right)^2 = \left(1 - \frac{3i\sum_{j=1}^{n}\phi_j A_{0j}}{(k_c r_j)^3}\right)\left(1 - \frac{9i\sum_{j=1}^{n}\phi_j A_{1j}}{(k_c r_j)^3}\right) \qquad (5.2)$$

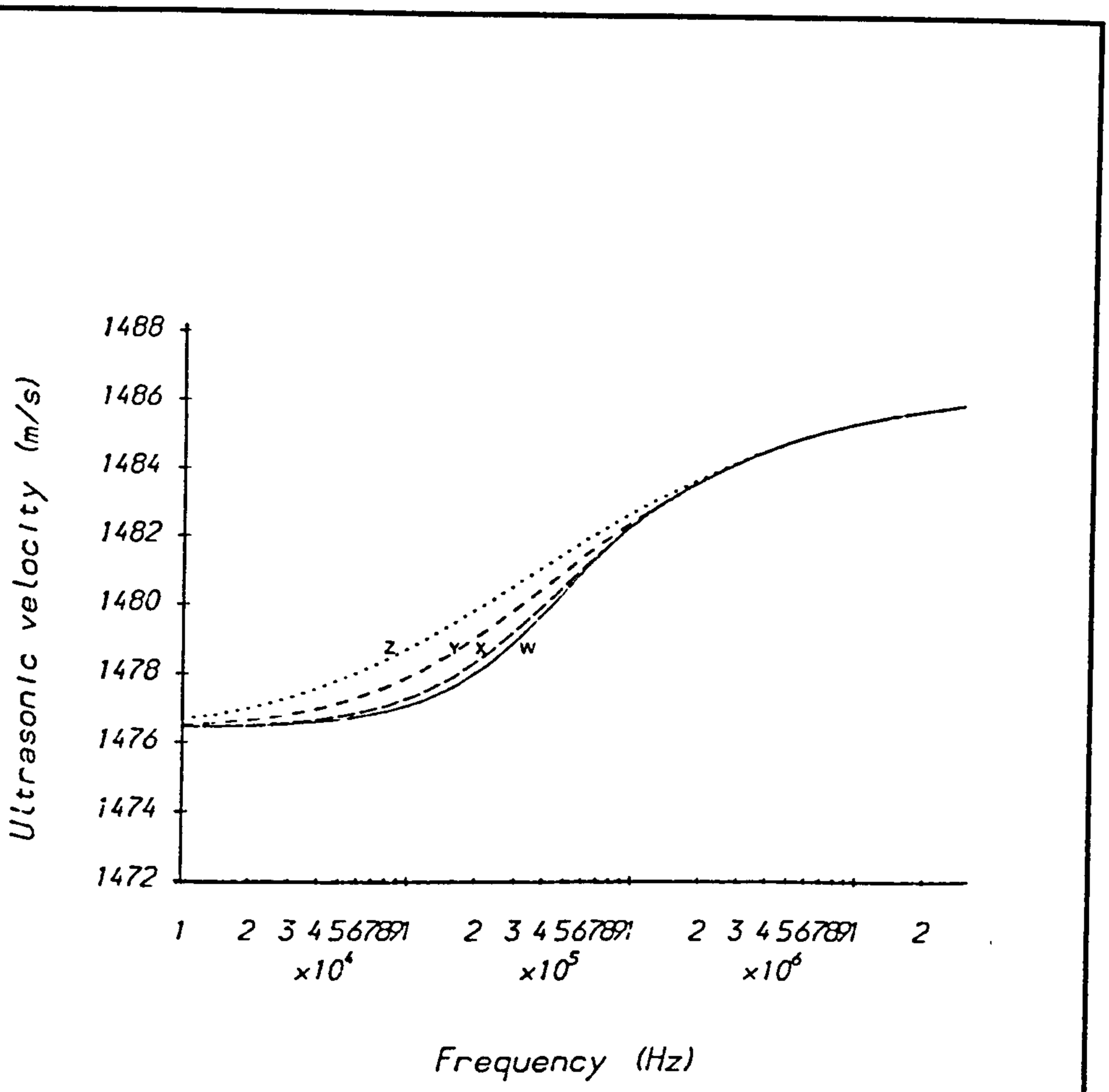

Figure 5.4: Effect of particle size distribution on velocity. Variation of ultrasonic velocity with frequency for a sunflower oil in water emulsion ($\phi = 0.1$ at 20°C and 1.25MHz). The four emulsions have similar Sauter mean radii ($r_{32} = 0.5\mu m$) but different geometric means (see table 5.2).

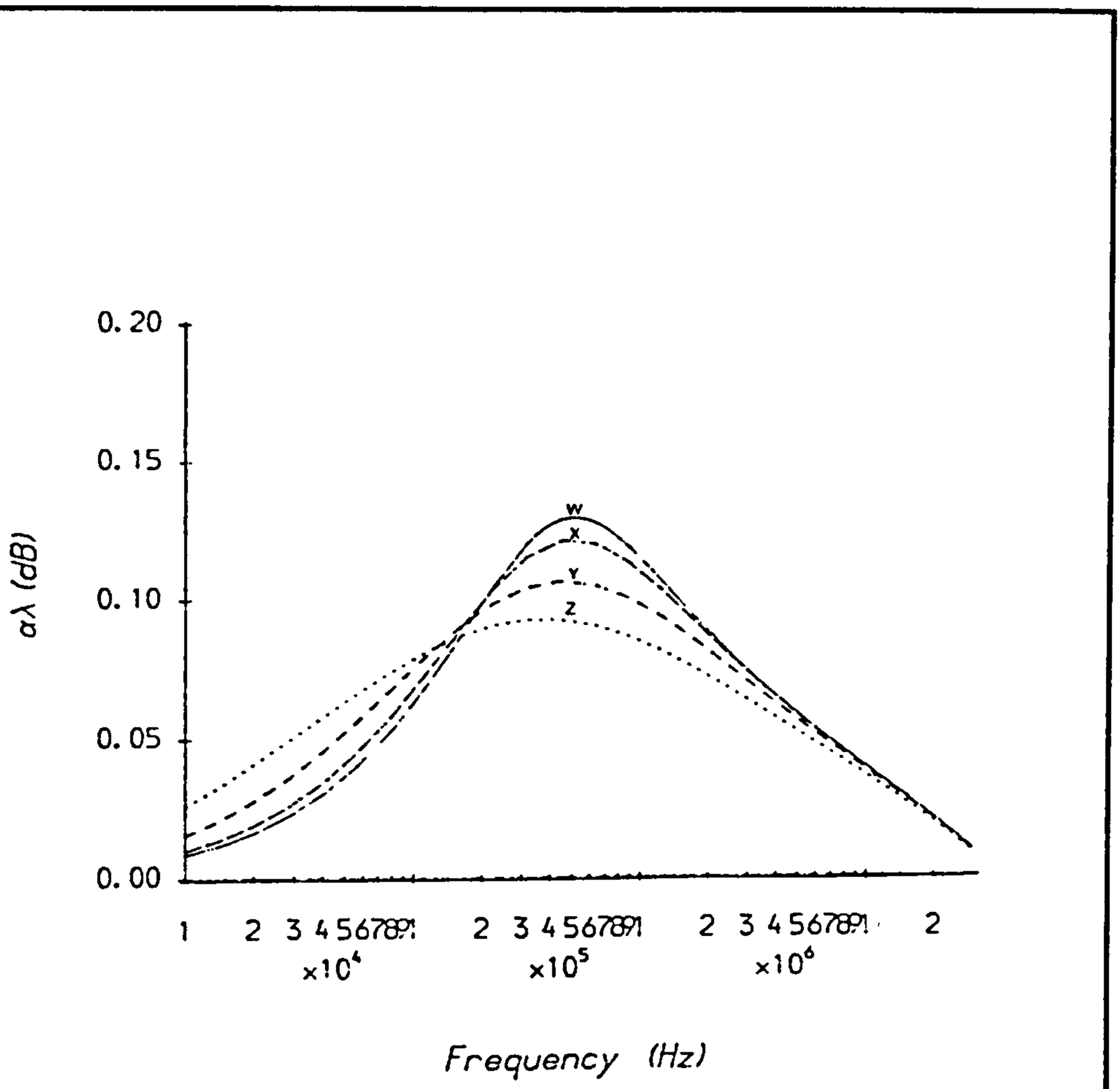

Figure 5.5: Effect of particle size distribution on attenuation. Variation of excess attenuation per cycle with frequency for a sunflower oil in water emulsion ($\phi = 0.1$ at 20°C and 1.25MHz). The four emulsions have similar Sauter mean radii ($r_{32} = 0.5\mu m$) but different geometric means (see table 5.2).

At the higher frequencies the velocities and attenuations of all the emulsions tend to the Sauter mean radius as suggested by Isakovich (1948). At lower frequencies the velocity of an emulsion with a particle size distribution is larger than that of a mono-disperse emulsion with the same Sauter mean radius (figure 5.4). The wider the particle size distibution the greater the difference. The excess attenuation per cycle curve flattens as the particle size distribution increases and the frequency where its maximum value occurs decreases (figure 5.5). This probably explains why the measured attenuation values presented in figure 5.3 were lower than the values predicted using the Sauter mean radius.

The dependence of the ultrasonic velocity and attenuation on emulsion droplet size means that the ultrasonic technique should prove a useful way of determining particles sizes in emulsions. Velocity measurements would appear to be the most suitable since they can be measured more accurately and appear to fit the theory better. A number of workers have investigated the possibility of using attenuation measurements to determine particle sizes in emulsions (e.g. Ohsawa 1969, Rozhlenko et al 1974, Javanaud et al 1986, Rokhlenko 1986), however no workers appear to have investigated the use of velocity dispersion due to thermal scattering for this purpose. By measuring the velocity of an emulsion as a function of frequency it should be possible to determine the disperse phase volume fraction, the average particle size and an indication of the particle size distribution. A measurement of the velocity at a frequency where the ultrasonic velocity is independent of particle size (e.g. below 10kHz or above 20MHz in figure 5.4) will allow its volume fraction to be determined from a knowledge of the thermophysical properties of the component phases only (see equations 2.16 and 2.17). A measurement of the velocity in a region where the velocity is dependent on particle size (r_{32}) but independent of the particle size distribution (e.g. 2-20MHz in figure 5.4) will allow the average particle size of the emulsion to be determined. Whilst a measurement in the region where the ultrasonic velocity depends on the particle size and the particle size distribution (e.g. 10kHz-2MHz in figure 5.4) will give an indication of the particle size distribution. (The larger the difference between the measured velocity

and that predicted using the Sauter mean radius the wider the particle size distribution). To carry out this sort of determination an instrument would have to be developed which can measure the ultrasonic velocity (and/or the excess attenuation) accurately over a wide range of frequencies (10kHz-100MHz).

There is a limited range of particle sizes the technique is sensitive to because the dependence of ultrasonic velocity on particle size has an upper and lower limit (figure 5.2). If we assume that the practical limits of ultrasonic measurement are 0.01-100MHz and take the upper and lower limits of velocity dispersion to be at the values $\sqrt{fr} \approx 2 \cdot 10^{-4}$ and $2 \cdot 10^{-3} ms^{-\frac{1}{2}}$ then the lower limit of particle size the technique will be sensitive to will be 20nm (at 100MHz) and the upper limit will be 60μm (at 0.01MHz). These limits will depend on the emulsion investigated and will be extended to larger particle sizes in systems where viscous scattering is important. The accuracy to which the particle size can be measured depends on the accuracy to which the velocity can be measured. The magnitude of the change in ultrasonic velocity per μm change in particle size in figure 5.2 is about $10 ms^{-1} \mu m^{-1}$ at the steepest point on the velocity-$\sqrt{fr}$ curve. Thus if the velocity can be measured to within 1m/s it should be possible to determine the particle size to within 0.1μm. There are a number of commercial instruments which can measure the ultrasonic velocity to within 0.1m/s and so it should be possible to determine the particle size to within 0.01μm using these instruments. However, many of these instruments work at a single fixed frequency which may not be in the required range.

To demonstrate the potential of the ultrasonic technique for determining particles sizes, the radii of the sunflower oil in water emulsions listed in table 5.1 were calculated from the velocity measurements listed in Appendix VI, table VI.1. This was done by finding the particle size needed in equation 2.11 to give the same prediction of the ultrasonic velocity as the measured values. The best accuracy was obtained by using measurements for each emulsion at a frequency where the velocity dispersion was greatest (≈ 1480m/s, figure 5.2). The results are compared with the values determined by the other techniques in table 5.3.

Table 5.3: Particle sizes determined from ultrasonic velocity measurements

	Ultrasonic technique			Other techniques
	f (MHz)	v (m/s)	r (μm)	r (μm)
A	1.25	1484.3	0.83	0.75
B	1.25	1481.0	0.47	0.42
C	2.25	1480.0	0.25	0.27
D	6.0	1480.6	0.15	0.18
E	6.0	1477.7	0.09	0.14

The droplet radii measured by the ultrasonic technique agree to within 0.1μm of those determined by the other techniques which is reasonable considering the errors in the velocity measurements (±1.0m/s). Also the particle radii determined by the ultrasonic technique will not be the same as the Sauter mean radii (r_{32}) since the velocity measurements are close to the mid-point of the velocity-$\sqrt{fr}$ curve (figure 5.4). However, the particle size distributions are fairly narrow and so the radii determined by the ultrasonic technique should be close to the r_{32} value. The ultrasonic technique has a number of advantages over existing techniques for particle sizing since it can be used to make measurements in emulsions which are optically opaque, in a non-invasive, non-intrusive manner, without dilution.

5.2.3.2 Variation of velocity and attenuation with droplet concentration

The variation of ultrasonic velocity and excess attenuation with droplet mass fraction at 1.25 MHz is presented in figures 5.6-5.13. There is good agreement between the experimental velocity measurements and those predicted using the scattering theory up to relatively high droplet mass fractions (ca. 0.5 w/w) for both O/W and W/O emulsions. The difference between the ultrasonic velocity predicted using equation 2.5 (which assumes no scattering) and the measured velocity increases as the droplet mass fraction increases. In emulsion B (figure 5.8) for example the difference is over 20m/s at a droplet mass fraction of 0.5. The Wood equation should therefore not be used in systems where scattering is important. The

excess attenuation measurements agree reasonably well with the theoretical predictions at the lower droplet mass fractions, considering the experimental errors involved, however, they fall increasingly below the theoretical predictions as the droplet concentration increases. This phenomenon has also been observed by other workers (Abramzon et al 1975, Rozhlenko et al 1974, Javanaud et al 1986). Possible reasons for this deviation are some form of interaction between the droplets, lack of self-consistency in the equations or breakdown of the assumptions underlying the equations (e.g. $\delta t > d$). The variability in the velocity and attenuation measurements in the W/O emulsions (figures 5.12 and 5.13) appear larger than those in the O/W emulsions. This is because this emulsion has the largest particle size and so the effects of scattering are not as dramatic as for the O/W emulsions. Thus the errors in the velocity and attenuation measurements appear larger.

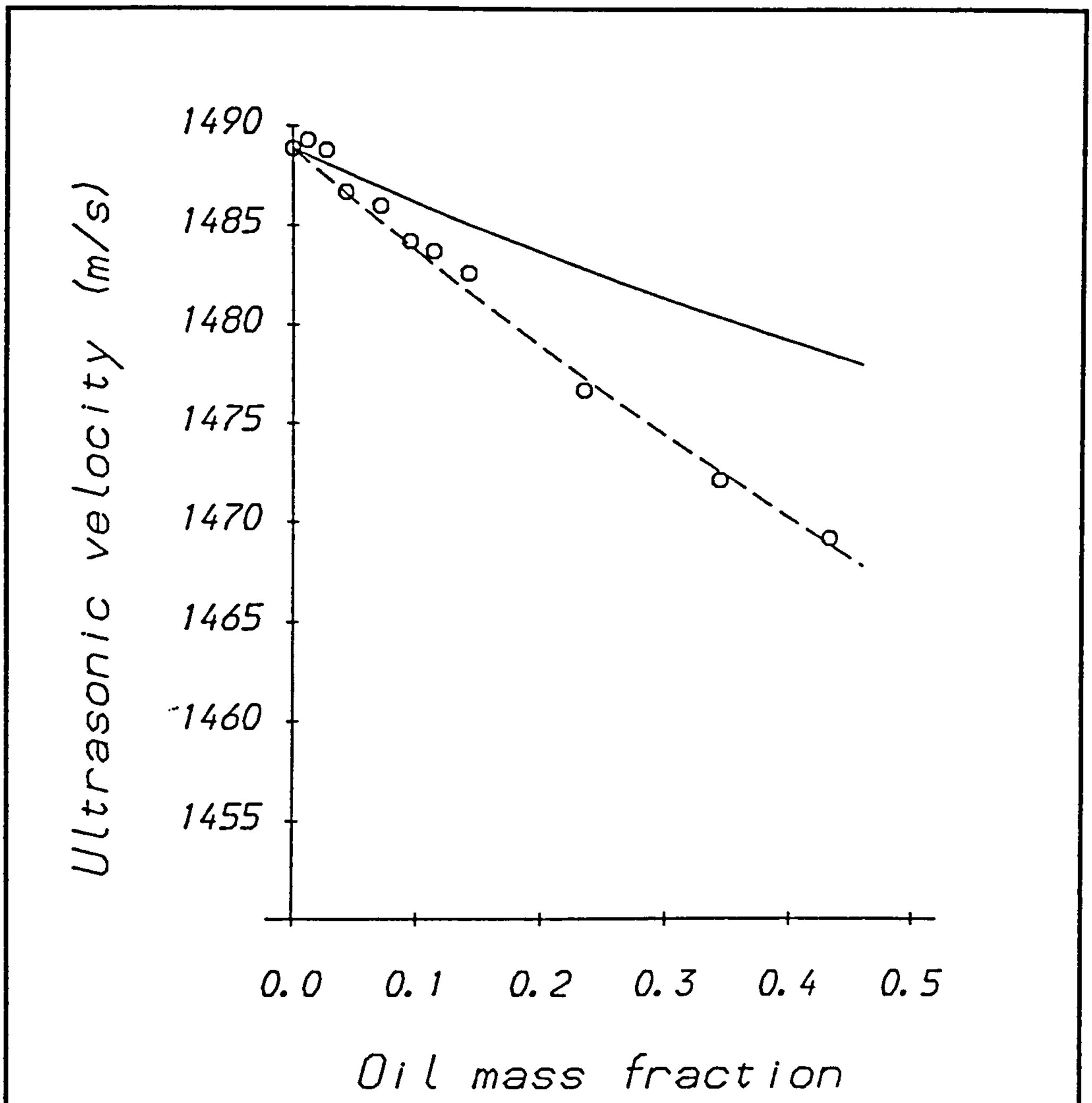

Figure 5.6: Velocity versus oil content (Emulsion A). Variation of ultrasonic velocity with oil mass fraction for a sunflower oil in water emulsion (at 20°C and 1.25MHz). Full curve is the velocity predicted assuming no scattering (equation 2.5), whilst the broken curve is that predicted using multiple scattering theory (equation 5.2).

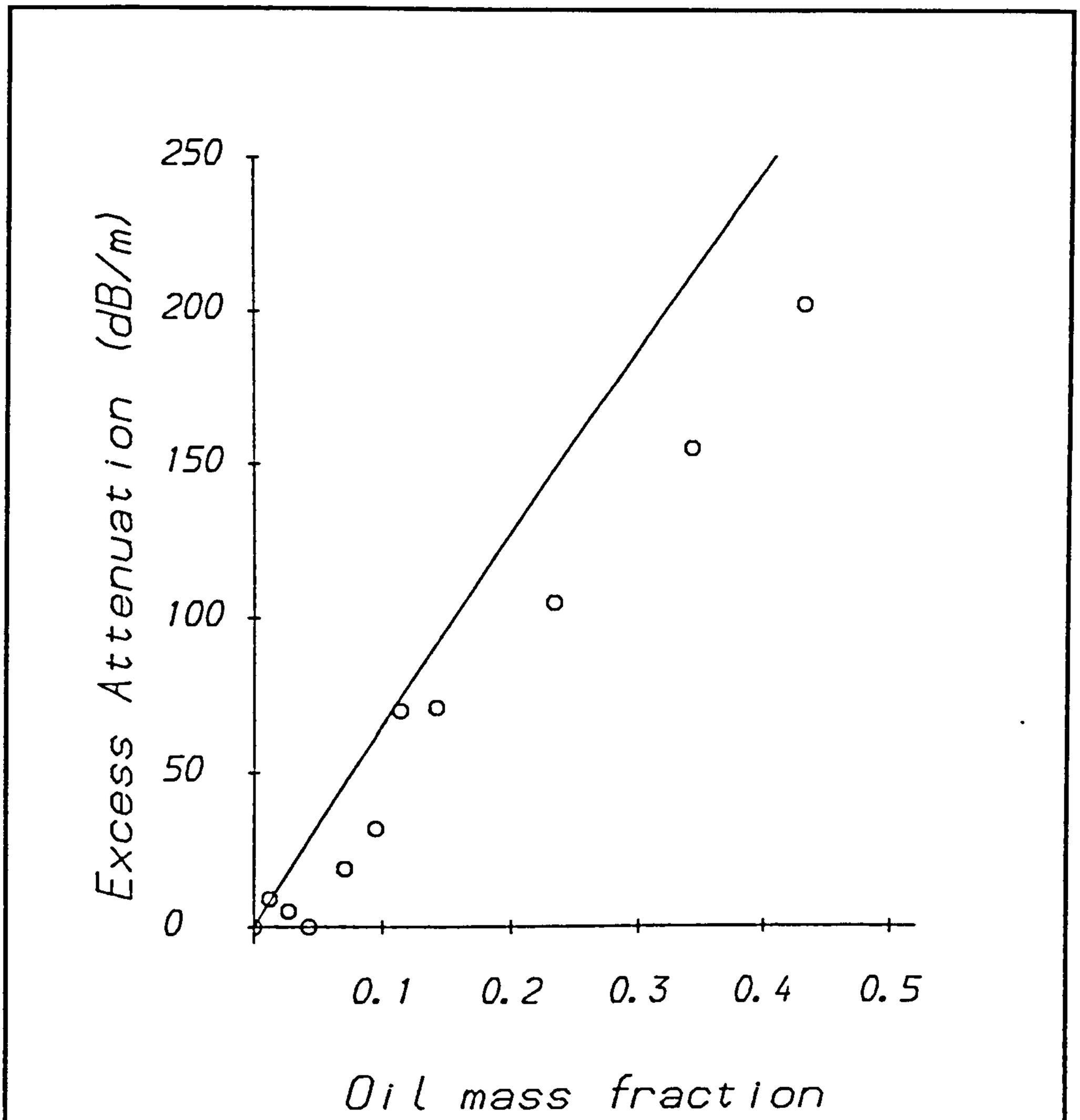

Figure 5.7: Attenuation versus oil content (Emulsion A). Variation of excess attenuation with oil mass fraction for a sunflower oil in water emulsion (at 20°C and 1.25MHz). Curve is the attenuation predicted using multiple scattering theory (equation 5.2).

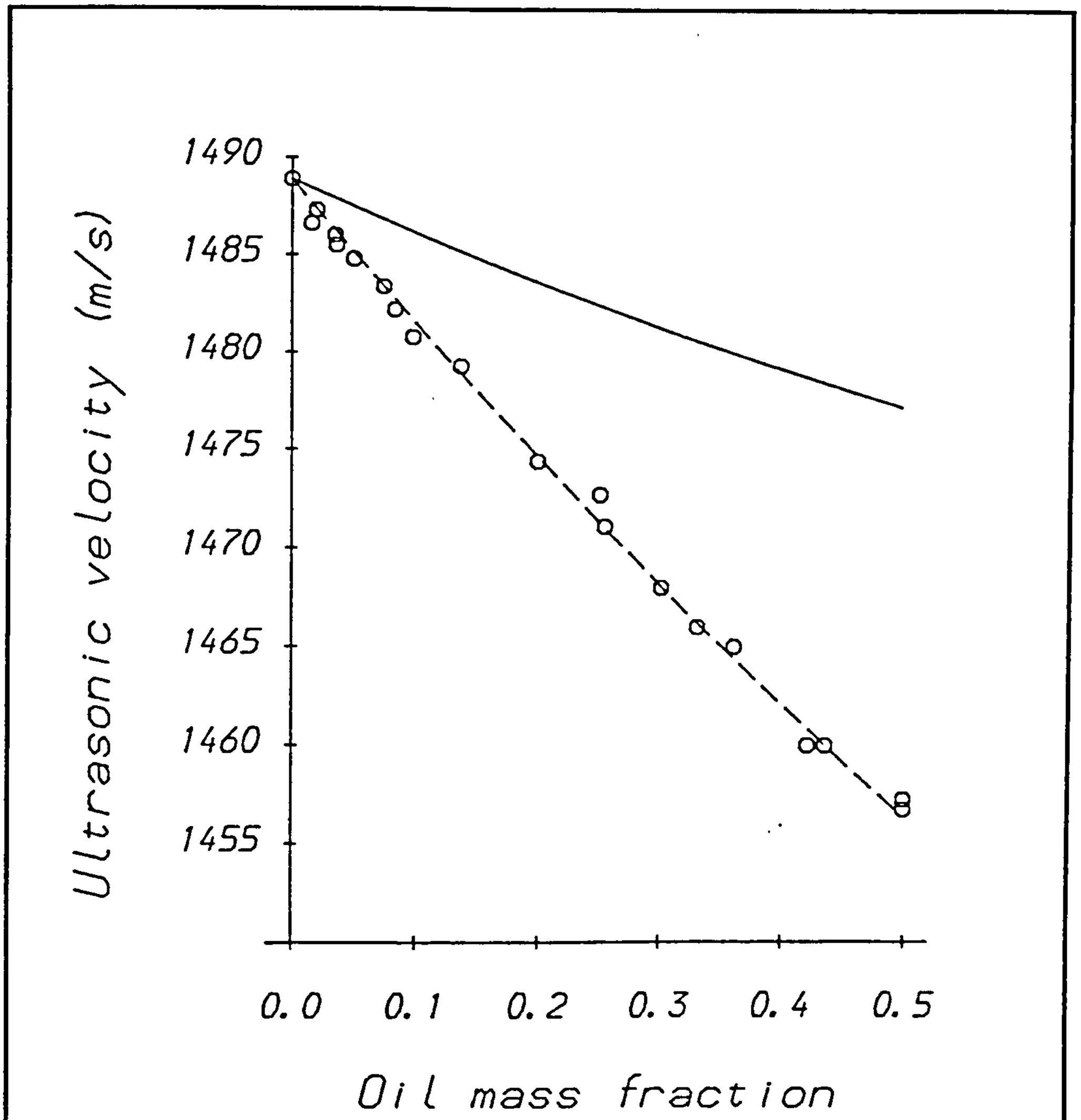

Figure 5.8: Velocity versus oil content (Emulsion B). Variation of ultrasonic velocity with oil mass fraction for a sunflower oil in water emulsion (at 20°C and 1.25MHz). Full curve is the velocity predicted assuming no scattering (equation 2.5), whilst the broken curve is that predicted using multiple scattering theory (equation 5.2).

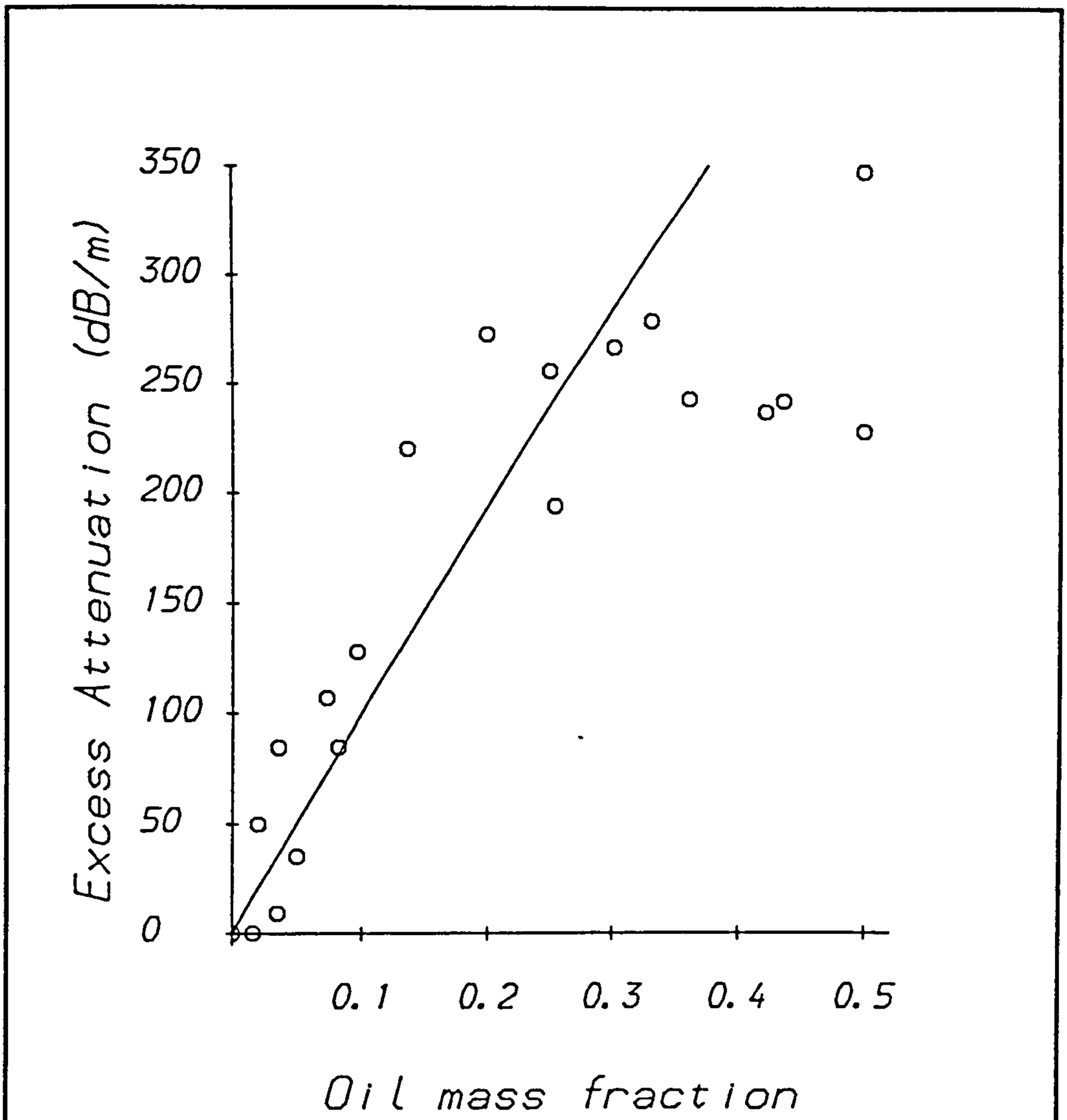

Figure 5.9: Attenuation versus oil content (Emulsion B). Variation of excess attenuation with oil mass fraction for a sunflower oil in water emulsion (at 20°C and 1.25MHz). Curve is the attenuation predicted using multiple scattering theory (equation 5.2).

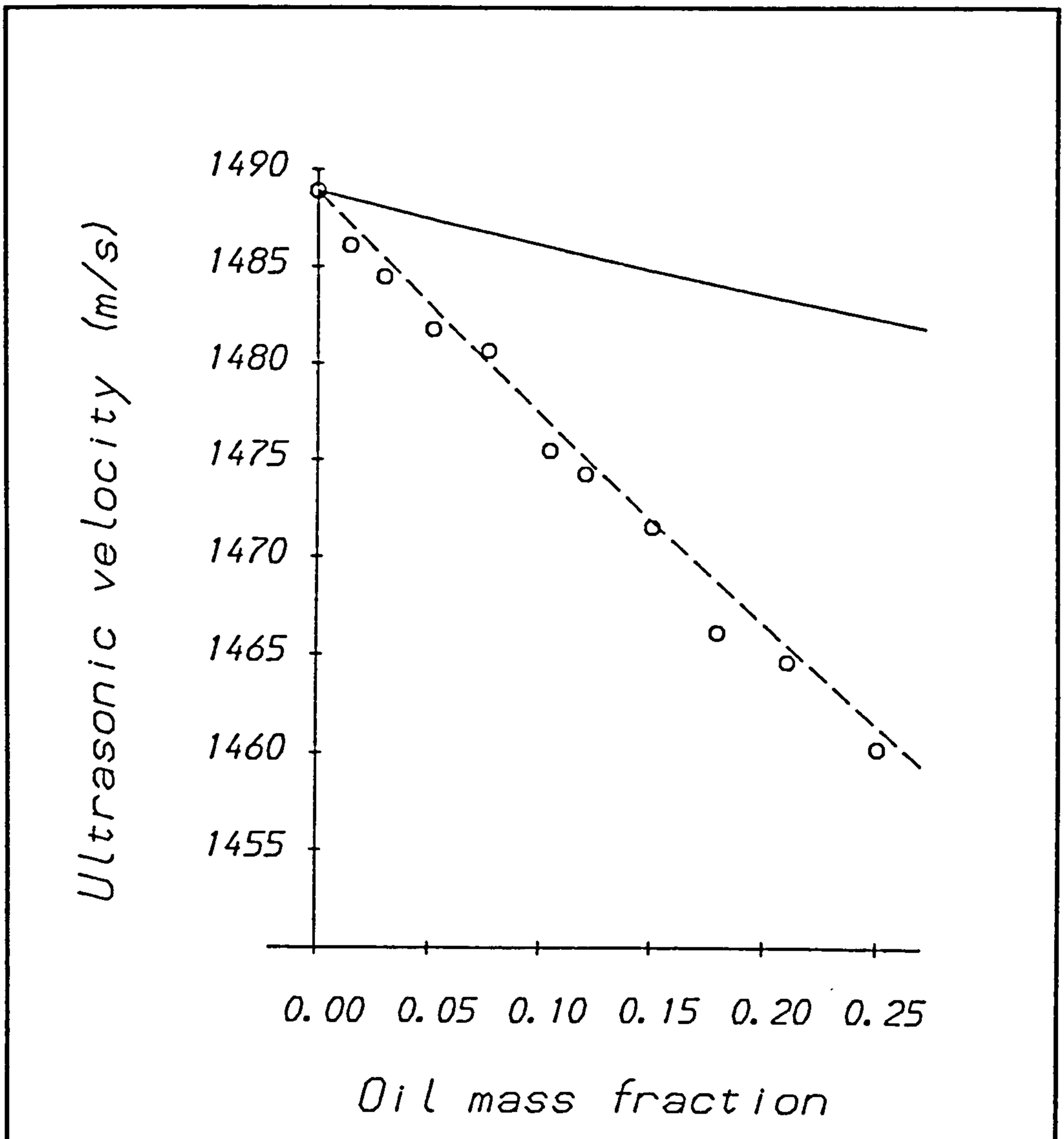

Figure 5.10: Velocity versus oil content (Emulsion D). Variation of ultrasonic velocity with oil mass fraction for a sunflower oil in water emulsion (at 20°C and 1.25MHz). Full curve is the velocity predicted assuming no scattering (equation 2.5), whilst the broken curve is that predicted using multiple scattering theory (equation 5.2).

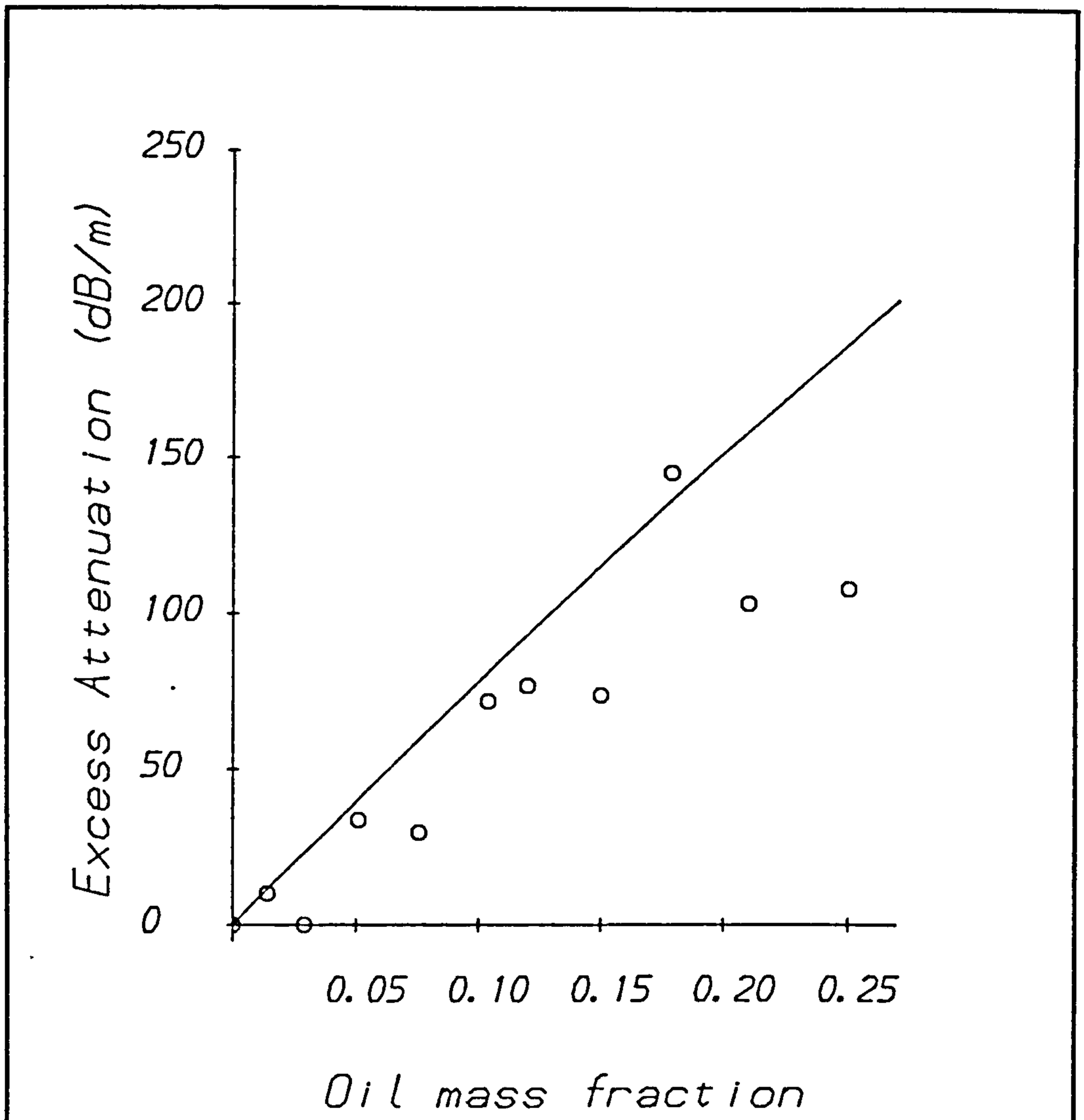

Figure 5.11: Attenuation versus oil content (Emulsion D). Variation of excess attenuation with oil mass fraction for a sunflower oil in water emulsion (at 20°C and 1.25MHz). Curve is the attenuation predicted using multiple scattering theory (equation 5.2).

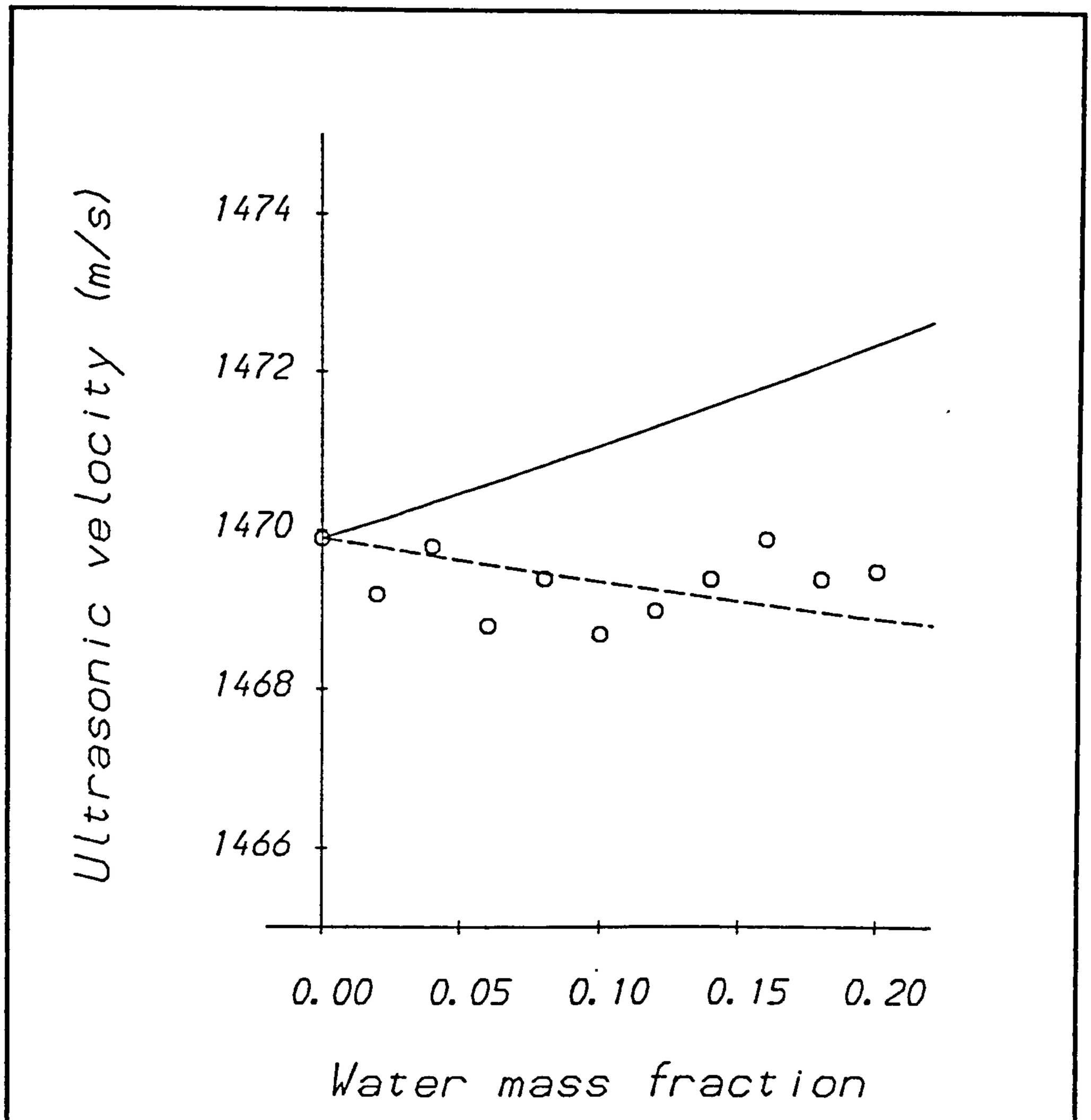

Figure 5.12: Velocity versus water content (Emulsion G). Variation of ultrasonic velocity with water mass fraction for a water in sunflower oil emulsion (at 20°C and 1.25MHz). Full curve is the velocity predicted assuming no scattering (equation 2.5), whilst the broken curve is that predicted using multiple scattering theory (equation 5.2).

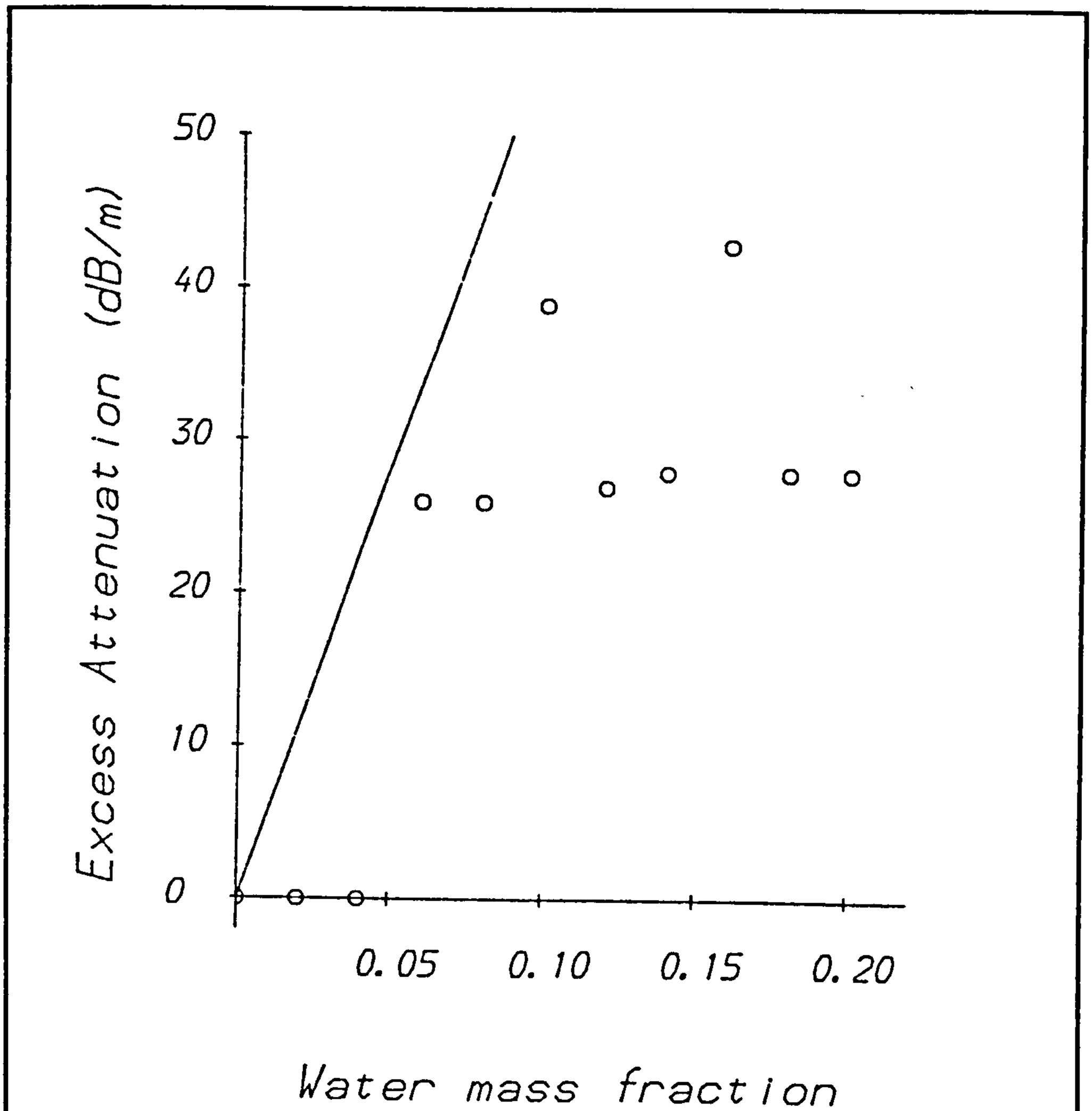

Figure 5.13: Attenuation versus water content (Emulsion G). Variation of excess attenuation with water mass fraction for a water in sunflower oil emulsion (at 20°C and 1.25MHz). Curve is the attenuation predicted using multiple scattering theory (equation 5.2).

The dependence of the ultrasonic velocity and attenuation on the disperse phase volume fraction of emulsions means that the ultrasonic technique should prove a useful means of determining this parameter. There is good agreement between the velocities predicted by the scattering theory and the measured values and so it should be possible to measure the concentration of droplets in an emulsion from ultrasonic velocity measurements using scattering theory. The oil contents of the serial dilutions of emulsion A were determined using the ultrasonic velocity measurements shown in figure 5.6 and the results are presented in table 5.4. There is good agreement between the disperse phase mass fractions determined by the ultrasonic technique and the actual values. The deviations are probably due to inaccuracies in the velocity measurements (± 1m/s). The accuracy to which the disperse phase mass fraction can be measured also depends on the magnitude of the change in velocity with change in droplet concentration, which in turn depends on the particle size and the difference in velocity between the component phases.

Table 5.4: Oil contents determined from ultrasonic velocity measurements.

Initial Oil content (% w/w)	v (m/s)	Predicted oil content (% w/w)
1.2	1489.3	-
2.7	1488.8	0.0
4.3	1486.7	4.4
7.1	1486.0	5.9
9.5	1484.2	9.7
11.4	1483.7	10.7
14.2	1482.6	13.2
23.4	1476.7	26.2
34.3	1474.3	37.0
43.2	1469.2	44.2

5.2.3.3 Effects of multiple scattering

It is useful to examine the effect of the multiple scattering (ϕ^2) terms in equation 2.11 on the theoretical predictions of velocity and attenuation. For droplet mass fractions up to 0.1 the multiple scattering terms make very little difference to the calculations of velocity and attenuation (figures 5.14-5.15). For larger values these terms become increasingly important. At a mass fraction of 0.5 the velocity predicted assuming single scattering is about 2.6 m/s below that predicted assuming multiple scattering, whilst the excess attenuation is greater by about 5%. Figure 5.14 shows clearly the need to include the multiple scattering terms in the equations so as to obtain a good fit between theory and experiment for emulsions with large droplet concentrations. The difference between the velocities and attenuations predicted by the Lloyd and Berry (1967) and the Waterman and Truell (1961) formulations is small; the velocity predicted by Waterman and Truell is about 0.2m/s larger than that predicted by Lloyd and Berry at a mass fraction of 0.5 whilst the attenuation values are within 0.5%. Thus either approach may be used to interpret results in the systems examined in this work.

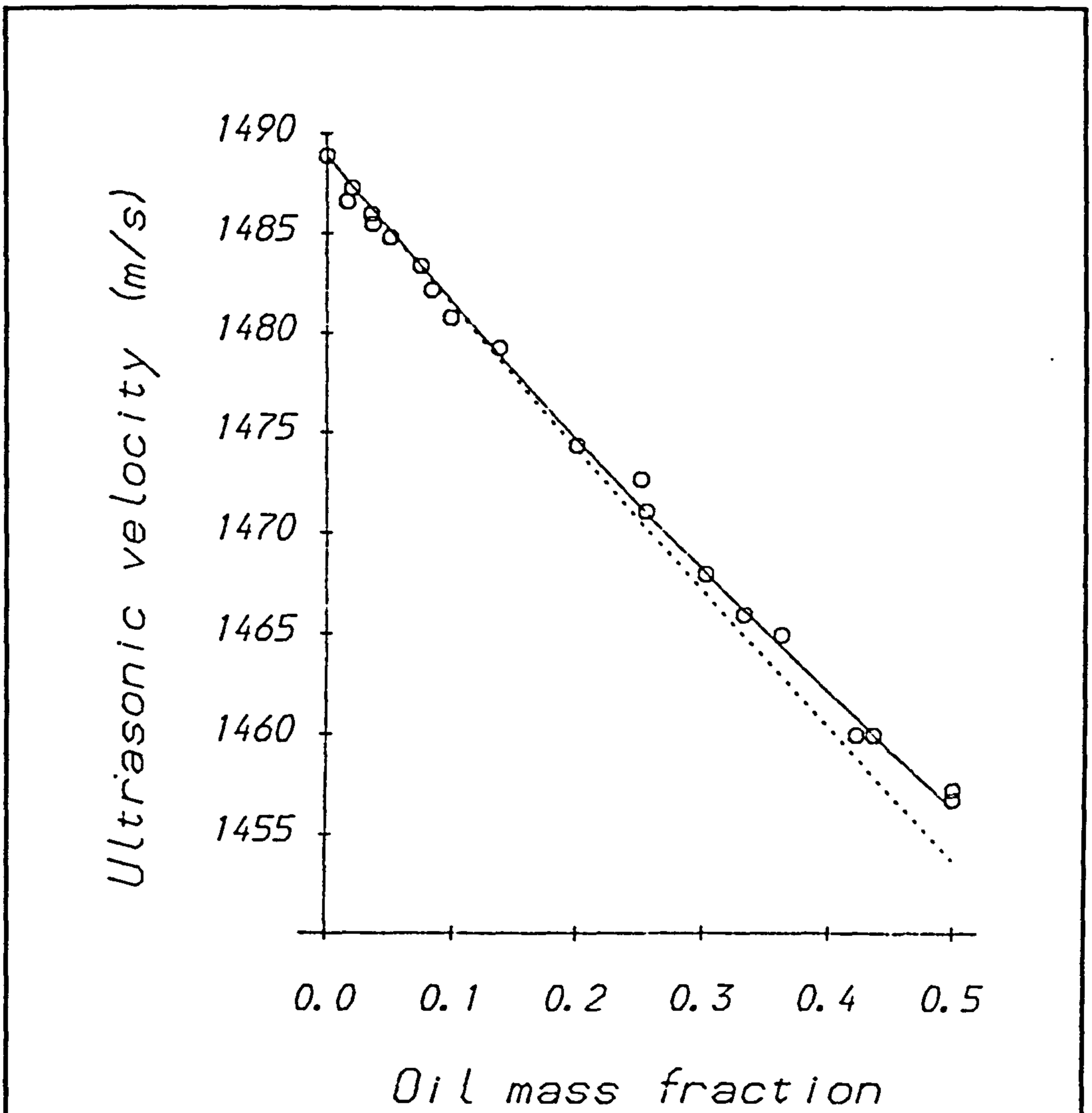

Figure 5.14: Effects of multiple scattering on velocity. Predictions of the ultrasonic velocity in emulsion B including (——) and excluding (- - -) the multiple scattering terms in equation 5.2.

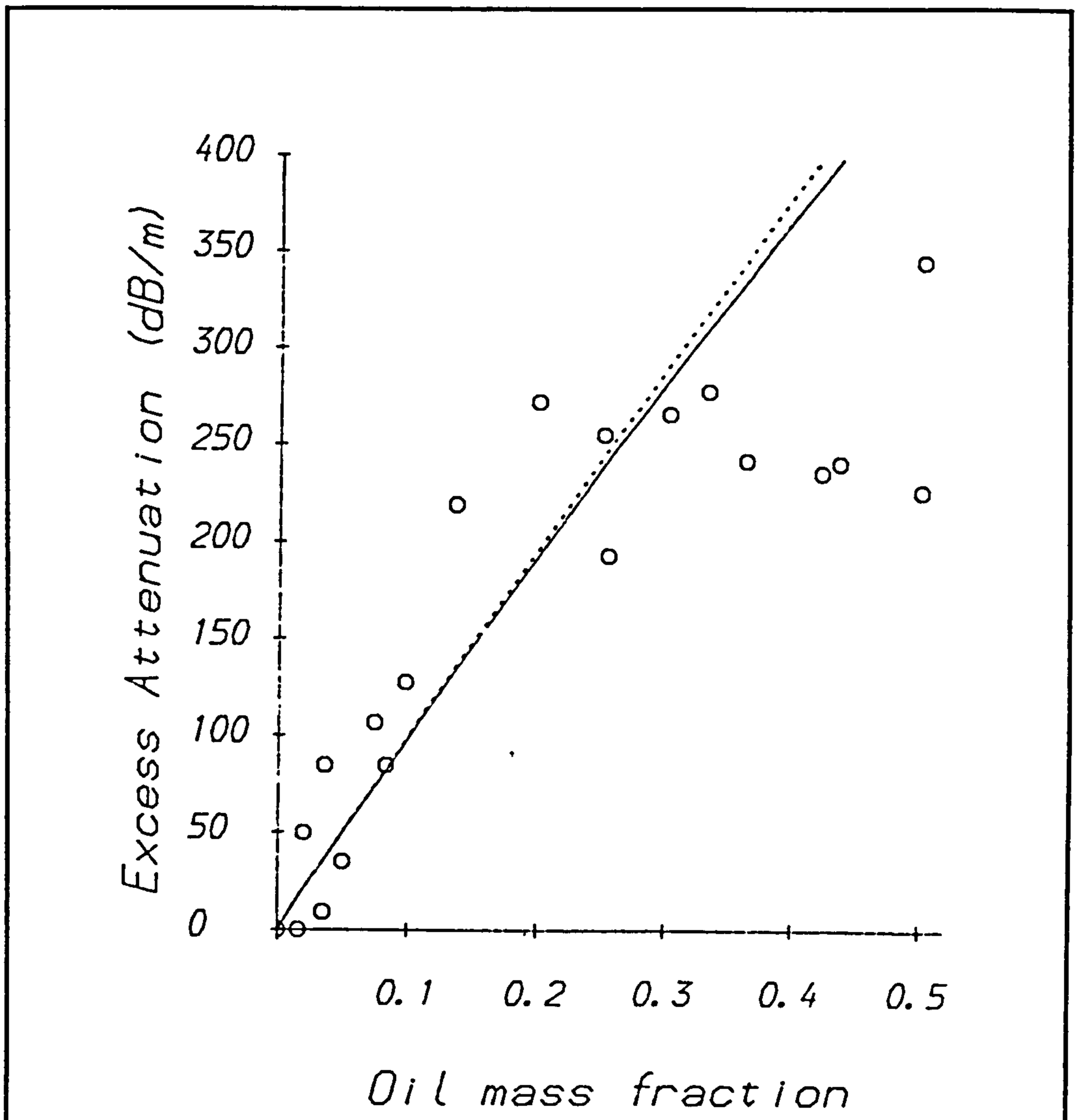

Figure 5.15: Effects of multiple scattering on excess attenuation. Predictions of the excess attenuation in emulsion B including (——) and excluding (- - -) the multiple scattering terms in equation 5.2.

5.3 Measurements in W/O emulsions containing solid fat crystals

5.3.1 Introduction

A number of food emulsions contain partially solidified fat, e.g. margarines, butters and low fat spreads contain aqueous droplets and fat crystals suspended in a continuous oil phase. The quality of these foods and their suitability for particular applications depend on their physical characteristics. For example the rheological properties of margarines depend on their SFC (Haighton 1976), whilst their organoleptic and microbiological properties depend on the size and concentration of the aqueous droplets (Dickinson and Stainsby 1982). The commercial importance of these products has led to the development of a number of techniques for measuring their properties. Most of the traditional techniques are laborious and time consuming: the water content of margarines and low fat spreads is usually measured gravimetrically by weighing a sample before and after the water has been evaporated off (Anderson and Williams 1954), whilst the particle size distribution of the water droplets is determined using light microscopy (Chrysam 1985). Consequently there has been considerable interest in the development of rapid instrumental techniques for measuring SFCs, water contents and droplet sizes of margarines, butters and low fat spreads. Pulsed NMR may be used to determine SFCs and water contents in a number of emulsions (section 4.1.3) and may also be used to determine droplet sizes. In this section the possiblity of using ultrasonics for characterising partially crystalline W/O emulsions is investigated. Measurements of the ultrasonic velocity were made with increasing temperature (5-65°C) for a series of water in tristearin/sunflower oil emulsions and for a number of margarines and low fat spreads.

5.3.2 Materials and Methods

5.3.2.1 Materials

The tristearin and sunflower oil were the same as those used in chapter 4. Echo margarine, Flora margarine and Outline low fat spread were obtained from the Co-operative wholesale society Ltd, Manchester. The ingredients listed on the packaging of the three commercial products are included below.

Flora Sunflower oil, vegetable oils, hydrogenated vegetable oils, whey salt, whey solids, emulsifiers (Lecithin E471), colours (annatto, curcumin), flavouring, vitamins A and D.

Echo Animal and vegetable oils, whey salt, whey solids, emulsifiers (Lecithin E471), colours (annatto, curcumin), flavouring, vitamins A and D.

Outline Water, vegetable oils, hydrogenated vegetable oils, butter milk, gelatine, salt, emulsifiers (mono- and di- glycerides), preservative (Potassium sorbate), colours (annatto, curcumin), lactic acid, flavouring, vitamins A and D.

5.3.2.2 Preparation of samples and ultrasonic measurements

The water/tristearin/sunflower oil emulsion was prepared using a procedure similar to that described in section 5.2.2 but with the following differences. The 'oil' phase was prepared by weighing tristearin powder (10%), sunflower oil (78%) and Admol Wol (2%) into a 150cm^3 conical flask, melting at 80°C, mixing thouroughly then degassing for 30mins at 600mmHg and 80°C. Distilled water was then added to some of the mixture to make up a 15% W/O emulsion (w/w) and this system was mixed and homogenised as described in section 5.2.2. Once the emulsion had been prepared serial dilutions were made with some of the original 'oil' phase. The emulsions were then cooled rapidly to 5°C in a water bath, and left over night, to ensure complete crystallization of the tristearin. Measurements of the ultrasonic velocity were then made with increasing temperature (5-65°C) at 1.25 MHz using the pulse echo technique described in chapter 3. The ultrasonic velocity of the margarine and

low fat spread samples were also measured at 1.25 MHz with increasing temperature (5-60°C), using the same method as described for the commercial fat/oil products in section 4.4.2. At the higher temperatures, where the fat crystals had melted, all the water/fat/oil emulsions had to be stirred vigourously before measurements were made since appreciable sedimentation of the aqueous phase droplets occured (see below).

5.3.2.3 Characterisation of samples

The water content of the Flora margarine, Echo margarine and the Outline low fat spread were determined gravimetrically by Unilever Research laboratories (URL), Colworth House, U.K. This was done by weighing a sample on a four decimal place balance before and after the water phase had been evaporated off. The water contents of the three products were determined to be 16.3% w/w for Flora, 16.2% for Echo and 58.5% for Outline. Values for the solids non fat (SNF) of the commercial products were also obtained from URL, typical values were 1% for the Flora and Echo margarines and 4% for the Outline. The variation of SFC with temperature of the samples was determined using the same pNMR method as that used for the commerical fat/oil samples (section 4.4.2).

The Sauter mean radius of the water in tristearin/sunflower oil emulsion was determined by light microscopy, by measuring the diameter of at least 1500 particles per sample, and was found to be 2.15μm. The particle size distribution of the margarines and the low fat spread are illustrated in photographs 5.1 to 5.3. The droplets in the low fat spread (photograph 5.3) are considerably larger than those in the margarines (photographs 5.1 and 5.2). The average particle size of the water/tristearin/sunflower oil emulsions, the margarines and the low fat spread samples are all much greater than those of the sunflower oil in water emulsions examined in section 5.2. Thus the effects of scattering should not be as important. However, the relatively large droplet size meant that sedimentation was appreciable at high temperatures where the fat crystals had melted. At these temperatures the samples had to be stirred vigoursly before ultrasonic measurements were made so as to redisperse the aqueous droplets. Sedimentation is not a problem at temperatures where the

fat phase is partially crystalline since the water droplets are restrained mechanically by the crystal matrix (e.g. photograph 5.4).

Photograph 5.1. Bright-field photograph of Echo margarine (x1000 magnification).

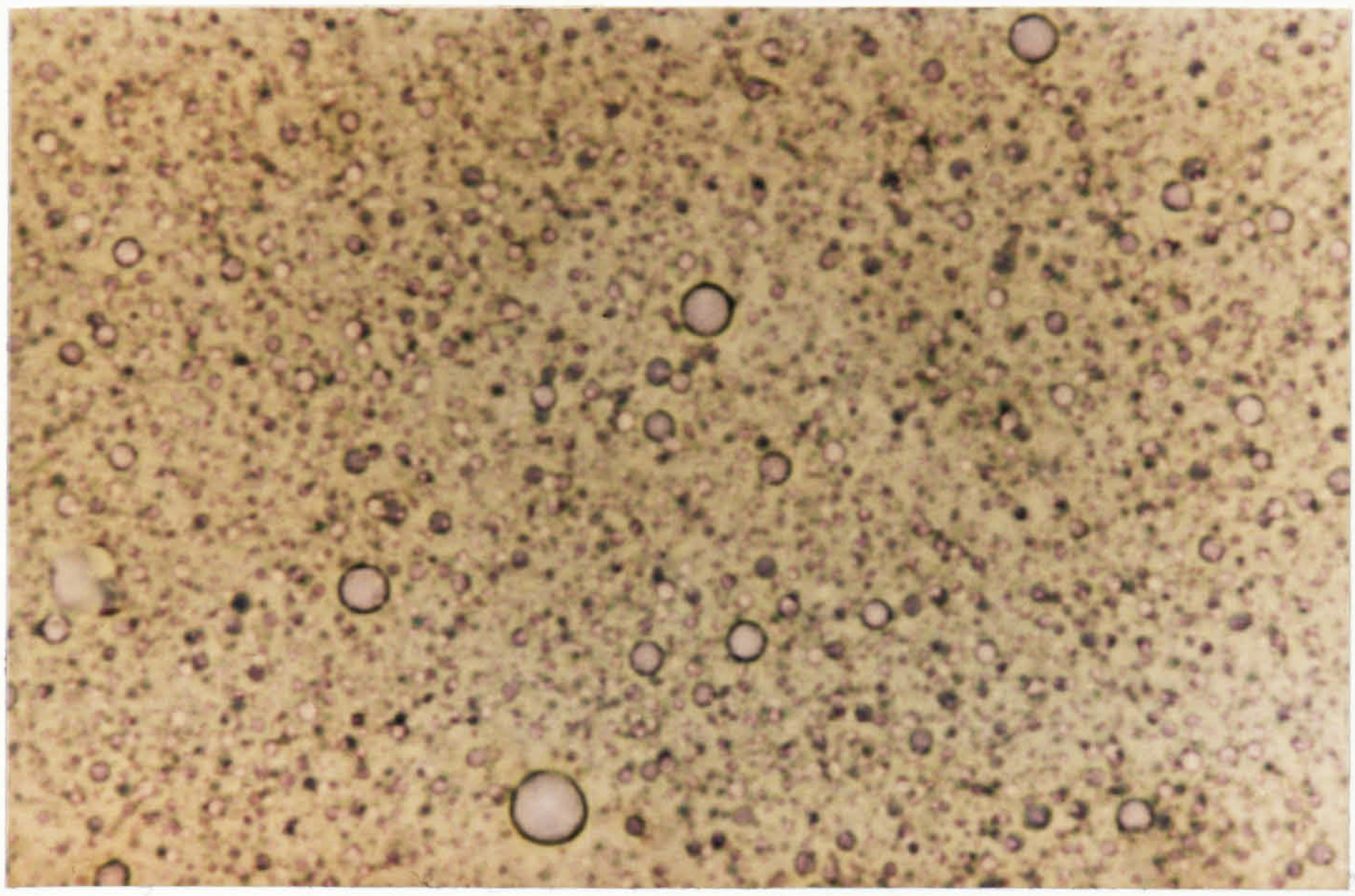

Photograph 5.2. Bright-field photograph of Flora margarine (x1000 magnification).

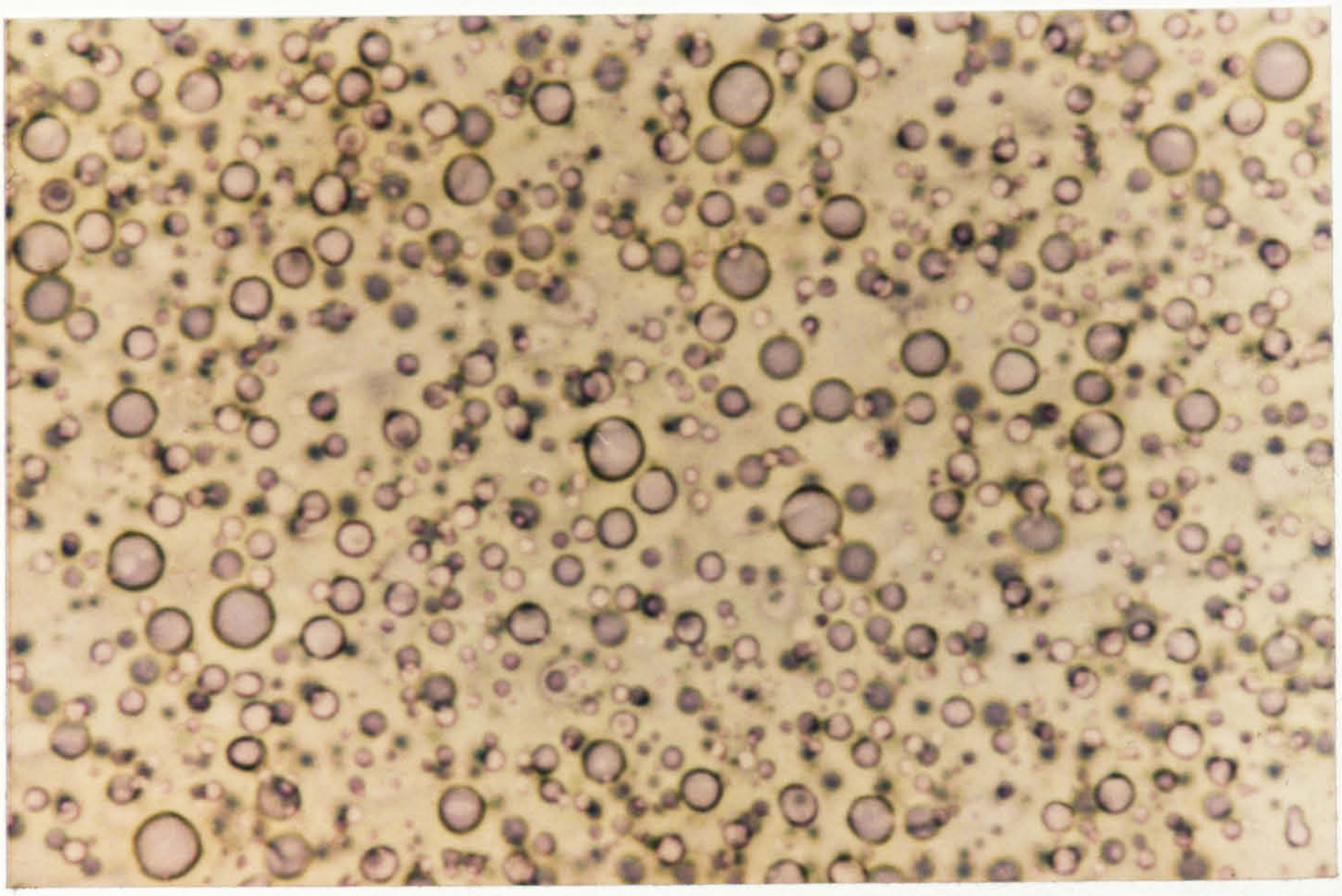

Photograph 5.3. Bright-field photograph of Outline low fat spread (x 500 magnification).

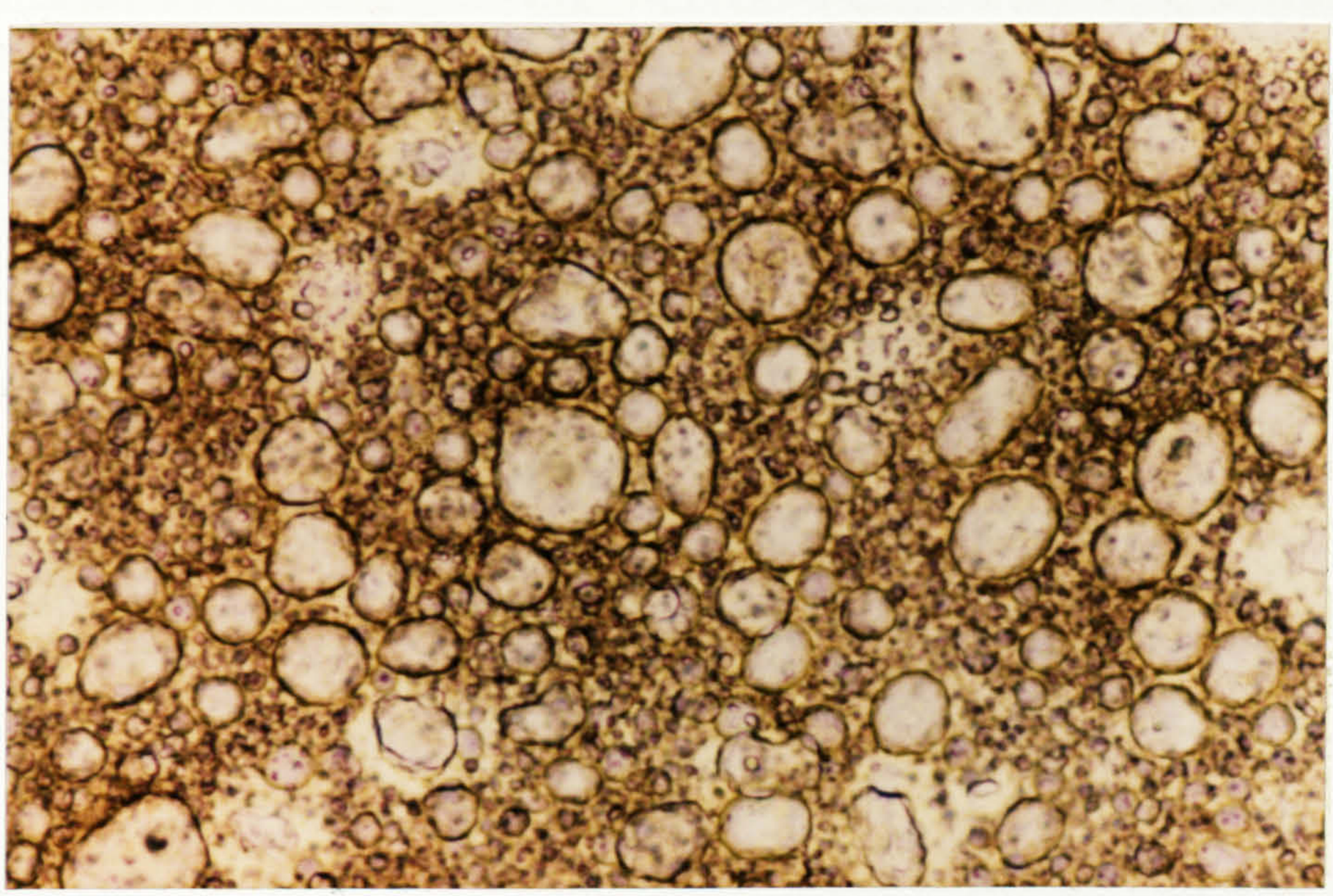

Photograph 5.4. Photograph of Outline low fat spread under polarised light (x 500 magnification). The water droplets are constrained mechanically by the matrix of fat crystals.

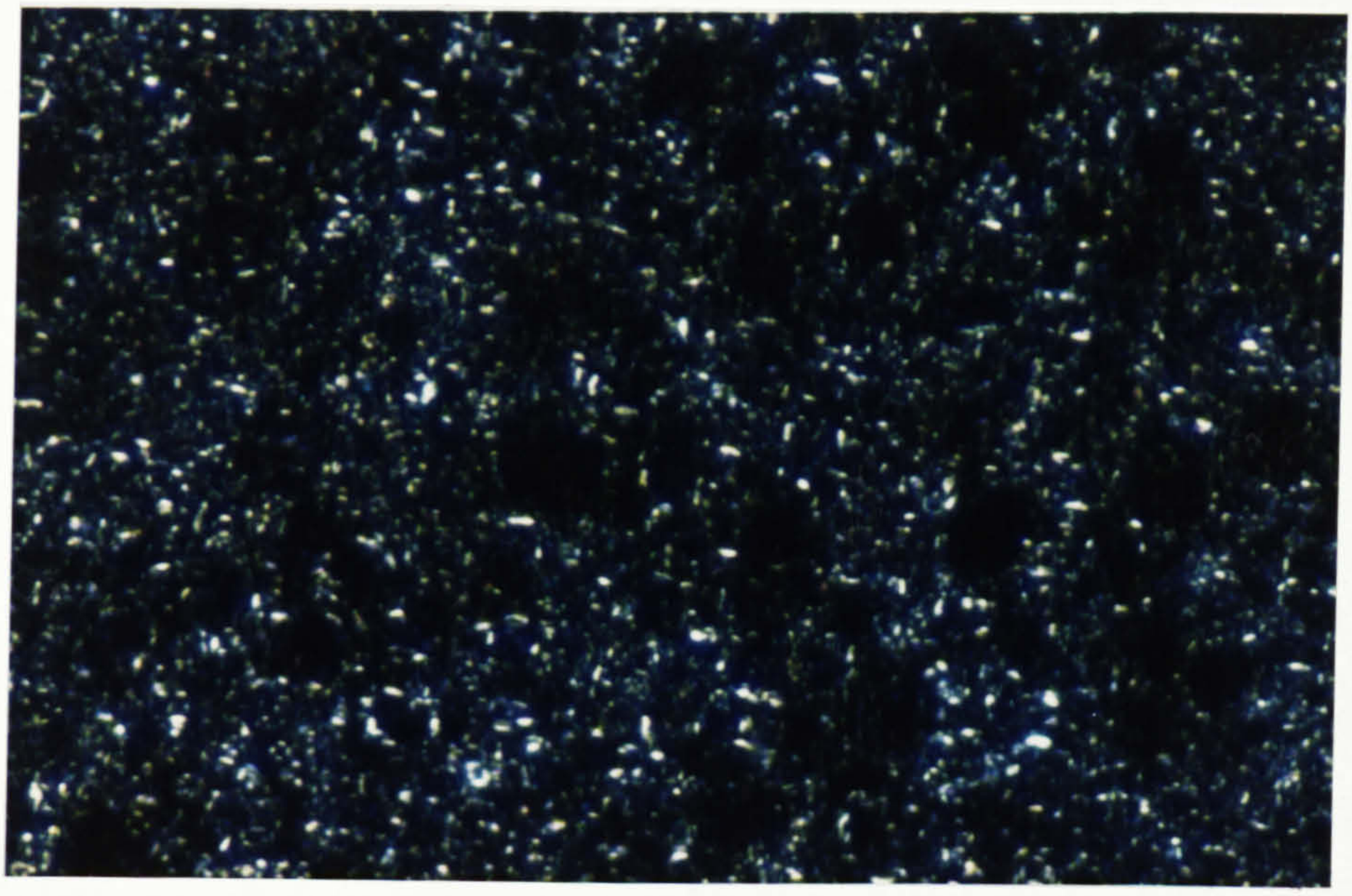

5.3.3 Results and discussion

5.3.3.1 Water/tristearin/sunflower oil emulsions

Measurements of the ultrasonic velocity with increasing temperature for a series of 10% tristearin in sunflower oil mixtures of varying water content (0-15%) are included in table VI.3, Appendix VI. The results for the tristearin in sunflower oil mixture and the 15% water/tristearin/sunflower oil emulsion are plotted in figure 5.16 with the values for sunflower oil (table 4.5). These measurements show that, although there is still a region where the velocity decreases rapidly with increasing temperature due to the melting of the

triglyceride phase (section 4.2.3.3), the addition of water to the tristearin/oil mixtures modifies the velocity-temperature profiles. The overall decrease in ultrasonic velocity with temperature is less in the emulsions than in the fat/oil mixture. This is because water has a positive temperature coefficient of velocity (up to 74°C), i.e. its velocity increases with increasing temperature, whereas fats and oils have negative temperature coefficients and so a mixture of fat and water has a less negative temperature coefficient than that of pure fat.

Table VI.3, Appendix VI, shows that there is no significant change in ultrasonic velocity with increasing water content in the emulsions at a temperature of about 23.3°C. The temperature at which this phenomenon occurs will be called the constant velocity temperature (CVT). At temperatures greater than the CVT the velocity of the emulsions is larger than that of the tristearin/sunflower oil mixture and the velocity increases with increasing water content. At temperatures lower than the CVT the velocity of the emulsions is lower than that of the tristearin/sunflower mixture and the velocity decreases with increasing water content. The temperature at which the CVT occurs depends on a number of factors. The most important of these are the velocities of the fat and aqueous phases and the magnitude of any scattering effects. In systems where scattering is not important the CVT occurs when the velocities of the fat and aqueous phases have similar velocities. In a system where scattering is important the fat and aqueous phases may have similar velocities, but the velocity of an emulsion may still vary significantly with water content due to scattering effects. It can be seen that the CVT of the emulsions included in table VI.3, Appendix VI occurs at a temperature where the 10% tristearin in sunflower oil mixture and distilled water have similar ultrasonic velocities and so the effects of scattering must be small. This is because the particle size of the emulsions is relatively large (2.15μm) and so the velocity dispersion due to thermal scattering is not appreciable. Indeed the velocities of the emulsions predicted by the Wood equation, which assumes no scattering, and those predicted using the scattering theory agreed to within 1m/s. The velocity of a fat phase depends on the type and amount of triglycerides present, the SFC and the presence of any

additional ingredients such as surfactants, colourings or vitamins. If a fat phase had a higher velocity than the one used in this work, e.g. a larger SFC, then the temperature where the water and the fat phase have the same velocity would occur at a higher temperature i.e. the CVT occurs at a higher temperature. Conversely, if a fat phase had a lower velocity than the one used in this work the CVT would occur at a lower temperature. The actual temperature would also depend on the presence of any additional ingredients in the aqueous phase. The velocity-temperature profile of a particular water/fat/oil system therefore depends primarily on the magnitude of scattering, the solid fat content and the amount of water phase present.

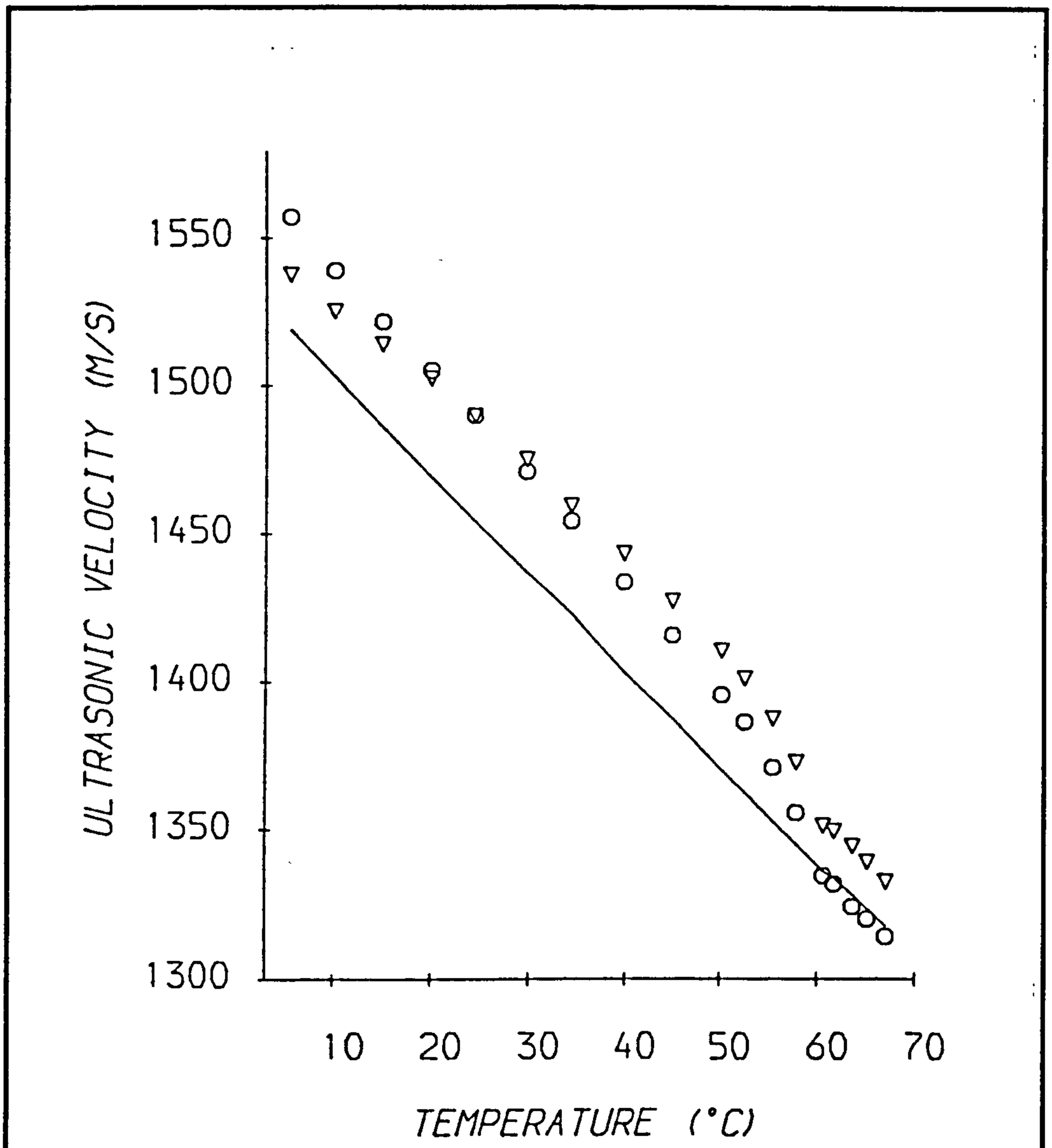

Figure 5.16: Velocity-temperature profile of water/tristearin/sunflower oil emulsion. Annotation: O = 10% w/w tristearin in sunflower oil mixture, ∇ = 15% w/w water in tristearin/sunflower oil mixture and curve is sunflower oil.

Water content and droplet size determination The water content and droplet size of the water/tristearin/sunflower oil emulsions could be determined at temperatures where the tristearin is partially crystalline, once the SFC and the thermophysical properties of the water, tristearin and sunflower oil are known, by measuring the velocity and/or attenuation as a function of frequency as described in section 5.2.3. It should also be possible to determine the water content and particle size irrespective of the SFC by measuring the ultrasonic velocity at a temperature where all the fat crystals have melted, since the system can then be thought of as a two phase W/O emulsion. The Sauter mean radius of the emulsions as determined by light microscopy was 2.15μm and so the effects of scattering were small, even at 1.25MHz. To measure the particle size of these systems ultrasonic measurements would have to be made at much lower frequencies than were possible in this work. The water content of the emulsions used in this work were determined at 10°C, a temperature well below the CVT so that the change in velocity with water content was significant, and at 65°C where all the solid fat had melted out, using the thermophysical properties of the component phases at these temperatures and ultrasonic scattering theory (equation 2.11). The results are listed in table 5.5.

Table 5.5: Ultrasonic water content determinations in fat/oil/water mixtures

Initial water content (w/w)	Measured water content (w/w) 10 °C	65 °C
5%	4.8%	4.5%
10%	8.7%	8.5%
15%	13.3%	13.7%

The measured water contents are significantly lower than the amount of water added initially at both temperatures. At 10°C this is probably because some sedimentation of the water droplets occured before the tristearin had time to crystallise when the samples were prepared initially. Indeed when samples were taken from the top and bottom of the 15%

water/tristearin/sunflower oil mixture and their water content measured gravimetrically, it was found that the water content at the top of the samples was about 13% whereas that at the bottom was about 16%. The low values at the higher temperature is probably because some sedimention of the water droplets occured between stirring the samples and making the ultrasonic measurements. To measure the water content at these higher temperatures it would be necessary to design an experimental apparatus which stirred the samples continuously during measurements.

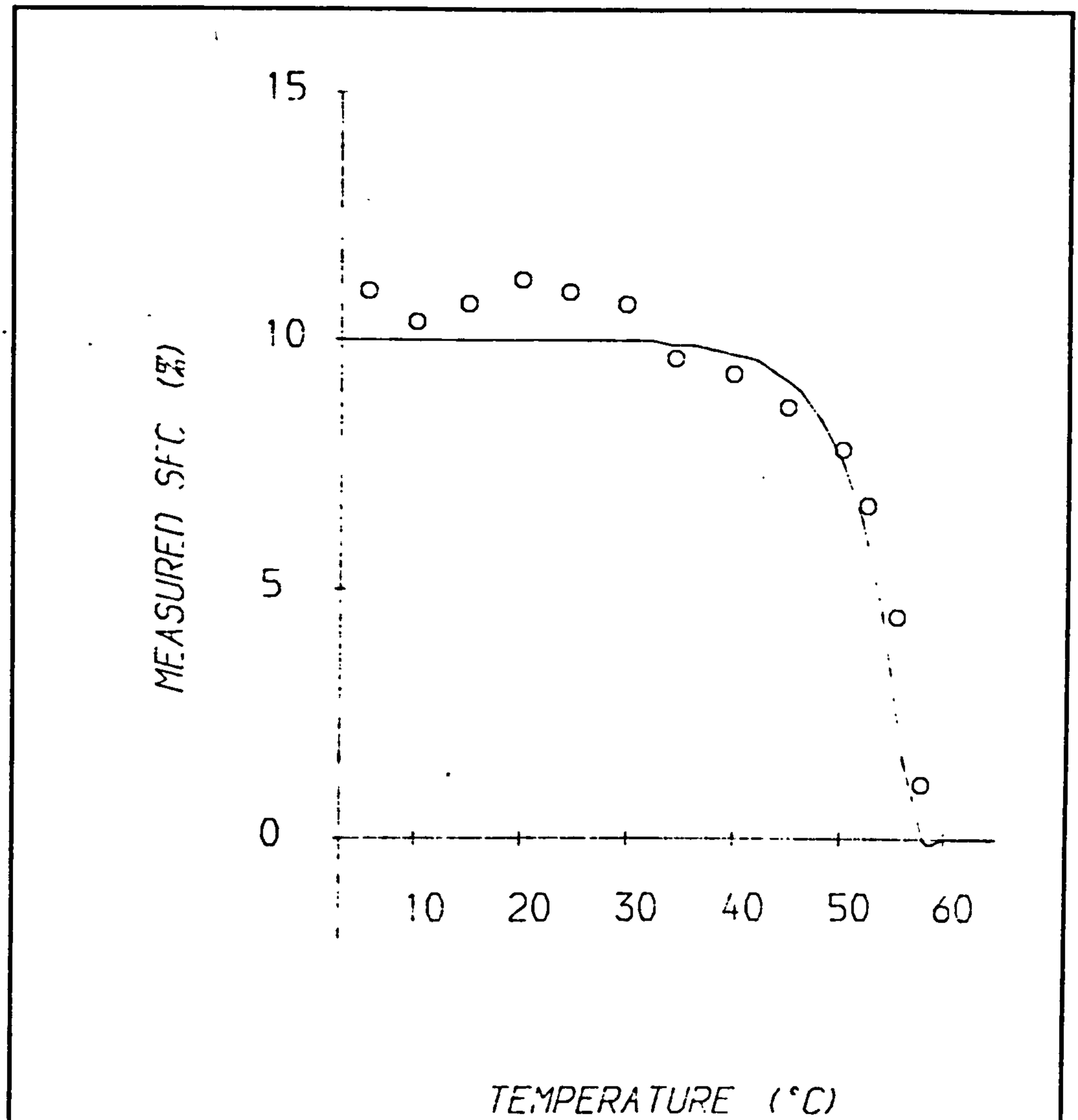

Figure 5.17: SFC versus temperature for water/tristearin/sunflower oil mixture. Annotation: O = SFCs determined from ultrasonic velocity measurements, whilst the curve is a prediction of the SFC assuming ideal solubility (equations 4.11 and 4.12).

SFC determination Due to the sedimentation of the water droplets at the higher temperatures it is not possible to use the same method of calculating the SFC as was used for the tristearin in oil mixtures described in section 4.2.3.3, because the velocity of the systems at the higher temperatures could not be measured reliably. However, a modification of the empircal approach described in section 4.2.3.1 can be used. For a water/fat/oil system the ultrasonic velocity can be described to a first approximation by the following equation (see equation 4.10):

$$\frac{100}{v_{mix}^2} = \frac{SFC}{v_{fat}^2} + \frac{\phi}{v_{aq}^2} + \frac{(100-SFC-\phi)}{v_{oil}^2} \qquad (5.3)$$

where ϕ is the aqueous phase content (% w/w), v_{aq} is the velocity of the aqueous phase, v_{oil} is the velocity of the oil phase, and v_{fat} is the empirical parameter determined in section 4.2.3.1. This equation assumes that the densities of the various phases are similar and that the effects of scattering are small. Equation 5.3 can be rearranged in the following manner:

$$SFC = \frac{100\left(\frac{1}{v_{mix}^2} - \frac{1}{v_{oil}^2}\right) + \phi\left(\frac{1}{v_{oil}^2} - \frac{1}{v_{aq}^2}\right)}{\left(\frac{1}{v_{fat}^2} - \frac{1}{v_{oil}^2}\right)} \qquad (5.4)$$

Thus the SFC of a water/fat/oil mixture can be determined at any temperature by measuring the velocity of the mixture, once the water content and the velocity of the oil and aqueous phases are known. Using the velocity of distilled water taken from Del Grosso and Mader (1972), assuming the velocity of the oil phase to be similar to that of sunflower oil (table 4.5) and using the value of ϕ determined at 10°C the variation of the SFC of the water/tristearin/sunflower oil mixture was calculated from the velocity measurements shown in figure 5.16. The results are included in figure 5.17, where they are compared with the values of SFC predicted using the ideal solubility equation (equations 4.11 and 4.12). There is reasonable agreement considering the assumptions made in the calculations, the values determined ultrasonically being within 1% of the predicted values. The reason the measured values are slightly above the predicted values at the lower temperatures is probably because

some impurities in the sunflower oil crystallised out with the tristearin. This phenomena was also observed for the tristearin in sunflower oil mixtures examined in section 4.3.3 (see table 4.10).

Ultrasonics would therefore appear to be a useful means of investigating phase transitions in water/fat/oil systems as well as the fat/oil systems examined in section 4.2.3.3 and may prove a useful adjunct or alternative to existing methods for this type of determination.

5.3.3.2 Margarines and Low Fat spread

Measurements of the ultrasonic velocity of Flora margarine, Echo margarine and Outline low fat spread with increasing temperature at 1.25MHz are shown in figure 5.18. It can be seen that they all have different velocity-temperature profiles. The velocities of the Echo and Flora margarines are similar at the higher temperatures (> 35 °C), however, at the lower temperatures the velocity of the Echo is considerably larger than that of the Flora. This is because at the higher temperatures all the solid fat crystals have melted and so the systems are effectively W/O emulsions. Since the effects of scattering are small, and both margarines have similar water and SNF contents their velocities would be expected to be similar. The slightly lower velocity of the Echo at high temperatures is probably because the velocity of its oil phase is lower than that of the Flora margarines. As the temperature decreases the velocity of the Echo increases significantly above that of the Flora since it has a larger SFC (see later). The overall decrease in velocity with increasing temperature of the Outline is significantly less than that of the two margarines; this is because it has a larger water content (see section 5.3.3.1).

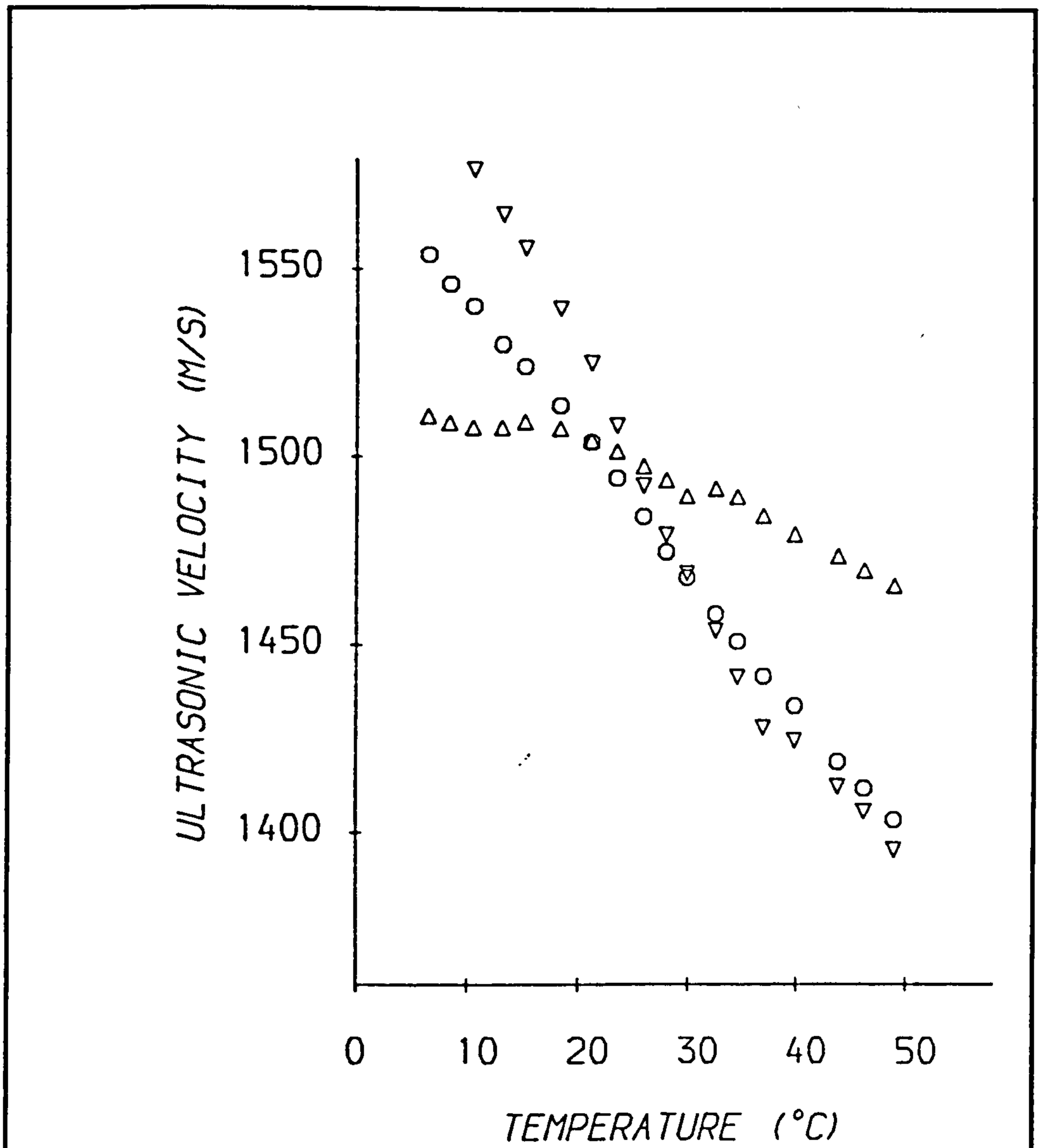

Figure 5.18: Velocity-temperature profile of commercial fats. Annotation: O = Flora margarine, ∇ = Echo margarine, Δ = Outline low fat spread.

It should be possible to determine the water content and particle size of these products, without a knowledge of their SFC, by measuring the velocity as a function of frequency at a temperature where all the solid fat crystals have melted. However, the relatively large particle size of the aqueous phase droplets meant that sedimentation in the samples was so rapid than reliable measurements could not be made at these temperatures. To determine the droplet size at lower temperatures one would need to know the thermophysical properties of the component phases and the SFC. Due to the relatively large particle size of the margarines and low fat spread it would be necessary to measure the ultrasonic velocity at much lower frequencies than were possible in this work to determine their droplet size.

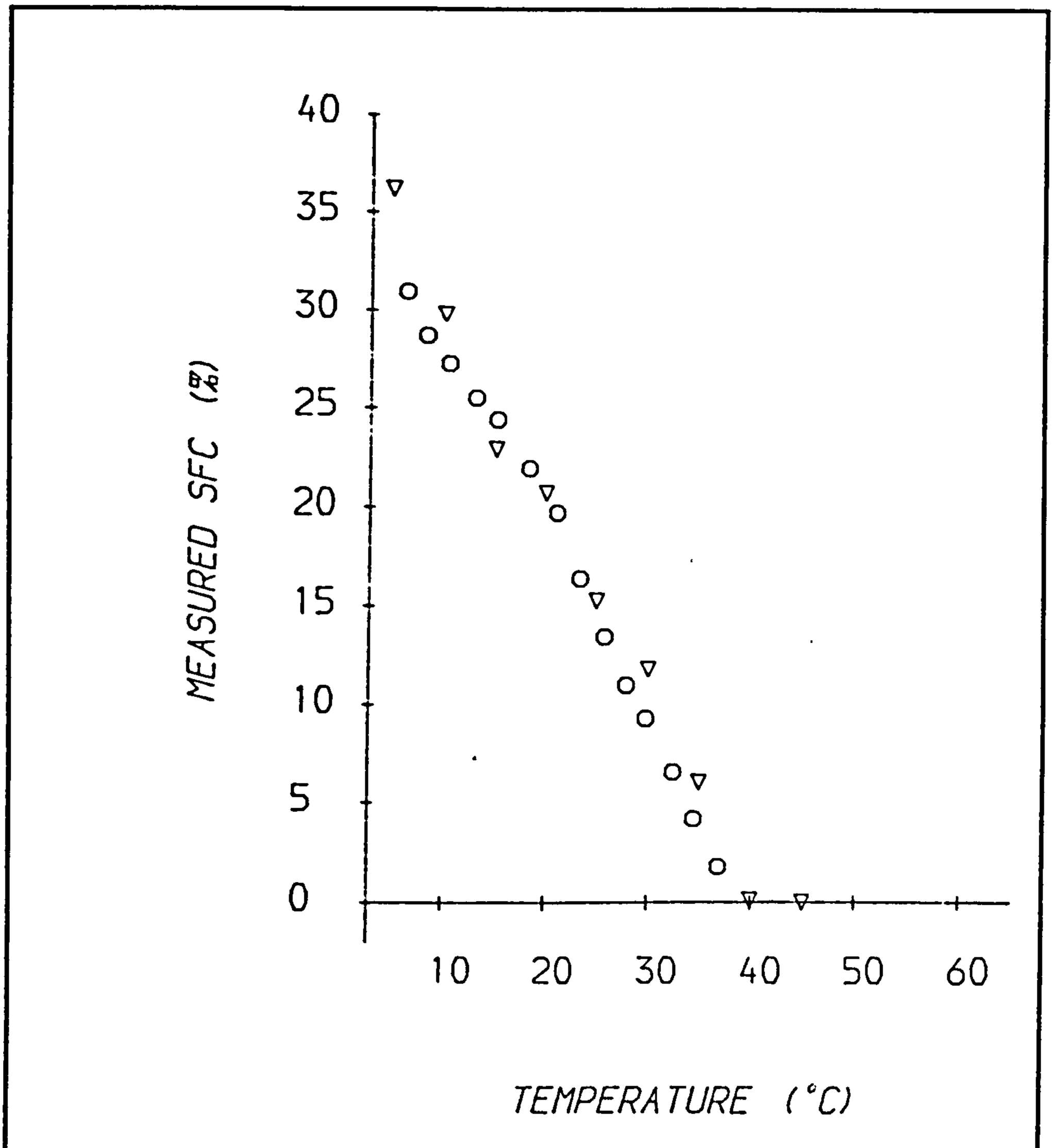

Figure 5.19: SFC versus temperature for Echo margarine. Annotation: O = values determined from ultrasonic velocity measurements, ∇ = values determined by pulsed NMR.

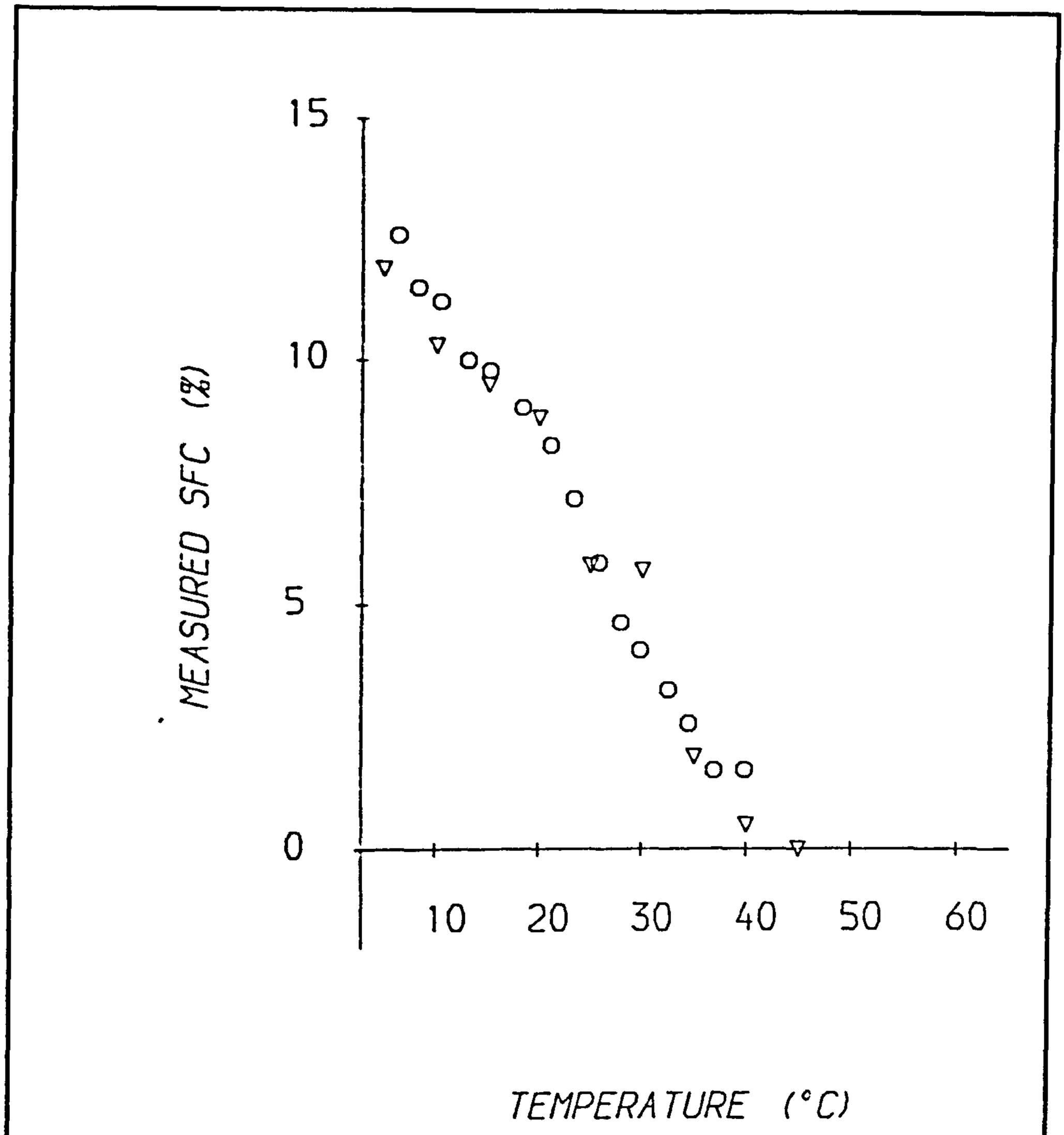

Figure 5.20: SFC versus temperature for Flora margarine. Annotation: O = values determined from ultrasonic velocity measurements, ∇ = values determined by pulsed NMR.

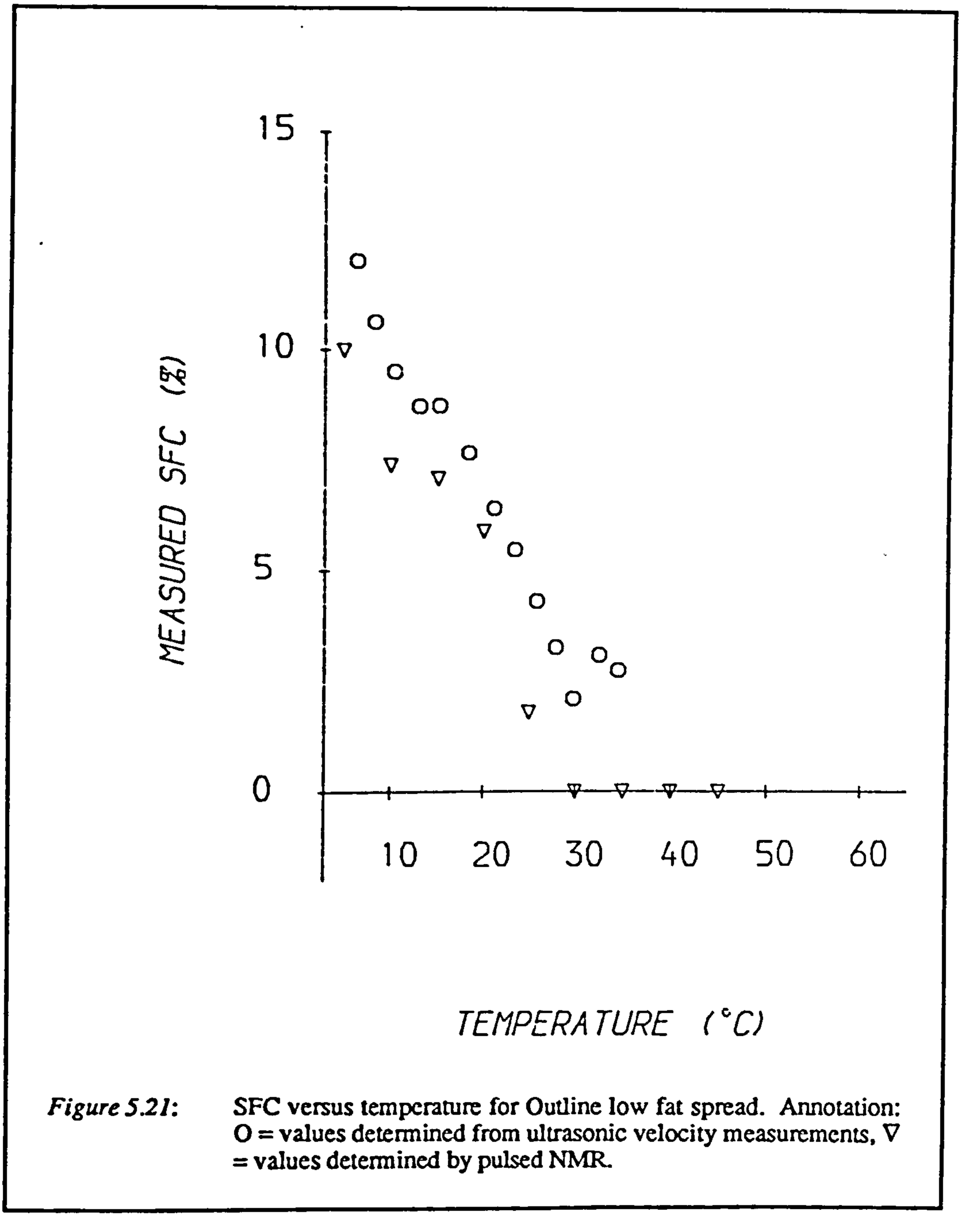

Figure 5.21: SFC versus temperature for Outline low fat spread. Annotation: O = values determined from ultrasonic velocity measurements, ∇ = values determined by pulsed NMR.

SFC determination The SFC of the margarines and low fat spreads can be determined using the same method as was used for the water/tristearin/sunflower oil emulsions described in section 5.3.3.1, i.e. by using equation 5.4. The velocity of the oil phase in the Flora margarine was assumed to be the same as that of sunflower oil (table 4.5). The velocity of the oil phase in the Outline was assumed to be the same as the average oil velocity calculated in section 4.3.3. The velocity of the oil phase in the Echo margarine, which is predominantly animal fats, was assumed to be the same as that for Co-op cooking oil which is made up of animal fats (table 4.13). The aqueous phase in margarines was traditionally made from cows' milk, however as can be seen from the ingredients list in section 5.3.2, they now contain a complex mixture of various other ingredients. The acoustic properties of these ingredients are not known and so for the purposes of this work it was assumed that the SNF in the margarines and low fat spreads are the same as those in cows milk. Saraf and Samal (1984) have measured the variation of ultrasonic velocity with temperature (30-80°C) for a series of SNF-water mixtures with varying SNF content (0-500g/l). From these measurements the following empirical equation was derived which assumes that there is a linear increase in velocity with increasing SNF content and that the increase in velocity with SNF is linearly related to temperature:

$$v_{aq} = v_{water} + (2.609 - 0.0213T)SNF$$

Thus the ultrasonic velocity of the aqueous phase can be calculated at any temperature and SNF content. The SNFs of the aqueous phase is equal to the total SNF of the products given in section 5.3.2 divided by (1 - water mass fraction).

Using the above parameters for the various commercial products their SFCs were determined as a function of temperature using equation 5.4 and the velocity measurements shown in figure 5.18. These values are compared with the SFCs measured using pulsed NMR in figures 5.19-21. There is good agreement between the values determined by the two techniques considering the assumptions made in the equations. The values obtained using the ultrasonic technique could be improved if the velocities of the oil and aqueous

phase$^{s}_{\lambda}$ were known. This would be possible if the technique were used in the factory or research laboratory where the product was manufactured since the separate oil and aqueous phases would be available for measurement. Ultrasonics would therefore seem to have considerable potential as a tool for characterising this type of system.

5.4 Ultrasonics as a tool for characterising emulsions

In this chapter the potential of ultrasonics as a tool for characterising food emulsions has been demonstrated. In binary O/W and W/O emulsions the technique can be used to determine the disperse phase volume fraction and the particle size distribution by measuring the ultrasonic velocity and/or attenuation as a function of frequency. In systems which contain solid fat crystals ultrasonics may also be used to determine SFCs. Ultrasonics has advantages over many existing techniques for charactersing emulsions since it can be used to make non- intrusive, non-invasive measurements in systems which are optically opaque. The technique may therefore prove useful as an analytical technique for use in the laboratory or as a sensor capable of monitoring the properties of emulsions during manufacturing.

Chapter 6

CONCLUSIONS

Previous workers have investigated the possibility of using ultrasonics to characterise food materials, but few of these investigations have led to the development of ultrasonic techniques for commercial application in the food industry. This is surprising since ultrasonics has found widespread use for characterising materials in areas such as medical physics, materials testing and geology. The main reasons for this apparent discrepancy are the lack of information about how ultrasound interacts with foods, the complexity and diversity of many food materials and the shortage of ultrasonic instrumentation for use in the food industry. In this work I have shown how a good understanding of the theories describing ultrasonic propagation in heterogeneous materials, coupled with careful experimental design, leads to many new applications of the technique for characterising fats and emulsions. Table 6.1 lists some of the applications of the technique developed in this thesis, as well as some possible areas for future applications.

Solid fat crystals have larger ultrasonic velocities than liquid oils and so ultrasonic velocity measurements can be used to determine SFCs, investigate phase transitions or measure crystal solubilities (section 4.2.3). To do this it was necessary to relate the velocity of a fat/oil mixture to its SFC, which could be done using either an 'empirical' or a 'theoretical' approach. In the first approach, empirical relationships between SFC and velocity were established by measuring the variation of ultrasonic velocity with SFC for a series of glyceride/oil mixtures of known SFC. Predictions of the SFC using this approach agreed well with known values for the various fat/oil mixtures examined. The empirical approach should therefore prove useful for determining SFCs in systems where a value for the SFC is required without the need for precise information about the properties of the

Table 6.1: Summary of applications of ultrasonic technique

	Present	Future
Fat/oil suspensions	SFC determinations, investigation of phase transitions, crystal solubility measurements	Particle sizing of fat crystals, determination of size and number of vacuoles
Oil mixtures	Determination of composition	
O/W and W/O emulsions	Determination of volume fractions and particle size distributions	Investigation of phase inversion, measurement of interfacial properties
O/W and W/O emulsions containing solid fat	Determination of water content and SFC, investigation of phase transitions	Particle sizing of droplets and fat crystals

component phases. In the theoretical approach the equations describing ultrasonic propagation reviewed in chapter 2 were used to relate the velocity to the SFC. The effects of scattering on the ultrasonic velocity of fat/oil mixtures are small and so it should be possible to use the Wood equation, which assumes no scattering, to interpret results. This equation gave good predictions of the SFCs up to SFCs of about 15%, however, there were significant deviations above this value. This was probably due to interaction between the particles or difficulties in measuring the velocity of the solid tristearin and further work is needed in this area to establish which. A theoretical approach is most useful for fundamental investigations of fat/oil mixtures, since more information about the properties of a system can be extracted than by using empirical equations. For example, although the effects of scattering on the velocity and attenuation of fat/oil mixtures are small they could be measured using more accurate ultrasonic instruments than were used in this work (e.g. ± 0.1m/s). Thus it may be possible to determine the particle size of fat crystals by measuring the velocity (or attenuation) accurately as a function of frequency (section 2.4.6.3).

There were very significant correlations between the SFCs determined by the ultrasonic technique and those determined using pulsed NMR, which is the established means of determining SFCs in the fats and oils industry at present. Both techniques have similar precisions and can be used for either on-line or off-line measurements. The ultrasonic technique is capable of faster sampling rates and has a considerably lower capital cost, however, it may have limited use for samples which contain air cells or vacuoles since these can strongly attenuate ultrasound. Even so, ultrasonics should prove a useful adjunct or alternative to pNMR for determining SFCs in many fat/oil mixtures. Attenuation measurements did not prove a useful means of characterising fat/oil mixtures since they were subject to large variability. This was partly due to the difficulty in isolating the attenuation due to the sample from that associated with the experimental design and partly because the attenuation of ultrasound caused by cracks or vacuoles in the samples obscured the signal from the sample alone. Cracks or vacuoles in fats play an important role in their overall bulk properties and so information about their number and size would be very useful. By utilising their effect on the attenuation of ultrasound it may be possible to determine these properties and this may prove a fruitful area for future work.

The ultrasonic velocity of a series of liquid triglyceride in oil mixtures and of some commercial oils was found to depend on the type and proportion of the triglycerides present and could be described using simple empirical equations. Thus the technique may also prove useful for characterising liquid oils or for measuring the composition of binary liquid oil mixtures.

In chapter 5 it was shown experimentally that thermal scattering of ultrasound may lead to appreciable velocity dispersion and excess attenuation in O/W and W/O emulsions, especially at low frequencies and particle sizes. There was good agreement between measured ultrasonic velocities and those predicted by scattering theory, however, the attenuation measurements agreed less well, particularly at high disperse phase volume fractions. This was probably due to some form of interaction between the particles or due to

breakdown of the assumptions underlying the scattering theory. By measuring the ultrasonic velocity or attenuation of an emulsion as a function of frequency it was shown how both the particle size distribution and the disperse phase volume fraction could be determined once the thermophysical properties of the component phases were known. A number of workers have investigated the possibility of using attenuation measurements to determine particle sizes in emulsions, however, the author could find no examples of the use of velocity dispersion due to thermal scattering for this purpose. The results of this work suggest that velocity measurements are more suitable for particle sizing since they can be measured more accurately and are easier to interpret.

The measurements in this work were in the frequency range 1.25-55 MHz. In this range droplets with radii between 0.1 and 1 μm can be sized. Most food emulsions contain droplets with larger particle sizes than this, typically between 1 and 10 μm, and so measurements at lower frequencies would be needed to size them. If ultrasonics is going to prove a useful tool for particle sizing many food emulsions it is necessary to design and develop an instrument which can measure the velocity and attenuation accurately over a wide frequency range (10kHz - 100MHz). Although there was good agreement between the velocity measurements and the scattering theory in this work only one system (sunflower oil and water) was examined and this over a limited range of particle sizes and frequencies. To establish the limitations of the scattering theory and to assess where it needs to be improved, theoretical predictions should be compared with experimental measurements for a variety of different emulsions with varying frequency (10kHz-100MHz), particle radii (0.01-100μm) and disperse phase volume fraction (0-1).

Ultrasonic scattering occurs due to viscous and thermal transport mechanisms which occur over distances of the order δ_s and δ_t from the interface between the particle and surrounding fluid. These distances can be varied by varying the ultrasonic frequency and so it should be possible, in theory, to obtain information about the thermophysical properties of the material close to the interface. This type of information would be very useful for

investigating the properties of substances adsorbed at the interfaces of emulsions and suspensions. However, such an experiment would require accurate velocity and attenuation measurements over a wide range of frequencies using well characterised systems and is beyond the scope of the present work. Ultrasonic velocity and attenuation measurements may also prove useful for investigating phase transitions in emulsions since there will be a change in emulsion type (O/W → W/O or vice versa), as well as a change in particle size, both of which will change the magnitude of the scattering effects and therefore the ultrasonic velocity and attenuation.

Preliminary experiments with some W/O emulsions containing a partially crystalline fat phase (e.g. margarines and low fat spreads) suggested that ultrasonics may also be used to determine their SFCs as well as their water content and droplet size, however, further work is required in this area using well characterised commercial products. Ultrasonics has a number of advantages over existing techniques for characterising emulsions, such as those based on light scattering or electrical conductivity, since no dilution of samples is required, and measurements can be made non-intrusively.

The theoretical and experimental work presented in this thesis should serve as a firm foundation for future work in this area. However, foods are complex systems which contain a variety of components and a considerable amount of work is still required in order to establish how ultrasound interacts with these components. For instance many foods contain strong scatterers such as sugar crystals or air cells which can have a dramatic effect on ultrasonic measurements, and these effects need to be examined experimentally and theoretically. Even so, the results of this thesis suggest that ultrasonics has many potential applications in the food industry. In research laboratories it may be used to characterise the properties of many food fats and emulsions. In industry it may be used to monitor the properties of foods stored in tanks or flowing through pipes in a non-intrusive, non-invasive manner, thus rapidly providing the food manufacturer with precise information about the properties of the product during processing. This type of information should lead to better

control over processing conditions and consequent improvements in product quality and reduction in manufacturing costs. One of the major factors holding back the development of ultrasonic sensors in the food industry has been the lack of suitable instrumentation. Until instrument manufacturers can provide accurate ultrasonic equipment at reasonable costs, suitable for use in the food industry, the ultrasonic technique will not fulfil its potential for characterising food materials.

Appendix I

LIST OF SYMBOLS

a, b, c = radius of particle times the wave number of the compressional, thermal and shear waves

C_p = specific heat at constant pressure

$d \approx r(\frac{4\pi}{3\phi})^{\frac{1}{3}}$ ≈ distance between particles

E = Young Modulus

f = frequency

$f(\phi)$ = far-field scattering amplitude

G = Shear Modulus

j_n, h_n = spherical Bessel functions

k_c, k_t, k_s = wave numbers of compressional, thermal and shear waves

$P_n(\cos\theta)$ = Legendre polynomials

r = radius of suspended droplets

T = absolute temperature

v = ultrasonic velocity

α = attenuation coefficient

A = shear wave potential

β = coefficient of cubical expansion

B = complex propagation constant

$\gamma = \frac{C_p}{C_v}$ = ratio of specific heats

$\delta_t = \sqrt{\frac{2\sigma}{\omega}}$ = thermal skin depth

$\delta_s = \sqrt{\frac{2\nu}{\omega}}$ = viscous skin depth

η = coefficient of shear viscosity

θ = polar angle

κ = adiabatic compressibility

$\lambda = \frac{\nu}{f}$ = wavelength of compressional wave

μ = coefficient of shear rigidity

$\nu = \frac{\eta}{\rho}$ = kinematic viscosity

ρ = density

$\sigma = \frac{\tau}{\rho C_p}$ = thermal diffusivity

τ = thermal conductivity

ϕ = volume fraction of droplets

$\phi_o, \phi_c, \phi_r, \phi_t$ = incident, compressional, reflected and thermal wave potentials

ω = angular frequency

Subscripts Primed (') quantities refer to the droplet whilst unprimed quantities refer to the suspending fluid, except for the Bessel functions where primes refer to differentiation.

Appendix II

DERIVATION OF WAVE EQUATION

Consider a compressional wave travelling through a small element of an infinite liquid which has bulk modulus K and cross sectional area A (figure II.1). At equilibrium the end faces of the element are at x and $x + \delta x$. In the presence of a compressional wave a force F(x) acts on point x of the element and the ends are displaced by ξ and $\xi + \delta\xi$, respectively. Since δx is the original length of the element and $\delta\xi$ is the overall increase then the strain on the element is $\frac{\delta\xi}{\delta x}$. By considering an infinitesimally small element we can assume that the bulk modulus is constant over the whole element:

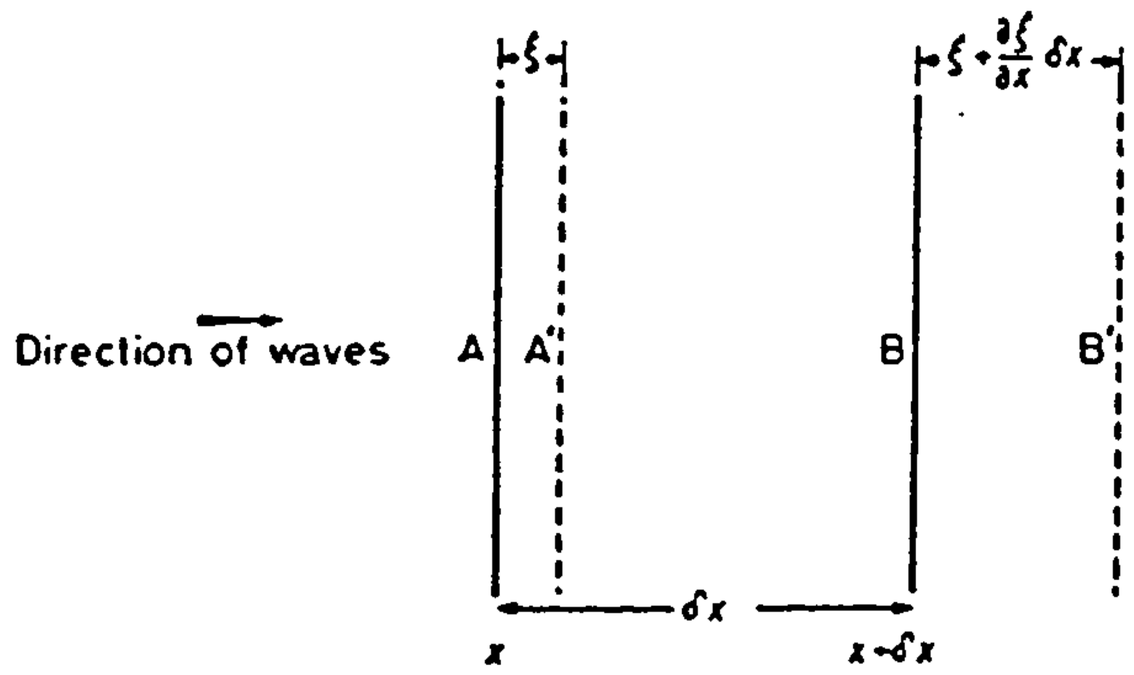

Figure II.1: Strain on a layer of homogeneous material. Caused by propagation of plane compressional waves through it (Blitz 1963).

$$K = \frac{Stress}{Strain} = \left(\frac{\frac{F(x)}{A}}{\frac{\delta\xi}{\delta x}} \right)$$

so

$$F(x) = KA\frac{\delta\xi}{\delta x}$$

The difference between the forces acting on the front (A') and back (B') faces of the element provides the restoring force, which is also equal to the mass x accelaration of the element (by Newtons laws of motion). Thus

$$KA\left(\frac{\delta\xi}{\delta x}\right)_{B'} - KA\left(\frac{\delta\xi}{\delta x}\right)_{A'} = A\delta x\rho\frac{\delta^2\xi}{\delta t^2}$$

where ρ is the density. For an infinitesimal element

$$\frac{\left(\left(\frac{\delta\xi}{\delta x}\right)_{B'} - \left(\frac{\delta\xi}{\delta x}\right)_{A'}\right)}{\delta x} = \frac{\delta^2\xi}{\delta x^2}$$

and so

$$K\frac{\delta^2\xi}{\delta x^2} = \rho\frac{\delta^2\xi}{\delta t^2}$$

This equation is the appropriate equation for one dimensional propagation in an ideal, lossless liquid mediumThe general equation for propagation in three dimensions is;

$$\varepsilon\left(\frac{\delta^2\xi}{\delta x^2} + \frac{\delta^2\xi}{\delta y^2} + \frac{\delta^2\xi}{\delta z^2}\right) = \rho\frac{\delta^2\xi}{\delta t^2}$$

Where ε is the appropriate elastic modulus. There are many possible solutions of u(x,y,z,t) that satisfy this equation, these depend on the type of wave propagation e.g. plane waves, cylindrical waves, spherical waves. The general solution for planes waves takes the form:

$$u(x,y,z,t) = ae^{i[\omega t \pm (k_1 x + k_2 y + k_3 z)]}$$

This plane wave is characterised by the wave vector k which has components k_1, k_2 and k_3 in the x, y and z directions. The direction of k is the direction the wave is travelling and its magnitude is related to the wavelength by the relation:

$$k = \frac{2\pi}{\lambda} = \frac{\omega}{v}$$

Appendix III

SPHERICAL BESSEL FUNCTIONS

In order to solve equation 2.9 it is ne c essary to calculate the values of the spherical Bessel functions and their derivitives. The expressions for the zero and first order Bessel functions are:

$$j_0(x) = \frac{\sin x}{x}$$

$$h_0(x) = \frac{-ie^{ix}}{x}$$

$$j_1(x) = \frac{\sin x - x\cos x}{x^2}$$

$$h_1(x) = -\left(1+\frac{i}{x}\right)\frac{e^{ix}}{x}$$

The derivitives of these expressions and the higher order values are calculated using recursion formulae (Bell 1968):

$$R_{n+1}(x) = \frac{2n+1}{x}R_n(x) - R_{n-1}(x)$$

$$R'_n(x) = \frac{n}{x}R_n(x) - R_{n+1}(x)$$

$$R''_n(x) = R_n(x) - \frac{n(n-1)}{x^2}R_n(x) + \frac{2}{x}R_{n+1}(x)$$

Where $R_n(x)$ represents either $j_n(x)$ or $h_n(x)$.

Appendix IV

COMPUTER PROGRAM FOR SOLUTION OF SCATTERING THEORY FORMULATIONS

All the computer programs used in this work were written in Fortran 77 and were run on an Amdahl 580 Mainframe computer which is operated by the Leeds University Computing Service. The example program included in this Appendix calculates the variation of ultrasonic velocity and attenuation with disperse phase volume fraction for mono-disperse emulsions. However, it can easily be modified to include particle size distributions or for use with suspensions of solid particles in fluid continuum. It can also be modified to calculate the dependence of velocity and attenuation on particle size and frequency. The program uses equations 2.9 and 2.11 to calculate the velocity and attenuation using multiple scattering theory and compares these values with those predicted assuming no scattering (equations. 2.5 and 2.8). The program is summarized in figure IV.1 in the form of a flow diagram.

The method used to calculate the scattering coefficients from equation 2.9 is not clear from the computer program and needs clarifying. Equation 2.9 can be rearranged in the following manner:

$$a_{11}A_n+a_{12}A'_n+a_{13}B_n+a_{14}B'_n+a_{15}C_n+a_{16}C'_n=b_1$$

$$a_{21}A_n+a_{22}A'_n+a_{23}B_n+a_{24}B'_n+a_{25}C_n+a_{26}C'_n=b_2$$

$$a_{31}A_n+a_{32}A'_n+a_{33}B_n+a_{34}B'_n+a_{35}C_n+a_{36}C'_n=b_3$$

$$a_{41}A_n+a_{42}A'_n+a_{43}B_n+a_{44}B'_n+a_{45}C_n+a_{46}C'_n=b_4$$

$$a_{51}A_n+a_{52}A'_n+a_{53}B_n+a_{54}B'_n+a_{55}C_n+a_{56}C'_n=b_5$$

$$a_{61}A_n+a_{62}A'_n+a_{63}B_n+a_{64}B'_n+a_{65}C_n+a_{66}C'_n=b_6$$

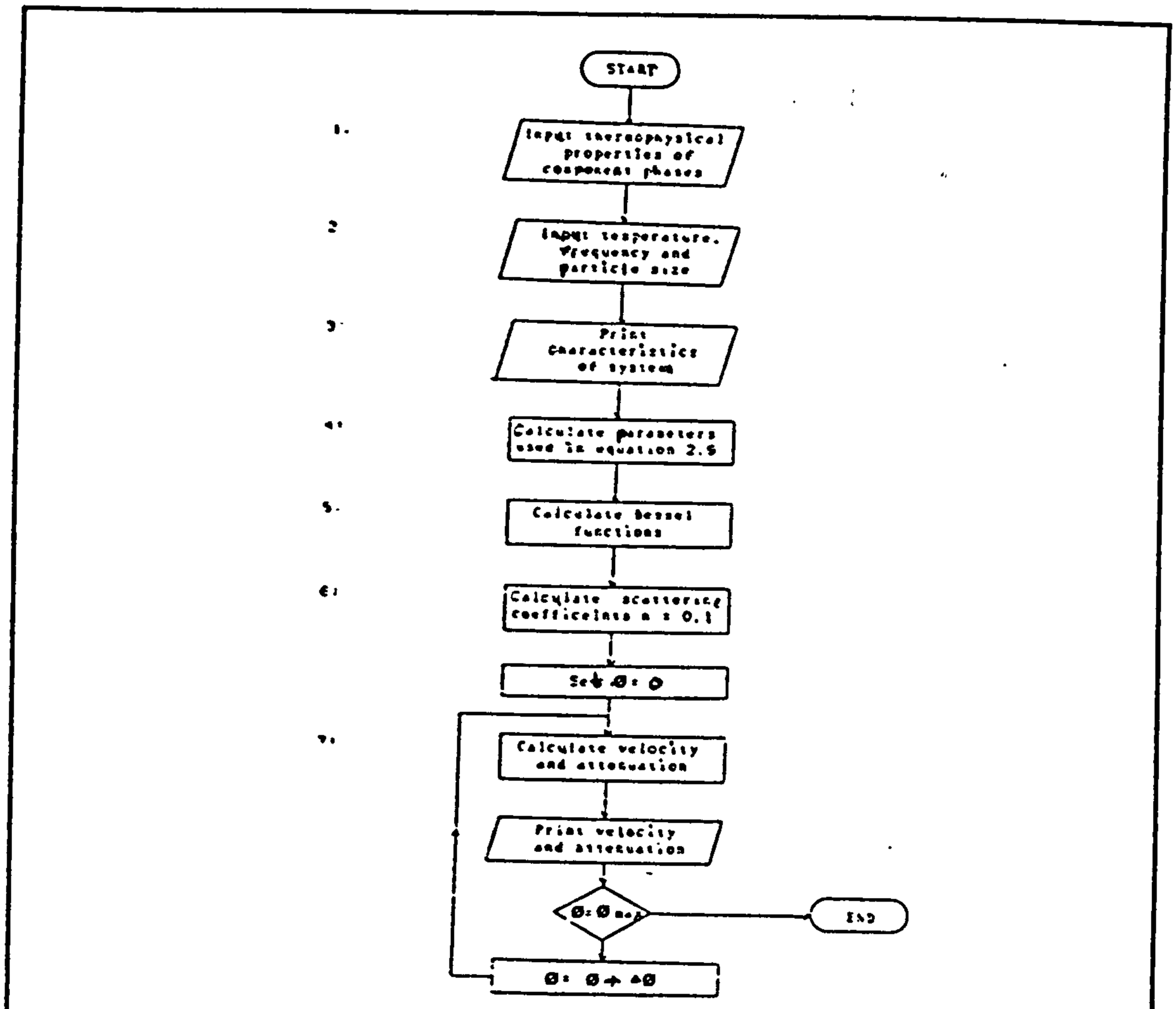

Figure IV.1: Flow diagram of computer program. The program is used to calculate the variation of ultrasonic velocity and attenuation with disperse phase volume fraction for a mono-disperse emulsion.

where A_n, A'_n, B_n, B'_n, C_n and C'_n are the scattering coefficients and a_{ij} and b_j ((i=1,6)j=1,6) are evaluated numerically from the appropriate quantities in equation 2.9. The scattering coefficients can then be determined by solving these complex linear equations simultaneously. The Amdahl mainframe computer at Leeds University supports a library of programs which can be used for the numerical solution of problems such as this. These programs were written by the Numerical Algorithms Group (NAG). The program used in this work, F04ADF (NAG 1987), calculates the solution of a set of complex linear equations by Crout's factorisation method. The main program passes the values of a_{ij} to the NAG

routine in the form of a two dimensional matrix and the values of b_j in the form of a one dimensional matrix. The NAG routine then returns the values of A_n, A'_n, B_n, B'_n, C_n and C'_n in the form of a 1-D matrix. Only the value of A_n is required for the subsequent calculations and so the rest of the scattering coefficients are disregarded.

PROGRAM THEORY

```
*  ================================================================  *
*  THIS PROGRAM CALCULATES THE VARIATION OF ULTRASONIC VELOCITY AND     *
*  ATTENUATION WITH DISPERSE PHASE VOLUME FRACTION FOR EMULSIONS.       *
*  ================================================================  *

*       ** DEFINITION OF VARIABLE TYPES **

        IMPLICIT REAL*8  (A-H,O-Z)
        REAL*8  M1,M2
        COMPLEX*16 GL1,GL2,XI
        COMPLEX*16 A,AA,B,BB,C,CC
        COMPLEX*16 AZ(6,6),BZ(6,1),CZ(6,1),AS(0:2)
        COMPLEX*16 J(0:3,3,6),H(0:3,3,6)

*       ** 1) INPUT THERMOPHYSICAL PROPERTIES OF COMPONENT PHASES **

        READ(1,*) V1,V2,P1,P2,VIS1,VIS2
        READ(1,*) ALPHA1,ALPHA2,SH1,SH2,T1,T2
        READ(1,*) ATTN1,ATTN2

*       ** 2) INPUT TEMPERTURE, FREQUENCY AND DROPLET RADIUS **

        READ(1,*) TEMP,FREQ,R

*       ** 3) PRINT THERMOPHYSICAL PROPERTIES OF COMPONENT PHASES **

        CALL TPDATA(V1,V2,P1,P2,VIS1,VIS2,SH1,SH2,ALPHA1,ALPHA2,
       *T1,T2,ATTN1,ATTN2,TEMP,FREQ,R)

*       ** DEFINE PI, I AND ANGULAR FREQUENCY, W **

        PI = 3.14159265D0
        XI=(0.0D0,1.0D0)
        W=2*PI*FREQ

*       ** 4) CALCULATE PARAMETERS USED IN EQUATION 2.9 **

        Y1=1+(273.16+TEMP)*ALPHA1**2*V1**2/SH1
        Y2=1+(273.16+TEMP)*ALPHA2**2*V2**2/SH2

        M1=1-2*VIS1*SH1/T1
        M2=1-2*VIS2*SH2/T2

        GL1=-W*(Y1-1)/(ALPHA1*V1**2)*XI
        GL2=-W*(Y2-1)/(ALPHA2*V2**2)*XI

        GB1=-P1*SH1/(ALPHA1*T1)
        GB2=-P2*SH2/(ALPHA2*T2)

*       ** CALCULATE WAVE NUMBERS TIMES PARTICLE SIZE **

        A=(W/V1+XI*ATTN1)*R
        AA=(W/V2+XI*ATTN2)*R
        B=SQRT(W*P1*SH1/(2*T1))*(1+XI)*R
```

```
      BB=SQRT(W*P2*SH2/(2*T2))*(1+XI)*R
      C=SQRT(W*P1/(2*VIS1))*(1+XI)*R
      CC=SQRT(W*P2/(2*VIS2))*(1+XI)*R

*     ** 5) CALL SUBROUTINE WHICH CALCULATES BESSEL FUNCTIONS **

      CALL BESSEL(J,H,PI,XI,A,AA,B,BB,C,CC)

*     ** 6) CALL SUBROUTINE WHICH CALCULATES SCATTERING COEFFICIENTS **

        CALL SOLVE(M1,M2,GL1,GL2,GB1,GB2,VIS1,VIS2,A,AA,B,BB,C,CC,
     *  T1,T2,AS,J,H,XI)

*       ** 7) CALL SUBROUTINE WHICH CALCULATES VELOCITY AND ATTENUATON **

      DO 20 VOL=0.0,0.501,0.05
        CALL LB(V1,V2,P1,P2,ATTN1,ATTN2,R,VOL,W,XI,AS,V,V0,ALPHA,ABS)
        WRITE(2,30) 100*VOL,V0,ABS,V,ALPHA
20    CONTINUE

      STOP
30    FORMAT(4X,F6.2,2(6X,F6.1,3X,F6.2,3X))
      END

*     ** ================================================== **
*     ** THIS SUBROUTINE CALCULATES THE BESSEL FUNCTIONS OF THE **
*     ** PARAMETERS: A,AA,B,BB,C,CC USING RECURSION FORMULAE.   **
*     ** ================================================== **

      SUBROUTINE BESSEL(J,H,PI,XI,A,AA,B,BB,C,CC)

      IMPLICIT REAL*8  (A-H,O-Z)
      COMPLEX*16 XI,X(6),J(0:3,3,6),H(0:3,3,6),Z
      COMPLEX*16 A,AA,B,BB,C,CC

      X(1)=A
      X(2)=AA
      X(3)=B
      X(4)=BB
      X(5)=C
      X(6)=CC

      DO 10 L=1,6

        Z=X(L)

        J(0,1,L)=SIN(Z)/Z
        J(1,1,L)=1/Z*(SIN(Z)/Z-COS(Z))
        H(0,1,L)=-XI*EXP(XI*Z)/Z
        H(1,1,L)=-EXP(XI*Z)*(1+XI/Z)/Z

      DO 20 N=1,2
        I=N+1
        K=N-1
        J(I,1,L)=(2*N+1)/Z*J(N,1,L)-J(K,1,L)
        H(I,1,L)=(2*N+1)/Z*H(N,1,L)-H(K,1,L)
```

```
20      CONTINUE

        DO 30 N=0,2
           I=N+1
           J(N,2,L)=N/Z*J(N,1,L)-J(I,1,L)
           J(N,3,L)=1/Z**2*(J(N,1,L)*(N*(N-1)-Z**2)+2*Z*J(I,1,L))
           H(N,2,L)=N/Z*H(N,1,L)-H(I,1,L)
           H(N,3,L)=1/Z**2*(H(N,1,L)*(N*(N-1)-Z**2)+2*Z*H(I,1,L))
30      CONTINUE

10    CONTINUE

      RETURN
      END

*     ** ================================================== **
*     ** THIS SUBROUTINE CALCULATES THE SCATTERING COEFFICIENTS OF **
*     ** EQN. 2.9 USING CROUT'S FACTORISATION METHOD (NAG F04ADF)  **
*     ** ================================================== **

      SUBROUTINE SOLVE(M1,M2,GL1,GL2,GB1,GB2,VIS1,VIS2,A,AA,B,BB,C,CC,
     *T1,T2,AS,J,H,XI)

      IMPLICIT REAL*8 (A-H,P-Z)
      REAL*8 M1,M2,WKSPCE(7)
      COMPLEX*16 A,AA,B,BB,C,CC
      COMPLEX*16 GL1,GL2,XI
      COMPLEX*16 AZ(6,6),BZ(6,1),CZ(6,1)
      COMPLEX*16 J(0:3,3,6),H(0:3,3,6),AS(0:2)

      DO 10 N=0,1

*        ** FIRST EQUATION **

         AZ(1,1)=A*H(N,2,1)
         AZ(1,2)=-AA*J(N,2,2)
         AZ(1,3)=B*H(N,2,3)
         AZ(1,4)=-BB*J(N,2,4)
         AZ(1,5)=-N*(N+1)*H(N,1,5)
         AZ(1,6)=N*(N+1)*J(N,1,6)
         BZ(1,1)=-A*J(N,2,1)

*        ** SECOND EQUATION **

         AZ(2,1)=H(N,1,1)
         AZ(2,2)=-J(N,1,2)
         AZ(2,3)=H(N,1,3)
         AZ(2,4)=-J(N,1,4)
         AZ(2,5)=-(H(N,1,5)+C*H(N,2,5))
         AZ(2,6)=(J(N,1,6)+CC*J(N,2,6))
         BZ(2,1)=-J(N,1,1)

*        ** THIRD EQUATION **

         AZ(3,1)=GL1*AZ(2,1)
         AZ(3,2)=GL2*AZ(2,2)
```

```
      AZ(3,3)=GB1*AZ(2,3)
      AZ(3,4)=GB2*AZ(2,4)
      AZ(3,5)=(0.0D0,0.0D0)
      AZ(3,6)=(0.0D0,0.0D0)
      BZ(3,1)=GL1*BZ(2,1)

*     ** FOURTH EQUATION **

      AZ(4,1)=AZ(1,1)*GL1*T1
      AZ(4,2)=AZ(1,2)*GL2*T2
      AZ(4,3)=AZ(1,3)*GB1*T1
      AZ(4,4)=AZ(1,4)*GB2*T2
      AZ(4,5)=(0.0D0,0.0D0)
      AZ(4,6)=(0.0D0,0.0D0)
      BZ(4,1)=BZ(1,1)*GL1*T1

*     ** FIFTH EQUATION **

      AZ(5,1)=VIS1*(A*H(N,2,1)-H(N,1,1))
      AZ(5,2)=-VIS2*(AA*J(N,2,2)-J(N,1,2))
      AZ(5,3)=VIS1*(B*H(N,2,3)-H(N,1,3))
      AZ(5,4)=-VIS2*(BB*J(N,2,4)-J(N,1,4))
      AZ(5,5)=-0.5*VIS1*(C**2*H(N,3,5)+(N**2+N-2)*H(N,1,5))
      AZ(5,6)=0.5*VIS2*(CC**2*J(N,3,6)+(N**2+N-2)*J(N,1,6))
      BZ(5,1)=-VIS1*(A*J(N,2,1)-J(N,1,1))

*     ** SIXTH EQUATION **

      AZ(6,1)=VIS1*(C**2*H(N,1,1)-2*A**2*H(N,3,1))
      AZ(6,2)=-VIS2*(CC**2*J(N,1,2)-2*AA**2*J(N,3,2))
      AZ(6,3)=VIS1*(M1*C**2*H(N,1,3)-2*B**2*H(N,3,3))
      AZ(6,4)=-VIS2*(M2*CC**2*J(N,1,4)-2*BB**2*J(N,3,4))
      AZ(6,5)=VIS1*2*N*(N+1)*(C*H(N,2,5)-H(N,1,5))
      AZ(6,6)=-VIS2*2*N*(N+1)*(CC*J(N,2,6)-J(N,1,6))
      BZ(6,1)=-VIS1*(C**2*J(N,1,1)-2*A**2*J(N,3,1))

*     ** DEFINE WORKSPACE FOR NAG ROUTINE F04ADF **

      DO 20 I=1,7
         WKSPCE(I)=9000.0
20    CONTINUE

*     ** CALL NAG ROUTINE F04ADF (CROUTS FACTORISATION METHOD)    **

         IFAIL = 1
         CALL F04ADF(AZ,6,BZ,6,6,1,CZ,6,WKSPCE,IFAIL)

*     ** ONLY FIRST SCATTERING COEFFICIENT (A) IS NEEDED **

         AS(N)=CZ(1,1)

   10 CONTINUE

         RETURN
         END
```

```
*     ** ================================================== **
*     ** THIS SUBROUTINE CALCULATES THE VARIATION OF VELOCITY  **
*     ** AND ATTENUATION OF AN EMULSION WITH VOLUME FRACTION:  **
*     **   1) ASSUMING NO SCATTERING (EQUATIONS 2.5 AND 2.8)   **
*     **   2) ASSUMING MULTIPLE SCATTERING (EQUATION 2.11)     **
*     ** ================================================== **

      SUBROUTINE LB(V1,V2,P1,P2,ATTN1,ATTN2,R,VOL,W,XI,A,V,V0,ATTEN,ABS)

      IMPLICIT REAL*8 (A-H,P-Z)
      COMPLEX*16 XI,XA(20),A(0:2),X,Y,Z,KC
      REAL*8  K0,K1,K2

*     ** CALCULATION OF VEL. AND ATTEN. ASSUMING NO SCATTERING **

        K1=1/(V1**2*P1)
        K2=1/(V2**2*P2)
        K0=VOL*K2+(1-VOL)*K1
        P0=VOL*P2+(1-VOL)*P1

         V0=1/(SQRT(K0*P0))
         ABS=(ATTN1*(1-VOL)+ATTN2*VOL)*8.686

*     ** CALCULATION OF VEL. AND ATTEN. ASSUMING MULTIPLE SCATTERING **

         KC=W/V1+XI*ATTN1

         X=3*XI*VOL*(A(0)+3*A(1))/(KC*R)**3
         Y=27*VOL**2*(A(0)*A(1)+2*A(1)**2)/(KC*R)**6
         Z = SQRT(1-X-Y)*KC

          V=W/REAL(Z)
          ATTEN=IMAG(Z)*8.686

      RETURN
      END

*     ** ================================================== **
*     ** THIS SUBROUTINE PRINTS OUT THE THERMOPHYSICAL PROPERTIES **
*     ** OF THE EMULSIONS COMPONENT PHASES                      **
*     ** ================================================== **

      SUBROUTINE TPDATA(V1,V2,P1,P2,VIS1,VIS2,SH1,SH2,ALPHA1,ALPHA2,
     *T1,T2,ATTN1,ATTN2,TEMP,FREQ,R)

      IMPLICIT REAL*8 (A-H,P-Z)

      WRITE(2,10)
      WRITE(2,15)
      WRITE(2,*)
      WRITE(2,20) TEMP
      WRITE(2,30) FREQ/1D6
      WRITE(2,40) R*1D6
      WRITE(2,*)
      WRITE(2,50)
      WRITE(2,55)
```

```
      WRITE(2,*)
      WRITE(2,60)
      WRITE(2,70) V1,V2
      WRITE(2,80) P1,P2
      WRITE(2,90) VIS1,VIS2
      WRITE(2,100) SH1,SH2
      WRITE(2,110) T1,T2
      WRITE(2,120) ALPHA1,ALPHA2
      WRITE(2,130) ATTN1*8.686, ATTN2*8.686
      WRITE(2,*)
      WRITE(2,140)
      WRITE(2,145)
      WRITE(2,*)
      WRITE(2,150)
      WRITE(2,160)
      WRITE(2,*)

10    FORMAT(1X,'NUMERICAL CALCULATION OF VELOCITY AND ATTENUATION IN AN
     * EMULSION')
15    FORMAT(1X,'=================================================
     *=========')
20    FORMAT(1X,'TEMPERATURE    = ',F6.1,' C')
30    FORMAT(1X,'FREQUENCY      = ',F6.2,' MHZ')
40    FORMAT(1X,'PARTICLE SIZE = ',F6.2,' MICRONS')
50    FORMAT(1X,'THERMOPHYSICAL PROPERTIES OF COMPONENT PHASES:')
55    FORMAT(1X,'-----------------------------------------')
60    FORMAT(34X,'CONTINUOUS PHASE  DISPERSE PHASE')
70    FORMAT(1X,'VELOCITY (M/S)                    ',5X,F7.1,10X,F7.1)
80    FORMAT(1X,'DENSITY (KG/M3)                   ',5X,F7.1,10X,F7.1)
90    FORMAT(1X,'VISCOSITY (KG/M/S)                ',5X,F7.3,10X,F7.3)
100   FORMAT(1X,'SPECIFIC HT. CAPACITY (J/KG/C)    ',5X,F7.1,10X,F7.1)
110   FORMAT(1X,'THERMAL CONDUCTIVITY (J/M/S/C)    ',5X,F7.3,10X,F7.3)
120   FORMAT(1X,'VOLUME EXPANSIVITY (/C)           ',5X,F7.5,10X,F7.5)
130   FORMAT(1X,'ABSORPTION COEFFICIENT (DB/M)     ',5X,F7.3,10X,F7.3)
140   FORMAT(1X,'VELOCITY AND ATTENUATION VERSUS DISPERSE PHASE VOLUME F
     *RACTION')
145   FORMAT(1X,'-----------------------------------------------------
     *-------')
150   FORMAT(4X,'DROPLET       NO-SCATTERING                SCATTERING')
160   FORMAT(4X,'VOL.  %     V (M/S)   A (DB/M)        V (M/S)   A (DB/M)')

      RETURN
      END
```

Appendix V

EXPERIMENTAL RESULTS FROM CHAPTER 4

Table V.1: Measured velocities in tristearin/paraffin oil mixtures

Variation of ultrasonic velocity with increasing temperature and triglyceride content at 1 MHz.

Temp. (°C)	Tristearin content (w/w)					
	0%	5%	10%	15%	20%	30%
-0.3	1547.7	1563.5	1576.1	1594.4	1617.6	1667.6
5.0	1527.4	1541.6	1553.0	1576.5	1596.6	1645.7
10.3	1507.6	1521.4	1535.2	1554.6	1574.9	1620.4
15.5	1488.4	1502.8	1515.4	1534.4	1552.6	1599.7
20.6	1469.6	1482.5	1497.3	1513.6	1530.7	1579.6
25.1	1453.4	1464.9	1477.5	1498.9	1517.9	1555.1
31.3	1431.4	1446.7	1457.1	1475.8	1493.7	1536.0
36.5	1413.0	1425.8+	1438.3+	1455.5+	1476.9	1515.2
42.3	1393.1	1407.5	1420.0	1436.8	1454.0+	1494.8+
45.1	1383.4	1394.6	1407.1	1422.6	1440.2	1477.2
49.9	1367.2	1374.2	1385.7	1402.7	1420.5	1456.8
51.8	1360.6	1366.6	1377.1	1393.0	1410.3	1445.3
55.1	1349.5	1349.8	1359.4	1375.9	1393.3	1428.8
57.3	1342.1	1339.7	1345.7	1359.1	1376.8	1408.8
60.3	1332.2	1330.7*	1329.7*	1331.2*	1347.6	1378.7
62.8	1324.2	1324.4	1321.8	1321.6	1322.3*	1339.2*
64.9	1317.2	1318.2	1316.6	1314.7	1316.1	1312.4
66.8	1311.0	1310.4	1310.6	1309.6	1309.1	1307.7
70.1	1300.3	1299.1	1297.9	1398.3	1298.7	1300.1

+ highest temperature where triglyceride is at least 99% solid

* lowest temperature where triglyceride is completely liquid

Table V.2: Measured velocities in tripalmitin/paraffin oil mixtures

Variation of ultrasonic velocity with increasing temperature and triglyceride content at 1 MHz.

Temp. (°C)	Tripalmitin content (w/w)					
	0%	5%	10%	15%	20%	30%
0.6	1544.2	1564.8	1577.6	1599.0	1617.5	-
4.7	1528.6	1544.0	1556.8	1574.0	1596.4	1657.9
10.6	1506.4	1522.0	1536.5	1552.2	1574.8	1631.0
15.8	1487.1	1500.6	1516.8	1530.9	1553.7	1604.9
20.7	1469.4	1484.8	1501.0	1514.8	1536.7	1587.1
26.4	1448.8	1462.8+	1478.9+	1494.5	1515.5	1560.0
31.1	1432.0	1444.6	1459.5	1481.3+	1494.8+	1539.6+
35.5	1416.5	1428.9	1441.8	1461.9	1479.1	1522.1
41.3	1396.5	1408.1	1422.4	1438.9	1455.0	1497.1
44.7	1384.7	1390.7	1407.4	1424.6	1439.1	1481.6
46.7	1377.9	1382.9	1395.7	1414.6	1427.6	1466.4
49.5	1368.3	1365.7	1375.6	1391.1	1406.2	1444.3
53.4	1355.2	1353.5*	1352.5	1353.7	1370.0	1404.8
57.3	1342.2	1344.3	1343.4*	1341.1*	1340.2	1351.8
61.1	1329.6	1328.9	1327.5	1325.2	1324.9*	1322.4*
66.6	1311.9	1310.6	1309.3	1308.2	1309.1	1306.9
70.3	1299.7	1298.0	1296.7	1297.9	1297.8	1295.9

+ highest temperature where triglyceride is at least 99% solid
* lowest temperature where triglyceride is completely liquid

Table V.3: Measured velocities in trilaurin/paraffin oil mixtures

Variation of ultrasonic velocity with increasing temperature and triglyceride content at 1 MHz.

Temp. (°C)	Trilaurin content (w/w)				
	0%	5%	10%	15%	20%
0.0	1546.6	1559.8	1572.6	1594.0	1619.8
3.4	1533.7	1549.0	1562.7	1582.7	1607.0
5.2	1526.7	1540.4+	1554.2	1569.1	1596.6
8.3	1515.2	1528.4	1542.2+	1561.8	1582.5
10.7	1506.1	1521.4	1536.4	1552.2+	1571.2+
13.8	1494.8	1507.4	1522.3	1539.1	1560.0
15.8	1487.1	1498.3	1510.9	1528.6	1548.9
18.6	1477.1	1487.0	1500.7	1514.7	1536.8
20.7	1469.5	1478.1	1490.7	1509.1	1529.7
26.9	1447.1	1453.1	1463.5	1479.1	1497.1
28.0	1443.2	1443.5	1452.9	1467.2	1485.8
30.8	1433.0	1429.9	1436.2	1350.3	1467.0
33.2	1424.8	1421.7	1418.9	1430.7	1444.4
36.0	1414.7	1414.6*	1409.9*	1408.6	1413.3
38.0	1407.8	1406.5	1401.1	1398.8*	1401.3
43.1	1390.2	1386.7	1381.8	1380.6	1379.7*
48.4	1372.1	1367.5	1365.8	1362.8	1358.5
53.9	1353.6	1352.5	1349.2	1345.5	1345.7
57.4	1341.8	1334.5	1336.6	1335.7	1333.9
60.4	1332.0	1329.8	1325.1	1325.1	1324.0
65.6	1314.8	1313.0	1307.8	1307.9	1306.5
70.1	1299.1	1296.0	1292.0	1292.1	1290.4

+ highest temperature where triglyceride is at least 99% solid
* lowest temperature where triglyceride is completely liquid

Table V.4: Velocity measurements in some vegetable oils

Variation of ultrasonic velocity with increasing temperature at 1.25 MHz.

	Velocity of Oils (m/s)					
T (°C)	Corn	Grape	Ground	Olive	Rape	Safflower
20.5	1467.8	1469.3	1465.5	1462.5	1467.7	1469.4
26.2	1449.0	1449.7	1446.1	1444.0	1448.7	1450.5
30.5	1433.9	1435.5	1431.2	1428.6	1434.4	1435.7
35.2	1418.7	1419.0	1413.2	1415.5	1418.9	1419.9
40.1	1402.3	1403.8	1398.8	1396.0	1401.3	1404.8
40.5	1401.1	1401.6	1399.9	1395.8	1401.3	1403.3
46.4	1381.3	1383.4	1378.2	1375.7	1381.7	1384.5
46.7	1381.3	1382.3	1377.8	1375.8	1380.7	1383.8
50.3	1368.7	1369.6	1364.6	1461.3	1368.0	1369.9
50.9	1367.2	1369.4	1364.9	1361.7	1367.5	1369.2
55.1	1354.3	1354.5	1350.6	1346.7	1353.7	1354.8
55.4	1353.3	1355.2	1350.4	1347.7	1353.0	1355.0
59.9	1339.6	1340.4	1336.3	1332.5	1339.8	1340.9
60.3	1339.4	1338.2	1335.1	1333.5	1338.7	1340.6
64.7	1323.8	1324.9	1320.2	1316.9	1322.5	1326.1
65.4	1323.3	1324.8	1320.5	1317.1	1322.4	1324.8
70.0	1308.4	1309.3	1304.9	1301.5	1307.6	1310.1

Table V.5: Velocity measurements in some vegetable oils

Variation of ultrasonic velocity with increasing temperature at 1.25 MHz.

	Velocity of Oils (m/s)		
T (°C)	Palm	Soybean	Sunflower
5.1	-	1521.8	1523.3
7.6	-	1512.6	1514.8
10.2	-	1504.1	1506.1
15.4	-	1485.6	1487.4
20.0	-	1470.2	1471.3
27.1	-	1445.1	1447.1
32.3	-	1427.8	1429.9
37.2	-	1412.2	1414.0
42.4	-	1395.2	1397.4
47.5	-	1378.5	1380.4
52.6	1352.1	1362.1	1364.3
57.7	1336.2	1347.9	1348.3
60.5	1327.7	1337.8	1339.7
65.3	1312.9	1323.7	1326.2
70.0	1298.1	1308.6	1310.6

Appendix VI

EXPERIMENTAL RESULTS FROM CHAPTER 5

Table VI.1: Velocity and attenuation measurements in emulsions A - E

Variation of ultrasonic velocity and attenuation with particle size and frequency for a series of 0.1 mass fraction sunflower oil in water emulsions at 20°C. The velocity (v) is in m/s, the attenuation coefficient (α) is in dB/m.

	r	1.25MHz		2.25MHz		6.0MHz		10.0MHz	
	(μm)	v	α	v	α	v	α	v	α
A	0.748	1484.3	105	1483.6	266	1484.1	181	1485.1	202
B	0.422	1481.0	167	1481.4	139	1484.7	161	1484.1	564
C	0.270	1479.0	101	1480.8	162	1483.2	415	1483.1	678
D	0.170	1476.6	80	1477.5	142	1480.6	370	1482.2	544
E	0.138	1474.9	48	1476.6	104	1477.2	310	-	-

Table VI.2: Velocity and attenuation measurements in emulsion F.

Variation of ultrasonic velocity and attenuation coefficient of a 0.1 mass fraction sunflower oil in water emulsion ($r_{65} = 0.117\mu m$) with varying frequency at 20°C. These results are a combination of measurements carried out at the AFRC Institute of Food Research (Norwich) using a pulse interferometry technique and the pulse echo technique described in chapter 3.

	1.1% Tween 20		Sunflower oil		Emulsion	
f (MHz)	v(m/s) ±1	α(dB/m) (s.e.m)	v(m/s) ±1	α(dB/m) (s.e.m)	v(m/s) ±1	α(dB/m) (s.e.m)
1.25	1486.3	-	1469.9	16(20)	1473.3	30(20)
2.25	1485.9	-	1469.6	47(30)	1473.4	151(30)
6.00	1485.6	-	1471.1	271(30)	1476.0	370(30)
10.00	1485.7	20(30)	1470.2	676(30)	1476.9	495(30)
5.1174	1486.5	-	1469.9	170(5)	1474.4	410(10)
15.3060	1486.8	50(2)	1468.0	1261(6)	1477.2	1350(10)
25.4323	1486.7	165(3)	1473.0	3220(10)	1480.2	2230(10)
35.4375	1486.4	311(5)	1470.0	5790(30)	1478.7	2840(20)
45.5085	1486.3	490(5)	1470.1	8560(40)	1481.2	3330(80)
55.6949	1487.8	761(4)	1471.0	12420(50)	1481.6	4640(30)

Table VI.3: Velocity measurements in partially crystalline W/O emulsions

Variation of ultrasonic velocity with temperature for distilled water and a series of 10% tristearin in sunflower oil mixtures of varying water content.

	Ultrasonic velocity (m/s)				
T (°C)	water	0%	5%	10%	15%
5.5	1428.4	1557.2	1549.3	1454.0	1537.7
10.0	1447.3	1539.0	1534.1	1530.0	1525.3
14.9	1465.6	1521.7	1518.9	1515.6	1514.1
19.9	1482.0	1505.2	1504.0	1501.2	1502.5
23.3	1492.0	1492.2	1493.9	1492.2	1492.9
24.4	1495.1	1489.8	1489.8	1488.9	1489.9
29.7	1508.4	1470.8	1471.4	1472.0	1474.9
34.3	1518.4	1454.3	1454.6	1458.6	1459.4
39.8	1528.5	1433.8	1436.2	1442.3	1443.3
44.9	1536.3	1415.8	1418.9	1425.5	1427.3
50.1	1542.7	1395.4	1400.4	1407.7	1410.5
52.5	1545.1	1486.3	1387.7	1396.8	1401.0
55.4	1547.7	1371.1	1377.5	1383.0	1387.5
57.8	1549.5	1355.9	1359.6	1367.3	1372.9
60.6	1551.3	1334.6	1335.7	1346.9	1351.5
61.7	1552.0	1331.9	1336.9	1343.8	1349.7
63.6	1552.9	1324.1	1329.8	1336.9	1344.6
65.1	1553.5	1319.9	1327.1	1333.6	1342.6
67.0	1554.1	1314.1	1322.0	1324.8	1332.7

Appendix VII

PUBLICATIONS AND PRESENTATIONS

A number of publications and presentations at conferences which have resulted partially or wholly from this thesis are listed below.

McClements DJ (1986). 'Determination of solid contents in two and three phase systems'. Oral presentation at *Acoustics and Ultrasonics as probes of emulsions and dispersions* meeting organised by the Physical Acoustics group of the Institute of Physics at London.

McClements DJ and Povey MJW (1987). 'Ultrasonic velocity as a probe of emulsions and suspensions'. *Advances in Colloid and Interface Science 27, 285.*

McClements DJ and Povey MJW (1987). 'Solid fat content determination using ultrasonic velocity measurements'. *International Journal of Food Science and Technology 22, 491.*

McClements DJ and Povey MJW (1987). 'Ultrasonic solid fat content determinations'. Presented orally and included in *Ultrasonics International 1987 Conference proceedings p.43.*

McClements DJ and Povey MJW (1988). 'Investigation of phase transitions in glyceride/paraffin oil mixtures using ultrasonic velocity measurements'. *Journal of the Americal Oil Chemists Society. In press.*

McClements DJ and Povey MJW (1988). 'Ultrasonic velocity measurements in some liquid triglycerides and vegetable oils'. *Journal of the American Oil Chemists Society. In press.*

McClements DJ and Povey MJW (1988). 'Comparison of pulsed NMR and ultrasonic velocity techniques for determining solid fat contents'. *International Journal of Food Science and Technology 23, 159.*

McClements DJ and Povey MJW (1988). 'Scattering of ultrasound by emulsions'. *Journal of Physics D: Applied Physics. In press.*

McClements DJ (1988). 'Ultrasonics as a probe of fats and emulsions'. Oral presentation which won prize for best presentation by a member of the Royal Society of Chemistry, at the *Current reasearch topics in lipid chemistry* meeting, organised by the Lipid Group of the Royal Society of Chemistry at London.

Povey MJW and McClements DJ (1988). 'Ultrasonic measurements in food emulsions and dispersions'. Presented orally at the *Food Colloid Symposium 1988* organised by the Food Chemisty group of the Royal Society of Chemistry. Also to be published in the conference proceedings.

Povey MJW and McClements DJ (1988). 'Ultrasonics in food engineering: Part I Introduction and experimental methods'. *Journal of Food Engineering. In press.*

REFERENCES

Abramzon AA, Makagonova NN and Rokhlenko AA 1975 *Colloid J.USSR. 37, 476*

Agricultural Research Council 1982 *'Sensors in agriculture'. Report of ARC Working Party on transducers*

Ahuja AS 1971, *in: Physics of Sound in Marine Sediments (edited by L Hampton) p.1 (New York: Plenum Press)*

Ahuja AS 1972a *J.Acoust.Soc.Am. 51, 182*

Ahuja AS 1972b *J.Acoust.Soc.Am. 51, 916*

Ahuja AS 1973 *J.Appl.Phys, 44, 4863*

Ahuja AS and Hendee WR 1978 *J.Acoust.Soc.Am. 63, 1074*

Allegra JR and Hawley SA 1972 *J.Acoust.Soc.Am. 51, 1545*

Anderson AJC and Williams PN 1954, *Margarine (Oxford: Pergamon Press)*

Anderson AL and Hampton LD 1980 *J.Acoust.Soc.Am. 67, 1865*

Andreae JJ, Bass R, Heasell EL and Lamb J 1958 *Acustica 8, 131*

Asher RC 1982 *Measurement and Control, May, 169*

Asher RC 1983 *J.Phys. E: Sci. Instrumen. 16, 959*

Ballaro S, Mallamace F and Wanderlingh F 1980 *Phys.Letters. 77a, 198*

Barret-Gultepe MA, Everett DH and Gultepe ME 1980, *Polymer Colloids II (edited by RM Fitch) p.313 (New York: Plenum)*

Barret-Gultepe MA, Gultepe ME and Yeager EB 1983 *J.Phys.Chem. 87, 1039*

Bell WW 1968, *Special Functions for Scientists and Engineers (London: Van Nostrand)*

Berger KG, Jewell GG and Pollit RJM 1979, *in Food Microscopy (edited by JG Vaughan) p.445 (London: Academic Press)*

Berryman JG 1980 *J.Acoust.Soc.Am. 68, 1809*

Bhatia AB 1967, *Ultrasonic Absorbtion (New York: Dover Publications Inc.)*

Bhattacharya AC and Deo BB 1981 *Ind.J.Pure.Appl.Phys 19, 1172*

Bhatti SS, Bhatti R and Singh S 1986 *Acustica 62, 96*

Biot MA 1956a *J.Acoust.Soc.Am. 28, 168*

Biot MA 1956b *J.Acoust.Soc.Am. 28, 179*

Biot MA 1962a *J.Appl.Phys. 33, 1482*

Biot MA 1962b *J.Acoust.Soc.Am. 34, 1254*

Blitz J 1963 *Fundementals of Ultrasonics (London: Butterworths)*

Blue JE and McLeroy EG 1968 *J.Acoust.Soc.Am. 44, 1145*

Breazeale MA, Cantrell JH and Heymann JS 1981, *in: Methods of Experimental Physics: Ultrasonics (edited by PD Edmonds) p.67 (New York: Academic Press)*

Cebula DJ, Povey MJW and McClements DJ 1987 *'Structure and Phase Transitions in Triglycerides' Neutron scattering experiment 9-13-2 at I.L.L. Grenoble*

Chapman D 1969, *Introduction to Lipids (London: McGraw-Hill)*

Chow JCF 1964 *J.Acoust.Soc.Am. 36, 2395*

Chrysam MM 1985, *in: Bailey's Industrial oil and fat products Vol.3 (edited by TH Applewhite) p.41 (New York: John Wiley and Sons)*

Datta PK and Pethrick RA 1980 *J.Phys.D:Appl.Phys. 13, 153*

Davies MC 1978 *J.Acoust.Soc.Am. 64, 406*

Davies MC 1979 *J.Acoust.Soc.Am. 65, 387*

Del Grosso VA and Mader CW 1972 *J.Acoust.Soc.Am. 52, 1442*

Dickinson E 1987 *Ann.Rep.Prog.Chem.Sect.C. 84, 31*

Dickinson E 1988, *in: Food Structure - its creation and evaluation (edited by JMV Blanshard and JR Mitchell) p.41 (London: Butterworths)*

Dickinson E and Stainsby G 1982, *Colloids in Food (London: Applied Science)*

Edmonds PD 1981 *Methods of Experimental Physics: Ultrasonics (New York: Academic Press)*

Epstein PS and Carhart RR 1953 *J.Acoust.Soc.Am. 25, 553*

Fitzgerald JW, Ringo GR and Winder WC 1961 *J.Dairy.Sci. 44, 1165*

Foldy LL 1945 *Phys.Rev. 67, 107*

Food and Drink Federation 1985 *'Sensing and process control in tomorrow's food and drink industry'. Report of a Working Party of the Food and Drink Federation and the Food Manufacturers Federation.*

Formo MW 1979, *in: Bailey's Industrial oil and fat products Vol 1 (edited by D Swern) p. 177 (New York: John Wiley and Sons)*

Fox BA and Cameron AG 1970, *Food Science: A chemical approach (London: University of London Press)*

Garti N, Wellner E and Sarig S 1982 *J.Am.Oil.Chem.Soc. 59, 181*

Gassman 1951 *Geophysics 16, 673*

Gaunaurd GC and Uberall H 1981 *J.Acoust.Soc.Am. 69, 362*

Gaunaurd GC and Uberall H 1982 *J.Acoust.Soc.Am. 71, 282*

Gaunaurd GC and Uberall H 1983 *J.Acoust.Soc.Am. 74, 305*

Gibson 1970 *J.Acoust.Soc.Am. 48, 1195*

Gladwell N, Javanaud C, Peers KE and Rahalkar RR 1985 *J.Am.Oil.Chem.Soc. 62, 1231*

Gladwell N, Javanaud C, Anson LW and Chivers RC 1987 *Ultrasonics International Conference Proceedings p. 555 (Surrey: Butterworths)*

Gouw TH and Vlugter JC 1964 *J.Am.Oil.Chem.Soc 41, 524*

Gouw TH and Vlugter JC 1966 *Fette.Seifen.Anstrich. 68, 544*

Gouw TH and Vlugter JC 1967 *Fette.Seifen.Anstrich. 69, 159*

Graff KF 1981, *in: Physical Acoustics Vol. XV (edited by WP Mason and RN Thurston) p.2 (New York: Academic Press)*

Grigorev SB, Manucharov YS, Mikhailov IG and Khakimov O 1976 *Sov.Phys.Acoust. 21, 331*

Gunstone FD and Norris FA 1983, *Lipids in Foods: Chemistry, Biochemistry and Technology (Oxford: Pergamon Press)*

Habeger CC 1982 *J.Acoust.Soc.Am. 72, 870*

Hagemann JW, Tallent WH, Kolb KE 1972 *J.Am.Oil.Chem.Soc. 49, 118*

Hagemann JW and Rothfus JA 1983 *J.Am.Oil.Chem.Soc. 60, 1123*

Haighton AJ 1976 *J.Am.Oil.Chem.Soc. 53, 397*

Hampson GC and Hudson BJF 1961, *in: The chemistry and technology of edible oils and fats (edited by J Devine and PN Williams) p.1 (New York: Pergamon Press)*

Hannewijk J and Haighton AJ 1958 *J.Am.Oil.Chem.Soc. 35, 344 and 457*

Hannewijk J, Haighton A.J. and Hendrike P.W. 1964, *in Analysis and characterisation of oils, fats and fat products (edited by HA Boekenoogen) p.119. (London: Interscience Publishers)*

Harker AH and Temple JAG 1987 *J.Phys.D: Appl.Phys. In press*

Hay AE and Burling RW 1982 *J.Acoust.Soc.Am. 72, 950*

Hay AE and Mercer DG 1985 *J.Acoust.Soc.Am. 78, 1761*

Hibberd DJ, Howe AM, Mackie AR, Purdy PW and Robbins MM 1987a, *in Food Emulsions and Foams (edited by E Dickinson) p.219 (London: Royal Society of Chemistry).*

← Hibberd DJ, Howe AM, Mackie AR and Robins MM 1987b Ultrasonics International Conference proceedings p.54 (Surrey: Butterworths)

Hoerr CW 1955 *J.Am.Oil.Chem.Soc. 32, 372 and 659*

Howe AM, Mackie AR and Robbins MM 1986 *J.Sci.Tech. 7, 231*

Hueter TF, Morgan H and Cohen MS 1953 *J.Acoust.Soc.Am. 25, 1200*

Hussin ABBH 1982 *An investigation into the use of ultrasonics to monitor phase changes and dilation in fats and oils. PhD Thesis, Procter Department of Food Science, University of Leeds*

Hussin ABBH and Povey MJW 1984 *J.Am.Oil.Chem.Soc. 61, 560*

Hustad GO, Richardson T, Winder WC and Dean MP 1970 *J.Dairy.Sci. 53, 1525*

Hvolby A 1974 *J.Am.Oil.Chem.Soc. 51, 50*

Inoue N, Hirai M, Hasegawa T and Matsuzswa K 1986 *J.Phys.D: Appl.Phys 19, 1439*

Irani RR and Callis CF 1963 *Particle size: Measurement, Interpretation and Application (New York: John Wiley and Sons)*

Isakovich MA 1948 *Zh.Eksperim.I.Teor.Fiz. 18, 907*

Javanaud C, Lond P and Rahalkar 1986 *Ultrasonics 24, 137*

Javanaud C and Rahalkar RR 1988 *Fat Sci.Tech. 2, 73*

Javanaud C 1988 *Ultrasonics 26, 117*

Johnson DL and Plona TJ 1982 *J.Acoust.Soc.Am. 72, 556*

kaye GWC and Laby TH 1986, *Tables of Physical and Chemical Constants (London: Longman)*

Kinsler LE and Frey AR 1950 *Fundementals of Acoustics (London: Chapman and Hall)*

Koltsova IS and Mikhailov IG 1970 *Sov.Phys.Acoust. 15, 390*

Koltsova IS, Mikhailov IG and Saburov B 1974 *Sov.Phys.Acoust. 19, 455*

Koltsova IS and Mikhailov IG 1976 *Sov.Phys.Acoust. 21, 351*

Koltsova IS, Mikhailov IG and Trofimov GS 1980 *Sov.Phys.Acoust. 26, 319 Koltsova IS 1985 Sov.Phys.Acoust. 31, 158*

Kress-Rogers E 1986 *J.Phys E: Sci.Instrum. 19, 13 and 105*

Kuo HL 1971 *Jap.J.Appl.Phys. 10, 167*

Kuo HL 1975 *J.Am.Oil.Chem.Soc. 52, 166*

Kuster GT and Toksoz MN 1974 *Geophysics 39, 587*

Lambert W 1982 *The Chemical Engineer Aug/Sept, 320*

Lavery H 1958 *J.Am.Oil.Chem.Soc. 35, 418*

Lefebvre J 1983 *J.Am.Oil.Chem.Soc 60, 295*

Lin WH and Raptis AC 1983 *J.Am.Oil.Chem.Soc. 74, 1542*

Lister D 1984, *In vivo measurement of body composition in meat animals (London: Elsevier Applied Science Publishers)*

Lloyd P and Berry MV 1967 *Proc.Phys.Soc. 91, 678*

Lutton ES 1955 *J.Am.Oil.Chem.Soc. 32, 49*

Lutton ES 1972 *J.Am.Oil.Chem.Soc. 49, 1*

Lynnworth LC 1979, *in: Physical Acoustics Vol XIV (edited by WP Mason and RN Thurston) p.408 (New York: Academic Press)*

McCann JD 1986 *Report AERE-R 11271. Instrumentation and Applied Physics Division, Harwell Laboratory*

McClements DJ and Povey MJW 1987a *Adv.Colloid.Int.Sci. 27, 285*

McClements DJ and Povey MJW 1987b *Int.J.Food.Sci.Tech. 22, 491*

McClements DJ and Povey MJW 1987c *Ultrasonics International Conference Proceedings p.43 (Surrey: Butterworths)*

McClements DJ and Povey MJW 1988a *Int.J.Food.Sci.Tech. 23, 159*

McClements DJ and Povey MJW 1988b *J.Am.Oil.Chem.Soc. In press*

McClements DJ and Povey MJW 1988c *J.Am.Oil.Chem.Soc. In press*

McClements DJ and Povey MJW 1988d *J.Phys D: Appl.Phys. In press*

McSkimin HJ 1964, *in: Physical Acoustics Vol. 1A (edited by WP Mason) p.271 (New York: Academic Press)*

Medwin H 1974 *J.Acoust.Soc.Am. 56, 1100*

Mehta CH 1983 *Geophysics 48, 1359*

Merker DR, Brown LC and Wiedermann LH 1958, *J.Am.Oil.Chem.Soc. 35, 130*

Miles CA, Fursey GAJ and Jones RCD 1985 *J.Sci.Food.Agric. 36, 215*

Mohsenin NN 1980, *Thermal properties of Foods and Agricultural materials (New York: Gordon and Breach)*

Moy LF and Winder WC 1971, *J.Dairy Sci. 54, 756*

NAG 1987 *Numerical Algorithms Group Fortran Library Mannual-Mark 12, Volume 5 (Oxford: NAG Ltd)*

Nishi RY 1975 *Acustica 33, 65*

Norton IT, Lee-Tuffnell CD, Ablett S and Bociek SM 1985 *J.Am.Oil.Chem.Soc. 62, 1237*

Ogushwitz PR 1985 *J.Acoust.Soc.Am. 77, 441*

Ohsawa T 1969 *Jap J.Appl.Phys. 7, 795*

Papadakis EP 1976, *in: Physical Acoustics Vol. XII (edited by WP Mason and RN Thurston) p.277 (New York: Academic Press)*

Pierce AD 1981 *Acoustics: An Introduction to its Physical Principles and Applications (New York: McGraw-Hill Book Company)*

Pomeranz Y 1985, *Functional properties of Food components (London: Academic Press)*

Povey MJW 1984 *J.Am.Oil.Chem.Soc. 61, 558*

Povey MJW 1988, *in: Advances in Food Emulsions and Foams (edited by E Dickinson and G Stainsby) p.285 (Essex: Elsevier Applied Science Publishers)*

Povey MJW and McClements DJ 1988a *J.Food.Eng. In press*

Povey MJW and McClements DJ 1988b *Food Colloid Symposium In press*

Prentice JH 1984, *Measurements in the Rheology of Foodstuffs p.140 (London: Elsevier Applied Science Publishers)*

Pulle MW and Winder WC 1969 *J.Dairy Sci 52, 883*

Qashou MS, Vachon RI and Touloukian YS 1972 *ASHRAE Trans. 78, 165*

Rahalkar RR, Gladwell N, Javanaud C and Richmond P 1986 *J.Acoust.Soc.Am. 80, 33*

Rao CR, Reddy LCS and Prabhu CAR 1980 *Current.Sci. 49, 185*

Ratinskaya IA 1962 *Sov.Phys.Acoust. 8, 160*

Raznjevic K 1976, *Handbook of thermodynamic table and charts (Washington: Hemisphere Publishing)*

Rokhlenko AA, Trukshina TS and Abramzon AA 1980 *J.Appl.Chem. (USSR) 52, 2132*

Rohklenko AA 1986 *Meas.Tech.USA 29, 581*

Rossel JB 1986, *in: Analysis of Oils and Fats (edited by RJ Hamilton and JB Rossel) p.1 (London: Elsevier Applied Science Publishers)*

Rozhlenko AA, Firsov EI and Abramzon AA 1974 *Colloid.J.USSR. 36, 645*

Sajas JF, Zayas YF, Gorbatov WM and Gorbatov VM 1978 *Fleischwirtschaft 58, 1009 and 1143*

Sanderson ML 1982 *Electron.Power 23, 161*

Saraf B, Mishra SC and Samal K 1982 *Acustica 52, 40*

Saraf B and Samal K 1984 *Acustica 56, 61*

Sayers CM 1980 *J.Phys.D: Appl.Phys 13, 179*

Schwartz LM and Johnson DL 1984 *Phys.Rev. B 30, 4302*

Shung KK, Krisko BA and Ballard JO 1982 *J.Acoust.Soc.Am. 72, 1364*

Silk MG 1984, *Ultrasonic Transducers for Non-destructive testing (Bristol: Adam Hilger Ltd)*

Skoda W and Van den Tempel M 1963 *J.Colloid.Sci. 18, 568*

Sleeter RT 1985 *in: Bailey's Indistrial oil and fat products Vol. 3 (edited by TH Applewhite) p.167 (New York: John Wiley and Sons)*

Sonntag NOV 1979, *in: Bailey's Industrial oil and fat products Vol 1 (edited by D Swern) p.412 (New York: John Wiley and Sons)*

Stoll RD 1971, *in: Physics of Sound in Marine Sediments (edited by L Hampton) p.19 (New York: Plenum Press)*

Tonshev YV and Grekhova LD 1976 *Food Sci.Tech.Abs. 5P904, Vol. 8*

Twersky V 1962 *J.Opt.Soc.Am. 52, 145*

Urick RJ 1947 *J.Appl.Phys. 18, 983*

Urick RJ 1948 *J.Acoust.Soc.Am. 20, 283*

Urick RJ and Ament WS 1949 *J.Acoust.Soc.Am. 21, 115*

Van Boekel MAJS 1981 *J.Am.Oil.Chem.Soc. 58, 768*

Van Putte K and Van den Enden J 1974 *J.Am.Oil.Chem.Soc. 51, 316*

Waddington D 1986, *in: Analysis of Oils and Fats (edited by RJ Hamilton and JB Rossel) p.341 (London: Elsevier Applied Science Publishers)*

Walstra P 1987a, *in: Food structure and behaviour (edited by JMV Blanshard and P Lillford) p.67 (London: Academic Press)*

Walstra P 1987b, *in: Food structure and behaviour (edited by JMV Blanshard and P Lillford) p.87 (London: Academic Press)*

Waterman PC and Truell R 1961 *J.Math.Phys. 2, 512*

Weiss TJ 1983 *Food Oils and their uses (Chichester: Ellis Horwood Ltd)*

Wessenti-Pulle MP 1972 *Dissertation Abstracts International B 33, 1604*

Winder WC, Consigny NP and Rodriguez-Lopez B 1961 *J.Dairy.Sci. 44, 1165*

Wood AB 1941 *A Textbook of Sound (London: Bell)*

Wyn-Jones E, Pereira MC and Morris ER 1982 *Prog.Fd.Nutr.Sci. 6, 21*

Zemansky MW 1957, *Heat and thermodynamics (New York: McGraw Hill Book Company)*